Norad

A Hydrogeological Atlas of
Faryab Province
Northern Afghanistan

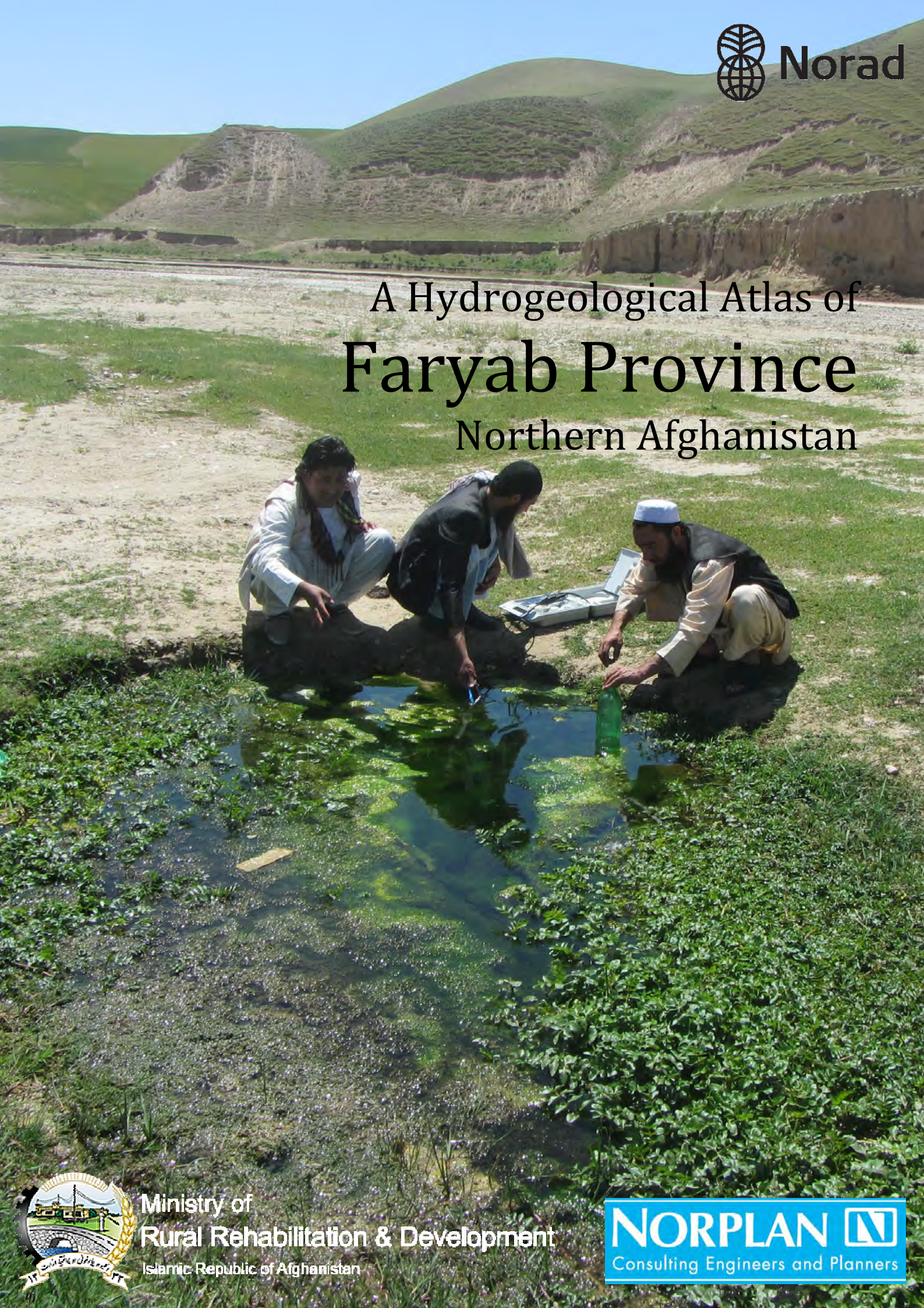

Ministry of
Rural Rehabilitation & Development
Islamic Republic of Afghanistan

NORPLAN
Consulting Engineers and Planners

Hydrogeological Atlas of Faryab Province

This Atlas was prepared in 2013-2014 by staff of NORPLAN (a trading name of Asplan VIAK AS, Kristiansand, Norway) under the auspices of the project:

Capacity Building and Institutional Cooperation in the field of Hydrogeology for Faryab Province, Afghanistan

The project client is the Afghan Ministry of Rural Rehabilitation & Development (MRRD), and the project was funded by Norwegian NORAD.

Author	David Banks (NORPLAN, Holymoor Consultancy Ltd.)

Data and assistance with figures were provided by

Data collection	Mohammed Hassan Saffi (DACAAR)
and facilitation	Mohammed Hadi (DACAAR)
	Ahmed Jawed (DACAAR)
	Jalil Anwari (MRRD)
	Ewaz Ali Poya (MRRD)
	Prof. Naim Eqrar (NORPLAN, University of Kabul)
	Ehsanullah Bayat (NCA)
GIS . Cartography	Prof. Shuaib Zarinkhail (NORPLAN, University of Kabul)
Project Management	Naqibullah Abrar (NORPLAN)
	Svein Stoveland (NORPLAN)
Geophysics diagrams	Andreas de Jong (NORPLAN, GeoSearch)
Hydrochemistry diagrams	Bjørn Frengstad (Norges geologiske undersøkelse)
Water analyses	Michael Watts (British Geological Survey)
	Cynthia Turner (British Geological Survey)
	NERC Isotope Laboratory, Keyworth, UK
Soil extractions	DACAAR wet laboratory, Kabul

We also acknowledge the assistance provided by colleagues in other Afghan Ministries in facilitating data provision, especially staff of the Ministry of Energy and Water (Dr Sayed Shaif Shobair and colleagues) and the Ministry of Mines (especially Fahim Zahir and Dr Naim Tookhey).

NORPLAN 2014

Contents and Key Diagrams

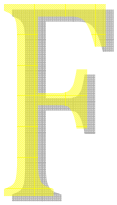

F

Note on use of external materials

The authors have made particular use of two sets of data in the preparation of this report:

1. The work and data-layers resulting from the collaboration between the United States Geological Survey and the Afghan Geological Survey, especially:
    - the 1:250,000 geological maps of McKinney & Sawyer (2005), McKinney & Lidke (2005) and Wahl (2005).
    - the data layers described in Steinshouer et al.'s (2006) Open File report **OFR-2006-1179**

As publicly funded products published by the USGS, we have assumed that these represent public domain sources. We gratefully acknowledge the use of these invaluable data sources.

2. Google Earth imagery. As our primary intention in using these images is ***not*** to present the Google Earth images themselves, but rather to use them as a geographical reference background on which we project our own data, we claim that this falls within the definition of "reasonable and fair use" of these images.

1. Faryab Province: A History of Water Resources

Faryab Province straddles several steep topographic, meteorological and geological gradients. The southern portion of the Province is dominated by the high topography of the Safed Koh / Band-e Turkestan mountains of the Hindu Kush: temperatures are modest and winter snow and rain provide adequate supplies of fresh water.

Towards the north, the lowland semi-desert plains of Oxiana predominate, underlain by the molasse-like and alluvial erosional deposits of the Hindu Kush uplift. The climate becomes more severe, with high evapotranspiration and limited rainfall. Water resources become scarcer and what water can be found is brackish. The northern portion of Faryab has thus been a marginal environment for human habitation during recent centuries.

Faryab not only occupies a physiographical and climatic divide, it also represents a cultural and political transition, between the Afghan and Persian heartlands to the south and the plains of Central Asia to the north. The semi-desert area north of the mountains and around the Amu Darya River (or Oxos) has often been referred to as Oxiana or Turkestan.

Maimana had been a prominent city since the early Islamic era, when it had been known in Arabic as *al-Yahudiyya* (city of the Jews - Lee 1987). It was destroyed during the Mongolian invasions of Turkestan and subsequently became a khanate that was a bone of contention between the Persians and Afghans to the south and the Turkic powers (such as the Emirate of Bokhara) to the north. From 1893 onwards, Maimana became a province of Afghanistan, with an Afghan governor.

Today, Faryab has an area of 20,293 km^2 a population of around 948,000, of which 114,000 are classified as "urban" and 834,000 are "rural" (CSO 2013). The Province is subdivided into 14 districts, as follows:

Table 1.1. The Districts of Faryab Province (as of 2013)

District	Population (CSO 2013)	Area (km^2) (Wikipedia)
Qaysar	138,400	2,502
Almar	68,300	1,525
Kohistan	53,100	2,254
Gurziwan	73,700	1,875
Pashtun Kot	183,500	4,000
Khwaja Sabz Posh	49,400	800
Bilchiragh	50,700	1,189
Maimana	78,500	133**
Shirin Tagab	79,100	3,500
Dowlatabad	47,200	2,598
Qaramqol	19,100	2,192
Qurgan	45,800	797
Andkhoi	38,700	381
Khani Chahar Bagh	22,500	1,056
Ghormach	52,566*	2,083

** Ghormach has been included in this Atlas, as there has been some recent discussion as to whether to transfer this district from Badghis to Faryab. The district's population was 52,566 in 2003, according to http://en.wikipedia.org/wiki/Ghormach_District*

*** Calculated in Google Earth*

A large proportion of the population, especially in rural districts, are from Uzbek or Turkmen linguistic groups, with significant numbers of Tajiks and Pashtuns, and a minority of Hazaras.

1.1 Vámbéry's (1865) Travels in Central Asia

When Arminius Vámbéry described his 1863 travels to the area in his *Reise in Mittelasien*, Maimana was a somewhat precarious khanate loyal to Turkestan. Indeed, Maimana was regarded as offering a first line of defence to any attempt on Bokhara from the south.

Vámbéry he entered Faryab from the north. He described the country between Zeid and Andkhoi as "*one dry barren plain, only occasionally producing a sort of thistle, the favourite fodder of the camels".* Vámbéry encamped at Khani Chahar Bagh and remarked of Andkhoi that "*it is astonishing what a quantity of fruit, corn and rice is raised in this desert-like neighbourhood, only scantily watered by a little salt stream* (the Shirin Tagab) *flowing hither from Maymene. In summer, a stranger finds the water - to the execrable taste of which the inhabitants are accustomed - quite undrinkable...it is said to produce many other evil consequences".* Vámbéry cites an old Persian verse:

Andkhuy has bitter salt water, scorching sand, venomous flies and even scorpions;
Vaunt it not, for it is the picture of a real hell.

In 1865, Vámbéry notes that a mere 30 years previously, Andkhoi had been a thriving city of 50,000 souls, with a widespread export of sheepskins and camels. Andkhoi, then a khanate in its own right, had subsequently been subsumed by Bokhara and forced to resist incursions by Afghans from the south. Caught between the jaws of Maimana, Bokhara and the Afghans, it had diminished to a ruinous town of 2000 houses and maybe 3000 tents in the surrounding area, with a total population of some 15,000.

Vámbéry progressed south via Khairabad, Bad Qaq and Akkale towards Maimana, strategically located at the boundary between plains and mountains (Figure 1.1). Vámbéry found Maimana to be a fortified town of some 1500 dwellings, inhabited by Afghans, Uzbeks, Tadjiks, Heratis, Jews and Hindus, with markets trading in horses, carpets, raisins, aniseed and pistachio. His journey continued via Almar, Nahrin, Qaysar, Chechaktu and on across the mountains to the valley of Bala (Upper) Murghab

1.2 Byron's (1937) Road to Oxiana

In 1933, some 70 years after Vámbéry, the irascible Robert Byron journeyed through Persia and Afghanistan to Oxiana. He entered Faryab via Bala Murghab, Karez (which he regarded as the beginning of "Turkestan"), Bukhara Qala and Maimana. He compared Maimana to the Wiltshire uplands of England, with strings of villages along a meandering river, flanked by mulberry and apricot trees. For Byron, the transition to semi-desert seemed to take place around Faizabad, where the landscape became lower, barren and sandy. The Governor of Maimana at that time described the ground as "*cooked*" between Faizabad and Mazar-e-Sharif, until one reached the fertile banks of the Amu Darya.

Like Vámbéry, Byron described Andkhoi as the centre of the lambskin (karakul and arabi) trade. Beyond (NE of) Andkhoi, Byron found the Oxianian landscape "*colourless and suburban*", turning progressively from "*leaden*" to the colour of aluminium.

1.3 Irrigation

In recent times, the situation has not changed so much. The main use of water in Faryab Province is for irrigation - much of this comes from the main rivers themselves.

Anecdotally, ever greater "takes" of water for irrigation have led to less and less water reaching Andkhoi in the summer months. Indeed, at Araba, a major irrigation channel takes the majority of the Shirin Tagab river's flow, leading it north to the Dowlatabad area, leaving the natural watercourse almost dry at some times of year (Figure 1.2).

Groundwater from springs and wells is also used in lesser quantities for irrigation and, historically, *karezes* (also called *qanats* or *aflaaj* in Arabia) were used to provide irrigation in many parts of Afghanistan. These karezes are horizontal adits, skimming groundwater from just below the water table in foothill areas and leading it several hundred metres, or even kilometres, to a point of use. In the last two decades, these karezes have fallen into disuse (Shobair & Alim 2004), as a result of:

- damage or lack of maintenance during the many years of civil war,
- disruption of social customs and management systems for irrigation usage, often traditionally coordinated by a village *mirab* (Thomas & Ahmad 2009), and
- in some cases, natural drought periods or the exploitation of deeper, pumped boreholes lowering the water table and drying up shallow karezes or dug wells (Banks 2001, Banks & Soldal 2002).

The economy of Faryab is based partly on livestock (cattle, sheep, goats, donkeys, occasionally camels), but largely on irrigated agriculture. Crops include wheat, barley, maize, potatoes and flax in fields, with fruit, nuts, vegetables, alfalfa, clover and (especially in Qaysar) grapes being cultivated in garden plots. Cotton, sesame and (in Almar, Qaysar and Gurziwan) tobacco are also produced as commodities. There was also a small (4% of rural population) opium poppy activity reported in 2005 (MRRD 2007).

Of the Shirin Tagab catchment area, around 40% is classified as rangeland, 36% is amenable to rain-fed agriculture while some 7.2% is irrigated (Ibrekk et al. 2006). Of the rural population of Faryab, around 81% had access to rain-fed land in 2005, with 37% having access to irrigated land (MRRD 2007). In the 1980s, Lee (1987) was able to write that "*There is still much semi-sedentary farming in the outlying areas, and during the summer many villages in Gurziwan are empty except for older men and the sick, the rest of the community have moved to the summer pastures and* lalmi *or non-irrigated lands where they grow their summer wheat and pitch their yurts and tents near a convenient source of water*."

Although Qureshi (2002) cites data suggesting that karezes have previously been a significant source of irrigation water in Faryab, his graphic materials suggest that canals are responsible for by far the largest area of irrigated land. During the NORPLAN surveys of 2013, no operational karezes were registered in Faryab (although the survey did not cover all areas or districts).

Table 1.2. Land cover in the catchments of the Murghab River in Afghanistan and the Shirin Tagab, after Favre & Kamal (2004).

Land cover	% of Murghab catchment	% of Shirin Tagab catchment
Rangeland (grass / low shrubs)	84.1	40.4
Rain-fed crops	12.9	35.8
Irrigated (intermittent)	1.4	4.7
Irrigated (intensive, 1 crop/year)	1.1	2.6
Irrigated (intensive, 2 crops/year)	0.01	-
Sand (semi desert)	-	15.5
Fruit trees	0.00	0.5

1.4 Potable Water Supply

There are three areas in the Province where saline groundwater has been a major issue:

1. the **Shor Darya Valley** (See Section), where both the Shor Darya river itself and the adjacent groundwaters are highly saline (>6000 µS/cm in the Shor Darya River). The main sources of potable water in this area (from which water is distributed by donkey or camel) are:

- the large Ateh Khan Khwaja spring, at the confluence of the Maimana and Qaysar Rivers, with a discharge of some 25 L/s and an electrical conductivity of only some 2660 µS/cm (Hassan Saffi 2010b).
- the Shirin Tagab river itself, with an electrical conductivity of <1000 µS/cm, but highly vulnerable to faecal microbial contamination (Hassan Saffi 2010b).

2. the **Astana Valley**, where both the Astana river itself (> 45,000 µS/cm) and the adjacent groundwaters are highly saline. The main sources of potable water in this area are:

- springs at Moghaito, on the southern flanks of a Cretaceous / Palaeozoic limestone/sandstone inlier, with discharges of around 3 L/s and an electrical conductivity of only some 3400-4500 µS/cm (Hassan Saffi 2010a).
- the Shirin Tagab river itself.

3. the area north of Faisabad and, in particular, the city of **Andkhoi** and surrounding urban areas. The groundwater is typically brackish in this area, and the surface water in the Shirin Tagab and its distributary irrigation canals is also brackish, contaminated and scarce, especially in the summer months. Alternative sources of potable water in this area include:

- a few wells or boreholes (typically located near irrigation ditches) where somewhat less brackish groundwater can be got (it is surmised that these may be recharged from irrigation canal infiltration).
- desalination (by electrically-powered reverse osmosis) of saline groundwater from dug wells. The NGO *Norwegian Church Aid* has been especially active in piloting such plants, although some question marks hang over the long-term technical and economic sustainability of such a strategy.
- collection and transport of water from distant sources, such as Shirin Tagab district, which is the northernmost district where relatively fresh groundwater can be got. A water trade, based on transport and sale of water collected from fresh sources, is in operation.

In recent years, a major engineering project was contracted by the Government for the construction of a major pipeline, carrying fresh groundwater from a well-field on the southern bank of the Amu Darya river, located a short distance NW of Kelif, across the desert to Andkhoi (MUMTAZ 2007). Several of these wells yielded relatively fresh calcium bicarbonate water of total dissolved solids <1000 mg/L, and in some cases <500 mg/L. This project appears to have been unsuccessful, allegedly due to issues with pipeline materials' quality and interference with the pipeline.

It is possibly worth noting that such large scale import of water to an urban area such as Andkhoi is fraught with difficulty unless an adequate disposal route can be identified. The import of water would likely lead to increased infiltration to the ground, via pit latrines, pipe leakages and irrigation. It would thus potentially lead to a rise in water table and further salinisation of groundwater, as salts are leached out of the unsaturated zone by the rising groundwater. It could even lead to problems with groundwater

inundation if allowed to continue unchecked. Such a scenario is recorded from many areas of the world where water has been imported to arid city environments, most notably in Riyadh, Saudi Arabia (Kreibich & Thieken 2008).

Figure 1.1. Irrigation pumps on the River Shirin Tagab at Char Shengo, Dowlatabad District. Photo taken by DACAAR on 12th May2013.

Figure 1.2. Irrigation channel, fed by water drawn from the River Shirin Tagab, near Araba, Dowlatabad District. Photo taken by DACAAR on 12th May2013.

Of Etymological Interest

The name ***Faryab*** is believed to mean *irrigated land.*

Figure 1.3. The channel of the River Shirin Tagab at Araba (Dowlatabad District), heavily depleted by the upstream offtake of irrigation water (Figure 1.3). Photo taken by DACAAR on 12th May2013.

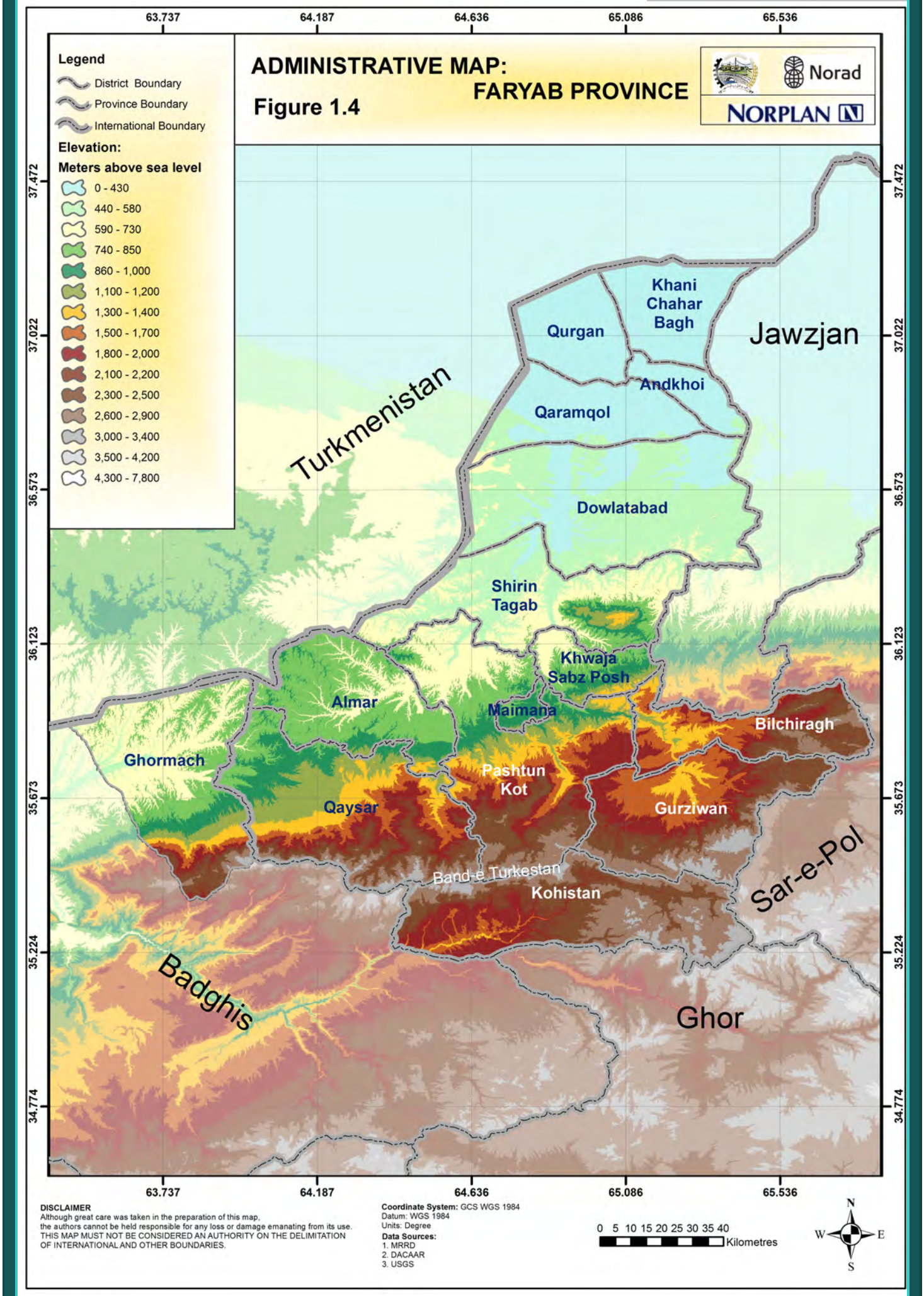
ADMINISTRATIVE MAP:
FARYAB PROVINCE
Figure 1.4
Norad
NORPLAN
Legend
District Boundary
Province Boundary
International Boundary
Elevation:
Meters above sea level
0 - 430
440 - 580
590 - 730
740 - 850
860 - 1,000
1,100 - 1,200
1,300 - 1,400
1,500 - 1,700
1,800 - 2,000
2,100 - 2,200
2,300 - 2,500
2,600 - 2,900
3,000 - 3,400
3,500 - 4,200
4,300 - 7,800
63.737
64.187
64.636
65.086
65.536
37.472
37.022
36.573
36.123
35.673
35.224
34.774
Turkmenistan
Jawzjan
Khani Chahar Bagh
Qurgan
Andkhoi
Qaramqol
Dowlatabad
Shirin Tagab
Khwaja Sabz Posh
Almar
Maimana
Bilchiragh
Ghormach
Pashtun Kot
Qaysar
Gurziwan
Band-e Turkestan
Kohistan
Sar-e-Pol
Badghis
Ghor
DISCLAIMER
Although great care was taken in the preparation of this map,
the authors cannot be held responsible for any loss or damage emanating from its use.
THIS MAP MUST NOT BE CONSIDERED AN AUTHORITY ON THE DELIMITATION
OF INTERNATIONAL AND OTHER BOUNDARIES.
Coordinate System: GCS WGS 1984
Datum: WGS 1984
Units: Degree
Data Sources:
1. MRRD
2. DACAAR
3. USGS
0 5 10 15 20 25 30 35 40
Kilometres
N
W
E
S

Figure 1.5. Physiography of Faryab Province showing selected settlements

Turkmenistan

63.287 63.737 64.187 64.636 65.086 65.536 65.985

37.022 36.573 36.123 35.673 35.224

Andkhoi
Khani Chahar Bagh
Qurgan
Qaramqol
Shirin Tagab
Pata Baba
Char Shengo
Dowlatabad
Khairabad
Shor Darya River
Araba
Faizabad
Koh-e Sayed (Deh-e Now)
Shirin Tagab Centre
Ateh Khan Khwaja Spring
Moghaito Spring
Bad Qar
Qaysar River
Bibi Aina borehole
Maimana
Dam Qul
Salmalik
3 new boreholes
Almar
Arab Aqsay
Surkhab
Bukhara Qala
Darrah-i-Akhzi
Bilchiragh
Karez
Nahrin
Chechaktu
Qaysar
Jar Qala (Gurziwan)
Maimana River
Sar-e Hawdz
Zyarat Gah
Bala Murghab
Telan
Qal'a (Kohistan)
Murghab River

63.287 63.737 64.187 64.636 65.086 65.536 65.985

DISCLAIMER
Although great care was taken in the preparation of this map, the authors cannot be held responsible for any loss or damage emanating from its use. THIS MAP MUST NOT BE CONSIDERED AN AUTHORITY ON THE DELIMITATION OF INTERNATIONAL AND OTHER BOUNDARIES.

File Path: Y:\2 RuWATSIP\1_RGIS\01_Project_Files\03_Working\forAtlas\Figure 1.5 Physiography of Faryab Province showing selected settlements v1.3.mxd

Coordinate System: GCS WGS 1984
Datum: WGS 1984
Units: Degree
Data Sources:
1. MRRD
2. DACAAR
3. USGS

Scale 1:1,000,000 @ A3 paper size

N W E S

Legend

- Towns
- Other Locations
- Major Springs
- Reservoir
- Wellfields / Boreholes
- Rivers
- International Boundary
- Province Boundary
- District Boundary

Elevation:
Meters above sea level

- 0 - 430
- 440 - 580
- 590 - 730
- 740 - 850
- 860 - 1,000
- 1,100 - 1,200
- 1,300 - 1,400
- 1,500 - 1,700
- 1,800 - 2,000
- 2,100 - 2,200
- 2,300 - 2,500
- 2,600 - 2,900
- 3,000 - 3,400
- 3,500 - 4,200
- 4,300 - 7,800

DRAWING:

Physiography of Faryab Province:

Showing selected settlements

Drawn by:	Shuaib Zarinkhail	Date:	Mar 2014
Checked by:		Date:	
Authorized by:		Date:	
Drawing No:	01		
Version:	1.3		

PROJECT:

Capacity Building and Institutional Cooperation in the field of Hydrogeology for Faryab Province, Afghanistan

CLIENT:

Norad

NORPLAN

2. Faryab: Location, Topography and Climate

2.1 Location

Faryab Province lies in the north of Afghanistan, with a northern border to the former Soviet republic of Turkmenistan. Faryab is bordered in the west by Badghis Province, to the east by Jawzjan and Sar-e-Pol and to the south by the mountainous province of Ghor.

2.2 Topography

At the core of Faryab province lies the Band-e-Turkestan, an east-west ridge of mountains. This is the westernmost spur of the Hindu Kush massif, which is in turn the Afghan portion of the great Himalayan orogenic belt.

The Band-e-Turkestan range is formed by a horst-like inlier of older lithified Permian and Triassic sedimentary rocks penetrating through the surrounding Cretaceous-Palaeogene limestones and clastic sedimentary rocks. Erosion in Miocene times has restricted the elevation of the summits of the Band-e-Turkestan to 3200-3500 m asl (Encyclopaedia Iranica 2013).

The Band-e-Turkestan forms a major watershed, separating the Shirin Tagab catchment to the north from the Murghab catchment to the south.

The terrain to the south of the Band-e-Turkestan (Kohistan district, in Faryab) is largely underlain by Cretaceous-Palaeogene limestones and is relatively elevated, much of it being at an altitude in excess of 1800 m asl. The terrain is deeply incised by the River Murghab and its tributaries, which form deep ravines. Limestone-fed springs are abundant.

To the north of the Band-e-Turkestan, the land falls away to the plains of the Dasht-e Shortepe (the salty desert), which stretch between Faizabad and the Amu Darya. Cretaceous and Palaeogene sedimentary rocks predominate until an elevation below c. 1500 m, below which the topography is dominated by foothills comprised of the erosional deposits from the Himalaya / Hindu Kush mountain building episode - namely Neogene molasse and alluvial fan deposits. These are often overlain by silty Quaternary wind-blown loess.

The main rivers (e.g. Maimana and Shirin Tagab) have flat valley floors, infilled with recent alluvium, and it is on these that much of the irrigated agriculture takes place.

Below Faizabad (c. 500 m asl) the terrain opens out into the flat semi-desert of Dasht-e Shortepe which is formed by Quaternary alluvial and wind-blown deposits. The terrain continues to fall gently northwards past Andkhoi (c. 310 m asl) and the Turkmenistan Border at Kolodets Imam Nazar (260 m asl), towards the Zeid depression (240 m asl, now occupied by a large Turkmen reservoir) and the Amu Darya itself at c. 245 m asl.

2.3 Climate: Temperature, Sunshine and Humidity

According to historic maps published by AIMS, many of which are reproduced in Favre & Kamal (2004), Faryab experiences between 2600 and 3000 sunshine hours per year, inversely depending on altitude.

The average temperature of the hottest month varies from >30°C in the northern semi-desert to <15°C in the Bund-e-Turkestan mountains.

The average temperature of the coldest month varies from <5°C in the northern semi-desert to below 0°C just south of Maimana and <-10°C in the Bund-e-Turkestan mountains. Figure 2.1 indicates that the average temperature in Maimana varies from

around 2°C in January to over 27°C in July, with a long term average of 14.7°C (Favre & Kamal 2004 cite an annual average temperature of 14.4°C).

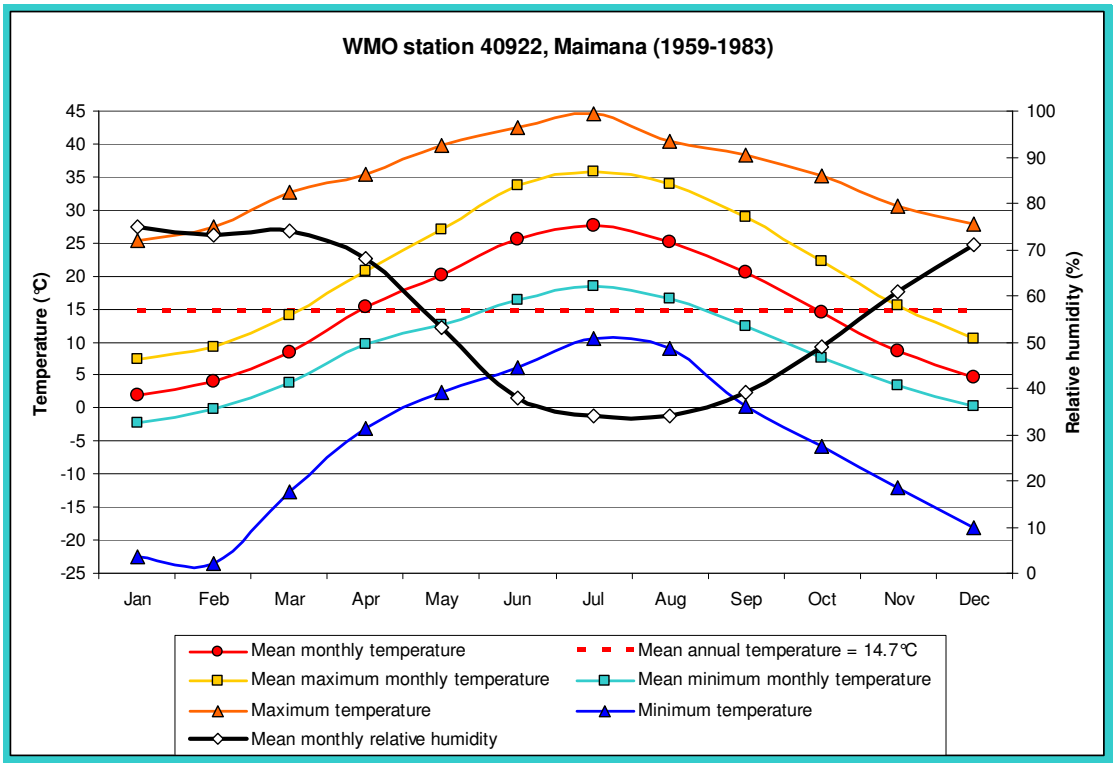

Figure 2.1. Long term dry-bulb air temperature data for WMO meteorological station Maimana (station 40922) in period 1959-83 (minimum temperature and relative humidity based on 1964-1983. Data derived from the NOAA website: ftp://dossier.ogp.noaa.gov/GCOS/WMO-Normals/RA-II/AH/40922.TXT

Arguably, the best regional sources of meteorological data for temperature are found at the NOAA website http://www.esrl.noaa.gov/psd/data/gridded/data.ghcncams.html. For air temperature, the following file has been used to calculate (Figure 2.2) long-term gridded monthly means, based on data from 1981-2010, on a 0.5 degree latitude x 0.5 degree longitude global grid (360x720):

- ftp://ftp.cdc.noaa.gov/Datasets/ghcncams/Derived/air.mon.1981-2010.ltm.nc.

These data are derived from the GHCN_CAMS Gridded 2m Temperature (Land) data set (Fan & Van den Dool 2008). Figure 2.3 compares the temperatures recorded at Maimana, with those in the calculated grid squares containing Andkhoi and mountainous Kohistan regions.

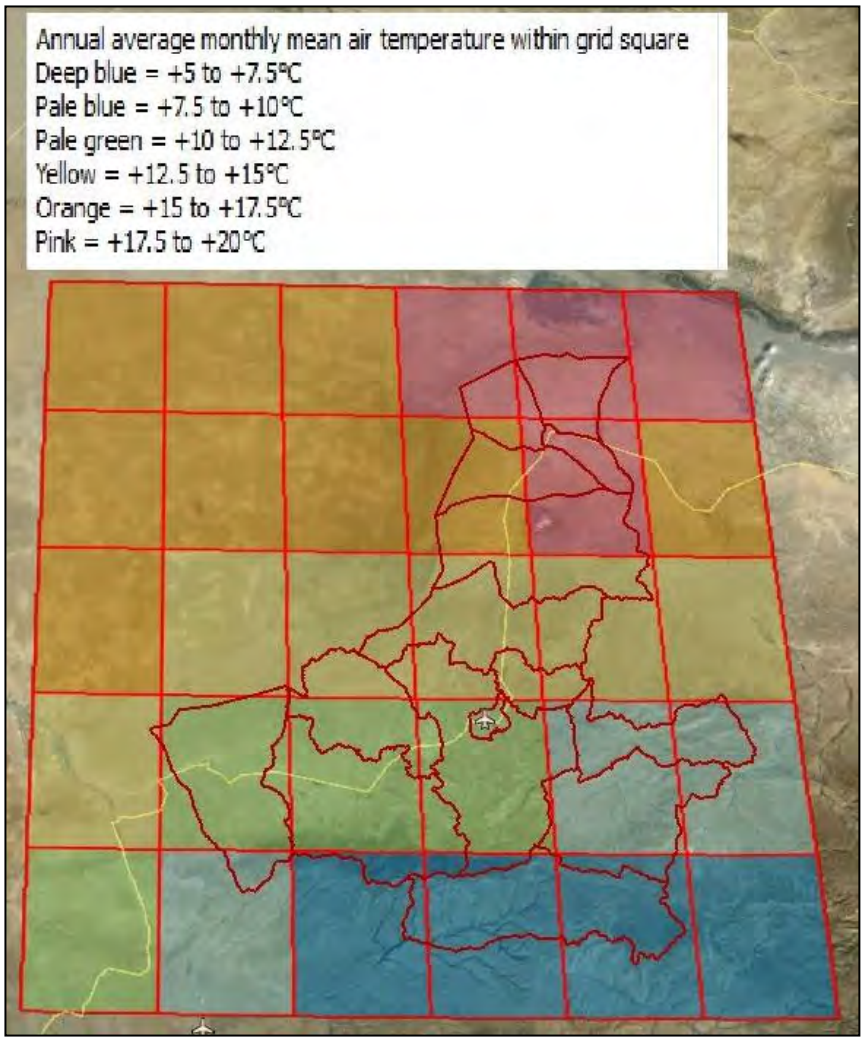

Figure 2.2. Average monthly mean air temperature within 0.5° grid squares, based on 1981-2010 data, after Fan & Van den Dool (2008).

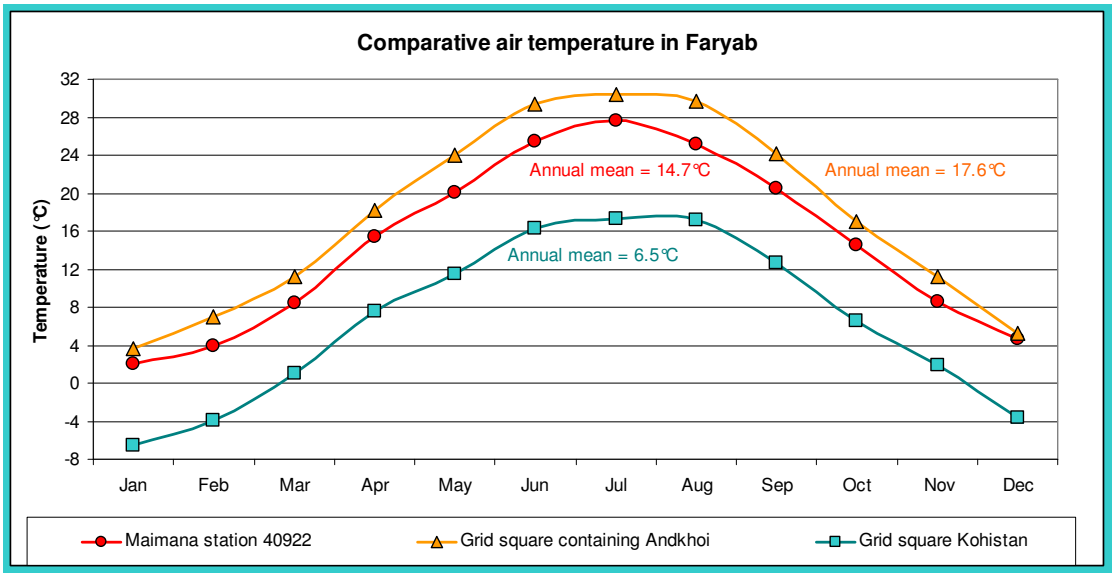

Figure 2.3. Long term annual mean air temperatures at Maimana (WMO station 40922) and in the grid squares containing Andkhoi and western Kohistan (from the NOAA dataset described in Fan & Van den Dool 2008).

2.4 *Climate: Precipitation and Evaporation*

According to historic maps published by AIMS, many of which are reproduced in Favre & Kamal (2004), average precipitation in Faryab ranges from 600-800 mm/a in the mountains, down to <300 mm/a in the semi-deserts of the north of the province.

Figure 2.4 shows that the bulk of precipitation in Faryab falls between November and May, with very little occurring between June and September.

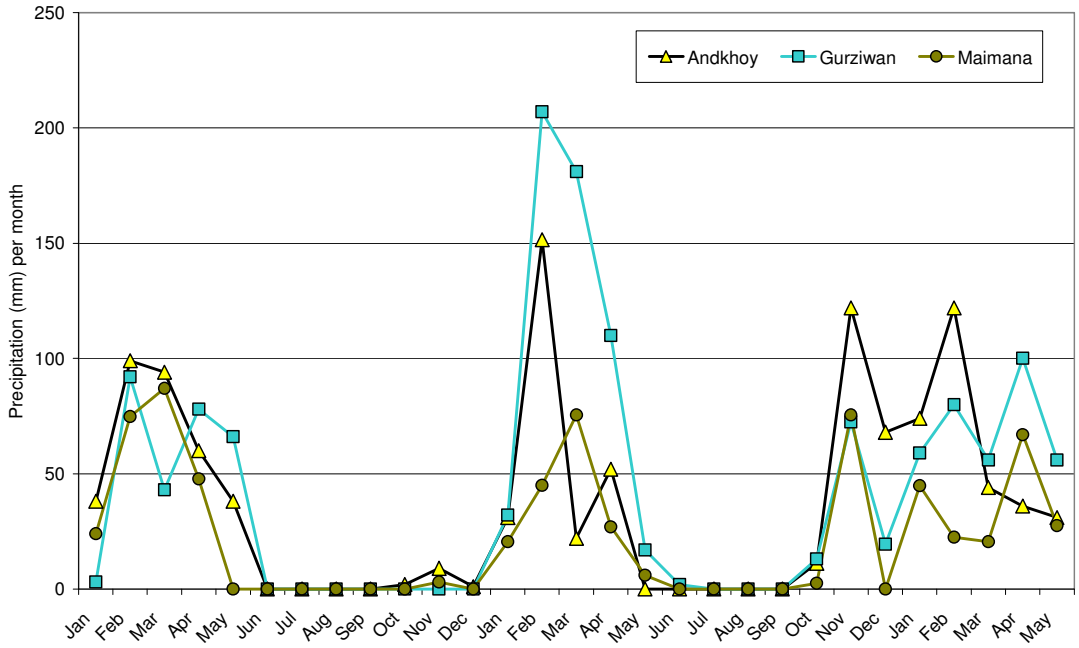

Figure 2.4. Monthly precipitation measured at Agromet stations in Maimana, Gurziwan and Andkhoi from January 2010 to May 2012, provided by the Afghan Ministry of Agriculture, Irrigation and Livestock (MAIL).

Station	Mazar-e-Sharif	Maimana	Lal-o-Sarjangal
Annual average precipitation	189 mm/a	354 mm/a	227 mm/a
Annual average potential evapotranspiration	1376 mm/a	1202 mm/a	695 mm/a
Monthly average potential evapotranspiration (coolest month)	0.6 mm/d	0.6 mm/d	0.2 mm/d
Monthly average potential evapotranspiration (hottest month)	8.5 mm/d	7.2 mm/d	4.3 mm/d

Table 2.1. Comparison of long-term precipitation and potential evapotranspiration data for Maimana with a semi-desert location (Mazar-e-Sharif) and a highland location (Lal-o-Sarjangal) - after Favre & Kamal (2004).

Figure 2.5 compares the precipitation and potential evapotranspiration in Maimana, with that at Andkhoi. It will be noted that, throughout Faryab, potential evapotranspiration greatly exceeds precipitation on an annual basis. In Maimana, precipitation typically only exceeds potential evapotranspiration in the window December to March. In Andkhoi, excess precipitation only marginally occurs in January, implying that opportunities for infiltration of excess rainfall as groundwater recharge will be very limited in the north of the Province.

The Watershed Atlas of Favre & Kamal (2004) indicates that the "normal" annual precipitation at Maimana is 354 mm, with a range from 200 mm to 582 mm. The annual

average potential evapotranspiration is cited as a massive 1202 mm/a (equivalent to 3.34 mm/d), with monthly means ranging from 0.6 to 7.2 mm/d. Table 2.1 compares these data with Mazar-e-Sharif (which would not be dissimilar to Andkhoi) and Lal-o-Sarjangal in Ghor Province (not dissimilar to the mountainous portions of Faryab).

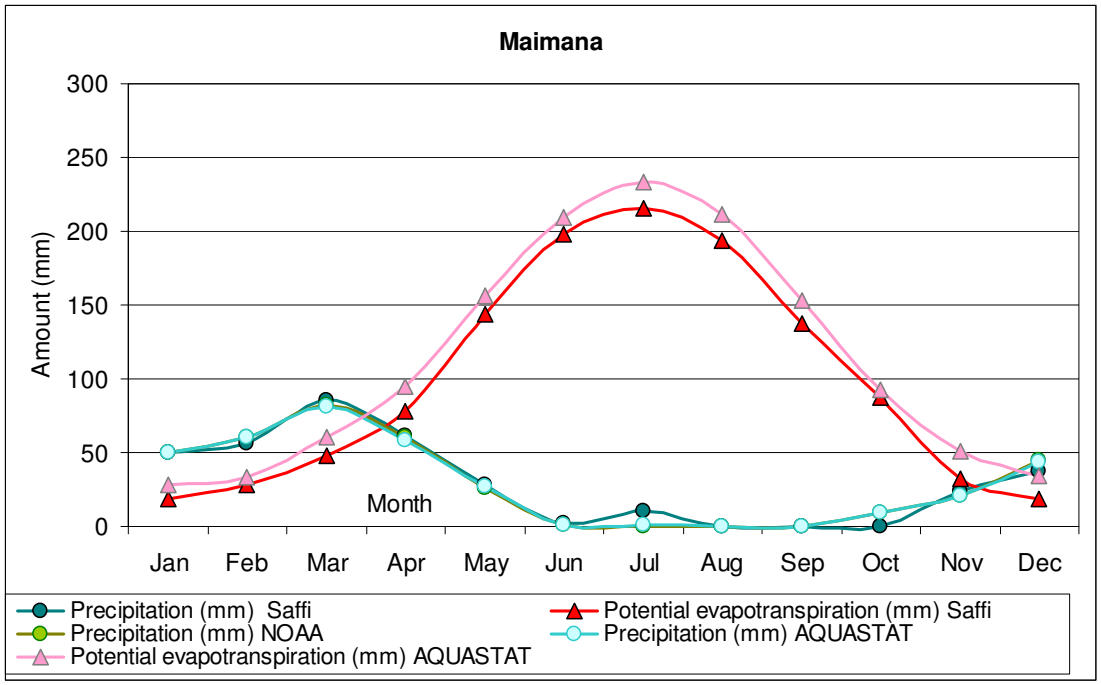

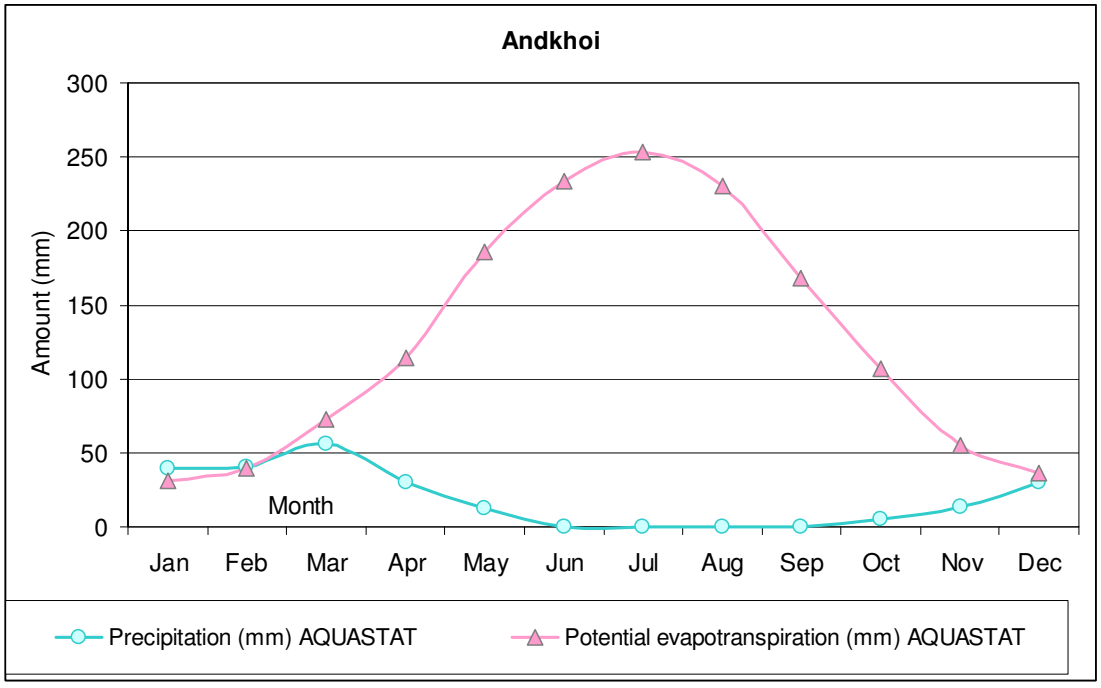

Figure 2.5. Monthly mean precipitation and evapotranspiration data for Maimana and Andkhoi. The data marked *Saffi* are long-term averages (annual mean total precipitation - 354 mm and potential evapotranspiration 1202 mm) from the Maimana meteorological station (1958-1978) cited by Hassan Saffi (2010a,b). *AQUASTAT* refers to data from the FAO Aquastat tool at http://www.fao.org/nr/water/aquastat/gis/index3.stm. *NOAA* refers to long-term averages (annual mean total precipitation - 356 mm) from the WMO station 40922 (1964-83) at Maimana, from ftp://dossier.ogp.noaa.gov/GCOS/WMO-Normals/RA-II/AH/40922.TXT. The *AQUASTAT* and *NOAA* data are almost identical.

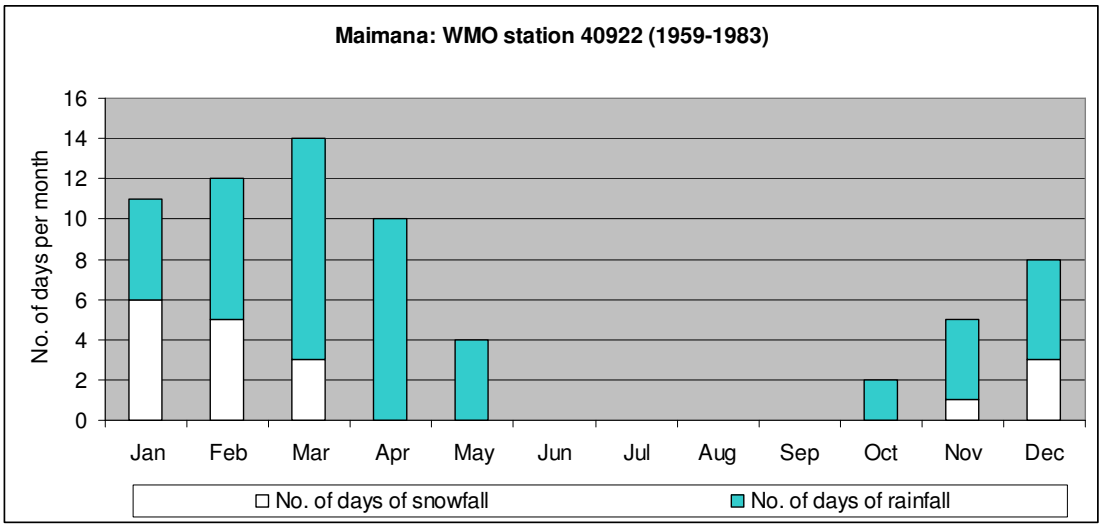

Figure 2.6. Average number of days of snowfall and rainfall recorded at WMO station 40922 Maimana for the period 1959-1983, according to data download from ftp://dossier.ogp.noaa.gov/GCOS/WMO-Normals/RA-II/AH/40922.TXT

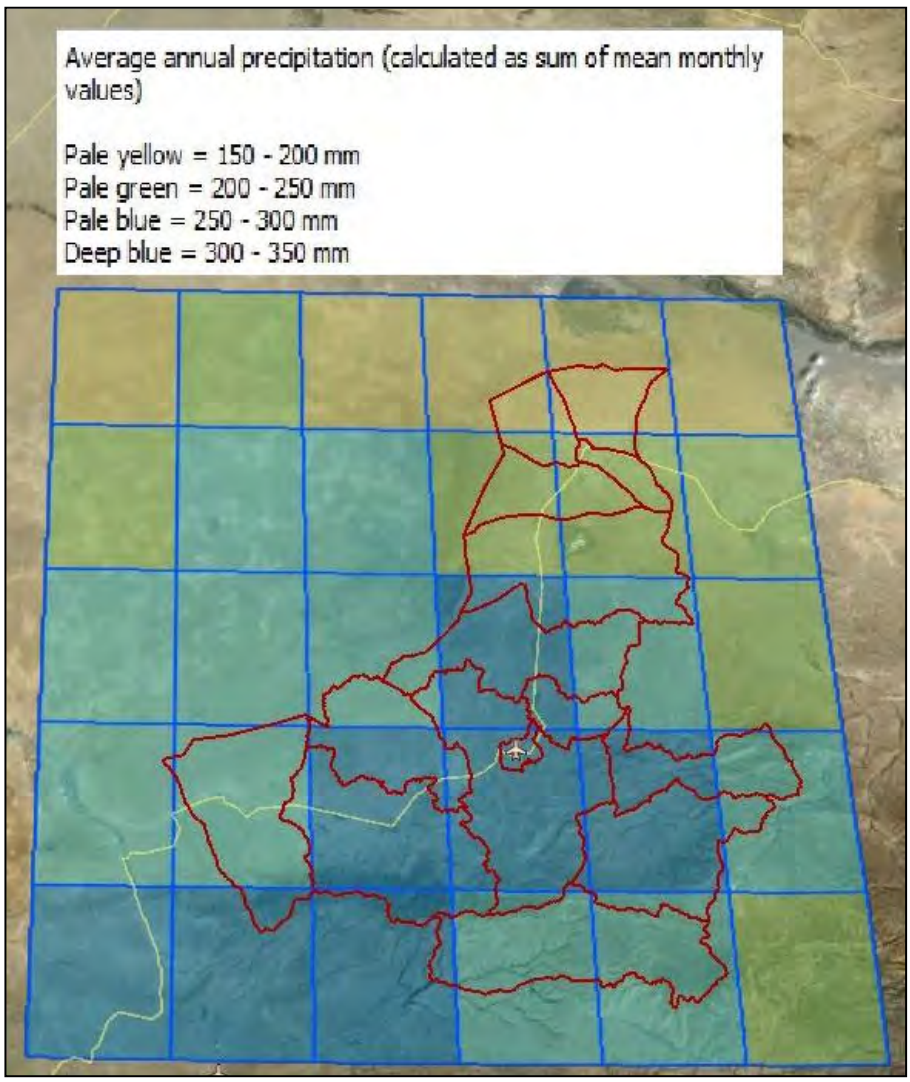

Figure 2.7. Average annual precipitation within 0.5° grid squares, based on 1981-2010 data, after Schneider et al. (2011).

Arguably, the best regional sources of meteorological data for precipitation are found at the NOAA website http://www.esrl.noaa.gov/psd/data/gridded/data.gpcc.html. For precipitation, the following file has been used to calculate long-term gridded (Figure 2.7) monthly means, based on data from 1981-2010, on a 0.5 degree latitude x 0.5 degree longitude global grid (180x720)

- ftp://ftp.cdc.noaa.gov/Datasets/gpcc/full_v6/precip.mon.1981-2010.ltm.v6.nc.

These data are derived from the GPCC Global Precipitation Climatology Centre data set (Schneider et al. 2011):

2.5 Chemical and Isotopic composition of precipitation

During winter 2013 and spring 2014, samples of rainfall and snowfall were collected at the premises of the Agricultural Departments in Maimana, Andkhoi and Gurziwan (near Jar Qala). These were couriered to the United Kingdom and analysed at the laboratories of the British Geological Survey (BGS) at Keyworth for a wide range of elements by ICP-MS techniques, anions by ion chromatography and stable O and H isotopes by mass spectrometry at the NERC isotope facility at Keyworth. The results are shown in Table 2.2.

It should be noted that, to avoid risk of contamination, the samples were *not* filtered in the field and might thus possibly contain traces of dust or other airborne materials. This effect could have resulted in elevated concentrations in, for example, the snow sample from Andkhoi.

In general, however, the samples have chloride concentrations of 1-2 mg/L at Andkhoi, 0.1 to 1.7 mg/L at Maimana and c. 0.6 mg/L at Gurziwan. The highest concentrations at Andkhoi presumably reflect evapo-concentration of salts during residence in the atmosphere. While precipitation in European maritime climates (e.g. Norway and the UK) is usually dominated by marine salts (e.g. NaCl) and atmospheric industrial contaminants (sulphate, nitrate from so-called "acid rain"), the precipitation in Faryab is characterised by calcium is the dominant cation and sulphate as the dominant anion, followed by chloride and nitrate. Thus may reflect a greater contribution from wind-blown dust (containing calcite and gypsum, and possibly halite). Sodium approximately balances chloride in the analyses, suggesting a derivation from halite in wind-blown dust, or possibly from distal marine salts.

As regards isotopic composition, the snowfall signatures are by far the isotopically lightest, with the signatures becoming "heavier" throughout spring. The heaviest isotopic rainfall signatures typically come from Andkhoi, as one would expect, due to greater isotopic fractionation by evaporation during its passage through the atmosphere.

Of Etymological Interest

The Faryab District of ***Kohistan*** means *mountainous land*.

Safed Koh means *White Mountains*, while ***Band-e-Turkestan*** refers to this range forming the *boundary wall to Turkestan*.

Dasht-e Shortepe: the ***dasht*** refers to a desert, while ***tepe*** probably derives from a Turkic word for hill, and ***shor*** means salty. Thus, *desert of salty hills* might be a rough translation.

Badghis means *Home of the wind.*

Table 2.2. Chemical and isotopic (VSMOW2) composition of rainfall sampled in Faryab in Winter 2012-13 and Spring 2013.

NORPLAN sample no. BGS sample number	Location Elevation	Type Date	Ca mg/L	Mg mg/L	Na mg/L	K mg/L	Sr µg/L	B µg/L	Cl^- mg/L	SO_4^{2-} mg/L	NO_3^- mg/L	$\delta^{18}O$ ‰	δ^2H ‰
Method			Inductively coupled plasma mass spectrometry						Ion chromatography			Mass spectrometry	
NOR-AND-SNW-03 13131-0003	Andkhoi c. 293 m asl	Snow 28/12/12	19.3	2.43	11.3	6.5	231	16	15.6	25.1	16.4	-18.01	-129.8
NOR-AND-RAIN-01 13131-0022	Andkhoi c. 293 m asl	Rain 15/3/13	15.0	1.38	2.5	0.6	57	12	2.0	6.9	6.8	-5.82	-35.3
NOR-AND-RAIN-02 13131-0023	Andkhoi c. 293 m asl	Rain 1/4/13	3.7	0.58	2.0	0.4	33	<10	1.4	3.9	1.0	-6.32	-32.9
NOR-GW-SNW-01 13088-0002	Gurziwan (Jar Qala) c. 1390 m asl	Snow 28/12/12	2.9	0.27	0.5	0.6	13	<10	0.60	0.75	0.38	-18.4	-122
NOR-GW-RAIN-01 13131-0001	Gurziwan (Jar Qala) c. 1390 m asl	Rain 26/2/13	5.3	0.33	0.5	0.8	19	<10	0.56	0.88	0.49	-12.24	-81.3
NOR-MAY-SNW-01 13088-0001	Maimana c. 847 m asl	Snow 28/12/12	5.2	0.14	<0.2	0.1	17	<10	0.10	0.58	0.46	-23.0	-165
NOR-MAY-RAIN-01 13131-0002	Maimana c. 847 m asl	Rain 26/2/13	2.5	0.18	0.5	0.4	13	<10	0.48	3.2	1.7	-8.64	-48.6
NOR-MAY-RAIN-02 13131-0021	Maimana c. 847 m asl	Rain 1/4/13	2.5	0.72	2.1	0.3	46	11	1.74	2.5	0.64	-5.32	-25.6

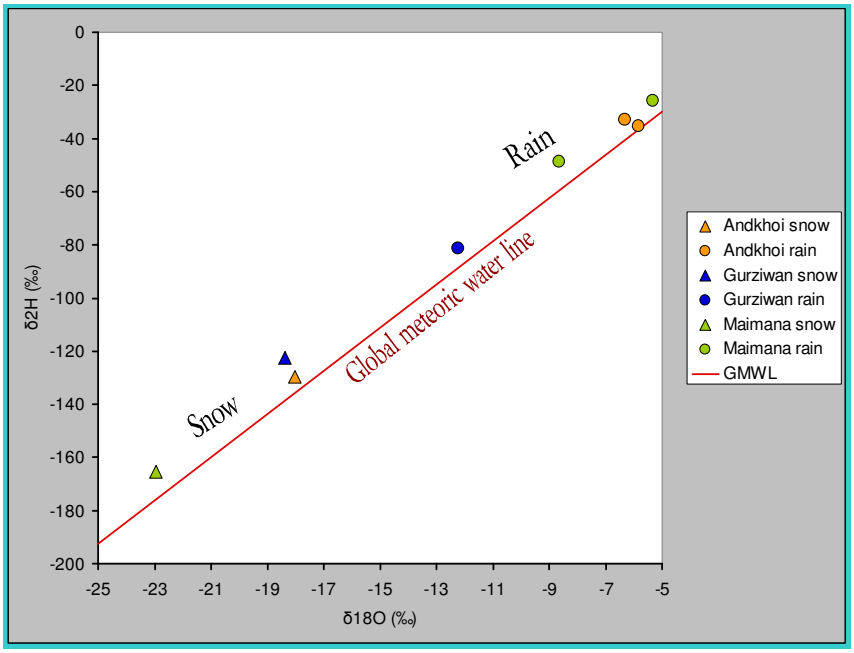

Figure 2.8. Stable isotope diagram comparing the isotopic composition of precipitation samples from Table 2.2. The GMWL is taken as $\delta^2H = (8.13 \times \delta^{18}O) + 10.8$ (Clark & Fritz 1997).

Figure 2.9. Typical topography of the northern plains area around Andkhoi. Photo by DACAAR, 3rd April 2013.

Figure 2.10. Typical topography of the piedmont area of Qaysar district. Photo by DACAAR, 6th March 2013.

Figure 2.11. Typical topography of the mountain area of Kohistan district. Photo by DACAAR, 23rd May 2013.

3. Faryab: Rivers and Surface Waters

3.1 The Amu Darya (Oxus)

The Amu Darya (or Oxos / Oxus, as it was called by the ancient Greeks) is the main watercourse running through northern Afghanistan, and forming the border with Turkmenistan. It is an "trans-boundary" watercourse and its use has been the subject of considerable international controversy. Usage of water from the Amu Darya has also been controversial as it is one of the two large watercourses (the Syr Darya being the other), which feeds the inland Aral Sea. As has been widely reported, the volume of water entering the Aral Sea has dramatically reduced over recent decades, leading to a catastrophic shrinking of the area of the sea, and desertification of the adjacent area (Zavialov 2005).

One of the main abstractions of water from the Amu Darya is the quantity drawn off by the Lenin (now renamed the Niyazov) Karakum Canal near the town of Khatab, in Turkmenistan, close to the northern extremity of Jawzjan Province.

The Karakum Canal traverses the Turkmen desert north of Faryab, via the Mary (Merv) inland delta (where it connects with the Murghab) and Gökdepe (near Ashgabat) to Bereket (Gazandjyk) only some 130 km short of the Caspian Sea. It was constructed by the Soviet Union between 1954 and 1988, with the objective of irrigating the Karakum desert, primarily for cotton production, but also supplying the city of Ashgabat with water. The canal is 1375 km long, is partly navigable and conveys some 13 km^3/a of water (an average of 412 m^3/s). A large proportion of the water is reported to be lost via seepage to the ground. Soil and groundwater salinisation is reportedly promoted by canal leakage, causing rises in groundwater level and dissolution of salts from the unsaturated zone, and evaporative accumulation of salts in irrigation water (Kharin 2002; Esenov 2014; Zonn 2014; http://en.wikipedia.org/wiki/Karakum_Canal). The Zeid Reservoir at the head of the canal, in the Lebap region of the Turkmen desert, has a reported capacity of 3.5 km^3, and the maximum off-take from the Amu Darya to the Karakum Canal is reported by Glantz (1999) as 580 m^3/s.

The salinity of the Amu Darya at Kelif gauging station is reported as around 0.5 g/L (Gapparov et al. 2011), while the annual flow is reported as 55.3 km^3 (1752 m^3/s; INTAS 2006). At Kerki gauging station, a short distance downstream from the Karakum Canal offtake, the annual flow is reported as 1696 m^3/s (period 1932-1989).

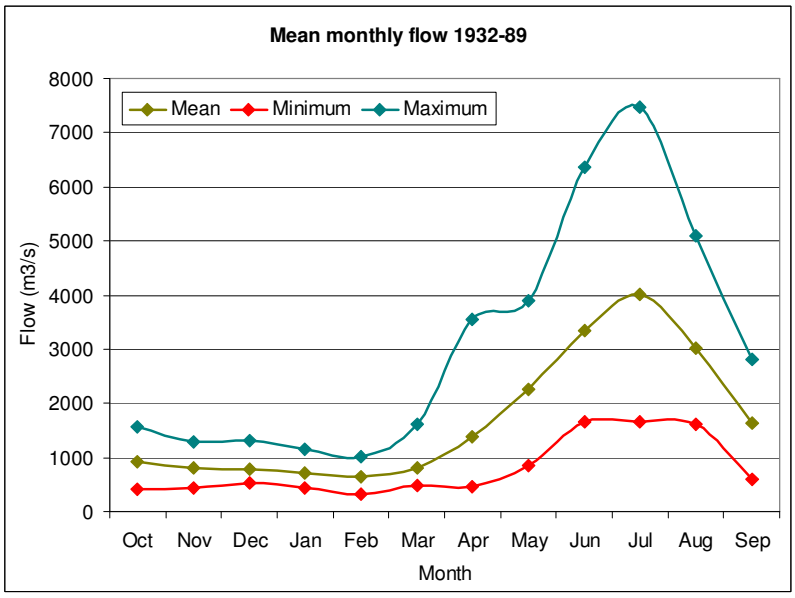

Figure 3.1. Mean monthly flows in the River Amu Darya at Kerki in Turkmenistan. *Source: UNH/GRDC from http://grdc.sr.unh.edu/html/Polygons/P2917110.html.*

Like the Balkh, Sar-e-Pol and Murghab Rivers, the Shirin Tagab system does not reach to the Amu Darya, but disperses within an inland delta system of distributary channels. There is no evidence that the Shirin Tagab ever discharged into the Amu Darya during historical or even recent geological (Holocene) times. The Amu Darya and Zeid depression does, however, form the base level towards which groundwater in the aquifers of northern Faryab drains.

3.2 The Murghab

The Murghab River flows westward through Afghanistan between the Band-e-Turkestan range to the north and the Safed Koh mountains to the south. Leaving Faryab, it passes through Badghis Province (and the town of Bala Murghab. It then enters Turkmenistan, before running out in the distributary channels of the inland delta in the desert around the town of Mary (historic *Merv*).

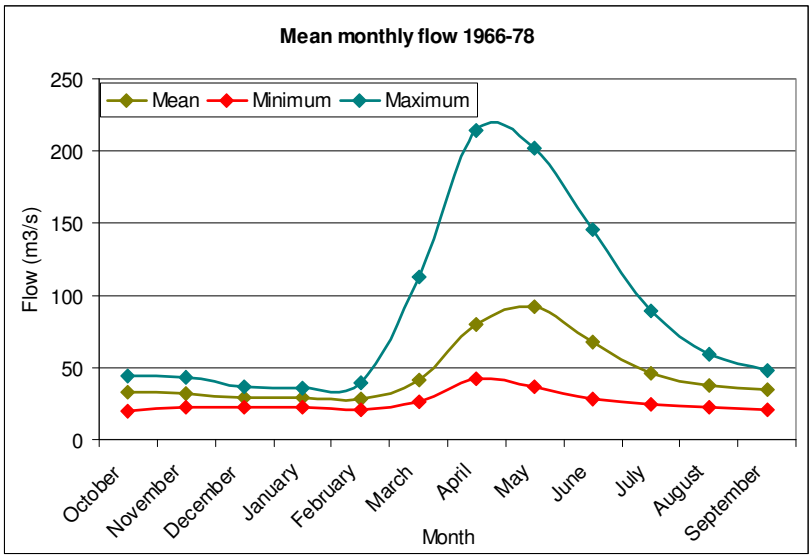

Figure 3.2. Mean monthly flows in the River Murghab at Qala-e-Niazkhan (station 40) in Badghis Province. *Source:*

1966-1978 data from the USGS suggest that the flow is strongly seasonal, with the greatest flows (exceeding 50,000 L/s at Qala-e-Niazkhan) between March and June, and being related to snowmelt. The river baseflow is likely to be substantially supported by groundwater discharge, especially from the large areas of Palaeogene-Cretaceous limestone aquifer outcrop that it traverses.

The long-term annual average flow at Qala-e-Niazkhan is 46,800 L/s, for an upstream catchment area of 13,805 km^2. This equates to an average run-off of 3.4 L/s/km^2 or 107 mm/a.

3.3 The Chechaktu (or Western Qaisar or Ghormach) River

The Chechaktu River (also referred to as the Western Qaisar river, the Ghormach River or the Karawal Kana) rises in the Ban-e-Turkestan mountains and exits the mountains onto the alluvial outwash plain at Zyarat Gah. The river has small tributary channel that rise very close to Qaisar town, within “spitting distance” of the true Qaisar River.

As the Chechaktu leaves Faryab and enters Ghormach district, it is joined by other tributaries flowing down from the Bund-e-Turkestan, notably the Shakh and Ghormach Rivers. The Chechaktu joins the larger Murghab River just downstream of Bala Murghab.

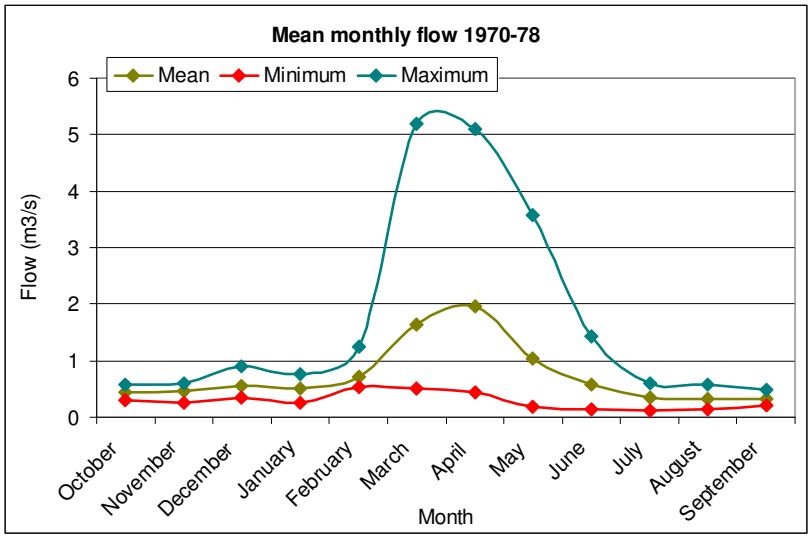

Figure 3.3. Mean monthly flows in the River Chechaktu at Chechaktu (station 44) in Qaisar District. Source:

1970-1978 data from the USGS suggest that the flow is strongly seasonal, with the greatest flows (exceeding 2,000 L/s at Chechaktu) between March and May, and being related to snowmelt.

The long-term annual average flow at Chechaktu is 760 L/s, for an upstream catchment area of 415 km^2. This equates to an average run-off of 1.8 L/s/km^2 or 58 mm/a.

3.4 The Shirin Tagab

According to Ahmad & Wasiq (2004) the Shirin Tagab has a total catchment area of 13,600 km^2. The annual run-off is estimated as between 100 and 132 Mm^3.

A major tributary joins the Shirin Tagab river near Pata Baba in Dowlatabad district. This is the Shor Darya, which carries the combined flow deriving from the Almar, Qaysar and Maimana Rivers. They are fed by snowmelt, rainfall and groundwater base-flow, especially baseflow from the productive Palaeogene-Cretaceous limestone aquifers up the mountains.

All these rivers rise in the northern slopes of the Band-e-Turkestan mountains. It has been argued that the Qaysar / Shirin Tagab river system may be the River *Ochus* referred to by writers of antiquity (Rawlinson 1879, Olbrycht 2010).

The rivers flow north down on the Neogene molasse and Quaternary loess plains, where they deposit their eroded sediment load and often form poorly defined braided river channels. They also change from a gaining (spring-fed) regime, to a losing regime, where flow temporarily or permanently infiltrates into the alluvial outwash sediments and starts to be lost to evaporation and irrigation take-off.

The Shirin Tagab is a so-called “blind” river system, which dissipates due to evaporation, irrigation off-take and infiltration to the ground, without ever reaching the Amu Darya. The River dissipates in an “inland delta” area, today comprising a network of irrigation channels around the city of Andkhoi.

The Shirin Tagab

The Shirin Tagab proper rises in the eastern part of Bilchiragh Province, although near Bilchiragh town, it is joined by the Chashma-i Khwab river, flowing out of a spectacular

gorge. The Chashma-i Khwab is, in turn, is fed by the streams of five valleys flowing out of Gurziwan: the Khwaja Ghar, the Shakh, the Zang, the Takhra and the Rabat (Favre & Kamal 2004)

There are three historic gauging stations on the course of the Shirin Tagab. In descending order these are:

1. At Khisht Pul, in Pashtun Kot district, shortly after the river has emerged from the pre-Neogene terrain onto the Neogene proluvial outwash deposits.
2. At Dawlatabad, prior to the confluence with the Shor Darya.
3. At Pata Baba, downstream of the confluence with the Shor Darya.

In the Shirin Tagab we can see that elevated flows are observed during the rainier months from October-November through to February. In March-May there is a strong snow-melt peak, and then the flow drops quickly to summer levels.

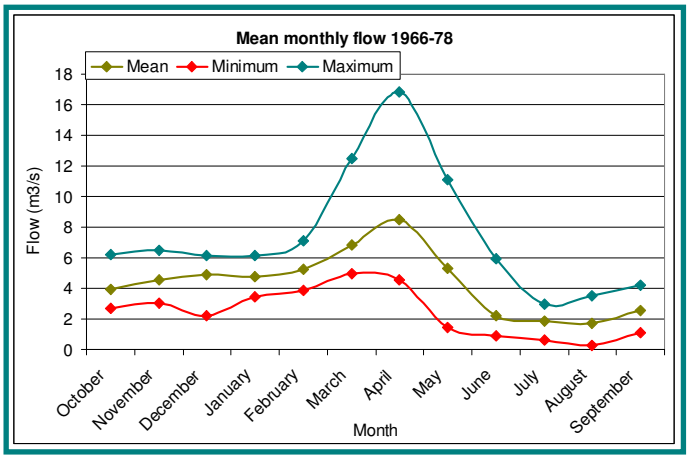

Figure 3.4. Mean monthly flows in the Shirin Tagab at Khisht Pul (station 48) in Pashtun Kot District. Source:

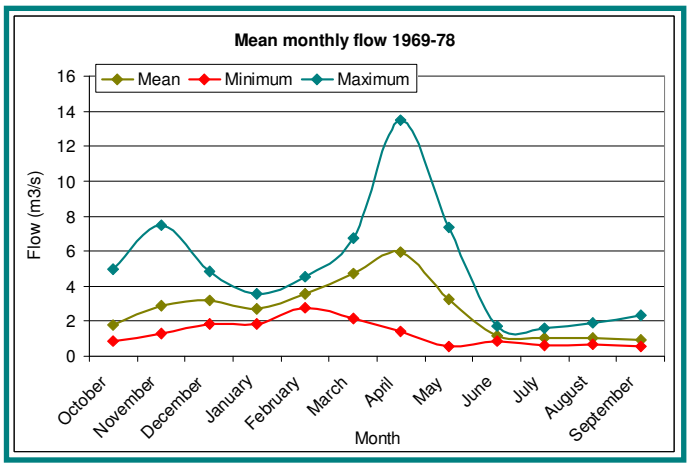

Figure 3.5. Mean monthly flows in the Shirin Tagab at Dawlatabad (station 47). Source:

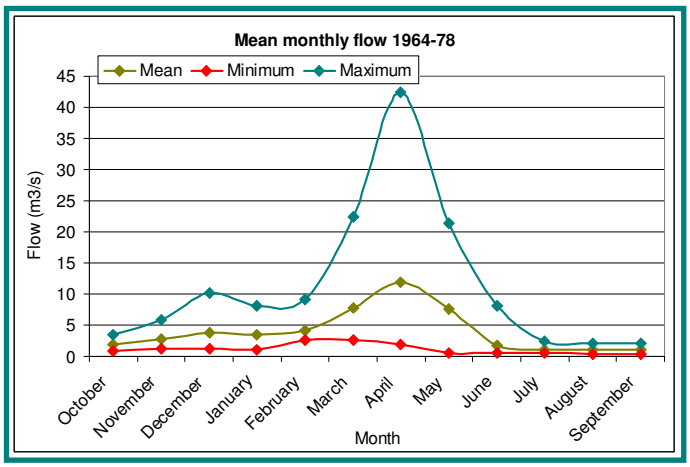

Figure 3.6. Mean monthly flows in the Shirin Tagab at Pata Baba (station 46,), Dawlatabad District. Source:

It is also important to note that the flows decrease downstream from Khisht Pul to Dowlatabad, by almost 50% on an annual average basis. As yet it is not clear whether this can be ascribed to:

- infiltration losses to groundwater
- abstraction for irrigation (and thereafter loss to evapotranspiration or infiltration to groundwater)
- evapotranspirative losses

or (as would be likely, a combination of all three).

The total flow at Pata Baba is, on average 1640 L/s greater than at Dowlatabad, presumably due to the confluence with the Shor Darya (average 2440 L/s, see below), but the specific areally distributed run-off rate decreases consistently downstream.

Table 3.1.

Gauging station	Long term annual mean discharge	Upstream catchment area	Areally distributed long term run-off
Khisht Pul (station 48)	4,450 L/s	3,280 km^2	1.4 L/s/km^2 43 mm/a
Dowlatabad (station 47)	2,340 L/s	4,645 km^2	0.50 L/s/km^2 16 mm/a
Pata Baba (station 46)	3,980 L/s	11,775 km^2	0.34 L/s/km^2 11 mm/a

The Astana River

The Astana is an east-bank tributary of the Shirin Tagab. It is unique in not rising on the pre-Neogene terrain of the Band-e-Turkestan, but rather, within the Neogene molasse sediments of Shirin Tagab District. The River itself is known to be extremely salty, due to the highly saline nature of the groundwaters in the Neogene aquifer, which feed it. A sample from Chel Quduq, taken in October 2005, has an electrical conductivity of 45,000 µS/cm.

The salinity of the ground and surface waters in the Astana Valley may be ascribed to (i) the very high rates of evaporation in the area, leading to up-concentration of precipitation derived salts in the soil and (ii) possibly, the suspected content of halite and gypsum in the Neogene soils.

To the north of the Astana River is a small inlier of Cretaceous and Palaeogene sedimentary rocks around Qara Qol. Somewhat fresher springs of groundwater drain from the southern flanks of this inlier (e.g. Moghaito, which has a reported discharge of up to 3 L/s and an electrical conductivity of 3400 µS/cm), but these have largely been captured for public water supply purposes.

3.5 The Qaisar / Maimana / Shor Darya Rivers

The Qaisar, Maimana and Almar Rivers all rise on the northern flank of the Band-e-Turkestan mountains.

The Maimana River

The Maimana is presumed to gain baseflow from groundwater discharge of the Cretaceous / Palaeozic limestone aquifers of its upper reaches. Shortly before arriving at Maimana, it crosses onto Neogene molasse deposits.

The Qaysar River

The Qaisar River also traverses onto Neogene / Quaternary deposits shortly upstream of Qaisar town.

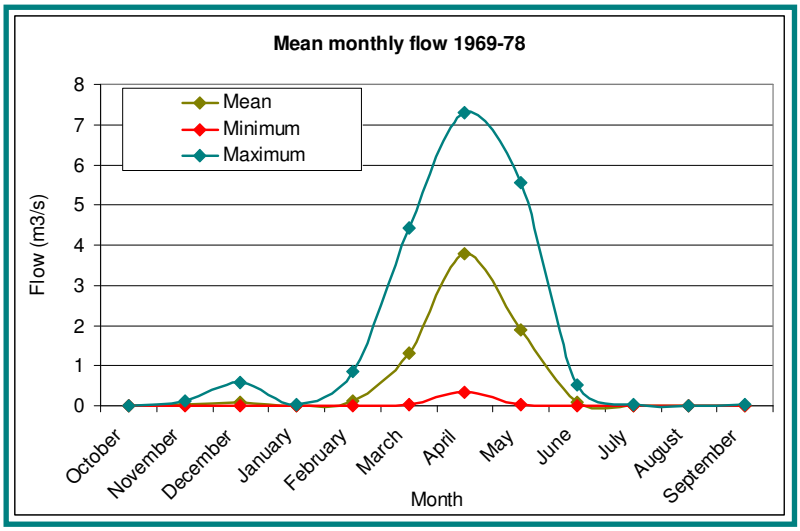

Figure 3.7. Mean monthly flows in the Qaisar River at Qaisar (station 49). Source:

1969-1978 data from the USGS suggest that the Qaisar River's flow is very strongly seasonal, with the greatest flows (typically up to 4,000 L/s at Qaisar town) between March and May, and being related to snowmelt. The river often effectively dries up at Qaisar between July and February, suggesting a lack of groundwater baseflow to the upper sections.

The long-term annual average flow of the Qaisar at Qaisar town is 540 L/s, for an upstream catchment area of 425 km^2. This equates to an average run-off of 1.3 L/s/km^2 or 40 mm/a.

The Almar and Aqsay Rivers

Several south bank tributaries join the Qaisar, of which the most important are the Almar River(s) and the Aqsay, all arising on the pre-Neogene rocks on the northern flanks of the Band-e-Turkestan mountains. In particular, the Almar River emerges from the pre-Neogene bedrock terrain through a canyon near Yaka Khana and immediately forms a wide alluvial fan and takes on a very diffuse, braided nature around Almar.

The Shor Darya

The Shor Darya is the name given to the combined flow of the Qaysar and Maimana Rivers, downstream of their confluence near Ateh Khan Khwaja. The Shor Darya section is known to be saline and this is belived to be due to discharge of saline or brackish groundwaters in the area.

At Ateh Khan Khwaja, there is a major spring (some 15- 35 L/s reported by DACAAR, varying seasonally) discharging to the Shor Darya. It represents some of the freshest water in the area, with an electrical conductivity of 2660 µS/cm (Hassan Saffi 2010b).

In May 2007, the Shor Darya was sampled at Ateh Khan Khwaja, where the electrical conductivity was found to be 6000 µS/cm. It was also sampled at Chokazi, near Jalair, and the electrical conductivity was found to be 8730 µS/cm (Hassan Saffi 2010b).

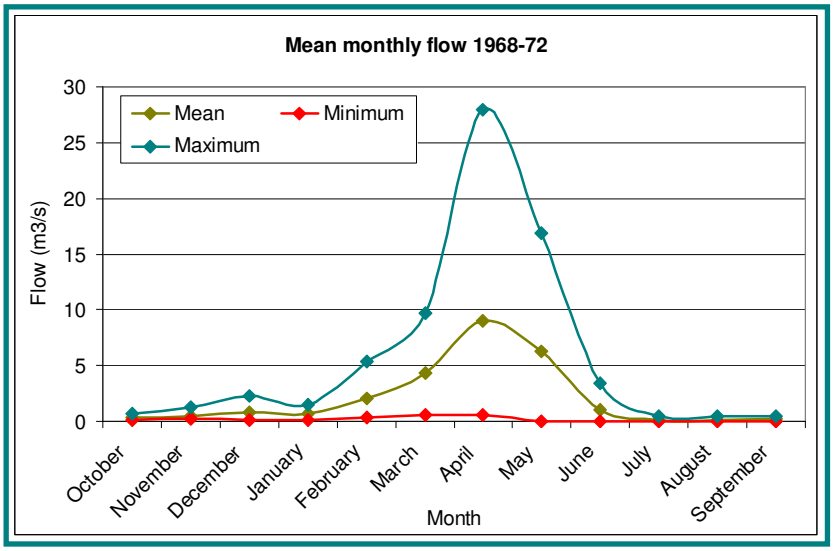

Figure 3.8. Mean monthly flows in the Shor Darya near Pata Baba (station 50,), Dawlatabad District. Source

1968-1972 data from the USGS suggest that the Shor Darya's flow is seasonal, with the greatest flows (typically up to 9,000 L/s near Pata Baba) between February and May. Flows are extremely low from July to November, suggesting a lack of groundwater baseflow.

The long-term annual average flow of the Shor Darya, prior to its confluence with the Shirin Tagab at Pata Baba 2440 L/s, for an upstream catchment area of 6685 km^2. This equates to an average run-off of 0.36 L/s/km^2 or only 12 mm/a.

The total flow in the Shirin Tagab at Pata Baba is, on average 1640 L/s greater than at Dowlatabad, presumably due to the confluence with the Shor Darya (av, but the specific areally distributed run-off rate decreases consistently downstream.

From these Figures and those from Table xx.xx we can calculate the accretion of flow:

(a) on the Qaisar / Shor Darya, between Qaysar and Pata Baba, as

(2440 - 540) L/s / (6685-425) km^2 = 1900 / 6260 km^2 = 0.30 L/s/km^2 = 10 mm/a

(b) on the Shirin Tagab, between Khisht Pul and Dowlatabad, as

(2340-4450) L/s / (4645-3280) km^2 = -2110 / 1365 km^2 = 1.5 L/s/km^2 = -49 mm/a

(c) on the joint system, between Shor Darya / Dowlatabad and Pata Baba, as

(3980-2440-2340) L/s / (11775-6685-4645) km^2

= -800 / 445 km^2 = -1.8 L/s/km^2 = -57 mm/a

3.6 The 2013 Maimana River Survey

On 1st May 2013, a stretch of the Maimana River was surveyed between Koh-e Khana, on the northern outskirts of Maimana, and Badghisy, representing a linear distance of almost 19 km and a river distance of just over 25 km. Flow, electrical conductivity, pH and temperature were taken at 5 stations along thos length (Figure 3.9), while chemical and isotopic samples, filtered at 0.45 µm, were taken at 3 stations and sent to the British Geological Survey, Keyworth, UK for analysis (see NORPLAN 2014 for methods).

The river temperature increased from 14.1 to 18.5°C downstream over the course of the survey, the electrical conductivity increased from 545 to 690 µS/cm, while the field pH was relatively constant at 8.4.

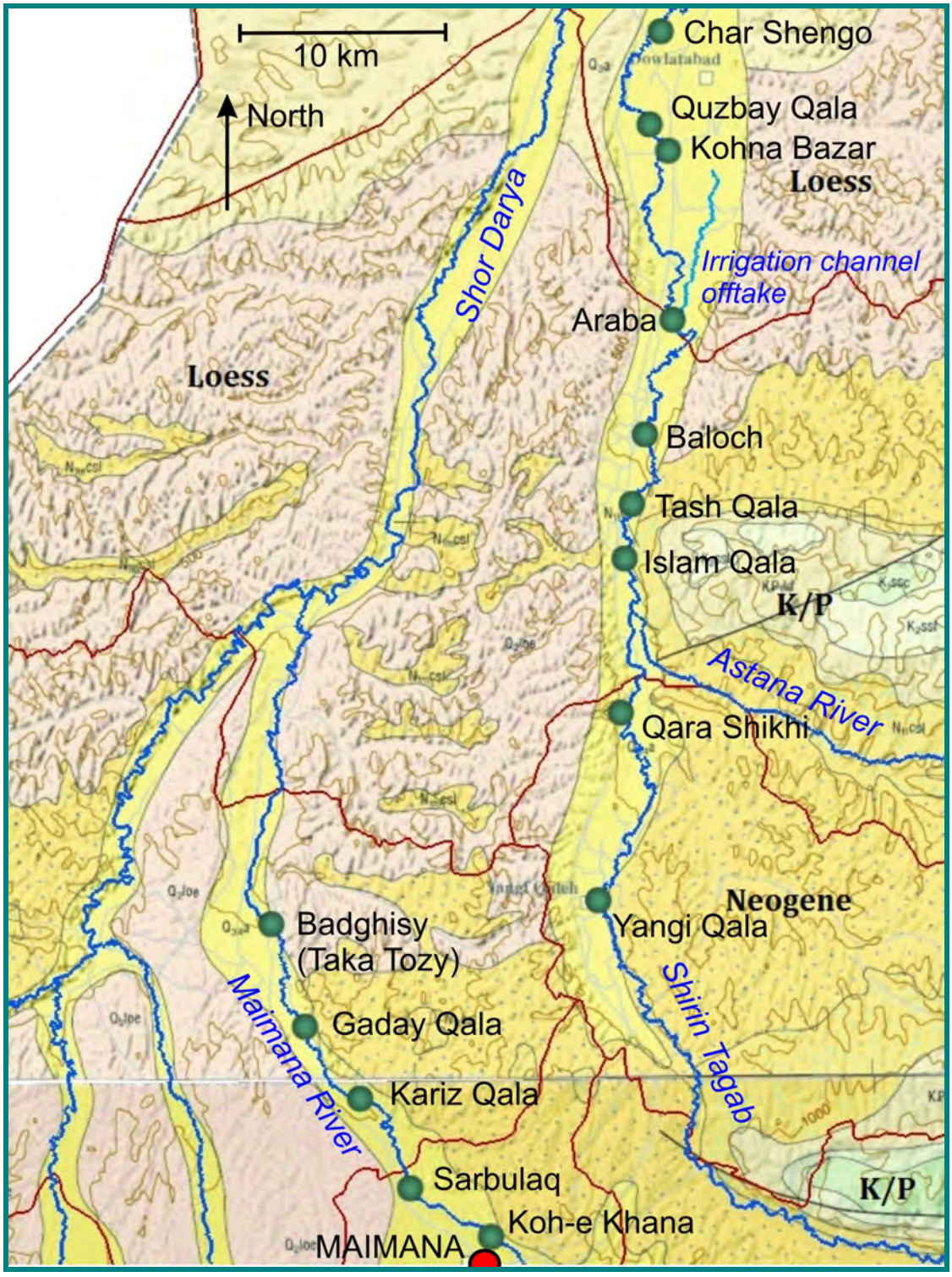

Figure 3.9. The locations for gauging and sampling during the 2013 survey of the Shirin Tagab and Maimana Rivers. The rivers are superimposed on the published 1:200,000 AGS/USGS geological maps (McKinney & Sawyer 2005; Wahl 2005), on which pink colours generally denote Quaternary loess, orange Neogene proluvial/molasse deposits, yellow Quaternary alluvium and green/brown Cretaceous / Palaeogene sedimentary rocks (K/P). These maps are believed to be public domain products.

At Koh-e Khana, the river contained around 8 mg/L nitrate (as NO_3^-) and <0.01 mg/L total phosphorus. The water chemistry was dominated by calcium and bicarbonate, with subsidiary sulphate.

Along the surveyed length, the flow rate (as estimated by impeller profile gauging) dropped from 2.1 m^3/s to 1 m^3/s, while the electrical conductivity rose by a factor of 1.27.

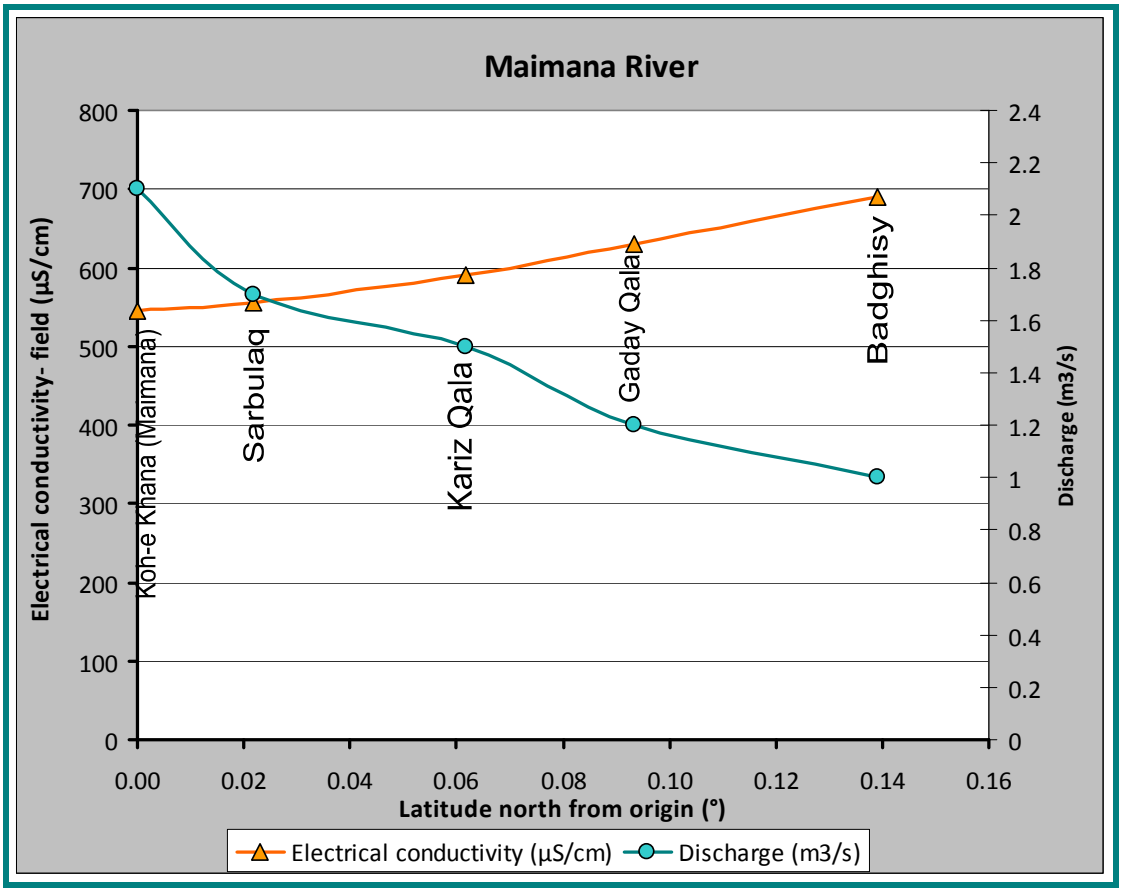

Figure 3.10a. Change in electrical conductivity and flow rate along the surveyed length of the Maimana River on 1st May 2013.

Different solutes were concentrated downstream at different rates, however, with calcium and bicarbonate accumulating relatively slowly, and solutes such as chloride, (followed by arsenic and potassium), which can be regarded as relatively conservative, accumulating by a factor of some 1.7.

The fact that the maximum solute upconcentration factor is only a little less than the flow loss factor (2.1) suggests that evaporation is a main driving force for loss of flow (abstraction and infiltration may also be factors in flow depletion).

If the channel is on average 6 m wide and 25 km long, the river stretch has a surface area of at least 150,000 m^2 (and probably more, given that narrow, straight sections were specifically chosen for gauging). The total flow loss over this section was 1.1 m^3/s = 3960 m^3/hr, implying the loss of 26 mm/hr from the open surface area.

From Chapter 2, we see that potential evapotranspiration in early May is around 140 mm per month; we could thus suppose that daytime evapotranspiration is approximately 0.375 mm/hr. Thus, we can conclude that direct evaporation from the river surface is unlikely to be adequate to account for the flow loss over the surveyed distance.

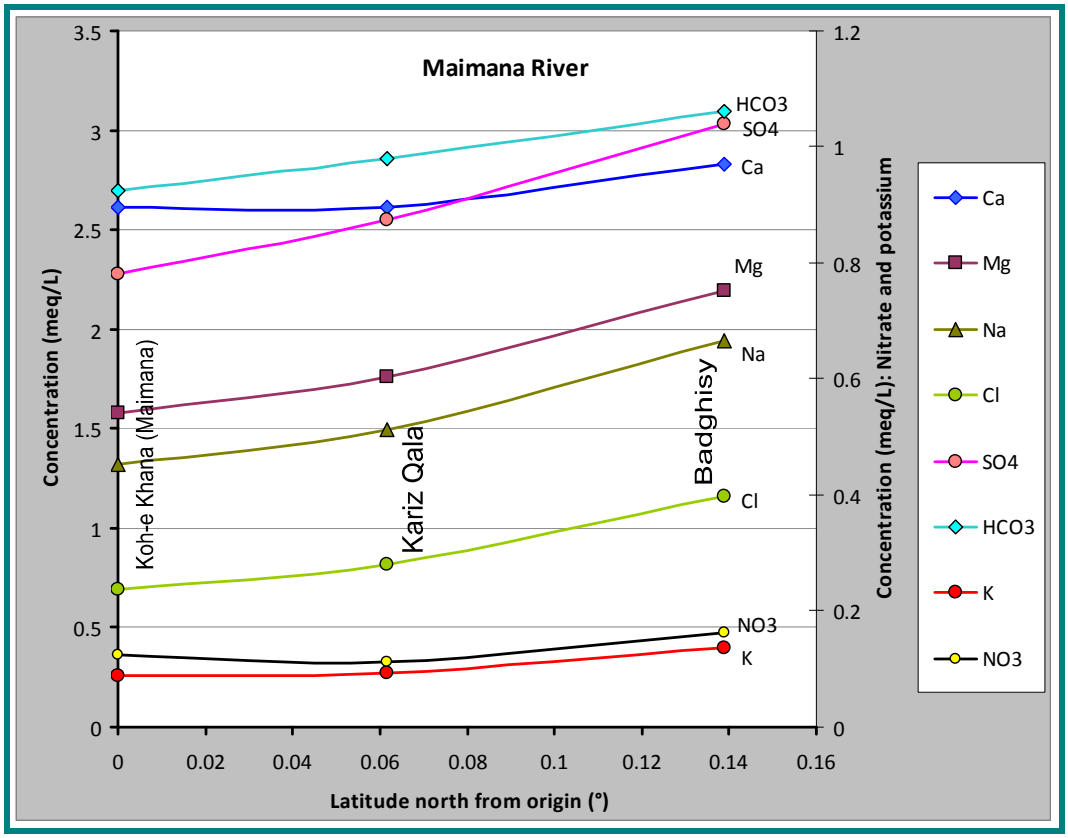

Figure 3.10b. Change in major ion concentrations (meq/L) along the surveyed length of the Maimana River on 1st May 2013. Samples analysed at British Geological Survey, Keyworth, UK.

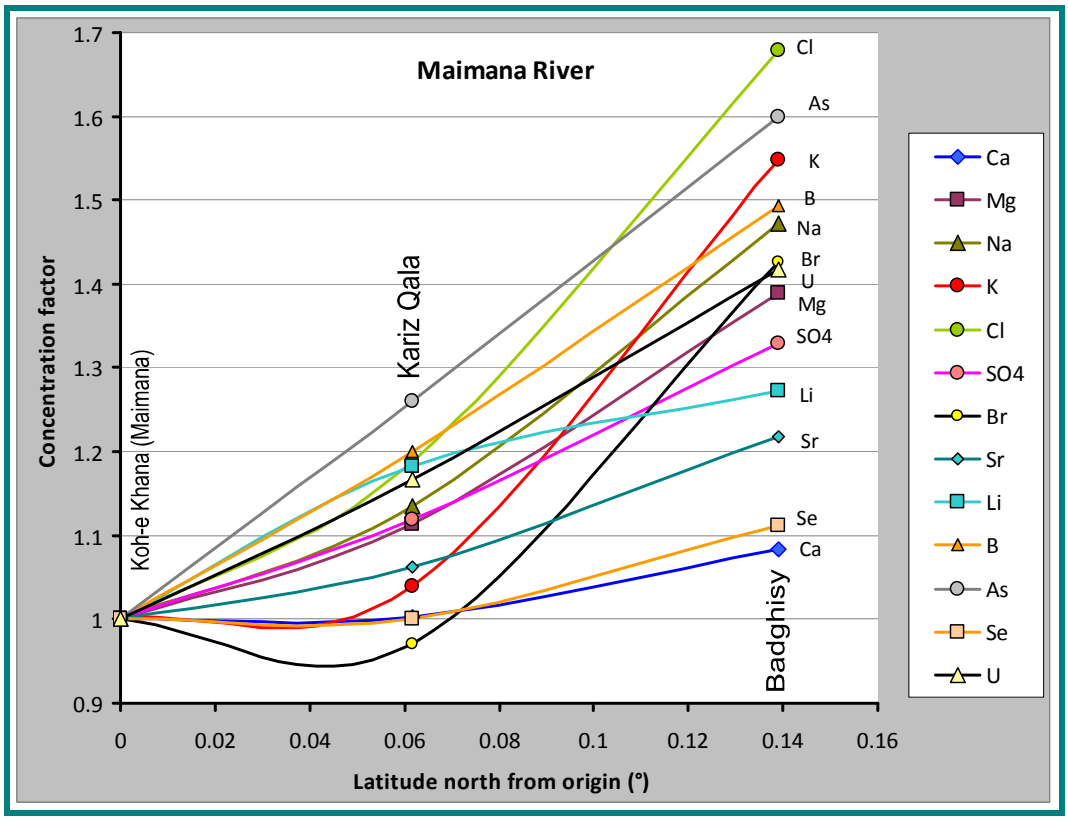

Figure 3.10c. Upconcentration of selected solutes (relative to Koh-e Khana) along the surveyed length of the Maimana River on 1st May 2013.

Stable isotopes of oxygen and hydrogen were also analysed at the NERC facility at the British Geological Survey and they show (Figure 3.10d) a steady enrichment in heavier isotopes downstream, indicative of evaporative fractionation. The isotopic values plot in the same area as rainfall in Figure 2.8.

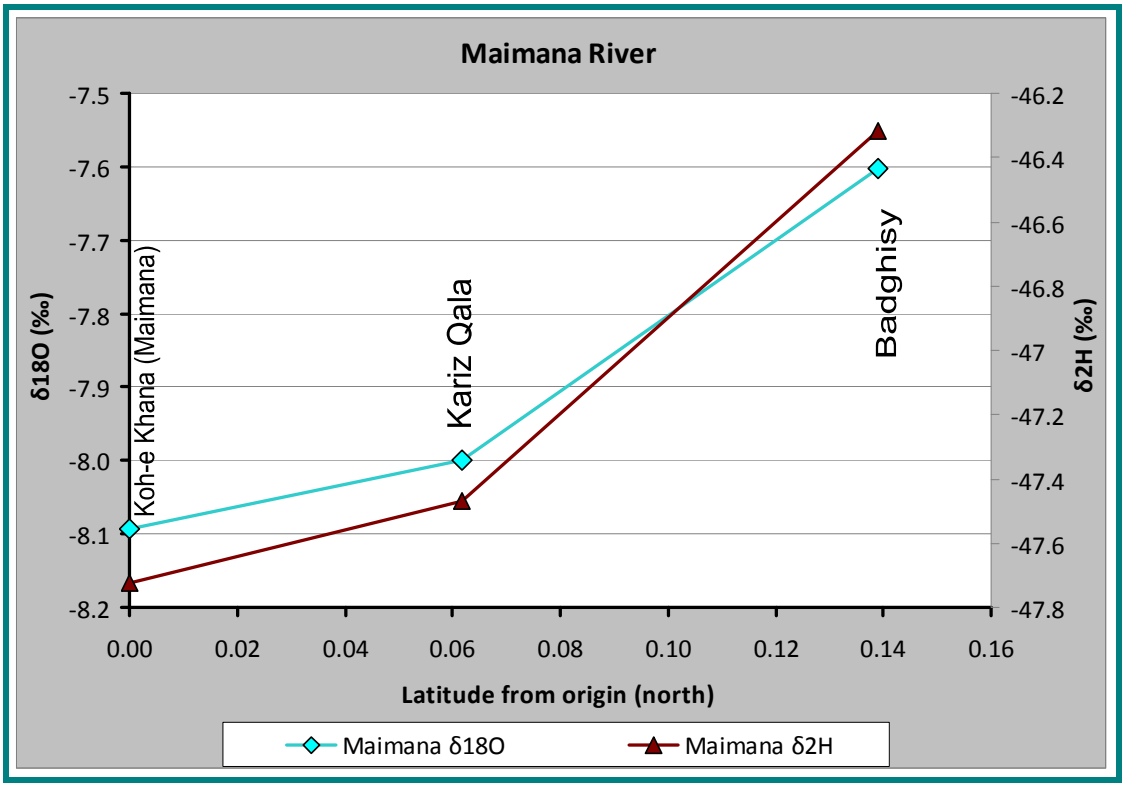

Figure 3.10d. Change in stable isotopic signature along the surveyed length of the Maimana River on 1st May 2013. Samples analysed at the NERC isotope facility at the British Geological Survey, Keyworth, UK.

3.7 The 2013 Shirin Tagab River Survey

On 11th-12th May 2013, a stretch of the Shirin Tagab River was surveyed between Yangi Qala and Char Shengo, representing a linear distance of c. 43 km and a river distance of c. 70 km. Flow, electrical conductivity, pH and temperature were taken at 9 stations along this length (Figure 3.9), while chemical and isotopic samples, filtered at 0.45 µm, were taken at 5 stations and sent to the British Geological Survey, Keyworth, UK for analysis (see NORPLAN 2014 for methods).

The river temperature varied between 16 and 18°C over the course of the survey, with 17°C being typical. The field pH was relatively constant at 8.4-8.5 upstream of Araba, and 8.1 to 8.2 downstream of Araba.

Along the surveyed stretch, the highly saline Astana River enters the Shirin Tagab just upstream of Islam Qala: it has no significant mitigating effect on the loss of flow in the Shirin Tagab, but *may* contribute to the step up in electrical conductivity at Islam Qala (Figure 3.11a).

Along the surveyed length, the flow rate (as estimated by impeller profile gauging) dropped from 1.9 L/s to 1 L/s between Yangi Qala and Baloch, while the electrical conductivity rose by a factor of 2.3 from 697 top 1605 µS/cm. The fact that the salinity increase exceeds the flow loss factor could be due to the saline input from the Astana area.

Just upstream of Araba, almost the entire flow of the Shirin Tagab is taken off into a major irrigation channel, leaving the natural channel of the Shirin Tagab effectively dry. The chemical and isotopic signature dips at Araba.

Downstream of Araba, the flow in the Shirin Tagab re-accretes: it is speculated that this is due to infiltration of irrigation water (i.e. the water taken off upstream of Araba) to the ground and thence discharging to the river. The flow rate does not reach its pre-Araba rate, however, with only 0.5 m^3/s being recorded at Kohna Bazar.

Salinity is re-acquired (irrigation water having been evapoconcentrated in the soil zone, and possibly also having picked up solutes from minerals in the unsaturated zone and aquifer), exceeding 2000 µS/cm in the lowermost stretches of the surveyed section

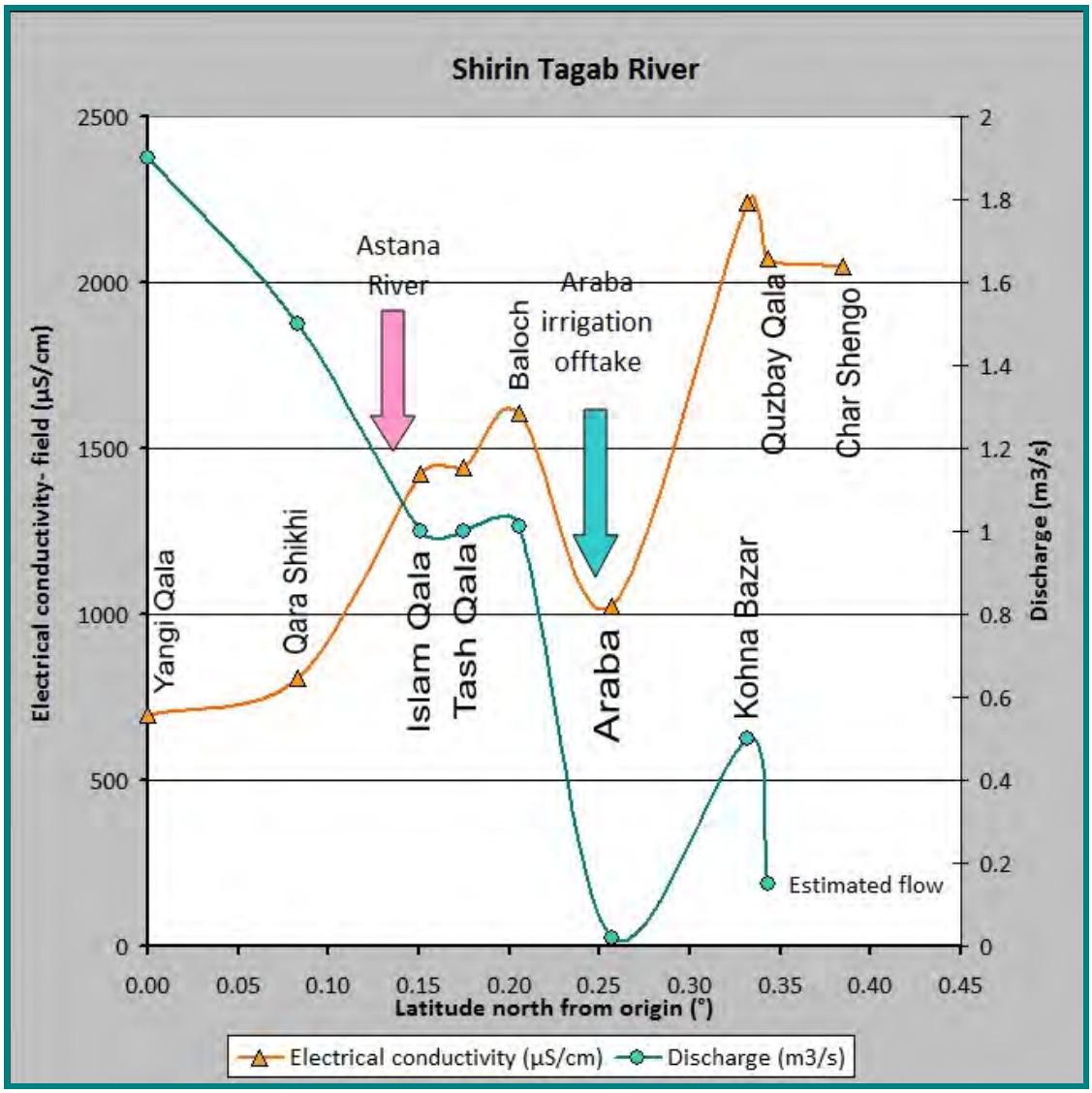

Figure 3.11a. Change in electrical conductivity and flow rate along the surveyed length of the Shirin Tagab River on 11th-12th May 2013.

At Yangi Khana, the river contained around 8.7 mg/L nitrate (as NO_3^-) which increases to c. 20 mg/L by Islam Qala and downstream. Total phosphorus is <0.01 mg/L along the entire surveyed length.

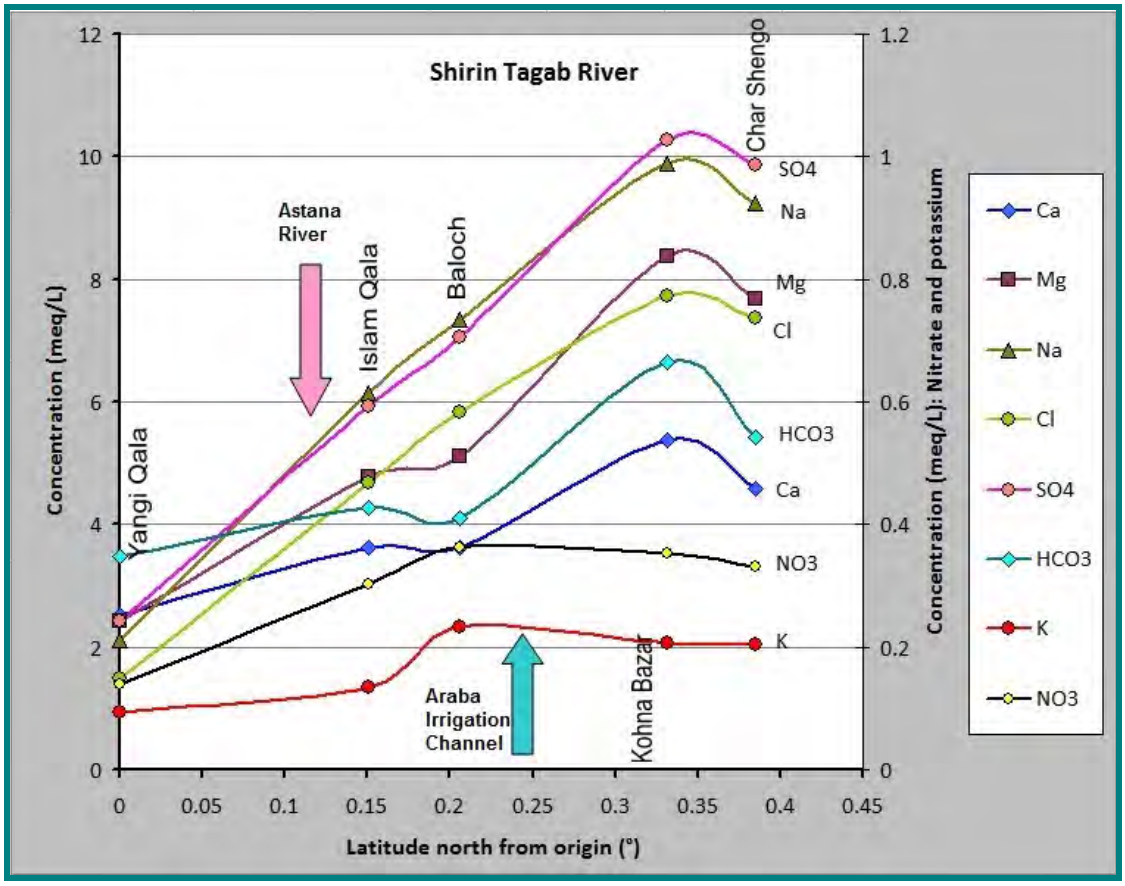

Figure 3.11b. Change in major ion concentrations (meq/L) along the surveyed length of the Shirin Tagab River on 11th-12th May 2013. Samples analysed at British Geological Survey, Keyworth, UK.

At Yangi Qala, the water chemistry is dominated by a Ca-(Na)-HCO_3^- composition. Downstream, concentrations of $SO_4^=$, Na, Mg and Cl^- increase rapidly and in parallel, whereas concentrations of Ca and HCO_3^- increase relatively slowly. Downstream, therefore, the water rapidly becomes dominated by Na and $SO_4^=$, with subsidiary Mg and Cl^-. It should be noted that this increase cannot be ascribed to simple dissolution of gypsum and halite, otherwise one would expect similar concentrations of Na and Cl and the increases in the ions would be unlikely to parallel each other. The parallel increases in soluble ion concentrations bear the signature of evaporative concentration, with increases in calcium and bicarbonate possibly being suppressed by calcite saturation.

Different solutes were concentrated downstream at different rates, however, with calcium and bicarbonate accumulating relatively slowly, and solutes such as chloride, (followed by sodium, bromide and sulphate), which can be regarded as relatively conservative, accumulating by a factor of some 3-4 by Baloch and 4-5 by K.ohna Bazar and Char Shengo (Figure 3.11c).

The fact that the maximum solute up-concentration factor is similar, though slightly greater than, the flow loss factor (1.9 to Baloch, c. 4 to Kohna Bazar) suggests that evaporation is a significant driving force for loss of flow (abstraction and infiltration may also be factors in flow depletion).

If the channel is on average 4 m wide and 34.1 km long between Yangi Qala and Baloch, the river stretch has a surface area of at least 136,400 m^2 (and probably more, given that narrow, straight sections were specifically chosen for gauging). The total flow loss over the Yangi Qala - Charshengo section was 0.9 m^3/s = 3240 m^3/hr, implying the loss of 23.8 mm/hr from the open surface area.

From Chapter 2, we see that average potential evapotranspiration in early May is around 150 mm per month at Maimana and 180 mm in Andkhoi; we could thus suppose that daytime evapotranspiration is approximately 0.44 mm/hr in the Shirin Tagab area. Thus, we can conclude that direct evaporation from the river surface is unlikely to be adequate to account for the flow loss over the surveyed distance.

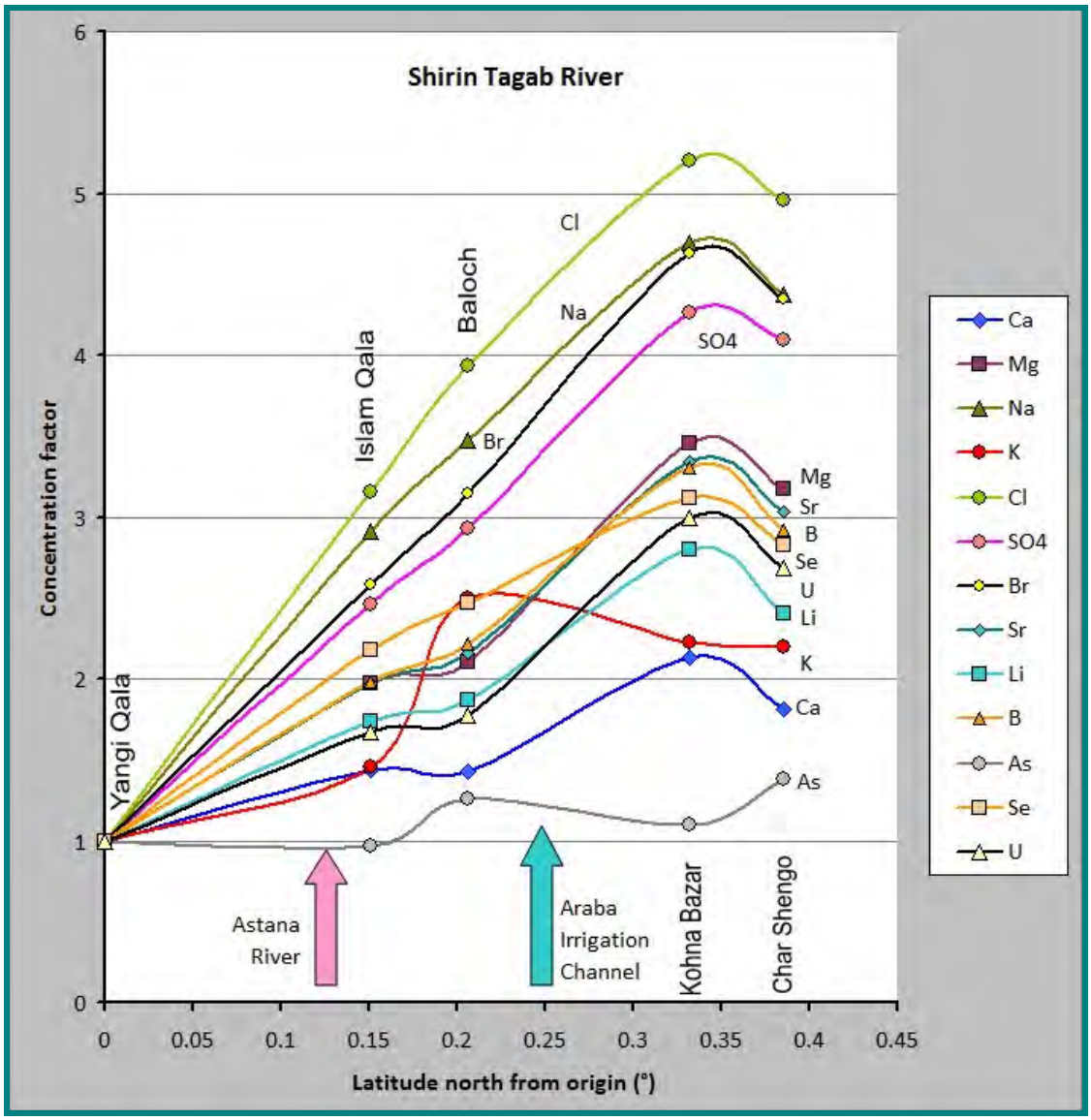

Figure 3.11c. Up-concentration of selected solutes (relative to Yangi Qala) along the surveyed length of the Shirin Tagab River on 11th-12th May 2013.

Stable isotopes of oxygen and hydrogen were also analysed at the NERC facility at the British Geological Survey. The isotopic values plot in the same area as rainfall in Figure 2.8. The isotopic values show (Figure 3.11d) a steady enrichment in heavier isotopes downstream in the reaches of flow depletion, from Yangi Qala to Baloch and from Kohna Bazar to Char Shengo, indicative of evaporative fractionation. In the zone of flow accretion, however, from Araba to Kohna Bazar, the isotopic values fall: this is presumably due to the river being fed with groundwater baseflow with a lighter isotopic signature. The reason that such groundwater has a lighter signature may be that it was recharged to the ground in upstream reaches of the river, during times of snowmelt (lighter signature, see Figure 2.8).

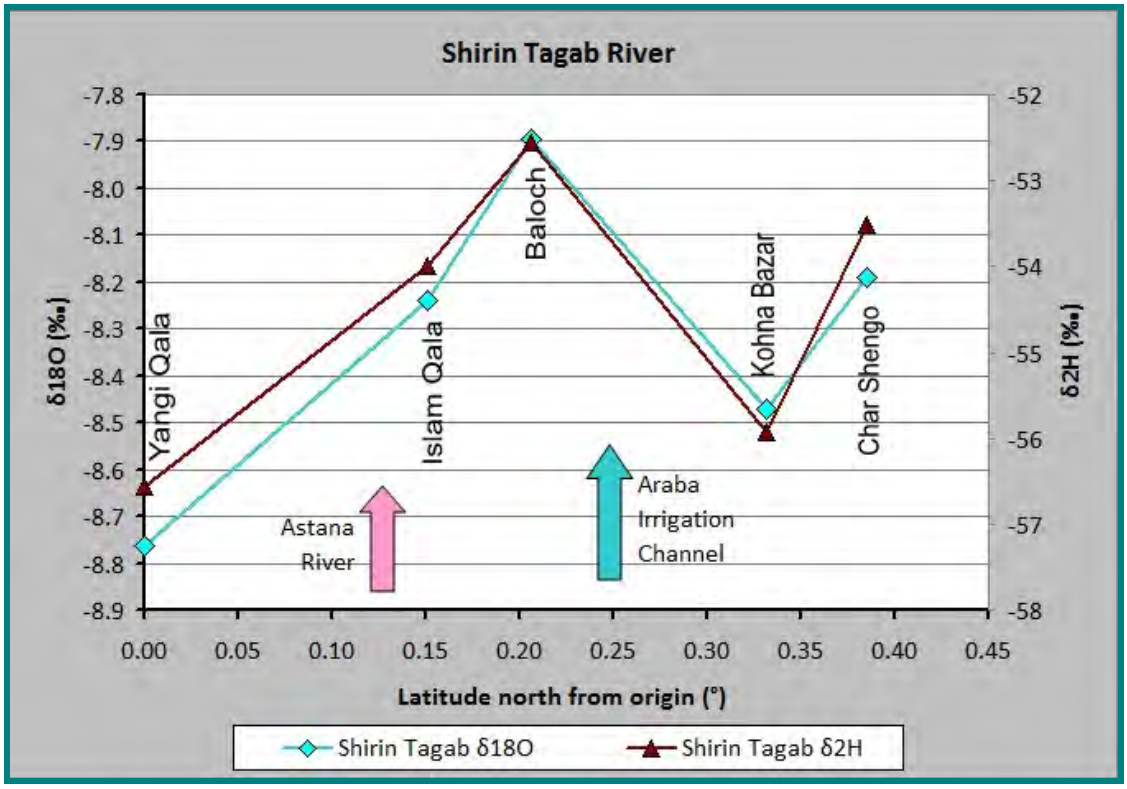

Figure 3.11d. Change in stable isotopic signature along the surveyed length of the Shirin Tagab River on 11th-12th May 2013. Samples analysed at the NERC isotope facility at the British Geological Survey, Keyworth, UK.

3.8 Summary: 2103 River Survey

The two River Surveys of 2013 reveal that, along the surveyed reaches, flows typically decrease downstream, with concentrations of solutes increasing. The fact that the solute up-concentration factors approximately mirror the flow loss factors strongly suggests that evapotranspiration is a major driving factor in this process. The steady enrichment of river waters in heavy stable isotopes is also strongly indicative of evaporative processes.

However, it would appear that direct evaporation from the river surface is inadequate to explain the flow loss. In fact, for both the Shirin Tagab and Maimana sections, around 50 times more surface area than appears to be available, would be required to result in the observed losses in flow due to open water evaporation. Even allowing for the fact that river widths measured at gauging stations may under-represent the average river width (as narrow, straight sections were preferentially chosen for gauging), we need to acknowledge that:

(i) abstraction and use for irrigation, and

(ii) river bed infiltration to groundwater

probably also contribute to loss in flow.

However, mechanism (i) could, in some circumstances be regarded as an evapotranspirative up-concentration mechanism. Water abstracted from the river is used to irrigate riparian crops: plants and soils efficiently lose water via evapotranspiration, but most non-nutrient solutes remain in the residual water, which either infiltrates to the soil. We will see in Chapter that, along these river reaches, the alluvial sand and gravel aquifer beneath the river valleys is effectively separated from the surafce via a layer of silty clay. This, infiltrating irrigation water may not reach the

deeper sand and gravel aquifer, but may discharge as shallow groundwater or interflow, back to the rivers, via natural seepages, field drains or ditches. The net result is loss of river discharge (abstraction and evapotranspiration), proportionate up-concentration of solutes and an effectively increased (additional areas of riparian irrigated land) for evaporative processes.

In the Shirin Tagab , just upstream of Araba, almost the entire flow of the Shirin Tagab is led off into an irrigation channel to water the land SE of Dawlatabad. We assume that the same evapo-concentrative processes occur in this irrigated land on a much larger scale. Eventually, the residual infiltrating water from the fields returns to the Shirin Tagab River and flow re-accretes (but never to pre-Araba levels) and with an increased load of solutes.

3.9 The Kelif Uzboy and the ancient course of the Amu Darya

The existence of enormous fresh groundwater resources in the Nubian sandstones below the Sahara Desert has drawn hydrogeologists' attention to the possibility that groundwater recharge could have taken place many thousands of years ago (during pluvial periods in the Pleistocene or early Holocene), bequeathing usable groundwater resources, even in terrains that are arid or brackish according to today's standards.

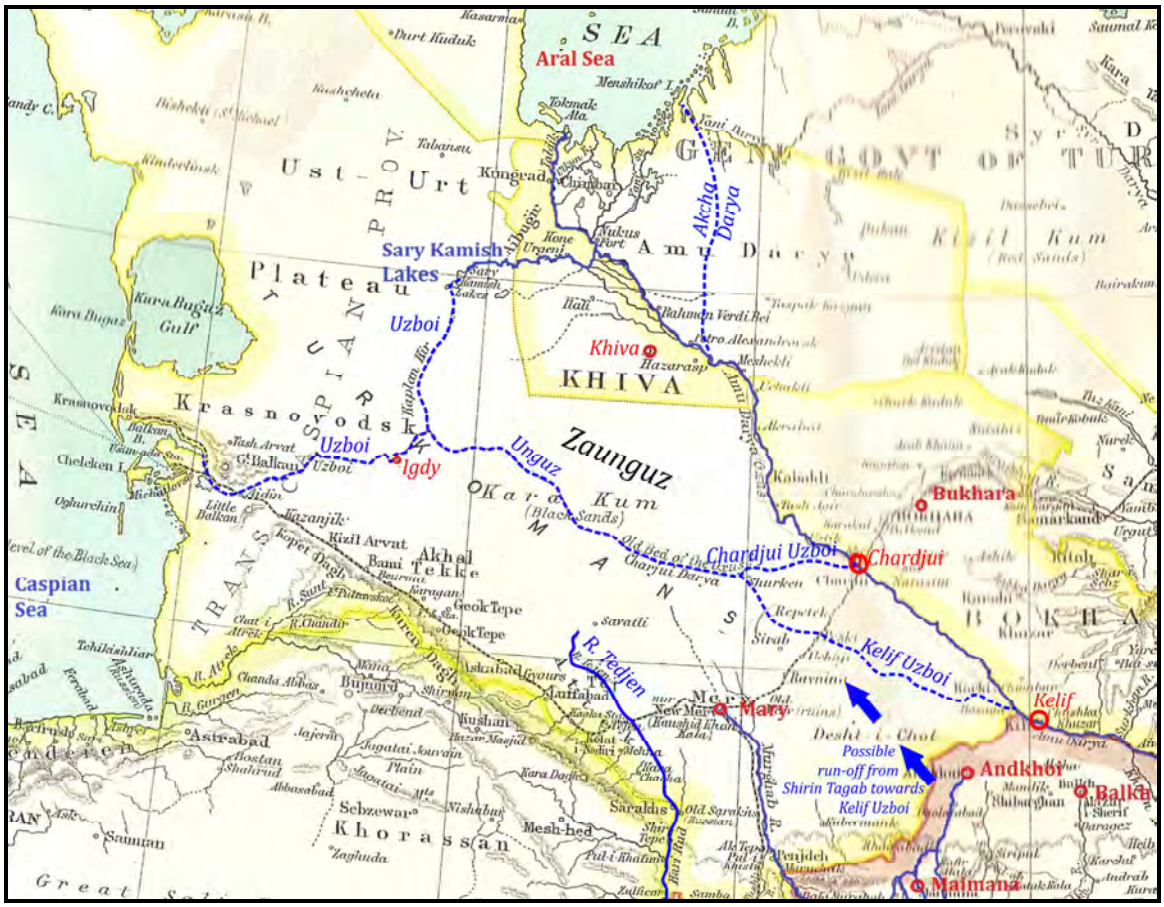

Figure 3.12. A map of Central Asia, showing the supposed former course of the Amu Darya (the Kelif Uzboi) and the borders of the Russian imperial territories of Khiva, Bukhara and Kokand around the time of 1902-1903. Source: http://en.wikipedia.org/wiki/Emirate_of_Bukhara. Believed to be public domain.

If we allow that, during such pluvial episodes, the river discharge in Faryab would have been greater and river water quality fresher, it seems reasonable that recharge of fresh groundwater resources might also have been greater, either by direct recharge

mechanisms or by increased infiltration of fresh river water in valleys, including river channels that are dry today.

The Aral Sea, the Sary Kamysh and the Unguz and the Uzbois

The Amu Darya, together with the Syr Darya, feeds the current inland Aral Sea. In large part, due to over-abstraction of the two rivers, the flows reaching the Aral Sea have decreased dramatically in recent decades, leading to a catastrophic desiccation of the Aral Sea (Zavialov 2005).

The palaeogeography of the Aral / Amu Darya system has long been a source of tremendous interest and controversy, because the system is associated with a number of apparent palaeochannels, which are largely inactive today. Amongst these are (Figure 3.12):

- The **Akcha Darya** channel: a minor palaeochannel system of the Amu Darya, by which water entered the Aral Sea slightly to the east of the recent main course.
- The **Sary Kamysh lakes**. These are a string of saline lakes to the south-west of the Aral Sea and have historically been fed by waters from the Amu Darya in a number of episodes. Up to the 15th-16th centuries AD, some of the Amu Darya's flow continued to the Sary Kamysh saline lakes and, at times of high flow, overspilled into the Western Uzboi and thence towards the Caspian (Aladin et al. 2005, Pravilova 2008). Even after, the 16th century some of the channels between the Amu Darya and the Sary Kamysh lakes were maintained as irrigation channels. Breckle & Geldyeva (2012) note that the Sary Kamysh Lakes and the Aral Sea represent two terminal receptors for the Amu Darya flow and that, in historical times, the Amu Darya rather often changed its outflow between the two. The reasons for this alternation may have been natural, but many authors have suggested that irrigation / damming projects by the Central Asian civilizations may also have been important in determining flow distributions.
- The (**Western) Uzboi,** a (now largely dry) palaeochannel running from Sary Kamysh, through the desert town of Igdy, to the Caspian Sea (Aladin et al. 2005, Létolle et al. 2007, Zonn et al. 2010). This channel was historically regarded as a major, and partly navigable, watercourse, carrying excess water (ultimately from the Amu Darya) from the Sary Kamysh depression. It thus provided an outlet for the Amu Darya's waters to the Caspian sea.
- The **Unguz** has the appearance of a palaeochannel crossing the Karakum towards the Caspian Sea, meeting the Western Uzboi just upstream of Igdy. It appears that it may have been linked to other apparent palaeochannels (the **Kelif Uzboi** or **Chardjui Uzboi**) further east. It has been widely speculated that these channels represent a former southern course of the Amu Darya, departing the current course near the towns of Kelif or Chardjui (respectively) and conveying the flow of the Amu Darya directly to the Caspian Sea.

The Unguz / Kelif Uzboi

Within various literature sources, it is widely (but, by no means, universally - see Boroffka 2010) claimed that the Amu Darya formerly left its current channel near Kelif (or possibly Chardjui), to cross the Karakum desert in a desiccated valley (supposed palaeochannel), referred to as the **Kelif Uzboi** (or Chardjui Uzboi) or **Unguz**, which joined the Western Uzboi upstream of Igdy and discharged to the Caspian Sea.

Fyedorovich (1979) states that the central and southern Karakum desert is composed of the alluvial deposits of the ancient Amu Darya and those of the deltas of the Murghab

and Tedzhen. The **Unguz** *consists of a chain of hollows up to 15 km long and 1–4 km wide, with flat bottoms of solonchak or takyr (*Great Soviet Encylopedia 1979 - entry for Unguz), running along the northern margin of the central Karakum, at the foot of the scarp (40-80 m high) of the elevated Zaunguz Karakum plateau to the north. [Fyedorovich suggests that the northern Zaunguz plateau itself is composed of Miocene and Pliocene sedimentary rocks, laid down by an earlier palaeo-Amu Darya]. The Great Soviet Encyclopedia (1979) believes that the Unguz is a palaeochannel of the former Amu Darya, and that some of its hollows are filled in sands from the river and later *deformed by tectonic movements and subjected to denudation.*

It is thus widely accepted that the palaeo-Amu Darya traversed the central Karakum in Neogene and Pleistocene times. However, the "myth" of the Kelif Uzboi as a more recent channel for the Amu Darya seems remarkably tenacious. The rumour of the Amu Darya discharging into the Caspian seems to have its route in some very hazy Greek geography by Herodotus, Strabo and Patrocles (Tarn 1901), which not only appears to confuse the Aral with the Caspian, but also introduces the nebulous River *Ochus* (easily confused with the *Oxus* - Olbrycht 2010), which might plausibly be construed an alternative southern course of the Amu Darya to the Caspian (Rawlinson 1879). Such rumours persisted for many centuries. Indeed, on the wall of the Doge's Palace in Venice, there is a 17th Century map showing the Amu Darya discharging to the Caspian rather than the Aral Sea. The ideas were kept alive by Russian and English adventurers and geographers such as Baron Aleksander V. Kaulbars, Arthur Conolly, General Mikhail N. Annenkoff and Sir Henry Creswicke Rawlinson (1879).

In 1714, Peter the Great was taken with the idea of turning the Amu Darya from its course to the Aral into its former (Sary Kamysh - Western Uzboi) course to the Caspian, and ordered an expedition to investigate this possibility (thus creating a waterway from Moscow to India). Eventually, the Russians convinced themselves that the Amu Darya had been deliberately diverted away from its old course via the Sary Kamysh lakes by the Turkmen nations (Zonn et al. 2010). In 1879, the Grand Duke Nikolaj Konstantinovich organized an expedition to survey the entire Amu Darya basin. By summer of that year, a group had arrived at the (then Bokhara-controlled) fortress on the Amu Darya at Kelif (just north of Faryab). A Turkmen guide (one Geldygog) informed the party that, close by, near the Afghan village of Aladat, a former channel of the Amu Darya (termed the "Shor") branched off the left bank of the Amu Darya and continued across the desert towards the Caspian Sea. Thus grew the myth of the **Kelif Uzboi** or **Chardjui Uzboi** as a recent southern course of the Amu Darya - possibly with a basis Pleistocene geological reality, but partly wishful thinking on the part of Russian adventurers!

The Recent Geological History of the Amu Darya / Aral Sea

The complex early Quaternary history of the Aral Sea is documented by Breckle & Geldyeva (2012) and its later history by Boomer et al. (2009) and Boroffka (2010). Boomer et al. (2000) probably provide the best overall overview of the evolution of the system, upon which the following is largely based:

- the Aral / Sary Kamysh depression was formed in the late Neogene, some 3 million years ago (Boomer et al. 2000). The Aral Sea may first have become water-filled by overflow from the Caspian Sea some 2-3 million years ago.
- During the latest Neogene (Pliocene) and early Pleistocene, the Amu Darya probably traversed the area known as the **Zaunguz Karakum** (between its modern course and the Unguz) towards the Caspian Sea, laying down broad expanses of sandy / clayey sediments. It is these sediments which, today, underlie the Zaunguz plateau (see above, and Fyedorovich 1979).

- Somewhere in the middle of the early Pleistocene, the Amu Darya's course shifted south to the *Nizmenie (Lower) Karakum*, i.e. to the area occupied by the apparent Kelif Uzboi / Unguz palaeochannel. The Amu Darya thus flowed towards the Caspian Sea and laid down the geological sequence of sediments known to Soviet geologists as the Karakumskaya Suite (sand, clay and carbonate muds). In this period, the Murghab and Tedjen Rivers would have been left-bank tributaries of the Amu Darya.
- Sometime during the late Pleistocene, the course of the Amu Darya began to migrate northwards towards its current channel, possibly in response to a gradual uplift and doming of the Karakum (Lyberis & Mering 2000). It may also have been in response to an increase in the flow and erosive power of the River (related to changes in climate or uplift patterns in the Pamir). The Unguz may thus have been one of the most recent Pleistocene palaeochannels in the area.
- During large parts of the Pleistocene, the Aral would likely have been dry for protracted periods.
- At the end of the late Pleistocene, or early Holocene, the course of the Amu Darya turned north and began to fill the Sary Kamysh depression and the Aral Sea. Fyedorovich (1979) suggests that the Amu Darya left the Karakum depression (the Unguz) some 20-30,000 years BP. Other authors place the filling of the Aral Sea at a later date (17,000 to 9,000 years BP; Zavialov 2005). Boomer et al. (2000) place the final diversion of the Amu Darya away from the Caspian towards the Aral / Sarykamysh / Khorezm Basin (the so-called "Great Aral Sea") at the onset of the Lavlakansky Pluvial period around 9000 years BP.
- During the warmer climate of 5000-7000 years BP, the Amu Darya's increased flow passed both into the Aral Sea (possibly via the Akcha Darya channel) and via the Sary Kamysh and Western Uzboi to the Caspian Sea. Fyedorovich (1979), Zavialov (2005) and Breckle & Geldyeva (2012) concur that the Amu Darya began to overflow from the Sary Kamysh lakes to the Caspian via the Western Uzboi in the early to mid Holocene (Fyedorovich suggests somewhere in the 5th-2nd millennia BC). Boroffka (2010) suggests that the Sary Kamysh / Western Uzboi route may have been active earlier than this, however.
- Up to the 15th-16th centuries AD, some of the Amu Darya flow continued to the Sary Kamysh lakes and, at times of high flow, overspilled into the Western Uzboi and thence towards the Caspian (Aladin et al. 2005, Pravilova 2008). During this period, the flow of the river was partially managed by the Khorezm civilization for irrigation. In 1558, an English merchant, Anthony Jenkins, observed that:

  > *`..the water that serveth all the country is drawn by ditches out of the river Oxus unto the great destruction of the said river, for which it falleth not into the Caspian Sea as it hath done in times past, and in short time all that land is like to be destroyed, and to become a wilderness for want of water, when the river Oxus shall fail."* (cited in Boomer et al. 2000).

- Even after, the 16th century some of the channels between the Amu Darya and the Sary Kamysh lakes were maintained as irrigation channels. In 1878, a major flood on the Amu Darya broke through to the Sary Kamysh, and re-filled the lakes.

So: What is the Kelif Uzboi / Unguz ?

Although many authors regard the Unguz as a former channel of the Amu Darya in the Pleistocene and even late Neogene (e.g. Lyberis & Mering 2000), there is not a complete consensus. Aladin et al. (2005) state that there is no trace of any flow of the Amu Darya

along the Kelif or Chardjui "Daryas" during the past five centuries. Furthermore, their assessment of the Unguz suggests that the "channel" shows no obvious traces of fluvatile activity and may be a wind-erosional feature.

According to Pravilova (2009) and Zonn (2014), the Kelif Uzboi was not (at least in the recent past) a southern channel for the Amu Darya, but rather an intermittent channel accepting discharge from the northern Afghan Rivers (such as the Balkh, Shirin Tagab and Sar-e Pol) at times of excessive flow. Indeed, Berg (1950) records that, in 1907, water from the rivers of northern Afghanistan penetrated into the Kelif Uzboy.

Of Etymological Interest

The name ***Shirin Tagab*** means *sweet water*.

Murghab means *River of the Birds*. In Greek it is believed to have been *Margiana*.

Amu Darya means the *River of Amul* (the city of Amul is the modern city of Türkmenabat, in Turkmenistan). In Greek the river was called the *Oxos* (Latin *Oxus*; Sanskrit *Vaksu*) and the plain between it and the mountains (including northern Faryab) was called *Oxiana*.

Shor Darya means *salty river* - a very apt description.

The Turkic name ***Unguz*** is believed to refer to an *old dry river bed* - see http://en.wikipedia.org/wiki/User:Yeniler/Hazar.

The ***Kelif Uzboi*** was believed to be the former channel of the River Amu Darya that diverged from the current channel near the town of Kelif and followed the initial line of the Lenin Canal, through Zeid and the Unguz towards the Caspian Sea. There is no evidence that the Amu Darya followed this course in historic times, and is based on a misunderstanding (see text).

Safed Koh means *White Mountains*, while ***Band-e-Turkestan*** refers to this range forming the *boundary wall to Turkestan*.

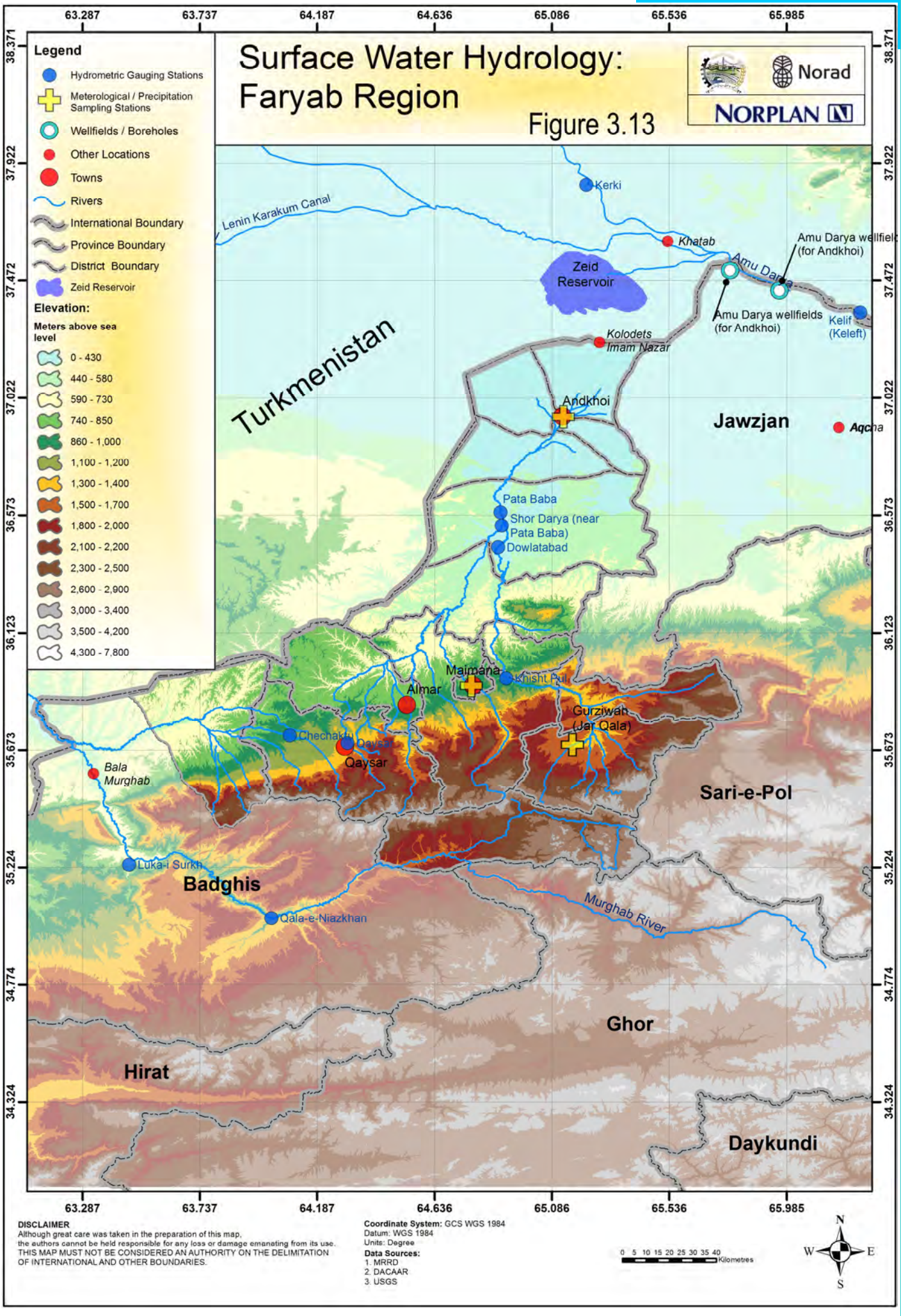
Surface Water Hydrology:
Faryab Region
Figure 3.13
Norad
NORPLAN
Legend
Hydrometric Gauging Stations
Meterological / Precipitation Sampling Stations
Wellfields / Boreholes
Other Locations
Towns
Rivers
International Boundary
Province Boundary
District Boundary
Zeid Reservoir
Elevation:
Meters above sea level
0 - 430
440 - 580
590 - 730
740 - 850
860 - 1,000
1,100 - 1,200
1,300 - 1,400
1,500 - 1,700
1,800 - 2,000
2,100 - 2,200
2,300 - 2,500
2,600 - 2,900
3,000 - 3,400
3,500 - 4,200
4,300 - 7,800
63.287
63.737
64.187
64.636
65.086
65.536
65.985
38.371
37.922
37.472
37.022
36.573
36.123
35.673
35.224
34.774
34.324
Kerki
Lenin Karakum Canal
Khatab
Amu Darya wellfield (for Andkhoi)
Amu Darya
Zeid Reservoir
Amu Darya wellfields (for Andkhoi)
Kelif (Keleft)
Kolodets Imam Nazar
Turkmenistan
Andkhoi
Jawzjan
Aqcha
Pata Baba
Shor Darya (near Pata Baba)
Dowlatabad
Maimana
Khisht Pul
Almar
Gurziwan (Jar Qala)
Chechaktu
Qaysar
Bala Murghab
Sari-e-Pol
Luka-i Surkh
Badghis
Murghab River
Qala-e-Niazkhan
Ghor
Hirat
Daykundi
DISCLAIMER
Although great care was taken in the preparation of this map, the authors cannot be held responsible for any loss or damage emanating from its use. THIS MAP MUST NOT BE CONSIDERED AN AUTHORITY ON THE DELIMITATION OF INTERNATIONAL AND OTHER BOUNDARIES.
Coordinate System: GCS WGS 1984
Datum: WGS 1984
Units: Degree
Data Sources:
1. MRRD
2. DACAAR
3. USGS
0 5 10 15 20 25 30 35 40
Kilometres
N
W
E
S

Figure 3.14

Hydrometry of Faryab Province

Legend

- Hydrometric Gauging Stations
- Meterological / Precipitation Sampling Stations
- Wellfields / Boreholes
- Other Locations
- Towns
- Rivers
- International Boundary
- Province Boundary
- District Boundary
- Khwaja Mod saline lake
- Chakan saline lake

Elevation:

Meters above sea level

- 0 - 430
- 440 - 580
- 590 - 730
- 740 - 850
- 860 - 1,000
- 1,100 - 1,200
- 1,300 - 1,400
- 1,500 - 1,700
- 1,800 - 2,000
- 2,100 - 2,200
- 2,300 - 2,500
- 2,600 - 2,900
- 3,000 - 3,400
- 3,500 - 4,200
- 4,300 - 7,800

DRAWING:

Surface Water Hydrology of Faryab Province

Drawn by:	Shuaib Zarinkhail	Date:	Feb 2014
Checked by:	David Banks	Date:	
Authorized by:		Date:	
Drawing No:	01		
Version:	1.5		

PROJECT:

Capacity Building and Institutional Cooperation in the field of Hydrogeology for Faryab Province, Afghanistan

CLIENT:

Norad

NORPLAN

DISCLAIMER
Although great care was taken in the preparation of this map, the authors cannot be held responsible for any loss or damage emanating from its use. THIS MAP MUST NOT BE CONSIDERED AN AUTHORITY ON THE DELIMITATION OF INTERNATIONAL AND OTHER BOUNDARIES.

File Path: Y:\2 RuWATSIP\1_RGIS\01_Project_Files\03_Working\forAtlas\Figure 3.14 Surface water hydrology- Faryab Province v1.5.mxd

Coordinate System: GCS WGS 1984
Datum: WGS 1984
Units: Degree

Data Sources:
1. MRRD
2. DACAAR
3. USGS

Scale 1:1,000,000 @ A3 paper size

0 5 10 15 20 25 30 35 40 Kilometres

N W E S

4. Faryab: Geology

4.1 Tectonic Overview

The geology of Afghanistan is dominated by the Mesozoic (Cimmeride) and Tertiary (Himalayan - Alpine) orogenic episodes that have given the nation its mountainous core and which have controlled recent sedimentary deposition in the adjacent areas.

During the late Permian, a number of tectonic plate fragments (micro-plates) broke away from the southern "super-continent" of Gondwanaland (Figure 4.1). One of these, the Afghan micro-plate, collided with the Eurasian continental plate in the Mesozoic. This "Cimmeride" (also loosely referred to as "Hercynian") orogenic episode commenced around the late Triassic and was complete by the Jurassic / Early Cretaceous (200-150 million years ago). The Cimmeride orogeny created the Paropamisus / Band-e Turkestan mountains, to the south of Faryab (Whitney 2006)

Around the Early Cretaceous, the Indian plate disengaged from Gondwanaland and subsequently collided with the Eurasian plate in the Palaeogene (late Palaeocene, early Eocene) resulting in further orogenesis, crustal thickening and crustal displacement (broadly referred to as the so-called Himalayan orogenic episode). South of the Harirud fault, the remnant of the Afghan micro-plate (the Afghan Block) has been (and is still being) squeezed south-westward at rates in excess of 1 cm/year by this crustal shortening (Whitney 2006).

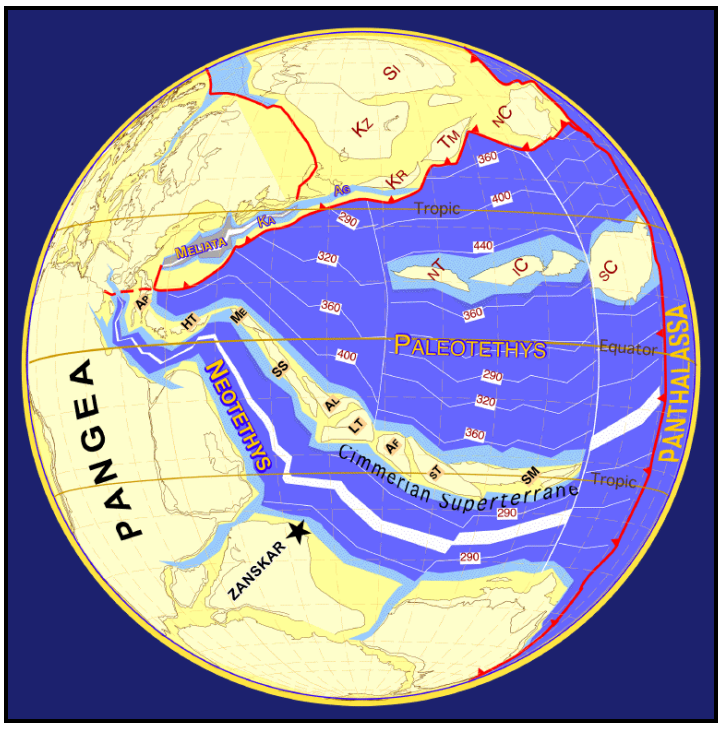

Figure 4.1. Plate tectonic reconstruction of the Himalayan region at 249 million years ago (late Permian / early Triassic). The Cimmerian superterrane, including the Afghanistan micro-plate (AF) is seen approaching Eurasia across the closing Palaeotethys Ocean. After Dèzes (1999); Available at http://en.wikipedia.org/wiki/Cimmerian_Orogeny.

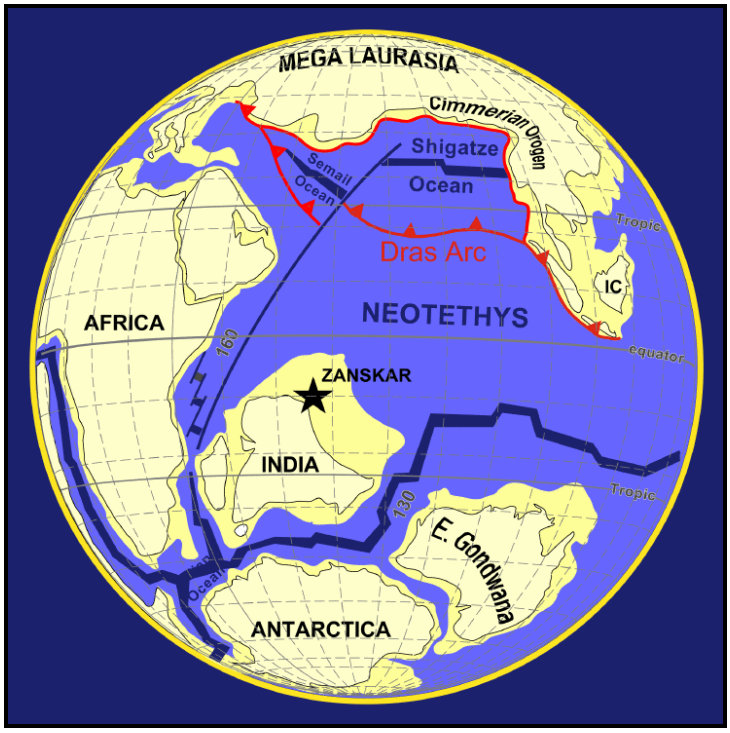

Figure 4.2. Plate tectonic reconstruction of the Himalayan region at 100 million years ago. The area of the Cimmeride orogen (now complete) is seen, as is the approaching Indian plate across the closing Neotethys Ocean. After Dèzes (1999); Available at http://en.wikipedia.org/wiki/Cimmerian_Orogeny.

The North Afghanistan Platform, on which Faryab is located, is thus an area of Cimmeride (pre-Jurassic) deformation. The Cretaceous and Palaeogene rocks are generally marine limestone and clastic sequences deposited in shallow basins. These uplifted during the Alpine / Himalayan orogenic episode. The huge thicknesses of Neogene and Quaternary sediments in the northern part of Faryab are the erosional result of the most recent (Himalayan) episode of uplift and mountain-building.

4.2 The North Afghanistan Platform

Faryab sits upon the *North Afghanistan platform* - an area including and to the north of the Band-e Turkestan mountain chain. The platform thus represents the extreme southern edge of the former Eurasian plate.

Tectonic Structure

The Platform is typically divided into two distinct areas:

- the northern Murghab-Upper Amu Darya ***Basin***, which is the main, subsiding sedimentary basin accumulating Neogene and Quaternary deposits.
- the southern Paropamisus-Band-e Turkestan ***Uplift*** area

These two features seem to have acquired their tectonic character (subsidence and uplift, respectively) during and after the Himalayan-Alpine orogeny, although it is acknowledged as probable that they evolved as down-warped ("intracratonic rift sag basin" - Klett et al. 2006) or uplifted structures during Jurassic-Palaeogene times.

The Paropamisus-Band-e Turkestan Uplift area is subdivided into three distinct fault blocks, stepping down towards the north into the Murghab-Upper Amu Darya Basin. These are:

- The Qala-e Naw Fault Block

- The Maimana fault block and
- The Shebergan fault block.

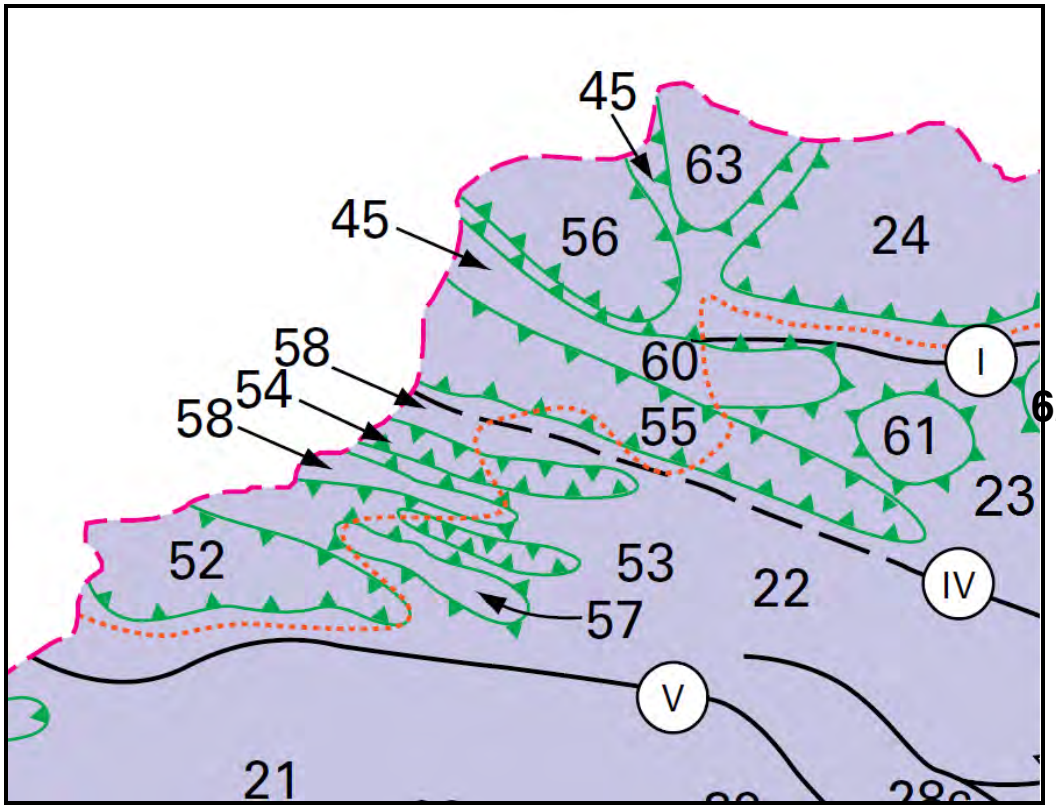

Figure 4.3. Tectonic map of the North Afghanistan Platform in the region of Faryab, after Abdullah & Chmyriov (2008), not believed to be copyrighted. The red dashed line shows the edges of the Murghab - Upper Amu-Darya Neogene-Quaternary basin. The green lines show areas of Alpine uplift or subsidence within the Cimmeride platform area.
Paropamisus-Band-e Turkestan Uplift: *21 - Qala-i Naw fault block; 22 - Maimana fault block; 23- Shebergan fault block; 61 - Sheram arch; 62 - Shadian arch.*
Afghanistan-South Turkmenistan Basin. *24 - Surkhan (Mazar-e Sharif) megasyncline*. Troughs: *52-Qala-i-Mor-Kaisar troughs, 53-Almar trough, 54- Ortepin trough, 55- North Karabil - Dawlatabad trough, 56- Obruchevskii trough.* Ramparts: *57 - Jekdalek, 58 - Khwaja Qol, 59 - Qara-Qol, 60 - Andkhoi, 63- Pericline of South-West Gissar.*
Neogene-Quaternary Basins: *45-Murghab - Upper Amu Darya*
Major Faults: *I - Alburz-Mormul; IV - Andarab-Mirza Wolang; V - Band-e Turkestan.* The *Band e-Turkestan Fault is approximately vertical and about 400 km long, separating the Qala-i Naw and Maimana fault blocks. It appears to be a right- lateral fault.*

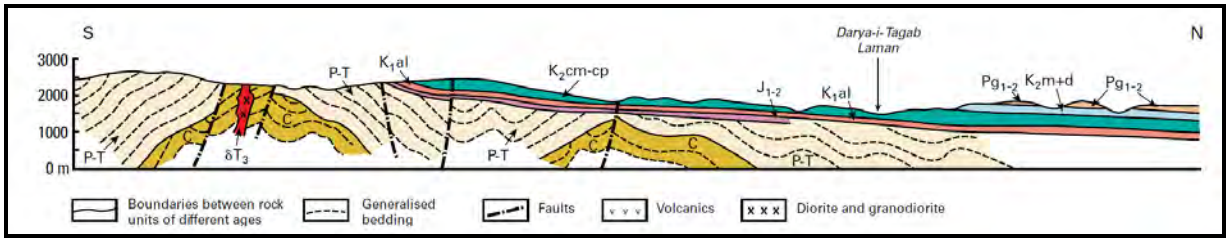

Figure 4.4. North-south cross section through the southern North Afghanistan Platform along the Darya-e Tagab Laman River, near Qala-e Naw, Badghis, after Abdullah & Chmyriov (2008a), not believed to be copyrighted. Note the relatively flat-lying Jurassic-Palaeogene sedimentary rocks sitting upon the folded Cimmeride basement.

Summary of Stratigraphy

According to Brookfield & Hashmat (2001), the stratigraphy of the North Afghanistan Platform can be roughly divided into three:

- Pre-Jurassic (pre-Cimmeride) folded basement of Palaeozoic to Triassic age.
- A post-Cimmeride, Jurassic to Palaeogene sequence of sedimentary rocks and some volcanic rocks, unconformably overlying the basement. These sedimentary rocks are relatively flat-lying, but show large scale flexure and deformation related to the Himalayan-Alpine orogeny.
- A syn- and post-Himalayan orogenic, Neogene to Quaternary continental clastic sequence.

The Jurassic-Palaeogene can be subdivided into four units:

1. A Late Triassic to Middle Jurassic rift succession, dominated by coarse, continental, coal-bearing clastics, laid down by braided and meandering streams in linear, rifting-related grabens.
2. Mid-Upper Jurassic mixed continental-marine clastic and carbonates, overlain by a regressive Upper Kimmeridgian–Tithonian evaporite-bearing sequence.
3. Lower Cretaceous red-beds and evaporites (unconformably overlying the Jurassic), succeeded by a transgressive sequence of Cenomanian to Maastrichtian shallow marine limestones.
4. Palaeocene to Eocene marine limestones with gypsum, succeeded by thin conglomerates and brackish-marine Upper Oligocene / Lower Miocene shales.

Information Sources

The most recent geological maps of Faryab are those at 1:250,000 scale, provided by the Afghan Geological Survey, assisted by the U.S. Geological Survey, although these are largely based on the mapping of earlier Afghan and Soviet geologists. The sheets covering Faryab are published by:

- McKinney & Sawyer (2005), covering the southern part of Faryab: Maimana, the Band-e Turkestan, Kohistan, Almar, Qaysar and Gurziwan.
- McKinney & Lidke (2005), covering the extreme east of the study area, including Ghormach.
- Wahl (2005), covering the northern part of Faryab, including Shirin Tagab, Dawlatabad and Andkhoi.

The British Geological Survey has also re-published the two volumes of the Geology of Afghanistan by Abdullah & Chmyriov (2008a,b). Originally written in Russian and published by Nedra in Moscow, the volumes reflect the Soviet unwillingness to fully embrace modern plate tectonic theory, but nevertheless remain an extremely comprehensive and systematic source work.

The following is largely derived from the sources mentioned above (and especially Dronov's 2008b overview).

4.3 Pre-Cimmerian Rocks in Faryab and the North Afghanistan Platform

At depth, the North Afghanistan Platform comprises a folded Palaeozoic-Triassic basement that was intruded by granites (not exposed in Faryab) during the last stages of

the subduction of the Palaeotethys Ocean (BGS 2014). In Faryab, the Cimmerian basement is most prominently exposed in the fault-bounded, horst-like Band-e Turkestan range. The units mapped in Faryab include:

C_2ls Late Carboniferous: dominated by limestones, with subordinate clastic sedimentary rocks (slates, sandstones, conglomerates, siltstones) and volcanic rocks (andesites, basalts).

Pssl Permian: dominated by red and variegated sandstones and siltstones, with subordinate conglomerates and mudstones.

T_1ssc Early Triassic: dominated by variegated marine sandstones and conglomerates, with subordinate chert and volcanic rocks (rhyolite, basalt).

T_{23}ssl Middle-Late Triassic sedimentary complex: dominated by marine sandstones and siltstones, with subordinate carbonaceous shales, mudstones, limestones, marls conglomerates, acidic and mafic volcanics. The late Triassic terrigenous deposits have been described as flysch.

4.4 Jurassic-Palaeogene Rocks in Faryab and the North Afghanistan Platform

The Cimmeride orogeny was largely complete in the Faryab area by the Jurassic. Following the orogeny, the mountain chain was eroded and peneplained. The northern part of the North Afghanistan Platform thus started subsiding and accumulating sediments.

Jurassic

Early to Middle Jurassic: Initially, erosion of the Cimmeride mountain chain produced a sequence of Jurassic clastic sediments on the new Cimmeride basement. The early-mid Jurassic clastic sequence contains some coal lenses and layers and is known to reach 100-1450 m in thickness, known as the **Sayghan Series.**

Middle to Upper Jurassic: Towards the end of the Middle Jurassic (167 Ma BP), conditions changed in the northern part of the platform, with marine carbonate sequences becoming predominant (Bathonian - Oxfordian). The carbonates are an important hydrocarbon reservoir rock and are referred to as the **Kugitang** or **Gissar Formation.**

Upper Jurassic: In the Upper Jurassic (Kimmeridgian-Tithonian), terrigenous red-bed (conglomerate, sandstone, siltstone) and evaporites again became predominant. One especially thick evaporite sequence forms the cap rock for the Middle-Upper Jurassic hydrocarbon reservoirs and is referred to as the **Gaurdak Salt Formation** (includes anhydrite, halite and some sylvite, Ulmishek 2004)**.** The Gaurdak salt generally increases in thickness to the north and pinches out to the south of Andkhoi (Figure 4.7).

The Jurassic strata are not exposed to any extent in Faryab, but are known at depth from drilled boreholes and are known to produce significant quantities of geothermal groundwater.

Cretaceous

Late Jurassic terrigenous clastic deposition continued into the Cretaceous.

K_1ssc Early Cretaceous: In Faryab, the early Cretaceous is represented largely by red sandstones and conglomerates, with less abundant siltstones, gypsum evaporites and clays. Near the Paropamisus-Band-e Turkestan Uplift in the south, the deposits are coarser-grained and of a terrestrial nature. To the north, in the Murghab-Upper Amu

Darya Depression, the sediments are finer, with some marine layers and lenses within the terrigenous sequence. The deposits can reach 1000 m in thickness.

The Hauterivian (Lower Cretaceous) sandstones of the Qezeltash Formation are an important hydrocarbon reservoir rock. Figure 4.5 shows structural contours on the top of the Qezeltash sandstone formation in Faryab.

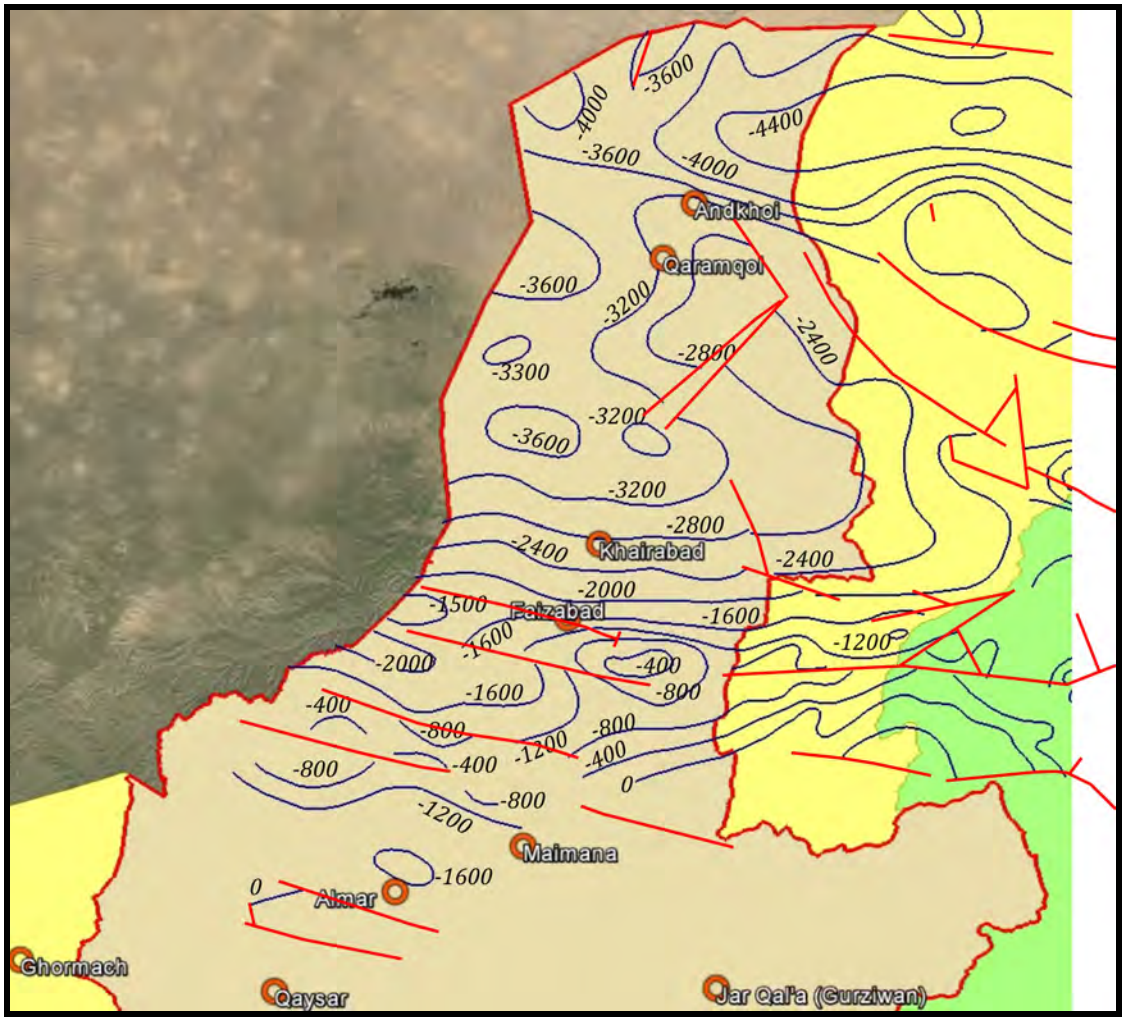

Figure 4.5. Structure contours on the top of the Hauterivian Qezeltash sandstone formation in m relative to sea level in Faryab. Based on data of Steinshouer et al. (2006). See also http://pubs.usgs.gov/of/2006/1179/metadata/qezeldpafg.htm. Red lines show faults transposed from Ghory Formation map of Klett et al. (2006).

Towards the end of the Early Cretaceous, marine conditions started transgressing from the north, with a finer grained, mainly clastic sequence accumulating in shallow marine basins, with the sediment supply coming from the Paropamisus-Band-e Turkestan Uplift.

K_2ssl Late Cretaceous clastic facies: In Faryab, the late Cretaceous is represented largely by shallow marine sandstones and siltstones, with less abundant clays, limestones, marls, conglomerates and gypsum evaporites.

From the start of the Cenomanian (start of the Late Cretaceous) onwards, marine carbonate facies start appearing, especially in the north and south-east of the area. By the end of the Cretaceous (Campanian-Maastrichtian), the marine transgression of the North Afghanistan Platform is almost complete, and marine platform deposits of limestone/dolomite sediments predominate. This deposition continued until the

Palaeogene. The Maastrichtian-Palaeocene in the southern (Paropamisus-Band-e Turkestan) part of the platform is dominated by a carbonate reef facies, which can reach up to 777 m thick. In the north, in the Murghab-Upper Amu Darya Depression, the deposits are more terrigenous in nature, with no reef facies and up to 600 m thick.

KP_1ld Late Cretaceous and Palaeocene carbonate facies (often referred to as the Ghory Formation): Deposits of marine limestones, marls and dolomites, with less abundant sandstones, clays, siltstones, gypsum, and conglomerates. The Ghory formation is some 150-170 m thick on the Maimana Step (Klett et al. 2006).

The Ghory Formation is a hydrocarbon reservoir rock in some areas, capped by Eocene mudstones. Figure 4.6 shows structural contours on the top of the Upper Campanian to Palaeocene Ghory formation in Faryab.

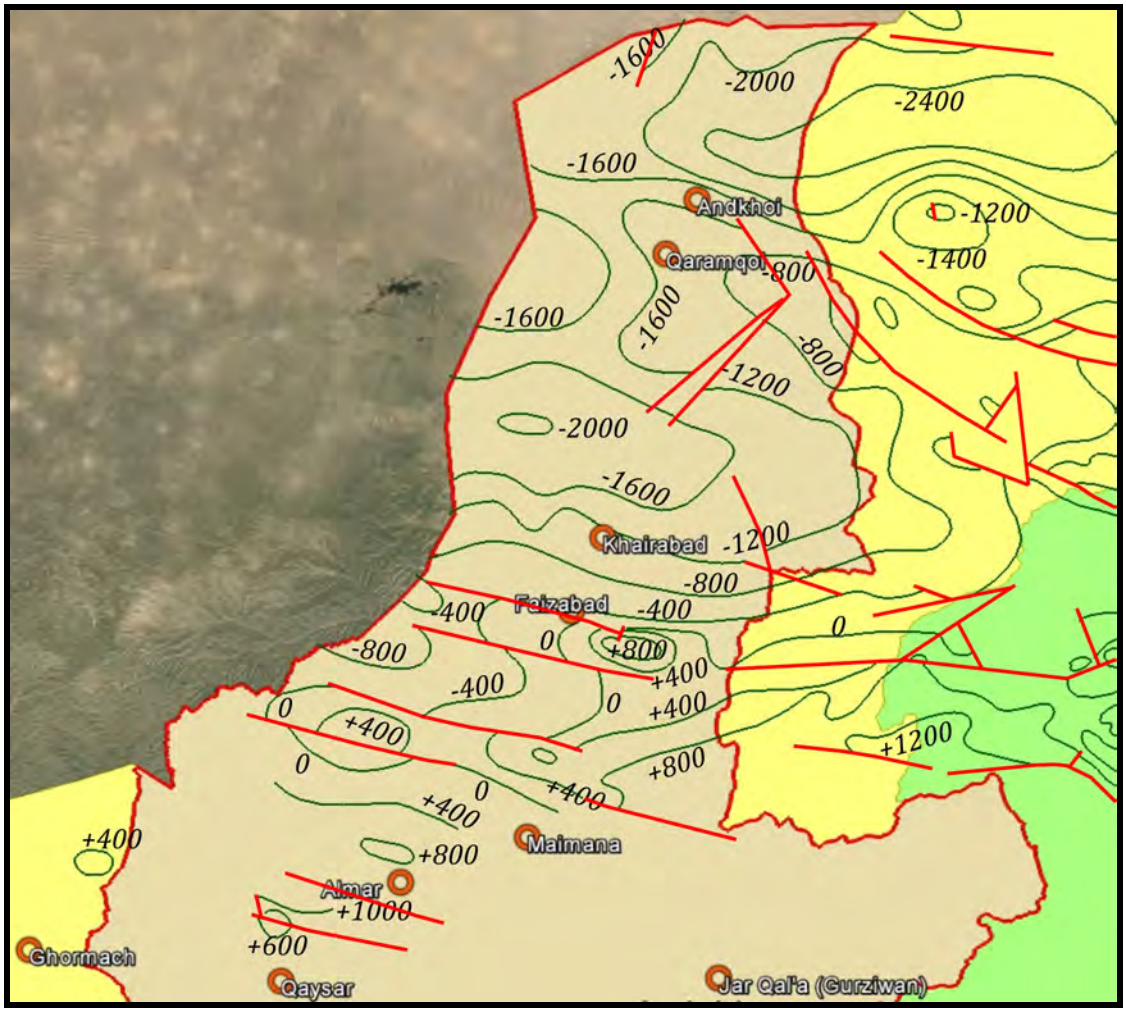

Figure 4.6. Structure contours on the top of the Campanian-Palaeocene Ghory carbonate formation in m relative to sea level in Faryab. Based Steinshouer et al. (2006). See also http://pubs.usgs.gov/of/2006/1179/metadata/ghorydpafg.htm. Red lines show faults (after Klett et al. 2006).

Palaeogene

KP_1ld Late Cretaceous and Palaeocene: see above.

During the Eocene, sedimentation was more dominated by terrigenous, fine clastic material, up to 800 m thick, in a marine basin.

P_2csh Eocene: In Faryab, Eocene deposits of clay, shale and siltstone are observed, with less abundant sandstone, limestone, marl, gypsum and conglomerate.

In the Eocene and Oligocene, some volcanic deposits are recorded from the North Afghanistan Platform, although these are not specifically mapped in Faryab.

4.5 Neogene and Quaternary Rocks in Faryab and the North Afghanistan Platform

The final stages of subduction of the Neotethys Ocean, as the Indian plate converged on the Afghan plate, took place in the Cretaceous and Tertiary, with volcanic activity further south and some intrusion of Oligocene/Miocene granites as far north as north-eastern Afghanistan. The Himalayan - Alpine orogenesis culminated in the late Palaeogene, early Neogene.

The focus of the Himalayan - Alpine orogeny was further south in Afghanistan than Faryab: nevertheless, the effects were felt in the North Afghanistan Platform area as an uplift of the southern part of the platform, commencing towards the end of the Eocene. Thus, Oligocene deposits are essentially absent in outcrop. Some Eocene-Oligocene shallow and partly fresh water sediments were deposited in the northern Murghab-Upper Amu Darya Depression.

The Uplift was coupled with dramatic erosion and deposition of Neogene and Quaternary proluvial and alluvial sediments in sedimentary basins to in the northern part of the North Afghanistan Platform, collectively referred to as the Afghanistan-South Turkmenistan Basin (or, in Faryab, as the Murghab-Upper Amu Darya basin).

Neogene

At the culmination of the Himalayan-Alpine orogeny, the Murghab-Upper Amu Darya Depression started subsiding very rapidly relative to the uplifted Paropamisus-Band-e Turkestan area and thus started accumulating vast thicknesses (up to 14,000 m) of predominantly terrigenous sediments. The upper Oligocene to Quaternary succession is probably no greater than 1.5 km thick in the Murghab depression (Figure 4.7) and adjacent areas (Ulmishek 2004, Klett et al. 2006). Within the southern uplifted area, minor, local sedimentary basin structures also developed (see Figure 4.3). The deposits commenced with finer material and coarsened as uplift continued. Adjacent to the main uplifted mountain areas, one might describe these deposits as “molasse”-type proluvial deposits, “dumped” in huge poorly-sorted alluvial fan structures washing out of the uplifted mountain areas.

The main stratal divisions mapped at outcrop in the AGS/USGS maps are:

N_1dig Miocene: in eastern Kohistan, a few small igneous intrusions of diorites, granodiorites and associated igneous rocks are noted.

N_{1l}csl Early Miocene: Predominant red clays and siltstones, with less abundant sandstones, conglomerates and limestones.

N_{1m}csl Middle Miocene: Predominant brown clay and siltstone, with less abundant sandstones, conglomerates and limestones.

Note that the AGS/USGS maps show the outcropping Neogene deposits in Faryab as Miocene, while the description of Abdullah & Chmyriov (2008a) implies that the Quaternary further north may be underlain by a thick Pliocene sequence, overlying the Miocene.

The AGS/USGS maps suggest that the outcropping Neogene deposits of Faryab are predominantly fine grained siltstones and clays. This is likely because the mapped outcrops represent only the **Lower Miocene Shafay Formation** and **Middle Miocene Kashtangi Formation**, both of which are dominated by red-brown finer grained clastics.

Other sources (Table 4.2 and Dronov & Chmyriov 2008) suggest that in large portions of the Neogene sequence, coarser sandstones and conglomerates may predominate. For example, in the **Upper Miocene Rustak Formation**, the **Lower Pliocene Kokcha Formation** and the **Upper Pliocene Keshm Formation**, coarser grained sandstones and conglomerates are more dominant (Dronov 2008a).

The lower Neogene sediments typically contain gypsiferous clays and siltstones and it is anecdotally reported that halite also occurs.

Quaternary

During the Quaternary, the northern Murghab-Upper Amu Darya Depression continued subsiding rapidly relative to the uplifted Paropamisus-Band-e Turkestan area, and alluvial sedimentation continued. As the tectonic situation began to stabilise intermittently, discrete "terrace" levels of alluvial sedimentation could be identified. The thickness of Quaternary sediments can reach several km in the deepest basins of the North Afghanistan Platform.

Q_1a Early Pleistocene alluvium: Predominantly gravels and sands (sometimes lithified), with silts and clays.

Q_2a Middle Pleistocene alluvium: Predominantly gravels and sands (sometimes lithified), with silts and clays. Occurs at high elevations in south of Faryab as a cover deposit overlying Cretaceous / Palaeogene and Neogene deposits. Some GIS data sets map this as late Pleistocene / Holocene Q_{34}t glacial till.

Q_2loe Middle Pleistocene loess: loess (silt) with some sand and clay. Wind-blown loess results from aeolian erosion of the vast alluvial plains during periglacial episodes of the Pleistocene. From published geological maps we must deduce that these can reach several tens of metres thickness.

Q_3a Late Pleistocene alluvium: Predominantly gravels and sands (sometimes lithified), with silts and clays.

Q_{34}e Late Pleistocene / Holocene aeolian sands: Occurs as cover deposits over alluvial plains in the semi-desert area in the north of the region.

Q_{34}a Late Pleistocene / Holocene alluvium: Predominantly gravels and sands (sometimes lithified), with silts and clays. Occurs mainly along modern river channels.

Q_4sm Recent Quaternary salt marsh deposits: Mud, silt, and clay, with some sand, limestone, gypsum and salt. The main salt basins (intermittent saline lakes) in Faryab are the **Khwaja Mod** (gypsum and halite), c. 20 km NNE of Khairabad, and the **Chakan** on the eastern border of Dawlatabad district. As of 1995, halite was being mined for table salt from the Khwaja Mod deposit on a small scale (Orris & Bliss 2002). The northern semi-desert area and the Karakum of Turkmenistan also contain takyrs or solonchaks.

The entire Neogene / Quaternary sequence of the northern Faryab plains and the Karakum of Turkmenistan can be regarded as the ancient proluvial / alluvial / lacustrine deposits of the precursors to the Shirin Tagab, Murghab and palaeo-Amu Darya rivers (see Chapter 3.9 and Fyedorovich 1979). The map of Krizhanovskii (1972) indicates the thickness of the Quaternary in the Turkmen desert, above the Neogene, as shown in Table 4.1.

Table 4.1. Depth to base of Quaternary in selected Soviet exploration boreholes in the Turkmen desert near Faryab, from Krizhanovskii (1972), see Figure 8.1 for locations.

Soviet borehole number	Estimated ground level (m asl)	Depth of borehole (m)	Depth to base of Quaternary (m)
182	251	82.7	Neogene not recorded
183	275	100.8	Neogene not recorded
188	722	301.4	170.0
189	519	252.3	Neogene not recorded
190	359	135.8	108.9
194	835	600.0	30.8
195	620	50.0	7.05

Table 4.2. Summary stratigraphic table of the sedimentary sequences on the North Afghanistan Platform. Modified after Annex 15 of Abdullah & Chmyriov (2008a). Not believed to be subject to copyright.

Tectonic Cycle	Structural Formation Complex	QALA-I-NAW FAULT BLOCK AND WEST MAYMANA FAULT BLOCK	SHEBERGHAN FAULT BLOCK	AFGHANISTAN - SOUTH TADJIKISTAN DEPRESSION
		Formations	Formations	
		Sedimentary and sedimentary-volcanogenic rocks	Sedimentary and sedimentary-volcanogenic rocks	Sedimentary and sedimentary-volcanogenic rocks
Orogenic	Quaternary	Q Grey, terrigenous, terrestrial	Q Grey, terrigenous, terrestrial	Q Grey, terrigenous, terrestrial
	Pliocene	N2 Variegated to grey, terrigenous, terrestrial 50 - 250m	N2 ?	N2 Variegated to grey, terrigenous, terrestrial 9,000m
	Miocene	N1 Variegated to red, terrigenous, terrestrial 300 - 800m	N1 Variegated to red, terrigenous, terrestrial 1,100 - 1,550m	N1 Variegated to red, terrigenous, terrestrial 1,100 - 5,750m
	Eocene - Oligocene	Pg2-3 Terrestrial volcanogenic (porphyry) 250 - 1,400m	Pg2-3 ?	Pg2-3 ?
Cratonic	Jurassic - Eocene	Pg2 Terrigenous 250 - 700m	Pg2 Terrigenous 400m	Pg2 Terrigenous 400 - 620m
		K2m-Pg1 Carbonate 150 - 1,150m	K2m-Pg1 Carbonate 200 - 600m	K2 Terrigenous-carbonate 150 - 1,700m
		K2 Carbonate-terrigenous 250 - 500m	K2 Carbonate-terrigenous 300 - 1,700m	
		K1 Carbonate-terrigenous 90 - 130m	K1 Green to variegated (marine in the upper portion, terrestrial in the lower portion) 550 - 850m	K1 Carbonate-terrigenous (marine in the upper portion, terrestrial in the lower portion) 170 - 850m
		J3 Terrigenous 800m	J3 Terrigenous-carbonate and evaporite 700 - 1,150m	J3 Terrigenous-carbonate and evaporite 250 - 1,150m
		J1-2 Terrigenous (coal-bearing) 60 - 100m	J1-2 ?	J1-2 Terrigenous (coal-bearing) 1,250 - 1,450m
In superimposed troughs	Triassic	T3r ?	T3r ?	T3r Terrigenous, terrestrial 350m
		T2-3 Dark-coloured, terrigenous, marine 2,200 - 4,000m	T2-3 Dark-coloured, terrigenous, marine 1,100m	T2-3 ?
		T1 Variegated volcanogenic-terrigenous, marine 150 - 2,000m	T1 ?	T1 ?

4.6 *Oil and Gas deposits of the North Afghanistan Platform*

Oil and gas resources are located in the huge Mesozoic-Tertiary sedimentary basin of northern Afghanistan, which can broadly be subdivided (Klett et al. 2006) into an eastern **Afghan-Tajik Basin** and a western **Murghab-Amu Darya basin**, separated by the **Gissar Mega-anticline** (Figure 4.7). According to Brookfield & Hashmat (2001), the oil and gas traps of the North Afghanistan platform are mainly associated with:

- Upper Jurassic carbonates, sealed by cap rocks of Upper Jurassic evaporite salt (Gaurdak salt formation). The Gaurdak salt generally increases in thickness to the north and pinches out to the south of Andkhoi (Figure 4.7). These evaporites occur at depths of c. 3 to 3.6 km in the North Karabil-Dawlatabad trough and at 4 to 5 km in the Obruchev trough (Klett et al. 2006).
- Lower Cretaceous sandstones, sealed by Aptian–Albian shales and siltstones.
- To a lesser extent, Upper Cretaceous / Palaeocene carbonates, sealed by cap rocks of Palaeogene shales.

The structural traps are typically anticlinal structures related to Neogene wrench faulting, and the hydrocarbon sources are mainly in the Jurassic, mostly the Lower-Middle Jurassic coal-bearing strata.

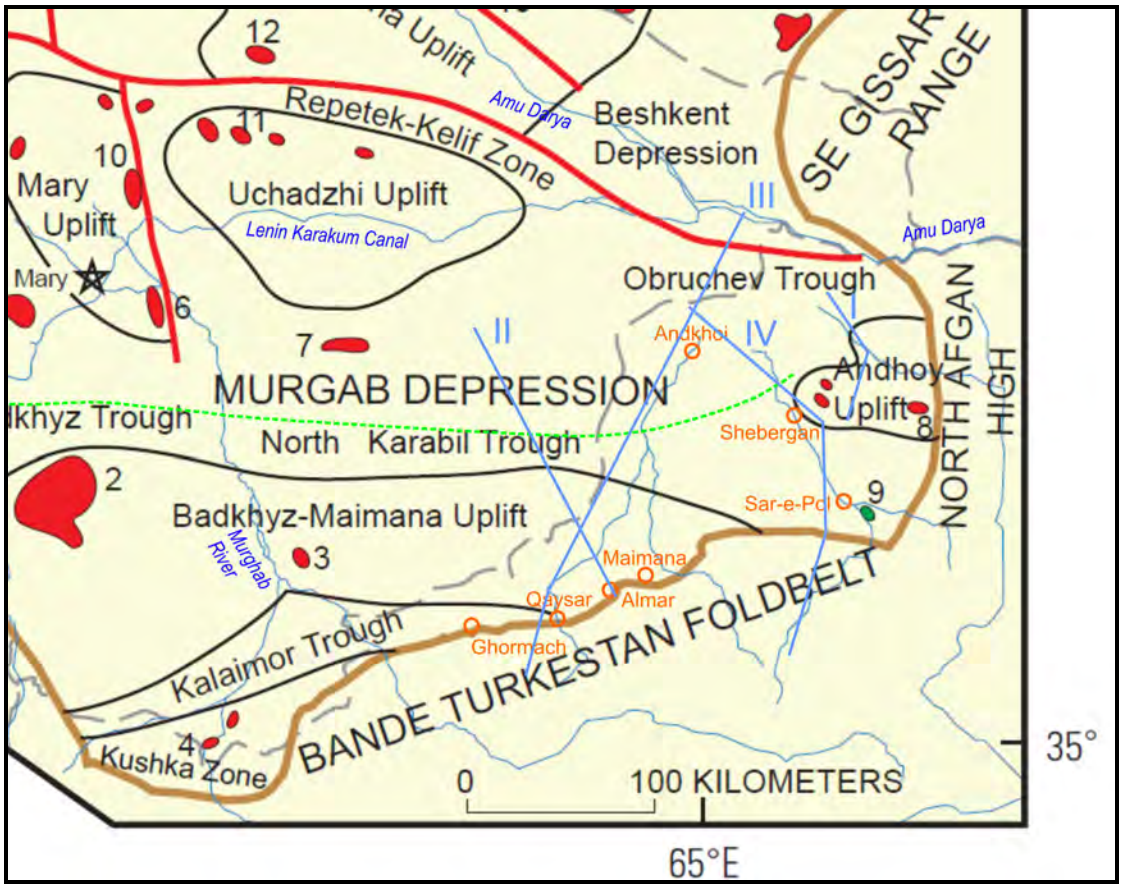

Figure 4.7. Structural map of northern Afghanistan and the Amu Darya basin, showing gas (red) and oil (green) reserves. The boundary of the Murghab-Amu Darya basin is shown as a thick brown line (note that many of the main towns of Faryab - orange circles - lie on the transition from the Band-e Turkestan uplift to the Murghab-Amu Darya depression). 8 = Hodja Gugerdag gas fields, 9 = Angot oil field. The dashed green line shows the pinch-out to the south of the Jurassic Gaurdak Salt Formation. The blueish lines marked I, II, III and IV show the approximate positions of Figures 4.8-4.11. After Ulmishek (2004). *Not believed to be subject to copyright (public domain USGS report).*

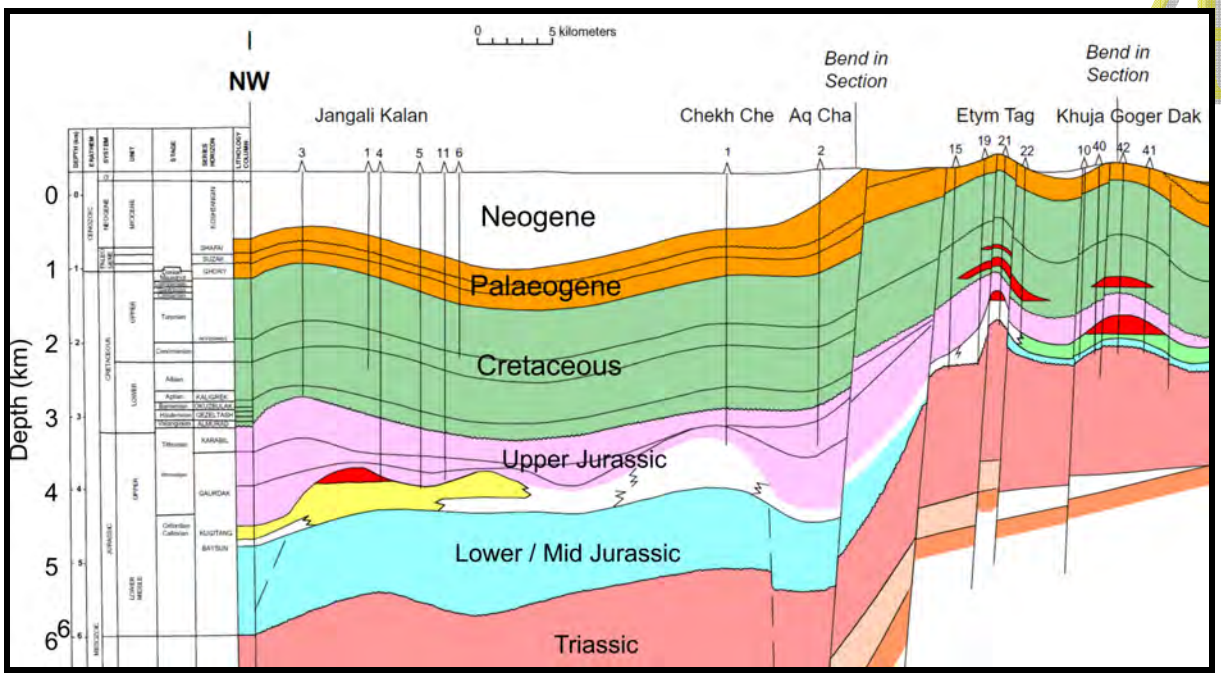

Figure 4.8. Cross-section over the Andkhoi uplift in Jawzjan Province from NW (left) to south (right). Approximate line of cross-section shown as I on Figure 4.7. Modified after Klett et al. (2006). Gas deposits are shown in red. USGS Public domain report, not believed to be subject to copyright.

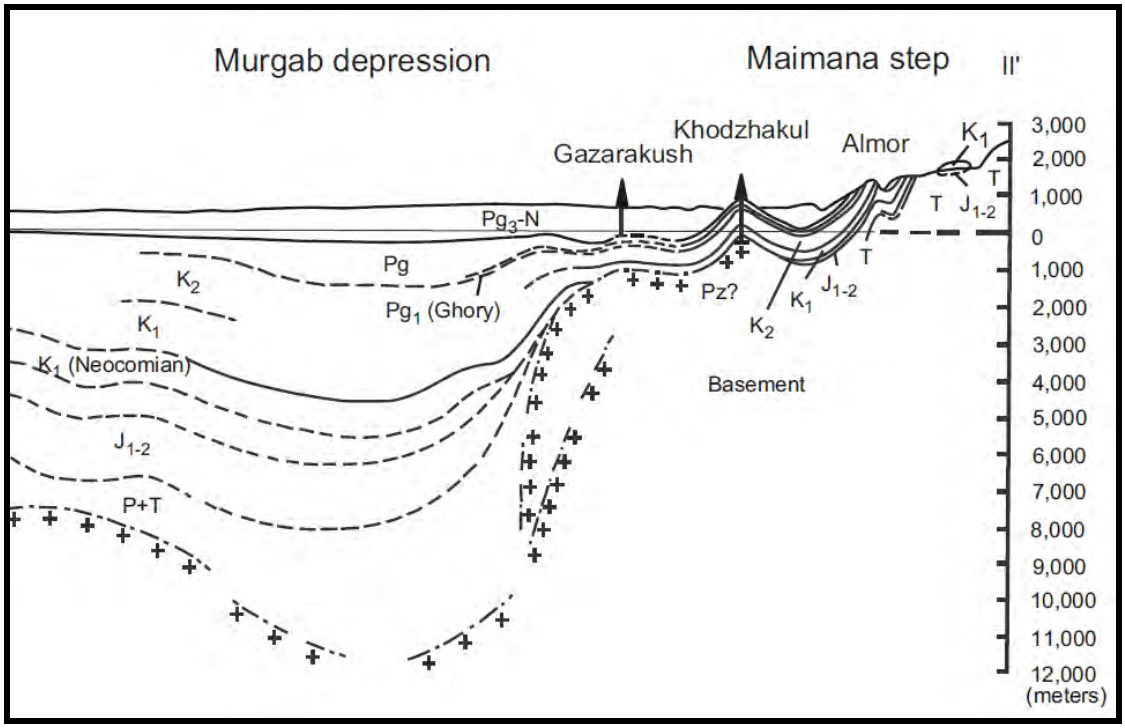

Figure 4.9. Cross-section north-west from Almar (south-east, right) into Turkmenistan (north-west, left). Approximate line of cross-section shown as II on Figure 4.7. After Klett et al. (2006). USGS Public domain report, not believed to be subject to copyright.

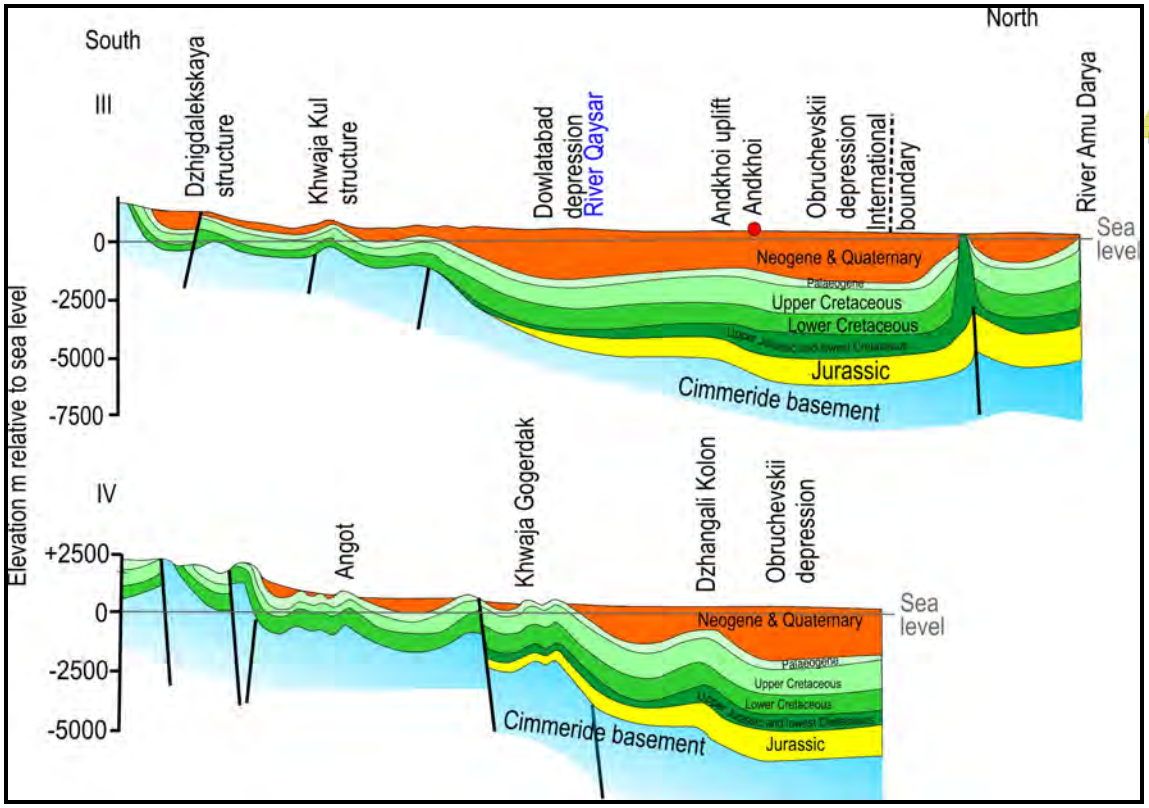

Figure 4.10. Cross-section NNE from the mountains south of Qaysar, through Andkhoi to the Amu Darya. Approximate line of cross-section shown as III on Figure 4.7.

Of Etymological Interest

The name **Band-e Turkestan** means *Boundary wall of Turkestan*. It is the main mountain range of southern Faryab and runs in a west-east direction for 200 km. According to Iranica Online (2014), the summit level (3,200-3,300 m; highest point 3,481 m) probably represents a pre-Miocene erosional, peneplained surface, which was subsequently uplifted during the Himalayan-Alpine orogeny.

The **Paropamisus** refers to the western part of the Hindu Kush range in Afghanistan (including the Siah Koh, Safed Koh, Chalap Dalan, and Malmand ranges). One possible derivation of the name is that it is from the Sanskrit "Para-Vami" - *the excellent and pure city of Vami (Bamyan).*

Flysch - marine clastic sediments, typically deposited as turbidites in a foreland basin of an incipient continental collision. These are often deformed during orogenesis by thrusting.

Molasse - typically coarser sands, conglomerates and shales eroded from a rapidly-rising mountain chain and deposited in the foreland basin. The molasse deposits thus succeed, and may be deposited on top of, flysch. Molasse is typically terrestrial proluvial, alluvial and occasionally lacustrine or shallow marine in nature.

Proluvium - a Soviet geological term used to describe alluvial fan deposits forming as outwash from mountain massifs. "*Proluvium forms alluvial fans and, where they merge, proluvial trains. The texture of the detrital material changes from pebbles and gravel with fanglomerates at the top of the fan to finer, more highly sorted sediments, frequently loess-like loams and sandy loams (proluvial loesses), at the bottom. Proluvium is most fully developed in the foothills of arid and semiarid regions where aleurite-clay sediments (frequently gypsumized and salinized) from flash floods sometimes form on the periphery of the area of proluvium distribution*". The Great Soviet Encyclopaedia (1978).

Takyr - is a shallow depression in a semi-desert area, with a clayey base, that fills with water when it rains. As the accumulated water evaporates, the clayey surface desiccates and fractured crust is formed, often containing filamentous cyanobacteria. Salinisation may develop at or below the surface, typically of gypsum and halite, as accumulated salts are leached out of the soil and concentrated. A saline takyr is often referred to as a **solonchak** (Berg 1950).

Figure 4.11 Geological Map of Faryab Province

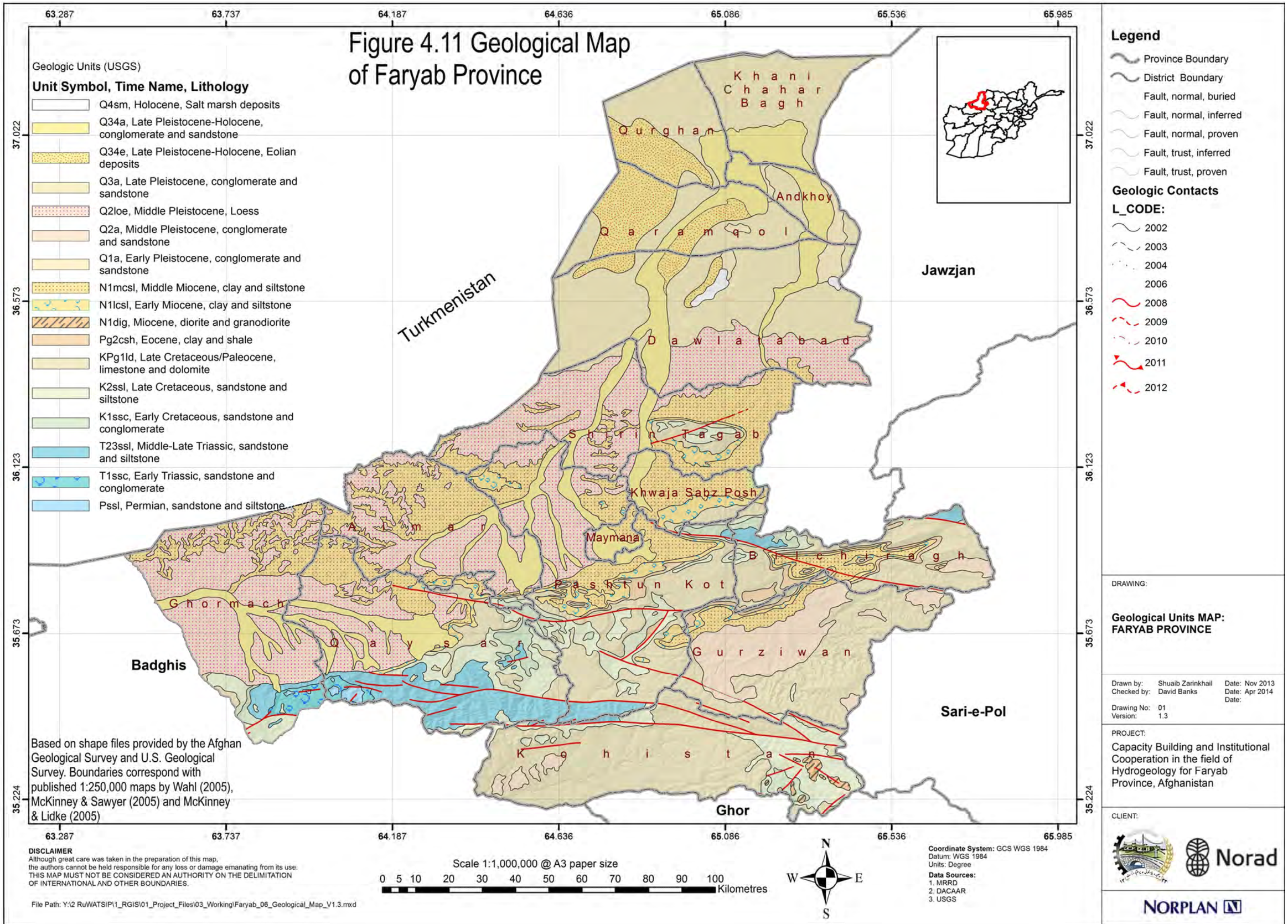

Geologic Units (USGS)

Unit Symbol, Time Name, Lithology

- Q4sm, Holocene, Salt marsh deposits
- Q34a, Late Pleistocene-Holocene, conglomerate and sandstone
- Q34e, Late Pleistocene-Holocene, Eolian deposits
- Q3a, Late Pleistocene, conglomerate and sandstone
- Q2loe, Middle Pleistocene, Loess
- Q2a, Middle Pleistocene, conglomerate and sandstone
- Q1a, Early Pleistocene, conglomerate and sandstone
- N1mcsl, Middle Miocene, clay and siltstone
- N1lcsl, Early Miocene, clay and siltstone
- N1dig, Miocene, diorite and granodiorite
- Pg2csh, Eocene, clay and shale
- KPg1ld, Late Cretaceous/Paleocene, limestone and dolomite
- K2ssl, Late Cretaceous, sandstone and siltstone
- K1ssc, Early Cretaceous, sandstone and conglomerate
- T23ssl, Middle-Late Triassic, sandstone and siltstone
- T1ssc, Early Triassic, sandstone and conglomerate
- Pssl, Permian, sandstone and siltstone

Based on shape files provided by the Afghan Geological Survey and U.S. Geological Survey. Boundaries correspond with published 1:250,000 maps by Wahl (2005), McKinney & Sawyer (2005) and McKinney & Lidke (2005)

Legend

- Province Boundary
- District Boundary
- Fault, normal, buried
- Fault, normal, inferred
- Fault, normal, proven
- Fault, trust, inferred
- Fault, trust, proven

Geologic Contacts

L_CODE:

- 2002
- 2003
- 2004
- 2006
- 2008
- 2009
- 2010
- 2011
- 2012

DISCLAIMER
Although great care was taken in the preparation of this map, the authors cannot be held responsible for any loss or damage emanating from its use. THIS MAP MUST NOT BE CONSIDERED AN AUTHORITY ON THE DELIMITATION OF INTERNATIONAL AND OTHER BOUNDARIES.

File Path: Y:\2 RuWATSIP\1_RGIS\01_Project_Files\03_Working\Faryab_06_Geological_Map_V1.3.mxd

Scale 1:1,000,000 @ A3 paper size

0 5 10 20 30 40 50 60 70 80 90 100 Kilometres

N W E S

Coordinate System: GCS WGS 1984
Datum: WGS 1984
Units: Degree

Data Sources:
1. MRRD
2. DACAAR
3. USGS

DRAWING:

Geological Units MAP: FARYAB PROVINCE

Drawn by:	Shuaib Zarinkhail	Date:	Nov 2013
Checked by:	David Banks	Date:	Apr 2014
		Date:	
Drawing No:	01		
Version:	1.3		

PROJECT:
Capacity Building and Institutional Cooperation in the field of Hydrogeology for Faryab Province, Afghanistan

CLIENT:

Norad

NORPLAN

5. Faryab: Hydrogeology

5.1 Previous hydrogeological maps

A hydrogeological map of Afghanistan was produced in 1977 by Abdullah & Chmyriov (1977a) at a scale of 1:2,000,000. This was accompanied by a map of mineral waters at a scale of 1:2,000,000 (Abdullah & Chmyriov 1977b), and a map of mineral and fresh water springs at a scale of 1:4,000,000 (Abdullah & Chmyriov 1977c).

Prior to this, however, Mishkin (1968) prepared a hydrogeological map of the Quaternary deposits of Northern Afghanistan (Faryab), which was subsequently reproduced in monochrome in Marinova's (1974) "*Hydrogeology of Asia*".

The hydrogeology of areas of Turkmenistan adjacent to Faryab province is discussed and shown in Krizhanovskii (1972).

Most recently, the Chinese Geological Survey (2012) includes the Faryab area in their set of hydrogeological and groundwater resources maps of Asia, broadly compiled according to the Standard International Association of Hydrogeologists' guidelines (Struckmeier & Margat 1995). The Chinese maps are at too coarse a scale to indicate much interesting detail regarding Faryab, however.

5.2 Overview

During the course of 2012-2014 an attempt has been made by the NORPLAN project team to register as many as possible groundwater features in Faryab. This has been performed largely by collating all available existing information - the majority being held by DACAAR. This information was supplemented by rapid field surveys carried out in

- Kohistan
- Bilchiragh
- Gurziwan
- Qaysar
- the area around Maimana Airport
- the four northern districts of Andkhoi, Qurgan, Qaramkol and Khani Chahar Bagh.

Springs

Figure 5.1 shows the distribution of registered springs in Faryab. It will be seen that these are especially abundant in the mountainous districts of Kohistan and Gurziwan, where they are largely derived from the late Cretaceous-Palaeogene limestone aquifer. In the mountain areas of southern Faryab, these springs form the backbone of potable water supply and also provide a valuable baseflow contribution to rivers.

Figure 5.1. Springs of Faryab province and adjacent areas.

Topographic background

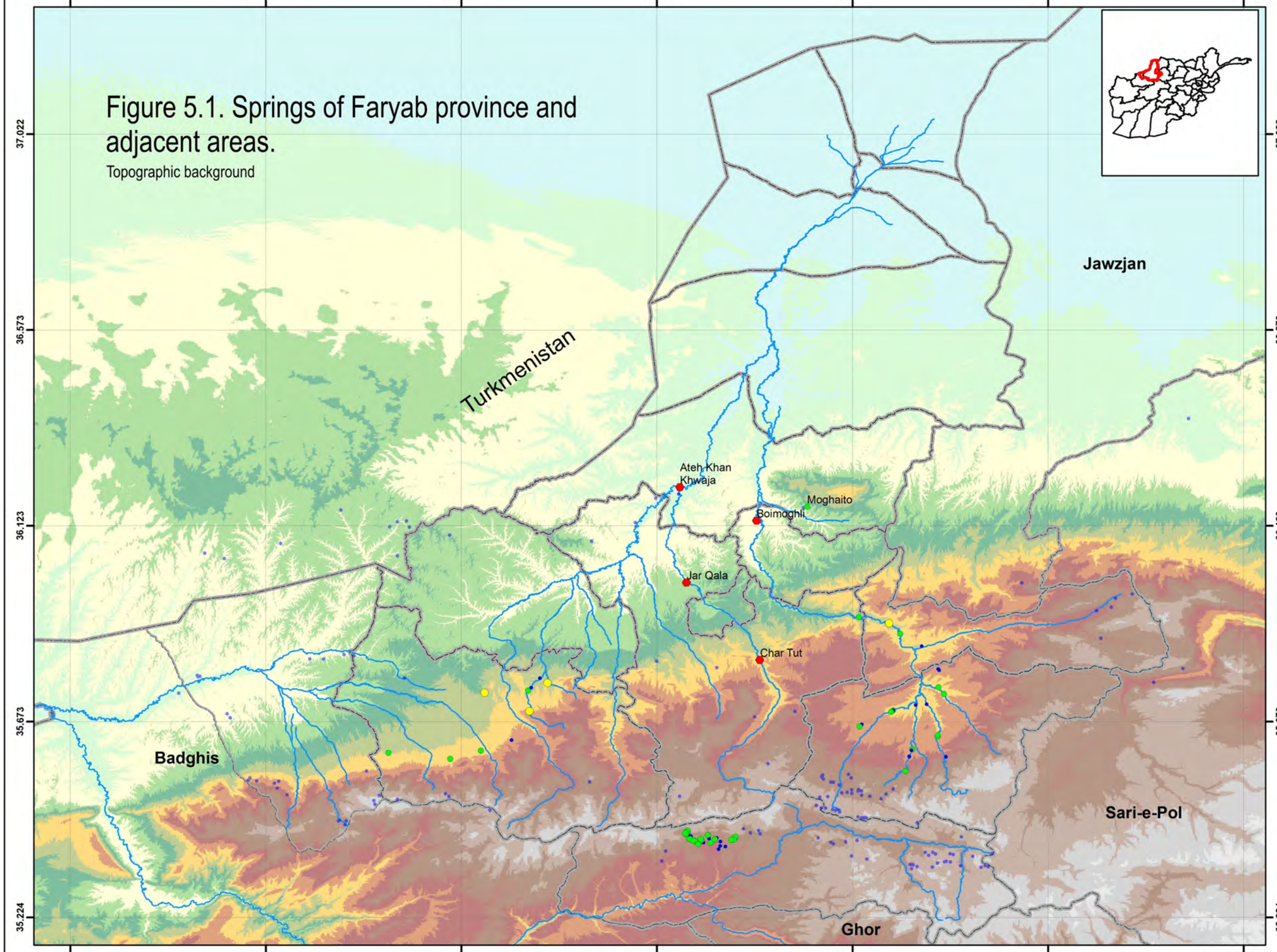

Legend

- Springs with no information
- Springs - discharge < 1 L/s
- Springs - discharge < 5 L/s
- Springs - discharge < 10 L/s
- Springs - discharge < 20 L/s
- Springs - discharge 20 L/s or more
- Rivers
- Province Boundary
- District Boundary

Elevation:

Meters above sea level

- 0 - 430
- 440 - 580
- 590 - 730
- 740 - 850
- 860 - 1,000
- 1,100 - 1,200
- 1,300 - 1,400
- 1,500 - 1,700
- 1,800 - 2,000
- 2,100 - 2,200
- 2,300 - 2,500
- 2,600 - 2,900
- 3,000 - 3,400
- 3,500 - 4,200
- 4,300 - 7,800

DRAWING:

Springs of Faryab and surrounding areas

Drawn by: Shuaib Zarinkhail Date: Apr 2014
Checked by: David Banks Date: Apr 2014

Drawing No: 01
Version: 1.3

PROJECT:

Capacity Building and Institutional Cooperation in the field of Hydrogeology for Faryab Province, Afghanistan

CLIENT:

Norad

NORPLAN

File Path: Y:\2 RuWATSIP\1_RGIS\01_Project_Files\03_Working\forAtlas\Figure 5.1 Springs of Faryab and surrounding areas v1.3.mxd

Coordinate System: GCS WGS 1984
Datum: WGS 1984
Units: Degree

Data Sources:
1. MRRD
2. DACAAR
3. USGS

Scale 1:1,000,000 @ A3 paper size

0 5 10 15 20 25 30 35 Kilometres

N W E S

63.287 63.737 64.187 64.636 65.086 65.536 65.985

37.022 36.573 36.123 35.673 35.224

Geologic Units (USGS)

Unit Symbol, Time Name, Lithology

- Q4sm, Holocene, Salt marsh deposits
- Q34a, Late Pleistocene-Holocene, conglomerate and sandstone
- Q34e, Late Pleistocene-Holocene, Eolian deposits
- Q2a, Middle Pleistocene, conglomerate and sandstone
- Q3a, Late Pleistocene, conglomerate and sandstone
- Q2loe, Middle Pleistocene, Loess
- Q1a, Early Pleistocene, conglomerate and sandstone
- N1mcsl, Middle Miocene, clay and siltstone
- N1lcsl, Early Miocene, clay and siltstone
- N1dig, Miocene, diorite and granodiorite
- Pg2csh, Eocene, clay and shale
- KPg1ld, Late Cretaceous/Paleocene, limestone and dolomite
- K2ssl, Late Cretaceous, sandstone and siltstone
- K1ssc, Early Cretaceous, sandstone and conglomerate
- T23ssl, Middle-Late Triassic, sandstone and siltstone
- T1ssc, Early Triassic, sandstone and conglomerate
- Pssl, Permian, sandstone and siltstone

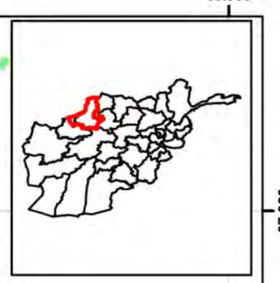

Turkmenistan

Jawzjan

Jalaier (Shor Darya) exploration boreholes

Astana valley exploration boreholes

Kariz Qala OBH

Badghis

Sari-e-Pol

Ghor

Figure 5.2. Wells and boreholes registered in Faryab Province and adjacent areas

Based on shape files provided by the Afghan Geological Survey and U.S. Geological Survey. Boundaries correspond with published 1:250,000 maps by Wahl (2005), McKinney & Sawyer (2005) and McKinney & Lidke (2005)

DISCLAIMER
Although great care was taken in the preparation of this map, the authors cannot be held responsible for any loss or damage emanating from its use. THIS MAP MUST NOT BE CONSIDERED AN AUTHORITY ON THE DELIMITATION OF INTERNATIONAL AND OTHER BOUNDARIES.

File Path: Y:\2 RuWATSIP\1_RGIS\01_Project_Files\03_Working\forAtlas\Figure 5.2 Wells and boreholes of Faryab and Surrounding areas v1.3.mxd

Coordinate System: GCS WGS 1984
Datum: WGS 1984
Units: Degree

Data Sources:
1. MRRD
2. DACAAR
3. USGS

Scale 1:1,000,000 @ A3 paper size

0 5 10 15 20 25 30 35 Kilometres

N W E S

Legend

- Groundwater point (unknown type)
- Drilled borehole
- Dug well
- Exploration borehole
- Observation borehole
- Rivers
- Province Boundary
- District Boundary

DRAWING:

Wells and boreholes of Faryab and Surrounding areas

Drawn by:	Shuaib Zarinkhail	Date:	Apr 2014
Checked by:		Date:	
Authorized by:		Date:	
Drawing No:	01		
Version:	1.3		

PROJECT:

Capacity Building and Institutional Cooperation in the field of Hydrogeology for Faryab Province, Afghanistan

CLIENT:

Norad

NORPLAN

Figure 5.3. A mountain spring in Kohistan emerging from a sedimentary rock sequence. Taken 23rd May 2013 by DACAAR.

Figure 5.4. A spring in a ravine, Qaysar district. Photo by DACAAR, 6th May 2013.

Figure 5.5. Kariz Qala spring emerging from the alluvial plain of the Maimana River in Pashtun Kot district around 10 km NW of Maimana city. Taken 5th May 2013 by DACAAR. The discharge is around 2 L/s of water with an electrical conductivity of 1350 µS/cm.

Boreholes and Dug Wells

Figure 5.2 shows the distribution of registered drilled boreholes and dug wells in Faryab.

Figure 5.6. A dug well in Kohistan district. Photo by DACAAR, 25th May 2013.

Figure 5.7. A dug well in Qaysar district. Photo by DACAAR, 5th May 2013.

Figure 5.8. A dug well in the northern plains area around Andkhoi. Photo by DACAAR, 4th April 2013.

Figure 5.9. Drilling a test borehole in the Astana Valley. Photo by Engineer Hassan Saffi, DACAAR, 8th April 2008.

Karezes

It is reported that karezes were formerly used to provide groundwater for irrigation in Faryab (see Chapter 1.3). During the 2012-14 NORPLAN survey, not a single karez was registered in Faryab.

5.3 Aquifers and aquitards of Faryab

Figure 5.xx shows the hydrogeological map that has been produced as a result of this project, broadly according to the standardised hydrogeological legend of Struckmeier & Margat (1995).

The following succession considers the allocation of each stratigraphic units (based on the digitised 1:250,000 USGS maps of McKinney & Sawyer (2005), McKinney & Lidke (2005) and Wahl (2005).

For many stratigraphical units, the real quantified hydrogeological data are extremely sparse and classification has been allocated on the basis of

- anecdotal evidence from Afghan hydrogeologists.
- hydrogeological evaluation of lithological descriptions.
- information provided in literature, especially from the section of Abdullah & Chmyriov (2008b) dealing with the hydrogeology of Northern Afghanistan, which information is used to supplement the descriptions that follow.

Map legend

The standardised hydrogeological legend of Struckmeier & Margat (1995) is broadly followed, in which

- aquitards / non-aquifers are protrayed in an orange-brown colour
- granular (clastic) aquifers are portayed in a blue colour
- fractured or karstic aquifers are portrayed in a green colour.

For the aquifers, the colours become more intense as the productivity of the aquifer increases. Additionally, in the context of this project:

- cover material, overlying other aquifer strata, but which may not be fully saturated themselves, are coloured grey.

It is very important to realise that **the Hydrogeological Map in Figure 5.xx only provides information about aquifer water productivity and not about water quality or salinity**. I.e. a "good" aquifer can produce saline water!

Pre-Cimmeride basement

Carboniferous-Triassic rocks are exposed largely in the Band-e Turkestan and almost no quantified information exists on their aquifer properties.

- **C_2ls** Late Carboniferous limestones, with subordinate clastic sedimentary and volcanic rocks. Presumed to represent a fractured aquifer of weak to moderate productivity. Colour coding - pale green.
- **Pssl** Permian sandstones and siltstones, with subordinate conglomerates and mudstones. Presumed to represent a fractured aquifer of weak to moderate productivity. Colour coding - pale green.
- **T_1ssc** Early Triassic sandstone and conglomerate, with subordinate volcanics. Presumed to represent a fractured aquifer of weak to moderate productivity. Colour coding - pale green.

- **T_{23}ssl** Middle-Late Triassic sedimentary complex. Fractured, complex aquifer system containing many lithologies, dominated by sandstone and siltstone, with subordinate shale, mudstone, limestone, conglomerate, volcanics. Presumed to represent a fractured aquifer of weak to moderate productivity. Colour coding - pale green.

  Abdullah & Chmyriov (2008b) state that groundwater in the Triassic of the upland areas is limited to sandstones and limestones and springs seldom exceed 1 L/s in discharge. Water is fresh and usually of Ca^{++}-HCO_3^- type (occasionally HCO_3^--$SO_4^=$ or Na^+-$SO_4^=$) Groundwater in the older Palaeozoic strata is broadly of a similar nature.

Post-Cimmeride / pre-Himalayan strata

- Jurassic strata are not exposed in outcrop in Faryab and thus are not designated a shading on the hydrogeological map. They do occur at depth beneath the northern portion of Faryab, however, and permeable sandstones and limestones within the sequence can yield substantial thermal water quantities in deep boreholes.

  For example, Abdullah & Chmyriov (2008b) note that "*Jurassic carbonate rocks with confined waters have been drilled through by deep wells on the Bayangor and Koh-i-Alburs structures* [both of these are anticlinal structures, east of Faryab, associated with the Sheram and Shadian arch structures - see Figure 4.3]*, with the flowing well yields of 0.09 L/s and 350 L/s, respectively. The water is of the chloride-sodium type; its dissolved-solids content ranges from 66 to 78 g/l.*"

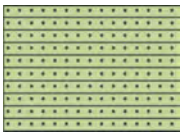

- **K_1ssc** Early Cretaceous sandstone / conglomerate complex. Fractured aquifer capable of supporting moderate spring-flow (may not be perennial). Also occurs at depth below northern part of Faryab province and may provide thermal saline groundwater. Presumed to represent a fractured aquifer of weak to moderate productivity. Colour coding - pale green.

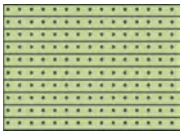

- **K_2ssl** Late Cretaceous sandstone / siltstone complex. Fractured aquifer capable of supporting moderate spring-flow (may not be perennial). Also occurs at depth below northern part of Faryab province and may provide thermal saline groundwater. Presumed to represent a fractured aquifer of weak to moderate productivity. Colour coding - pale green.

  Abdullah & Chmyriov (2008b) confirm that sandstone, conglomerate, limestone and marl strata within the K_1ssc and K_2ssl sequence can function as aquifers, with natural spring discharges in upland areas ranging from several hundredths to 1 L/s and water typically being of calcium-bicarbonate type. As the strata plunge northward beneath later cover, salinity and temperature increases. In the Mazar-e Sharif basin, boreholes can yield substantial quantities of thermal saline water

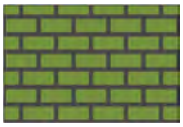

- **KP_1ld** Upper Cretaceous and Palaeocene limestone, dolomite and marl complex. Karst aquifer capable of supporting large perennial springs, providing significant baseflow to river headwaters. Karstic aquifer of strong productivity. Colour coding - medium green.

Abdullah & Chmyriov (2008b) confirm that the Upper Cretaceous-Palaeogene limestone forms a good, freshwater karstified aquifer. Springs from this aquifer often yield 0.1 to 7 L/s, with the possibility of considerably higher yields under favourable conditions. Waters in the upland areas are typically of HCO_3^-, $SO_4^=$-HCO_3^--Ca^{++} and Ca^{++}-Na^+ types, with mineralisations of 0.3 to 0.5 g/L. Abdullah & Chmyriov (2008b) caution, however, that in mountain regions, the highly dissected topography can drain the majority of the aquifer thickness, with springs only occurring at the very base of the aquifer against the boundary with underlying lower permeability rocks. In other words, the saturated aquifer thickness in such regions can be low. They state, "*For instance, in the upper reaches of the Maymana, Balkh and Samangan rivers, the limestone forms steep 300-400m high slopes without a single water manifestation, and it is only at the base that springs can be found discharging as much as 3-5 L/s.*"

Abdullah & Chmyriov (2008b) suggest that the Upper Cretaceous-Palaeogene limestone can retain its aquiifer character as it dips northward below the later cover, with substantial yields being recorded from deep wells. The water becomes increasingly saline however (several g/L) and reducing (H_2S).

- **P_2csh** Eocene clays, shales and siltstones. Presumed to behave predominantly as an aquitard. Local groundwater resources may be associated with minor sandstone / conglomerate / limestone horizons. Colour coding - orange.

<u>Post Orogenic Molasse, Alluvium and Igneous Rocks</u>

- **N_1dig** Miocene diorites, granodiorites and associated igneous rocks. Presumed to contain local occurrences of groundwater associated with fractures zones. Igneous bodies with local productivity only. Colour coding - pale orange.

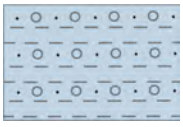

- **N_{1l}csl** Neogene (early Miocene) molasse-type deposits. Red clay and siltstone more abundant than sandstone, conglomerate, limestone. Well yields typically <1-3 L/s. Contains lenses of halite / gypsum and groundwater is often saline. Higher yields and fresher water can sometimes be obtained in valley areas. Designated a granular aquifer of weak productivity. Colour coding pale blue.

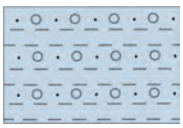

- **N_{1m}csl** Neogene (Mid Miocene) molasse-type deposits. Brown clay and siltstone more abundant than sandstone, conglomerate, limestone. Well yields typically <1-3 L/s. Contains lenses of halite / gypsum and groundwater is often saline. Higher yields and fresher water can sometimes be obtained in valley areas. Designated a granular aquifer of weak productivity. Colour coding pale blue.

  Abdullah & Chmyriov (2008b) appear to confirm that well yields from the Neogene tend to be lower than from recent Quaternary alluvium. They suggest that salinity increases as Neogene aquifers dip northward below the Quaternary cover.

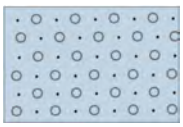

- **Q_1a** Early Pleistocene alluvium. Gravels and sands (sometimes lithified) dominate over silt and clay. Presumed to be less

productive than $Q_{34}a$. Contains predominantly saline water in north of region. Designated a granular aquifer of weak productivity. Colour coding pale blue.

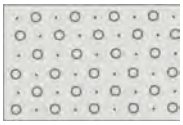

- **Q_2a (?)** Gravels and sands (sometimes lithified) dominate over silt and clay. Occurs at high elevations in south of area as a cover deposit overlying Cretaceous / Palaeogene and Neogene aquifers. It is not known whether it contains saturated portions and if it constitutes an aquifer in its own right. Either **Q_2a** mid-Pleistocene alluvium or **$Q_{34}t$** late-Peistocene-recent glacial till. Designated a granular cover material. Colour coding - pale grey.

- **Q_2loe** Pleistocene loess. Poor aquifer, silty and often yielding saline water. Where saturated, can support small yields from dug wells and is used by nomads in the Shor Darya area. Designated a granular aquifer of very weak productivity. Colour coding very pale blue.

  Of the loess aquifer, Abdullah & Chmyriov (2008b) state that yields of dug wells can be 0.1 to 0.4 L/s, while "*In the Qaysar and Maymana valleys, many ascension springs are observed at the foots of coniform hills built up of loess. Their discharges vary between 0.01 and 6.6 L/s.*" The salinity of loess waters is often very high, however, typically 5-10 g/L, with a range from 0.8 to 20.3 g/L and a sulphate-chloride-sodium-calcium type.

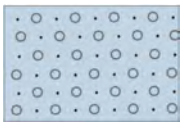

- **Q_3a** Late Pleistocene alluvium. Gravels and sands (sometimes lithified) dominate over silt and clay. Presumed to be less productive than $Q_{34}a$. Contains predominantly saline water in north of region. Designated a granular aquifer of weak productivity. Colour coding pale blue.

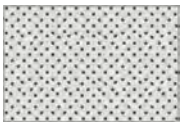

- **$Q_{34}e$** Late Pleistocene-recent aeolian sands. Occurs as cover deposits over alluvial plains in north of region. Not known if aeolian deposits contain saturated portions. Designated a granular cover material. Colour coding - pale grey.

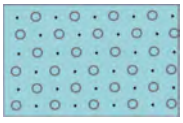

- **$Q_{34}a$** Late Pleistocene-recent Quaternary alluvium south of Pata Baba. Gravels and sands (sometimes lithified) dominate over silt and clay. Coarser grained and more productive south of confluence with Shor Darya. Individual boreholes can produce 10 L/s or more. Here, designated a granular aquifer of moderate productivity. Colour coding medium blue.

  Of this aquifer, Abdullah & Chmyriov (2008b) say, "*The ground water of the Maymana Valley occurs in sand and coarse gravel found at a depth from 3.5 to 67 m. The depth to water table varies between 16.6 and 21.0 m. The specific yield of the wells ranges from 3.5 to 4.0 l/s.".* The water is of a HCO_3^--$SO_4^=$-Na^+-Ca^{++} chemical type, mineralisation 0.7 - 0.9 g/L and temperature 16 - 17°C.

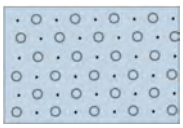

- **$Q_{34}a$** Late Pleistocene-recent Quaternary alluvium north of Pata Baba. Less productive, finer grained and containing saline groundwater towards the north. Here, designated a granular aquifer of weak productivity. Colour coding pale blue.

  Of this aquifer, Abdullah & Chmyriov (2008b) imply that in the northern areas of Shirin Tagab, Darreh-i Siyah and Balkh deltas,

groundwater can be found in sand layers with thick clayey-sandy sequences. They state that *"the specific yields* [without quite explaining what a "specific yield" is] *of the wells range from 1.2 to 3.7 L/s; the yield of the dug wells are from 0.1 to 0.7 L/s."* The water is reported as saline, with mineralisations 3-10 g/L and usually of sodium-sulphate character. Abdullah & Chmyriov (2008b) specifically state that "*Small lenses of sulphate and bicarbonate-sulphate-magnesium-calcium waters having the dissolved solids content from 1 to 3 g/L were tapped near irrigation canals and river channels*".

- **Q_4sm** Recent Quaternary salt marsh deposits. Coloured white.

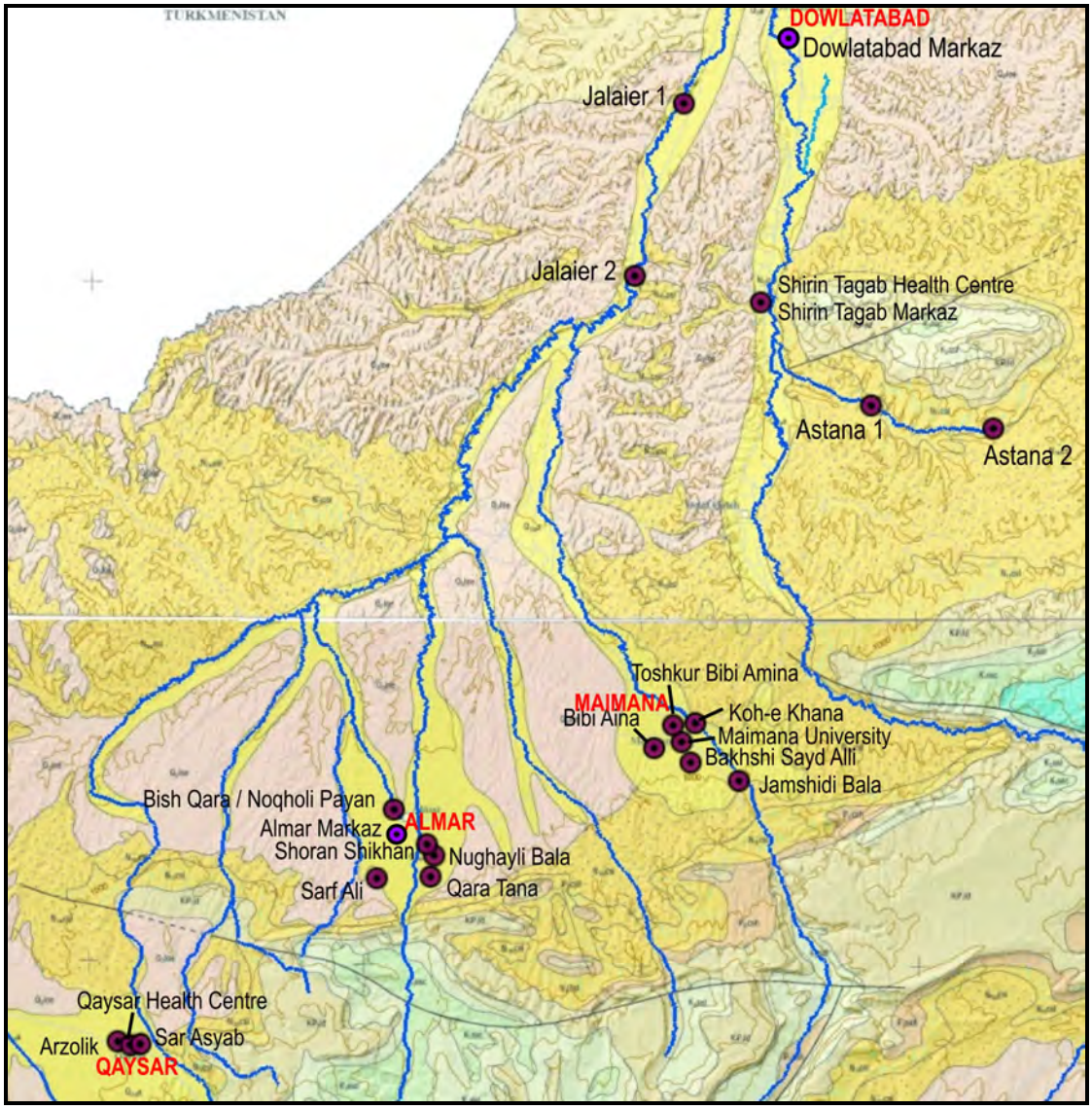

Figure 5.10. Geological map of Faryab, showing the locations of test-pumped boreholes. Background is formed by AGS/USGS 1:250,000 maps **by** McKinney & Sawyer (2005) and Wahl (2005).

5.4 Aquifer Properties in Faryab

Very few wells or boreholes have any yield data associated with them in Faryab. Even fewer have any form of test pumping data - of those, in no case is the test pumping data of adequate quality to permit any form of reliable interpretation using, for example Theis or Cooper-Jacob analysis.

In several cases, a yield (Q) figure is associated with a drawdown (s) and a pumping test duration. These boreholes are shown on Figure 5.1. This permits us to apply the Logan Approximation to estimate aquifer transmissivity (T). The Logan Approximation can be stated (Misstear et al. 2006) as:

$T = (Q/s) * 1.22$ for hydraulically ideal wells

$T = (Q/s) * 2$ for real "inefficient" wells

where T is in m^2/d, Q is in m^3/d and s is in m.

The results of these calculations are shown in Table 5.1, as "high" and "low" estimates of transmissivity, calculated from the above expressions. It should be recognised that, in no case does the transmissivity value calculated represent the transmissivity of the entire aquifer sequence, nor even the transmissivity of the Quaternary / Neogene sequence. It merely represents the transmissivity of the aquifer strata hydraulically accessible to the well.

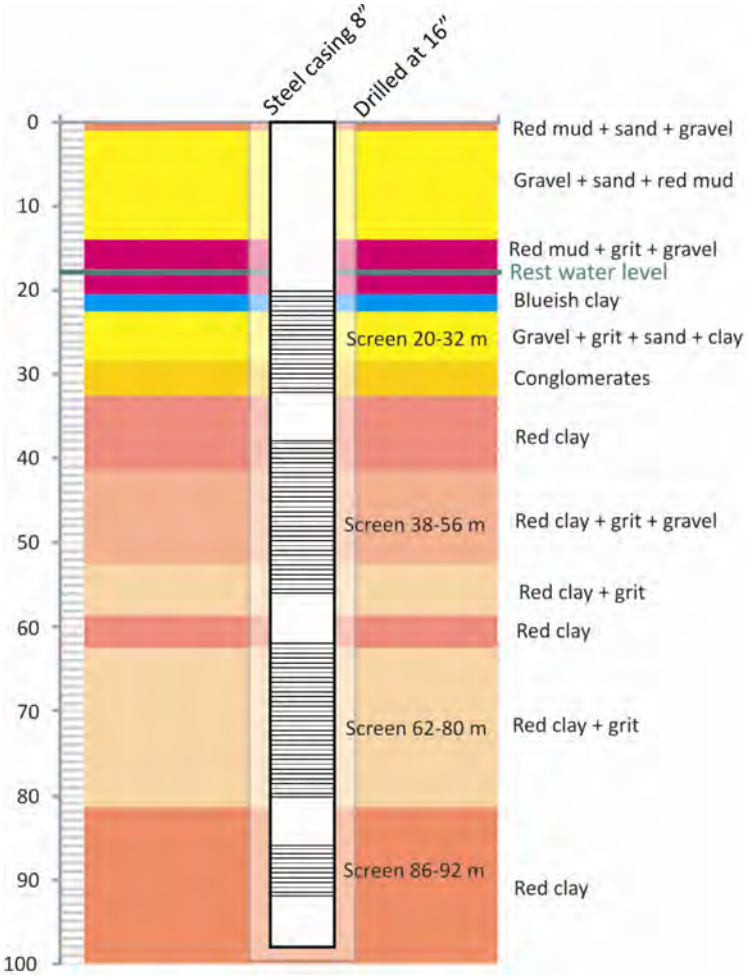

Figure 5.11. Borehole construction log for Koh-e Khana test well, District 1, Maimana city.

Table 5.1. Boreholes in Faryab with pumping / drawdown data. Transmissivity range estimated by Logan approximation. * = transmissivity very low (pump dry); $ = approximate grid reference only. SWL = static water level.

Borehole	Aquifer	Depth	Diameter	Date	SWL	Yield *Q*	Yield *Q*	Drawdown *s*	Duration	*T* (high)	*T* (low)
		m	mm		m bwt	L/s	m3/d	m	hr	m²/d	m²/d
Qaysar area											
Arzolik borehole		145	152	05/03/2008	91.4	4	346	13.6	8	51	31
Qaysar Health Centre$		104	254	31/03/1979	78.72		86	3.5	8	49	30
Sar Asyab borehole		150	152	04/03/2008	27.5	5	432	15.2	4	57	35
Almar area											
Sarf Ali borehole		160	152	01/06/2010	134.2	2.77	239	Pump dry	0.22	*	*
Qara Tana borehole		150	152	01/06/2010	87.1	2.9	251	Pump dry	0.27	*	*
Nughayli Bala borehole		150	152	06/03/2008	101	3	259	19	6	27	17
Shoran Shikhan borehole		150	152	03/06/2010	105	1.85	160	25	5	13	8
Almar Markaz (Centre)$	Quaternary	66	152	Aug-75	52	0.7	60	6		20	12
Bish Qara / Noqholi Payan borehole		122	152	29/05/2010	83.7	3.5	302	15.3	15	40	24
Maimana area											
Jamshidy Bala borehole	Neogene	92	203	18/03/2012	26.8	3.5	302	34.3	6	18	11
Bakhshi Sayd Alli borehole	Neogene	118	203	16/07/2012	61.8	2.5	216	47.32	7	9	6
Maimana University borehole	Quaternary	90	203	30/11/2011	41	0.7	60	1.5	6	81	49
NCA Maimana (Koh-e Khana) test borehole	Quaternary	98	203	16/10/2011	20.3		864	6.7	24	258	157
Bibi Aina borehole	Quaternary (some Neogene)	204	254	30/06/2008	65	8	691	6	5	230	141
Toshkur Bibi Amina (Maimana District)$		74	254	24/06/1979	50		216	0.7	13	617	376
Further north											
Shirin Tagab Health Centre$		42	203	21/06/1978	21.5		121	3.8	20	64	39
Shirin Tagab Markaz (Centre)$	Quaternary	41	203	Feb-75	22.9	5	432	1.32	5	655	399
Astana 1 deep bore (Mahad)	Neogene	200	152	08/09/2009	10	2	173	13	7	27	16
Astana 2 deep bore (Gul Qudoq)	Neogene	200	152	09/11/2009	9	1.5	130	121	0.73	2.1	1.3
Jalaier 1 deep bore (Chokazie village)	Neogene	200	152	24/12/2009	23	4	346	11.1	8.5	62	38
Jalaier 2 deep bore (Atomchi village)	Neogene	200	152	07/02/2010	16.7	0.75	65	129.1	6	1.0	0.6
Dowlatabad Markaz (Centre), borehole 2$	Quaternary	42	152	1976	13	5	432	6	19	144	88

For most of the boreholes in Table 5.1, it is reasonable to assume that the borehole has been installed with well-screen in the most transmissive portions of the aquifer (see a diagram of the Maimana University borehole construction in Figure 5.2) and thus that the calculated transmissivity represents the transmissivity of the saturated section of strata penetrated by the well.

The transmissivities of the Quaternary aquifer system range from several hundred m^2/d in northern Maymana (Bibi Aina, Toshkur Bibi Amina, Koh-e Khana) and the Shirin Tagab valley, down to a few tens of m^2/d around Qaysar and Almar. In an international perspective these transmissivities would probably be regarded as low to moderate.

In the desert of Turkmenistan, the 82.7 m deep Soviet borehole 182 (see Figure 8.1; Krizhanovskii, 1972) yielded 0.91 L/s for a drawdown of 1.61 m from Quaternary strata (static water level 26.9 m bgl). This indicates a transmissivity of 60-98 m^2/d.

For the Neogene, the transmissivities are even lower, ranging from around 1 m^2/d to 40-60 m^2/d.

In Table 5.2, the estimated transmissivity values have been divided by saturated depth to result in a very approximate estimate of depth-averaged hydraulic conductivity (permeability).

	Aquifer	T (high)	T (low)	Saturated depth	K (high)	K (low)
		m^2/d	m^2/d	m	m/d	m/d
Qaysar area						
Arzolik borehole		51	31	53.6	0.9	0.6
Qaysar Health Centre		49	30	25.28	2.0	1.2
Sar Asyab borehole		57	35	122.5	0.5	0.3
Almar area						
Sarf Ali borehole		*	*	25.8	*	*
Qara Tana borehole		*	*	62.9	*	*
Nughayli Bala borehole		27	17	49	0.6	0.3
Shoran Shikhan borehole		13	8	45	0.3	0.17
Almar Markaz (Centre)	Quaternary	20	12	14	1.4	0.9
Bish Qara and Noqholi Payan borehole		40	24	38.3	1.0	0.6
Maimana area						
Jamshidi Bala borehole	Neogene	18	11	65.2	0.3	0.16
Bakhshi Sayd Alli borehole	Neogene	9	6	56.2	0.16	0.10
Maimana University borehole	Quaternary	81	49	49	1.6	1.0
NCA Maimana (Koh-e Khana) test borehole	Quaternary	258	157	77.7	3.3	2.0
Bibi Aina borehole	Quaternary (some Neogene)	230	141	139	1.7	1.0
Toshkur Bibi Amina		617	376	24	25.7	15.7
Further north						
Shirin Tagab Health Centre		64	39	20.5	3.1	1.9
Shirin Tagab Markaz (Centre)	Quaternary	655	399	18.1	36.2	22.1
Astana 1 deep bore (Mahad)	Neogene	27	16	190	0.14	0.09
Astana 2 deep bore (Gul Qudoq)	Neogene	2.1	1.3	191	0.01	0.01
Jalaier 1 deep bore (Chokazie village)	Neogene	62	38	177	0.4	0.21
Jalaier 2 deep bore (Atomchi village)	Neogene	1.0	0.6	183.3	0.005	0.003
Dowlatabad Markaz (Centre), bore 2	Quaternary	144	88	29	5.0	3.0

Table 5.2. Boreholes in Faryab with pumping / drawdown data. Transmissivity range estimated by Logan approximation. * = transmissivity very low (pump dry).

It is important to remember that the saturated portion of the geological section will contain a range of strata of different permeabilities, aquitards and aquifers. Thus, this arithmetic average hydraulic conductivity will grossly underestimate the hydraulic conductivity of the most permeable horizons. In shallower boreholes, the saturated section is more likely to dominated by a specific sand/gravel aquifer, resulting in a high average hydraulic conductivity

Estimates of average hydraulic conductivity of the sequences fall in the range 1-3 m/d for northern Maimana, and in the shallower strata of the Toshkur Bibi Amina borehole it is in the range 15-26 m/d.

In the Quaternary strata of the Shirin Tagab valley, estimates of average hydraulic conductivity of the sequences are also >1.9 m/d, and in the shallower strata of the Shirin Tagab Markaz borehole it is in the range 22-36 m/d.

The aquifers in Qaysar and Almar appear to have typical average conductivities of <1.2 m/d, while the Neogene aquifers return typical average conductivities of <0.2 m/d.

Of Etymological Interest

Aquifer: From the Latin *aqua* (water) and *ferre* (to carry). This term denotes a geological body or stratum with sufficient transmissivity(or hydraulic conductivity) and storage to permit the economic abstraction of groundwater. Note that (1) in arid areas, groundwater is scarcer and has higher "value", thus the threshold for designating a stratum an aquifer may be lower; (2) the definition says nothing about the use of the water or the water quality.

Aquitard: From the Latin *aqua* (water) and *tardus* (slow). The opposite of an aquifer. This term denotes a geological body or stratum with **insufficient** transmissivity and storage to permit the economic abstraction of groundwater. This designation does not imply that the stratum is impermeable, however.

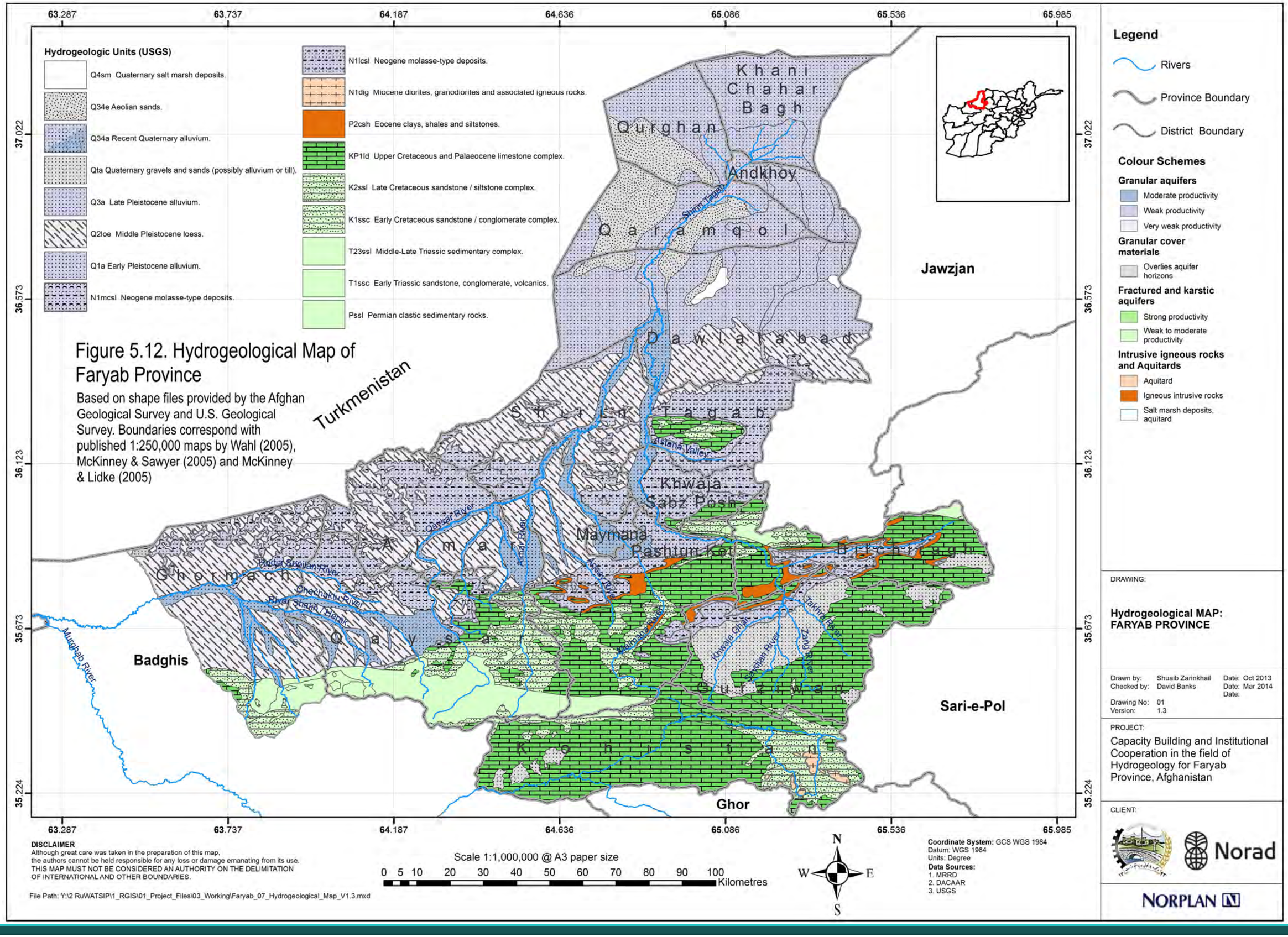

Figure 5.12. Hydrogeological Map of Faryab Province

Based on shape files provided by the Afghan Geological Survey and U.S. Geological Survey. Boundaries correspond with published 1:250,000 maps by Wahl (2005), McKinney & Sawyer (2005) and McKinney & Lidke (2005)

6. Faryab: Groundwater Levels and Flow

6.1 Regional Groundwater Flow

Abdullah & Chmyriov (1977b) discuss the regional groundwater flow in the North Afghanistan basin as a whole. In a hydrogeological basin, it is normal to experience downward head gradients in areas where recharge is dominant (mountain areas) and upward head gradients where discharge is dominant (heads increase with depth, often leading to artesian heads at depth).

Deep strata

Across the northern plains of Faryab, artesian conditions are reported in boreholes drilled through the Quaternary/Neogene succession into the underlying Palaeogene/Cretaceous and Jurassic aquifer horizons.

According to Abdullah & Chmyriov (1977b), in the deep Cretaceous and Jurassic strata (potentially oil-bearing), formation pressures decrease to the north, away from the Band-e Turkestan.

In the Upper Jurassic / Hauterivian aquifer / oil reservoir systems, Abdullah & Chmyriov (1977b) argue that fresher recharge water from the foothills of the Band-e Turkestan is gradually displacing fossil marine (connate) sedimentation water from the aquifers. Where this has happen to a large extent, the water has a sodium bicarbonate nature, with relatively low mineralization, grading into higher mineralization water of sodium sulphate waters and eventually calcium chloride bribes (50-150 g/L mineralization). In the higher Aptian/Albian/Cenomanian reservoir strata, lower permeabilities mean that displacement of brines by fresher water has not taken place to such an extent. Unhelpfully, Abdullah & Chmyriov (1977b) do not define what they mean by a low mineralization.

The main discharge area for the deep aquifers is believed by Abdullah & Chmyriov (1977b) to be the Khwaja Mod saline lake, which occupies a graben and whose west shore appears to follow a fault line.

Abdullah & Chmyriov (1977b) suggest that the uppermost (Quaternary) aquifer system is disconnected from deeper artesian aquifers. They note that, even on the plains "the Quaternary aquifer system is recharged by surface waters."

6.2 Mishkin's (1968) Map

Mishkin's (1968) map of the Quaternary aquifer system of the northern Afghanistan plains reveals a pattern of declining groundwater head contours towards the north. The contours are typically convex northwards along the line of the Shirin Tagab river, suggesting that the river is recharging the aquifer system. Mishkin also maps zones of fresher groundwater along the river valleys, underlining this interpretation.

Figure 6.1 shows Mishkin's (1968) contours superimposed on the geological map of Wahl (2005). A limited number of flow lines have been drawn on the map. The map suggests that the Khwaja Mod saline lake operates as a local focus for groundwater discharge from the Quaternary aquifer system, as well as possibly the deeper aquifers (see above).

Furthermore, the contours suggest that groundwater flow in the Quaternary aquifer system does not discharge towards the Amu Darya, but rather to the Zeid depression or towards the Kelif Uzboy depression in Turkmenistan to the NW. Indeed, the map

suggests that there is a component of groundwater flow *from* the Amu Darya towards the Zeid depression.

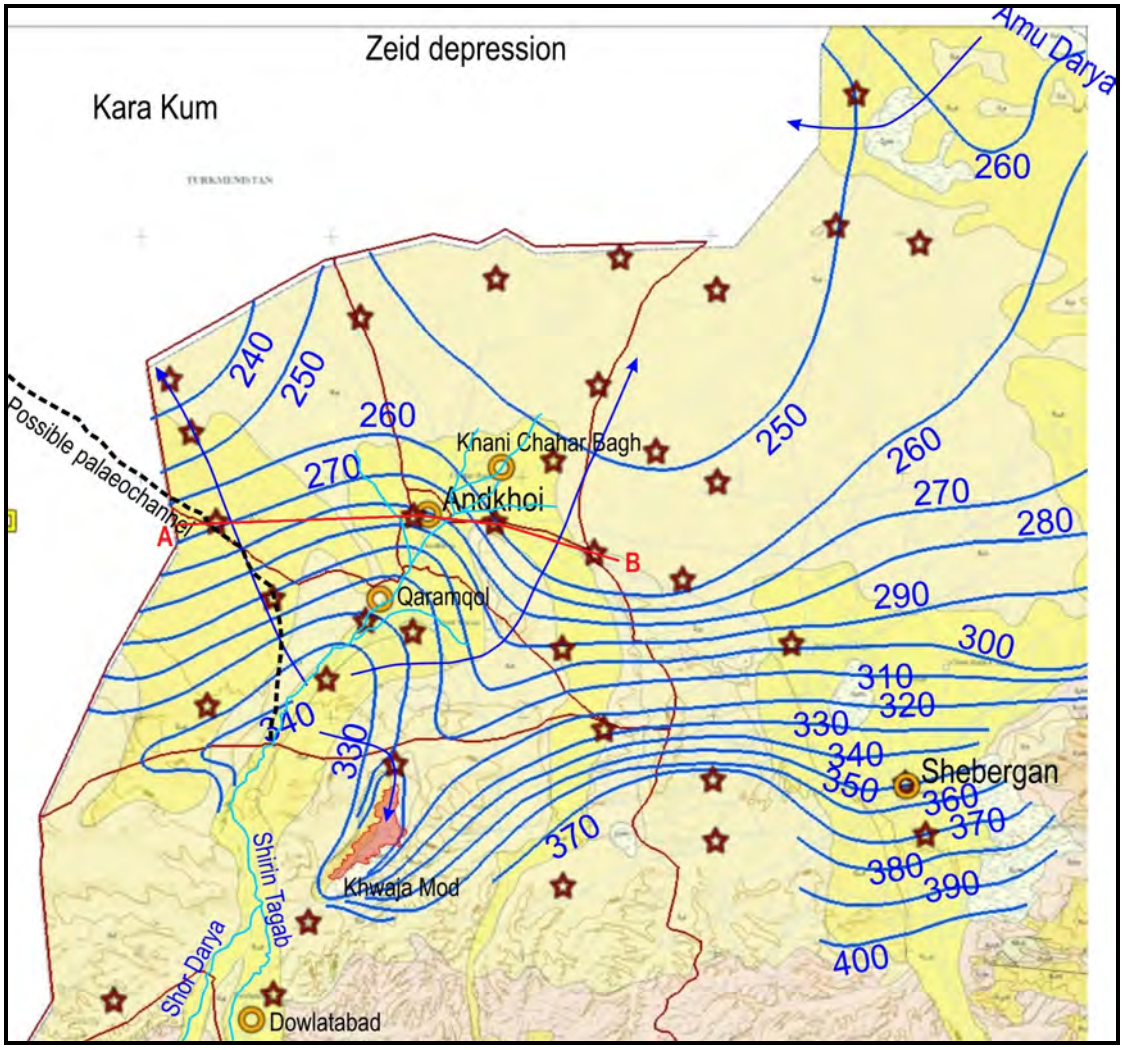

Figure 6.1. Mishkin's (1968) contours of groundwater head in the Quaternary aquifer system of Faryab, superimposed on the geological map of Wahl (2005). Groundwater flow lines and rivers are added in blue. Red stars show the locations of the wells and boreholes Mishkin used to calibrate his map. The red line A-B shows the line of the Andkhoi cross-section in Figure 6.8. The dashed black line shows a topographic depression which may be a palaeochannel of the Shirin Tagab.

6.3 Groundwater level map

Figure 6.2 shows the static groundwater, as measured in wells and boreholes registered in NORPLAN's project database. The data are kriged, but the kriged shading is restricted to a radius of within 5 km of the nearest "real" data point. This is because the vast majority of boreholes and wells occur within the valleys of the main rivers (Figure 5.1) and data from these cannot be extrapolated to higher-elevation interfluve areas, where there is no data and where the groundwater level may be much deeper.

The map indicates that, in the main river valleys, groundwater level is typically in the range 20-40 m below ground level (m bgl). This, in turn, implies that:

- there is a general tendency for rivers to recharge the aquifer by infiltration (thus losing water).
- the groundwater gradient broadly follows the topography from south to north along these valleys.

Also, in general, in the southern portions of the main valleys, towards the mountain foothills, (e.g. Gurziwan, Pashtun Kot), the groundwater level is generally somewhat deeper. This reaches an extreme situation in the Qaysar and Almar areas, where depth to groundwater may exceed 50 m and can even reach depths of over 100 m below ground level (Nughayli Bala and Shoran Shikhan boreholes).

To explore the relationship between topography, depth to groundwater and surface watercourses, four characteristic sections will be explored subsequently:

- in the southern part of the Quaternary valley fill aquifer, in Almar area
- across the Maimana River, near Maimana Airport
- across the Shirin Tagab River, near Islam Qala
- in the Shirin Tagab delta / northern plains area, near Andkhoi.

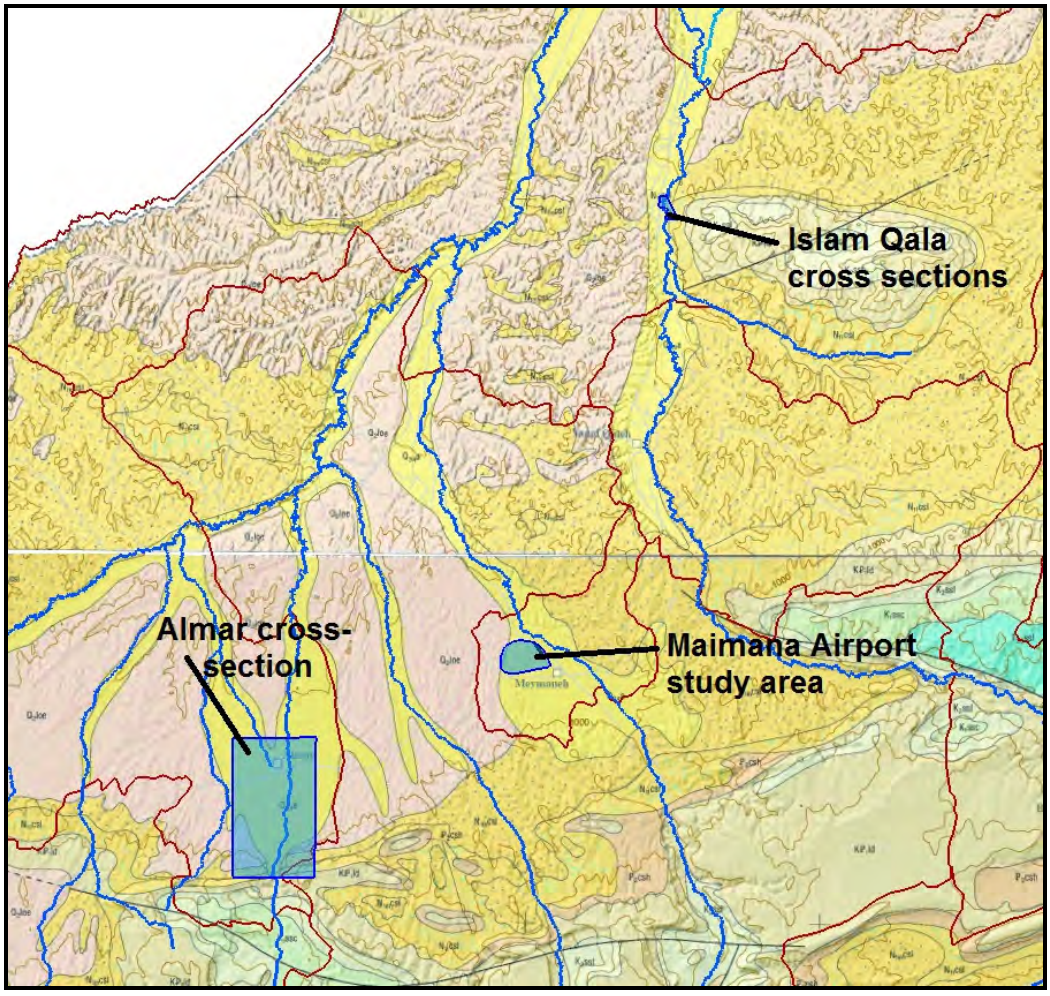

Figure 6.2. Locations of the Almar, Maimana Airport and Islam Qala cross-sections discussed in this chapter. Superimposed on the 1:250,000 scale geological maps of Wahl (2005) and McKinney & Sawyer (2005), published by the Afghan Geological Survey and US Geological Survey and believed to be public domain.

6.4 Almar section

Figure 6.3 shows the location of the section, encompassing the area where the Almar River emerges from the foothills of the Band-e Turkestan through a gorge (1000-970 m asl) onto alluvial terrain. As the river transits from the hilly Mesozoic and Terrain onto the alluvial area it has historically deposited (and continues to do so) huge amounts of eroded sands, gravels, silts and clays as alluvial fans ("proluvial deposits" in Russian terminology). The river Almar has a braided, branching and rejoining, character in this section. This river morphology is characteristic of either a high sediment load, or a high terrain slope (caused by the build-up of sediment in the alluvial fans) or both.

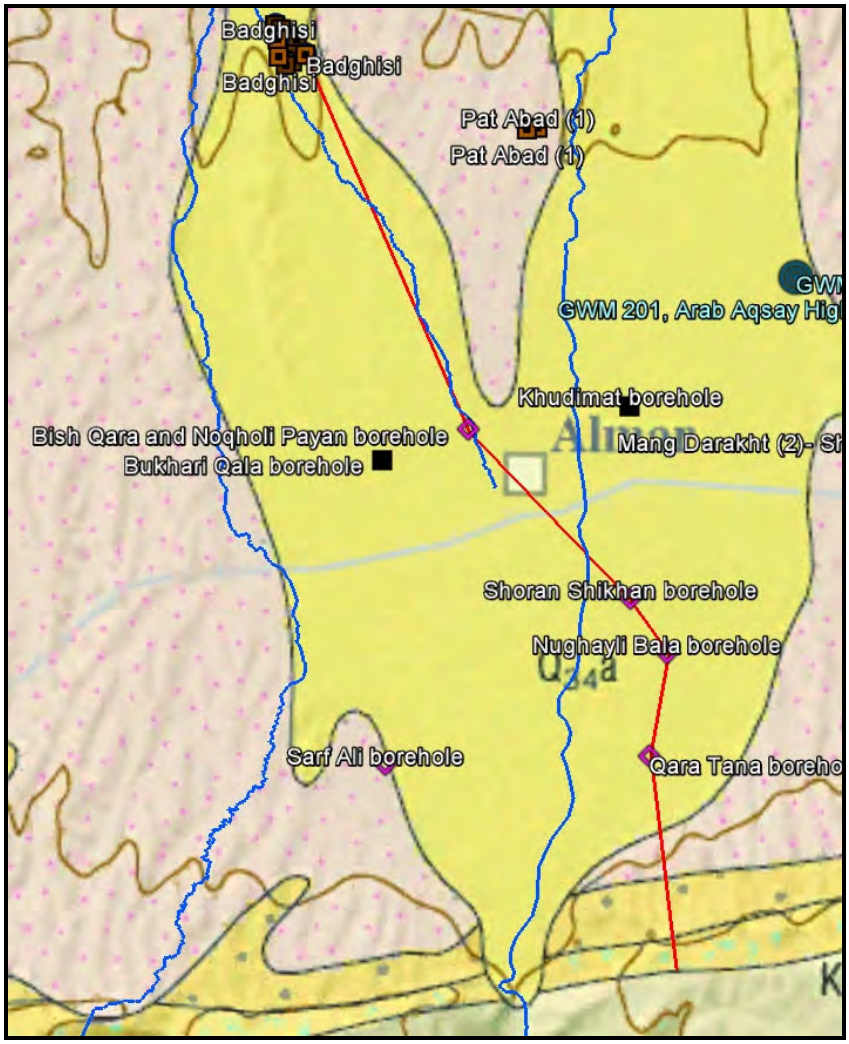

Figure 6.3. Line of cross-section in Figure 6.4, in Almar area, superimposed on the geological map of McKinney & Sawyer (2005), published by the USGS and believed to be public domain. See Figure 6.2 for location.

The sediment deposited as the rivers emerge from the mountains is generally relatively coarse (high content of sands and gravels) and the river water is thus able to infiltrate from the river into the alluvial deposits.

Figure 6.4 shows the south-north section from the Almar gorge to Badghisy. It clearly shows that:

- The groundwater gradient is from south to north, as one would expect. There is no mysterious "depression" in the groundwater levels corresponding to the high depth to groundwater!

- The groundwater gradient is relatively low (presumably due to the aquifer's coarse nature and high transmissivity).
- The topographic gradient is relatively high, due to the alluvial fan / braided river morphology.
- Thus, the terrain slopes more steeply than the water table. Thus, the depth to water table increases to the south (exceeding 100 m in places). The great depth to water table is thus *not* due to "low" groundwater levels, but rather due to "high" surface topography in these areas. To the north of the section, the depth to groundwater is around 30-40 m bgl.
- The water table is always below the level of the surface watercourses. There is thus a tendency for the rivers to infiltrate into the aquifer (although infiltration may be restricted by the generally clayey silty nature of the overbank sediments in the uppermost portions of the borehole logs.

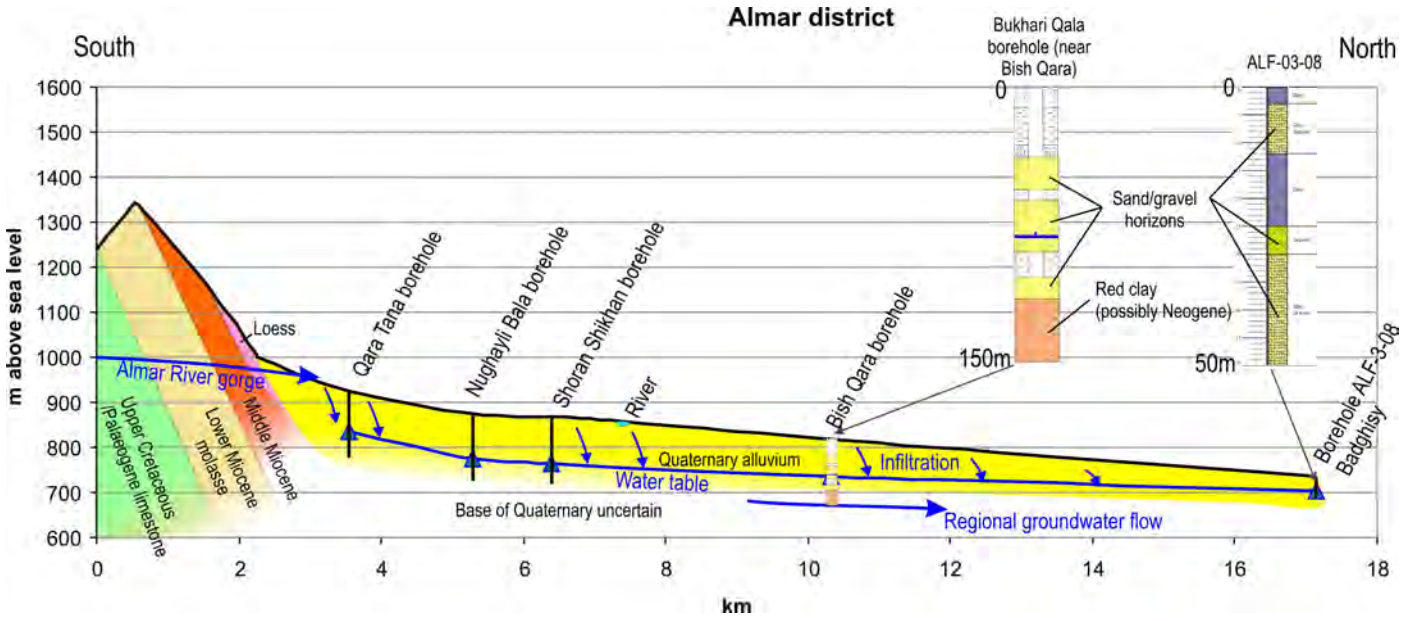

Figure 6.3. South-north section in Almar district (as indicated in Figure 6.2). The Almar river emerges from the mountains in a gorge at 100-970 m asl. The Bukhari Qala borehole (whose section is shown) is located slightly off the section, but is relatively close to Bish Qara borehole.

6.5 Maimana Airport section

An area to the north-west of Maimana city has been designated as a study area by NORPLAN - shown in blue in Figure 6.4. It occupies a flat alluvial plain, , underlain by significant thicknesses of Quaternary sand and gravel ,sloping gently from around 850 m asl in the west to around 830 m asl in the east, towards the Maimana River.

The study area contains several inhabited villages, especially in the west, of which the largest is Torpakhtu. The study area is largely occupied by agricultural land. The published Afghan Geological Survey / USGS maps show that the plain is underlain by Quaternary alluvial deposits of the Maimana River. These are described as:

- $Q_{34}a$ - Conglomerate and sandstone (Holocene and late Pleistocene) - Alluvium: shingly and detrital sediments, gravel, sand more abundant than silt and clay.

These alluvial deposits are underlain at unknown depth by Neogene sediments (and possibly also by loess), described as

- N_{1m}csl - Clay and siltstone (middle Miocene) - Brown clay, siltstone more abundant than sandstone, conglomerate, limestone.

Groundwater levels typically range from 40 m below ground level in the extreme west of the study area to around 30 m bgl in the east. It should be noted that this appears to be below the level of the Maimana River, suggesting:

1) There is a degree of discontinuity between river and aquifer

2) The River is likely to be infiltrating water into the ground.

The majority of boreholes drilled in the area yield groundwater of moderate electrical conductivity (1200 - 2000 µS/cm), implying a slightly brackish water quality. In the extreme SW of the area, higher conductivities of 2300-3600 µS/cm occur.

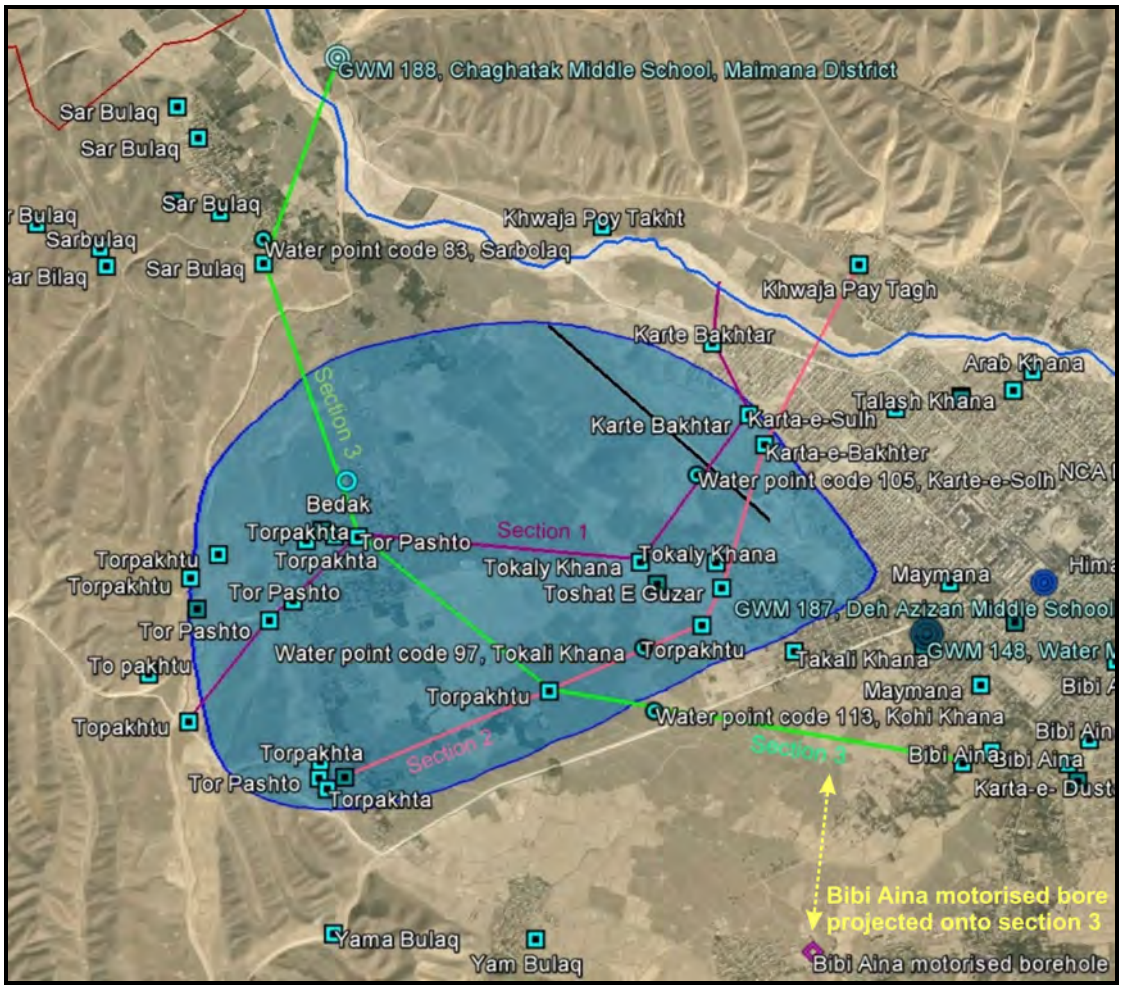

Figure 6.4. Maimana Airport (1.6 km long runway shown as black line) viewed in Google Earth, showing locations of selected drilled boreholes, and the River Maimana as a blue line. The purple, pink and green lines show the cross-sections in Figure 6.5. Note the Bibi Aina motorised borehole towards the bottom right of the map, projected onto the line of cross-section 3. North is up the page.

Cross section 1 suggests that, below the study area there is an initial clayey layer of thickness < 20 m. The origin of this layer is uncertain, but it may be a combination of overbank sediments and reworked wind/blown material. It is underlain by a substantial

gravelly/sandy aquifer unit, whose base has not been proved but which appears to be at least 30-40 m thick (saturated and unsaturated total thickness). This appears to disappear towards the Maimana River east, to be replaced by clayey sediments (at least within the depth range of 50-60 m penetrated by the boreholes).

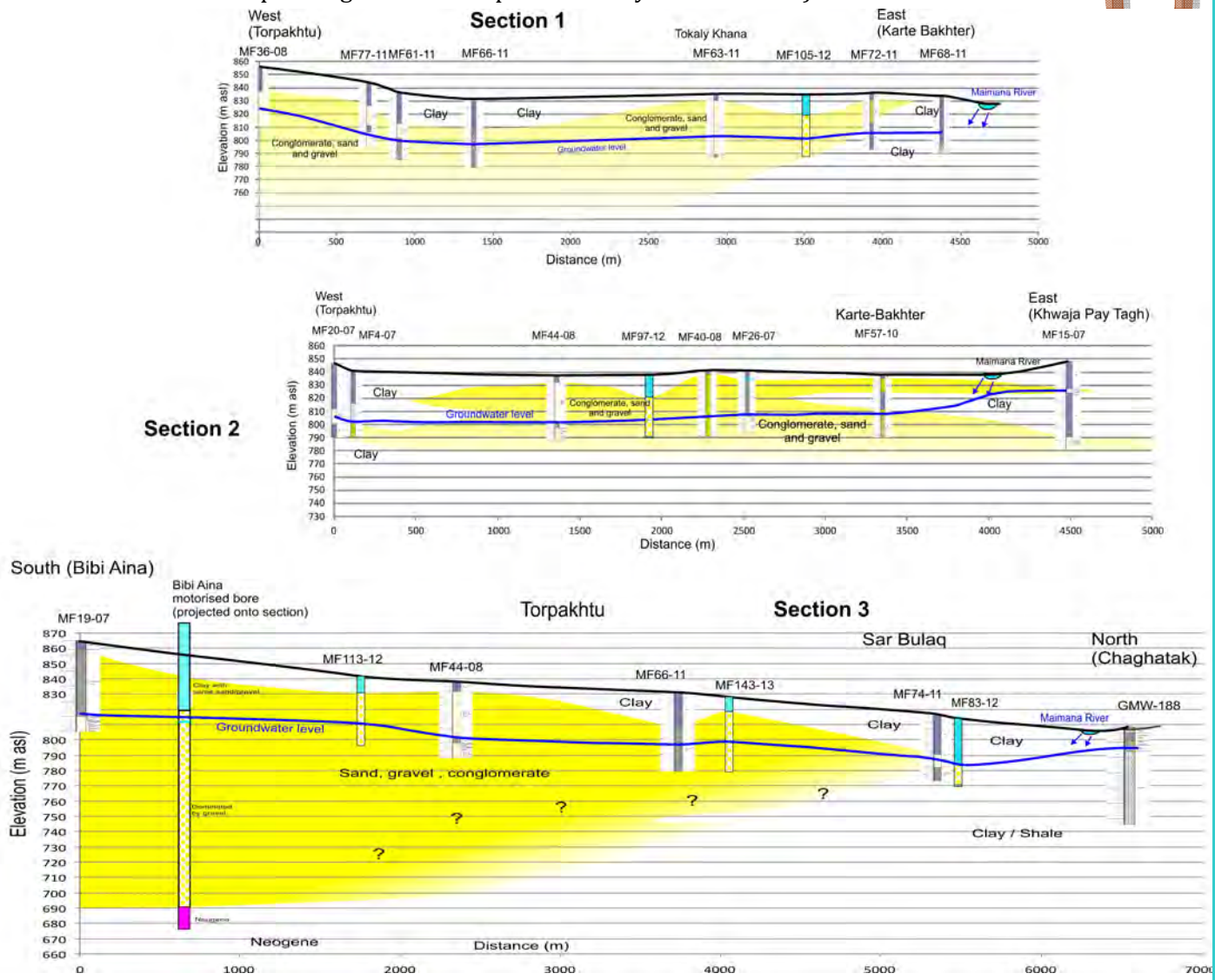

Figure 6.5. Cross-sections 1, 2 and 3, as marked on Figure 6.4, showing the relationships of the sandy/gravelly alluvial aquifer (shaded yellow) and the water table (blur line) to the surface and the Maimana River.

The groundwater level is around 30 m below ground level and appears to be below the elevation of the Maimana River, suggesting:

1) There is a degree of discontinuity between river and aquifer

2) The River is likely to be infiltrating water into the ground.

However, the sediments in the vicinity of the river are generally clayey, so the degree of river infiltration to the aquifer is likely to be rather limited.

Lack of good terrain elevation data renders the following observation very tentative, but it appears there is a slight slope of the groundwater level surface away from the Maimana River over much of the section, again suggesting an infiltrating river regime.

The second east-west cross-section, Cross-section 2 broadly supports the findings of cross-section 1.

Cross-section 3 is broadly is north-south. The 200 m deep Bibi Aina production borehole, supplying water to a piped network in Maimana, and test pumped at 8 L/s with only 6 m drawdown (specific capacity 115 m2/d, likely transmissivity around 200 m2/d (Table 5.1), with hydraulic conductivity between 1 and 1.7 m/d on average (Table 5.2)) is projected onto the cross section (although it lies some distance to the south of the section - see Figure 6.4). The Bibi Aina borehole encountered clayey dominated strata with some gravels to 56 m depth, then a gravel aquifer to 185 m (at least 129 m good aquifer thickness, of which 120 m is saturated). At 185 m depth, the borehole encountered lower permeability Neogene deposits (although there is some debate amongst hydrogeologists regarding where the Quaternary - Neogene boundary is located in the borehole).

Cross section 3 also confirms that groundwater levels are below the level of the River Maimana. Despite being disconnected from the River, they do have a gentle, broadly south-to-north gradient, confirming that the general direction of groundwater flow follows the topography from south to north.

Finally, the gravel aquifer seems to peter out (at least, at shallow depth) towards the River, in the region of Sar Bulaq, being replaced by clayey / shaley strata. The aquifer does not seem to extend, at shallow depth, to the eastern bank of the Maimana River.

In conclusion, there appears to exist a substantial aquifer storage of moderately fresh to brackish groundwater below the study area in a Quaternary alluvial sand/gravel/conglomerate unit of thickness at least 30-40 m. If the Bibi Aina borehole is representative of the Maimana Airport study area (including the rather tentative depth to Neogene), then the aquifer thickness could be in excess of 100 m. The aquifer's indicative transmissivity at Bibi Aina is around 200 m^2/d. The aquifer is overlain by clayey sediments ranging in thickness from a few metres to around 20 m.

The aquifer is generally unconfined with groundwater levels typically a little over 30 m bgl in shallow boreholes.

The river-aquifer system seems to be characterised by downward vertical head gradients, with the Maimana River seemingly disconnected from regional groundwater heads and presumably with a tendency to infiltrate river water into the ground.

BUT the source of recharge to the aquifer is not clear.

- The climate (and the clayey overburden) means that opportunities for direct recharge are very limited.
- The aquifer tends to be separated from the Maimana River by lower permeability clayey materials.

Thus, a large question mark must be placed over the ultimately sustainability of a major groundwater abstraction from this aquifer.

6.6 *Islam Qala (Shirin Tagab) section*

The third examples of hydrogeological cross-sections are taken across the Shirin Tagab River, near the settlement of Islam Qala in the southern part of Shirin Tagab district.

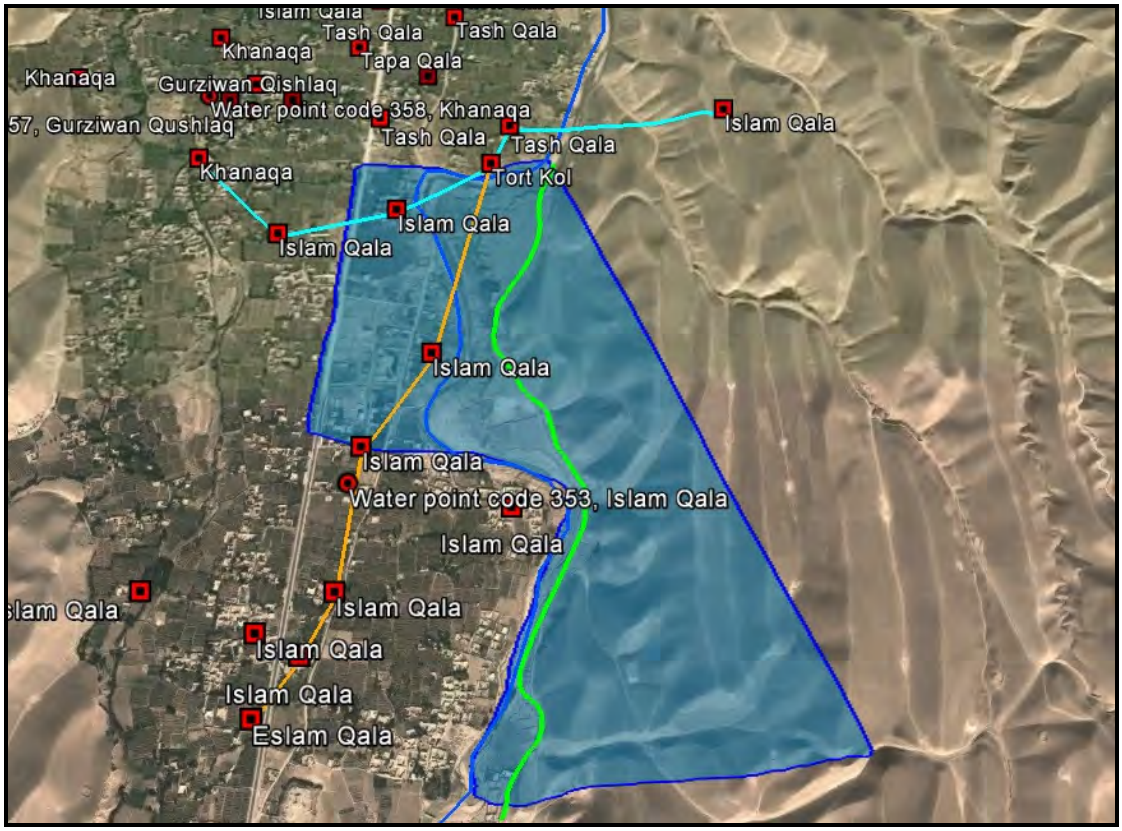

Figure 6.6. Location of Shirin Tagab study area (powered by Google Earth). The blue line shows the Shirin Tagab River, flowing north. The green line shows the edge of the alluvial plain and the boundary with the Neogene scarp. Water boreholes are shown as red dots and squares. Pale blue line = cross-section 1; orange line = cross-section 2.

The study area straddles the valley bottom of the Shirin Tagab river, at around 520 m asl. To the east of the study area, the terrain rises, as hills underlain by Neogene sedimentary rocks, to above 600 m asl. The valley bottom contains habitation (the diffuse village of Islam Qala) and irrigated fields. The Neogene hilly terrain is largely uninhabited and appears uncultivated.

The published Afghan Geological Survey / USGS map show that the valley floor is underlain by Quaternary alluvial deposits of the Shirin Tagab River. These are descried as:

- **Q34a - Conglomerate and sandstone (Holocene and late Pleistocene)** - Alluvium: shingly and detrital sediments, gravel, sand more abundant than silt and clay.

These alluvial deposits are underlain at presumed relatively shallow depth by Neogene sediments, which also outcrop as hilly terrain in the east of the study area. These are described as

- **N1lcsl - Clay and siltstone (early Miocene**) - Red clay, siltstone more abundant than sandstone, conglomerate, limestone

There are a number of registered drilled boreholes in the area. Groundwater levels in the valley floor typically range from 20-30 m below ground level. It should be noted that this appears to be below the level of the Shirin Tagab River.

There is a considerable amount of data on groundwater electrical conductivity within the study area. The groundwater appears to have a variable, but generally high, electrical conductivity, in the range 1800 - 4000 µS/cm.

Two hydrogeological cross-sections have been drawn across the study area, as shown on Figure 6.6.

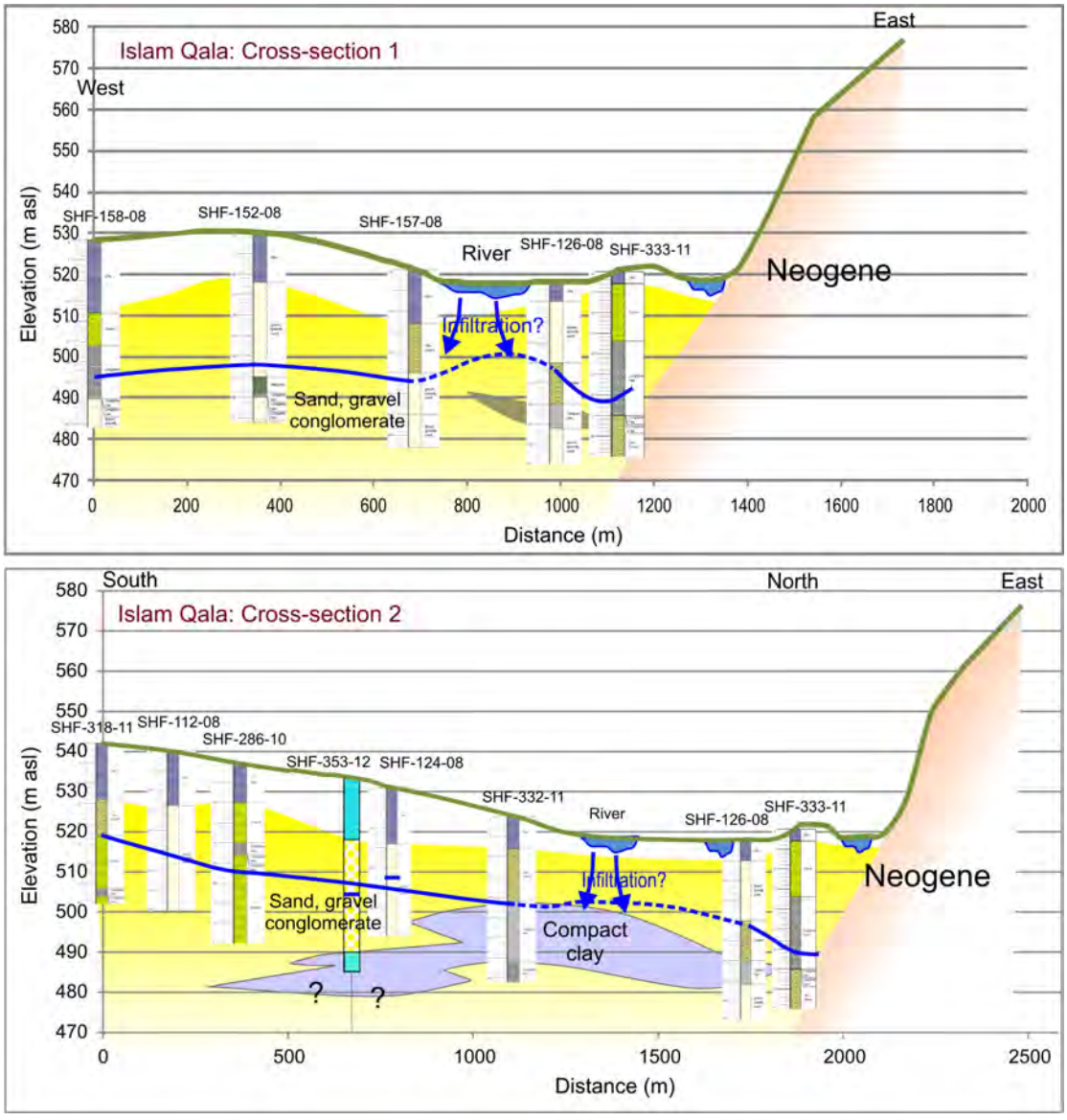

Figure 6.7. Cross-sections 1 and 2, as marked on Figure 6.6, showing the relationships of the sandy/gravelly alluvial aquifer (shaded yellow) and the water table (blur line) to the surface and the Shirin Tagab river. The unshaded surficial layer is clay/silt.

Cross section 1, approximately west-east, suggests that, below the study area, there is an initial clayey layer of thickness 3-18 m, underlain by a substantial sandy-gravel / conglomerate aquifer unit, whose base has not been proved but which appears to be at least 30-40 m thick (saturated and unsaturated total thickness). In no borehole has the top of the Neogene been unequivocally identified, despite its presumed outcrop in the east of the study area.

The groundwater level is around 20-30 m below ground level, at an elevation of 490-500 m asl. It thus appears to be at least 20 m below the elevation of the Shirin Tagab River.

- There is a degree of discontinuity between River and aquifer
- The River is likely to be infiltrating water into the ground.

However, the sediments in the vicinity of the river are generally clayey in their upper portion, so the degree of river infiltration to the aquifer may possibly be limited.

The second, south-north **cross-section 2** broadly supports the findings of cross-section 1. It confirms, however, that there is a groundwater hydraulic gradient along the course of the Shirin Tagab valley from south to north, with heads falling from +520 m asl to less than +500 m asl.

Two old pumped abstraction wells have formerly been drilled in the Shirin Tagab area (although it is likely that they were somewhat north of this study area). They suggest that yields in the range 2 to 12 L/s might be expected from this aquifer, with drawdowns of 5-7 m.

- Shirin Tagab Health Centre: Aquifer = 33 m thick. Drilled to 50 m but only completed to 42 m. Rest water level = 21.5 m below well top. Test pumped at 1.4 L/s with 3.8 m drawdown after 20 hrs. Optimum yield judged to be 2.6 L/s with 6.9 m drawdown. Electrical conductivity = 850 µS/cm. Constructed by cable tool methods 10/6/1978 to 21/6/1978. No exact grid reference given. Information from old Dari handwritten table from MRRD
- Shirin Tagab Markaz (Centre): Drilled to 43 m but only completed to 41 m. German PVC screen 2.0 mm slots. Aquifer = 16.9 m of sand, gravel, cobbles. Rest water level = 22.2 m below well top; Electrical conductivity = 1650 µS/cm. Tested at 5 L/s for 5 hrs with 1.32 m drawdown. Optimal yield calculated as 11.8 L/s with 5.3 m drawdown. Constructed by cable tool method in Feb 1975. No exact grid reference given. (Information from Radojicic, 1978). An older handwritten Dari summary suggests that the rest water level on completion was 22.9 m bgl, not 22.2 m bgl.

In conclusion, there appears to exist a substantial aquifer storage of brackish groundwater below the study area in a Quaternary alluvial sand/gravel/conglomerate unit of thickness at least 30-40 m, of which we know that at least 10-20 m are saturated. The aquifer is overlain by clayey sediments ranging in thickness from a few metres to around 18m.

The aquifer is believed to be underlain by Neogene lower permeability materials at unknown depth. None of the boreholes in the area have unequivocally encountered Neogene and nothing is conclusively known about their hydraulic properties.

The aquifer is generally unconfined with groundwater levels typically 20- 30 m bgl in shallow boreholes. In an east-west orientation (perpendicular to the River) there is no clear hydraulic gradient on the water table. There is, however, a clear north-south hydraulic gradient down the River valley, indicating the groundwater flow in the Quaternary alluvial aquifer is generally northwards.

The aquifer system seems to be characterised by downward vertical head gradients, with the Shirin Tagab River seemingly disconnected from regional groundwater heads and presumably with a tendency to infiltrate river water into the ground.

The climate (and the clayey overburden) means that opportunities for direct recharge are very limited. The clayey overburden may also hinder indirect recharge by infiltration from the river. Thus, a large question mark must be placed over the ultimate sustainability of a major groundwater abstraction from this aquifer.

6.7 *Andkhoi cross- section*

The cross-section through Andkhoi is taken from Mishkin's (1968) map, and the reproduction thereof in Marinova (1974). The line of the cross-section is shown in Figure 6.1.

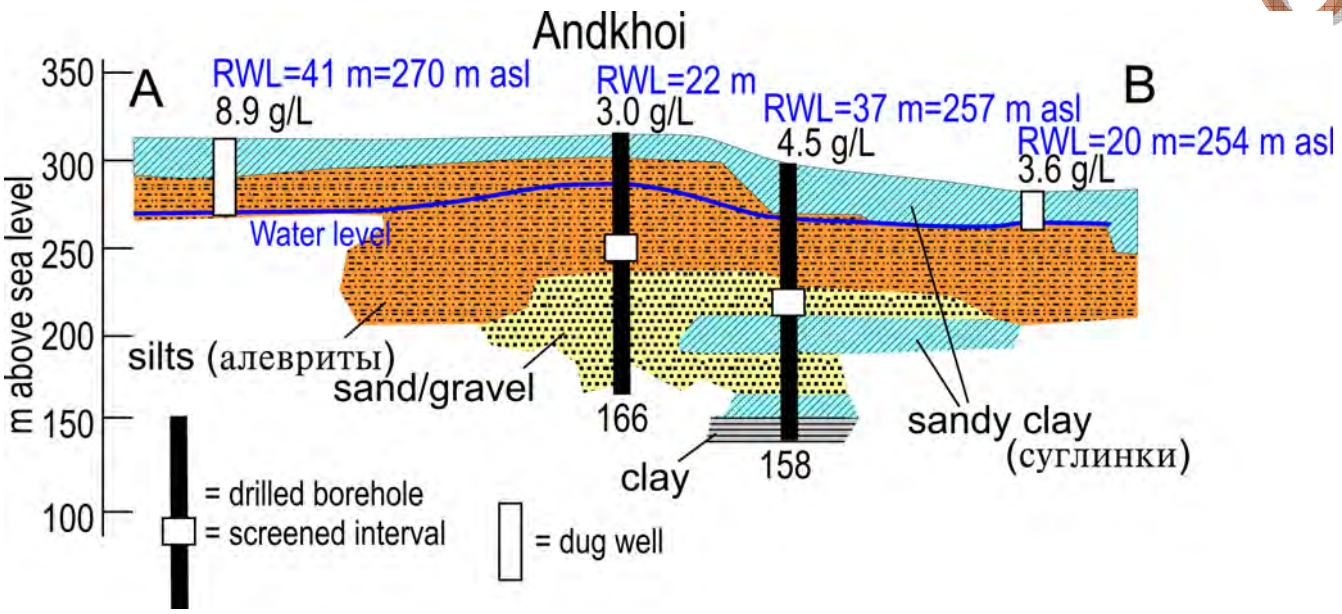

Figure 6.8. West (A) to east (B) section through Andkhoi, from the map if Mishkin (1968) and reproduced by Marinova (1974). RWL = rest (static) ground water level (m below ground level), converted also to m above sea level (m asl). The figure given as g/L is the total mineralization of the water from the dug well or screened interval of the borehole. For the two drilled boreholes, the figure at the base of the well is the depth in m.

The section shows that the ground level in Andkhoi is around 310-320 m asl. The static groundwater level in the deep borehole in the north of Andkhoi (where the well-screen is placed around 60 m down) is around 22 m bgl. This correspond with more recent data from dug wells collected during the 2013 survey, where groundwater levels in Andkhoi and the region immediately north of Andkhoi were typically 15-25 m bgl.

In the top 60-70 m of the section the dominant sediment types are sandy clays and silts, possibly enough to provide modest yields of groundwater. Below 60-70 m, a sand/gravel horizon of a few tens of m thickness is recorded in the two deep boreholes. The water in these boreholes is still brackish, however, in excess of 3 g/L.

It is interesting that the static groundwater level appears to "mound" beneath the Andkhoi delta area, which is indicative of recharge, possibly via infiltration from the distributary channels of the Shirin Tagab. Received wisdom amongst hydrogeologists working in the area is that the least saline groundwater resources are typically found in the vicinity of distributary and irrigation channels, where infiltration of fresher surface water to the ground may occur at some times of the year. This is tentatively supported by the fact that the least brackish water (3.0 g/L) is recorded immediately beneath the Shirin Tagab delta at Andkhoi, as compared with 8.9 g/L in the shallow well near the Turkmenistan border.

The ground surface and groundwater level fall away to the east, into what appears to be a valley formerly occupied by a river channel and now currently only marked by a strip of late Pleistocene/Holocene alluvium in Figure 6.1.

6.8 Groundwater level fluctuation

DACAAR operates a network of observation boreholes in Faryab (Figure). However, at present, it has only been possible to use data from one of these boreholes to construct a hydrograph. This borehole is at Kariz Qala school, Pashtun Kot district, just north of Maimana, in the vicinity of Kariz Qala / Jar Qala spring (Figures 5.2, 5.3). The borehole is 50 m deep, with a filter installed between 45-49 m depth in compact clayey gravels. The borehole is within a few hundred metres of the Maimana River. The hydrograph, from electronically logged data, is shown in Figure 6.9. Water level amplitude is modest (<60 cm annually). The hydrograph is not corrected for barometric fluctuations, thus the small-scale variations in logged pressure could be due to variations in atmospheric pressure and not water level. However, it is possible to observe

- a rise in water levels from Sept/Oct to April/May in 2009-2010, coinciding with autumn/winter rainfall and snowmelt, and thus with peak river flows.
- a fall in water levels from May to September.

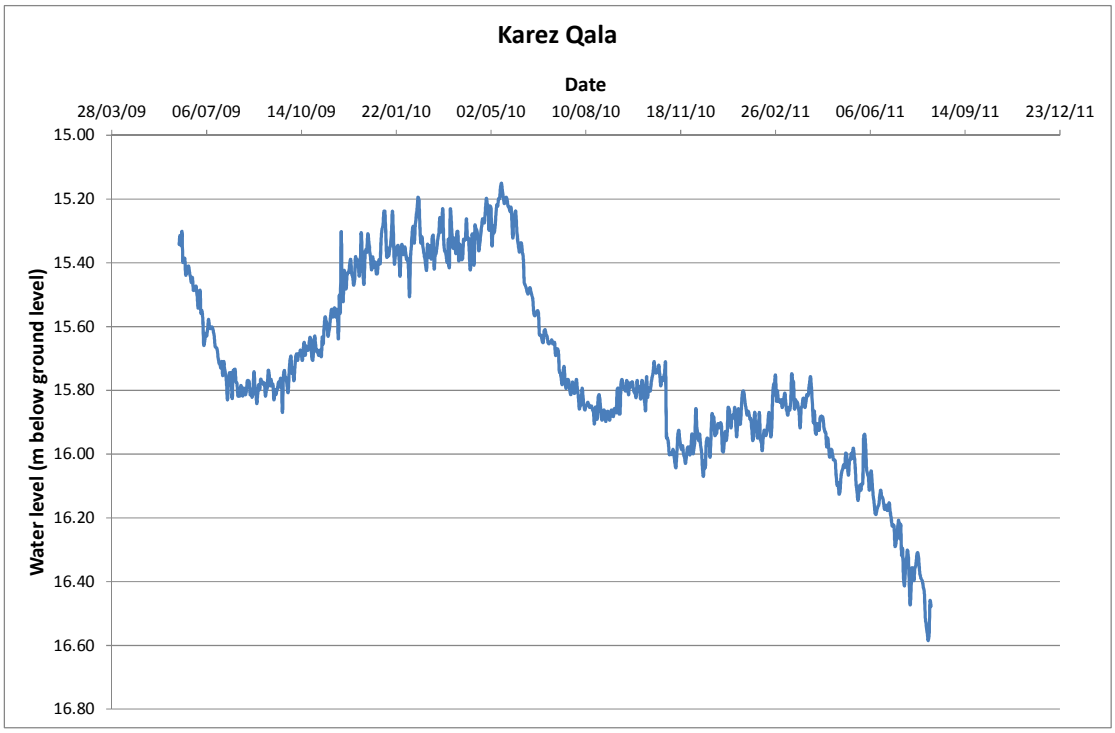

Figure 6.9. Reconstructed hydrograph for DACAAR's 50 m deep Kariz Qala school observation borehole in Pashtun Kot district for 2009-2011. The hydrograph is subject to some uncertainty due to a single manual calibration. The hydrograph is uncorrected for barometric pressure.

It is important to remember that the changes in water level may be due to actual recharge of the aquifer with water, but that they could also be simply due to "loading" of a confined aquifer by excess water in the nearby River Maimana, without any recharge taking place (and the compact sand / gravel aquifer in the borehole does have some confined nature, being overlain by around 10 m of compact clay).

If we take the rise in water level as representing recharge (either from the river or from rainfall), a rise in water level of 50-60 cm, combined with a specific yield of 10-20%, might imply a recharge of the order of 50-120 mm of water per year.

6.9 *Conclusions: Recharge and Discharge*

Groundwater Recharge

Thus far, the picture that we have gained from examining the example cross-sections in Sections 6.4 to 6.7 is one where:

- that direct infiltration of rainfall and snowfall probably takes place in the Band-e Turkestan mountains and their Mesozoic / Palaeogene foothills. The groundwater recharge emerges as spring flow (especially from the karstic limestone aquifers) and base-flow, supporting the discharge in the main rivers.
- as soon as there rivers cross from the mountain foothills onto the alluvial valleys and plains or central and northern Faryab, the main water table in the alluvial aquifers is consistently below the level of the main rivers.
- there would thus be a general tendency for the rivers to infiltrate into the ground, into the alluvial aquifers. The magnitude of this recharge would likely be limited by the modest permeability of the generally clayey / silty nature of the strata in the upper part of the alluvial geological succession.
- one might thus expect the groundwater in the immediate vicinity of the river channels to be fresher than elsewhere.
- the depth to groundwater gradually decreases northwards: from in excess of 50 m bgl in the Qaysar and Almar areas, to 20-30 m in the Maimana and Shirin Tagab areas, and to 10-20 m bgl around Andkhoi / Khani Chahar Bagh. Figure 6.9b suggests that rest water levels decline to depths in excess of 30 m again in the very north of the Andkhoi / Khani Chahar Bagh area.

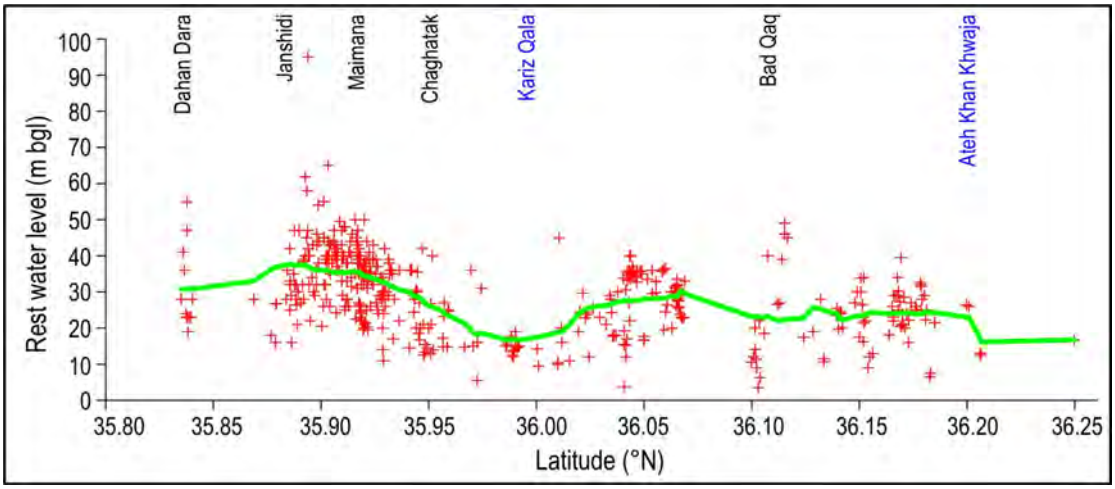

Figure 6.10a. Rest water levels in wells and boreholes registered along the valley of the Maimana River, from south (left) to north (right). Levels in metres below ground level (m bgl**).** The green line shows a moving average through the data. Kariz Qala / Jar Qala and Ateh Khan Khwaja springs are marked in blue.

Figure 6.9c suggests that groundwater levels also become shallower downstream along the Checkaktu valley from east to west, with groundwater levels <10 m deep becoming common in the Chechaktu valley in Ghormach.

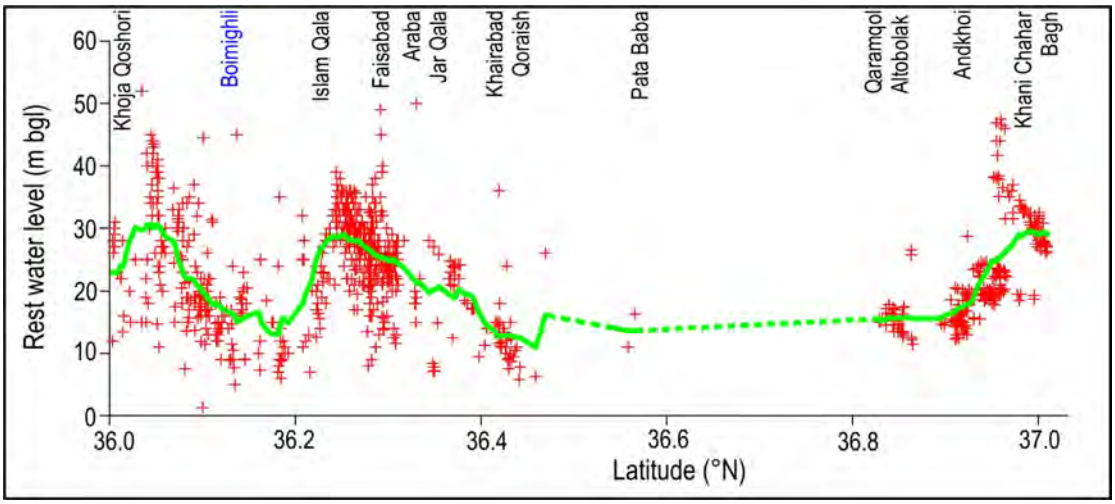

Figure 6.10b. Rest water levels in wells and boreholes registered along the valley of the Shirin Tagab River, from south (left) to north (right). The green line shows a moving average through the data. Boimoghli spring is marked in blue.

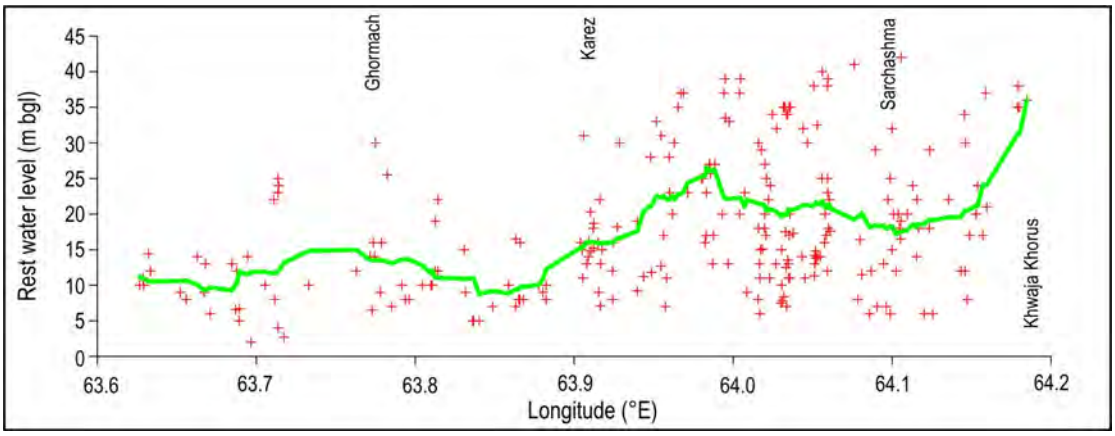

Figure 6.10c. Rest water levels in wells and boreholes registered along the valley of the Chechaktu River, from west (left) to east (right). The green line shows a moving average through the data.

Specific Loci of Groundwater Discharge

Despite the general impression of groundwater levels typically being >10 m below ground level in the main river valleys, there are loci of groundwater discharge in the northern regions of Faryab. The most obvious of these is the **Khwaja Mod saline lake**, which appears to act as a discharge locus for local groundwater flow in the alluvial / Neogene aquifers (Figure 6.1). It also is believed to act as a discharge for deeper regional groundwater flows via a major fault zone. The groundwater discharge at this location is evaporated away, leaving deposits of halite and gypsum.

There are other, very specific, springs in the northern part of Faryab, which act as important sources of water supply for the local population. Some of these are relatively easy to understand: the springs at Moghaito emerge from higher elevation aquifer strata in a Mesozoic inlier and are presumed to be fed by direct infiltration of modest amounts of precipitation.

The other springs, which are less easily understood, include (Figure 5.1):

- The **Boimoghli spring**, with an estimated discharge of some 35 L/s and electrical conductivity of 1510 µS/cm (2007 data), emerging from the side of the

Shirin Tagab valley in the northern part of Khwaja Sabz Posh district. A number of wells near the spring record water levels of c. 10 m bgl in the alluvial deposits. As the spring is approached, however, groundwater levels become shallower, with the nearest well (KHF-148-07, Turk Man Qishlaq) recording a water level of only 5 m bgl.

- The **Jar Qala spring**, with an estimated discharge of some 25 L/s and electrical conductivity of 1385 µS/cm (2007 data), emerging from the valley side of the Maimana River, in Pashtun Kot district, some 10 km NW of Maimana city. A spring in a similar location, on the alluvial floor of the Maimana River valley, was registered as **Kariz Qala spring** in 2013 (Figure 5.5), with a discharge estimated as only 2 L/s and an electrical conductivity of 1350 µS/cm. It is uncertain whether these represent two different springs. The location of the spring area is difficult to understand: a number of nearby dug wells and a DACAAR observation borehole at Karez Qala school all record a groundwater level of around 15 m bgl (Figure 6.9).
- The **Ateh Khan Khwaja spring**, at the junction of the Maimana and Qaysar rivers (i.e. at the start of the Shor Darya), in Shirin Tagab district. This has a discharge of some 35 L/s and electrical conductivity of 2450 µS/cm (2007 data). The location of the spring area is difficult to understand as the wells and boreholes in the vicinity exhibit groundwater levels of >20 m bgl in the alluvial deposits. These are upstream of the spring, so we have no good data on groundwater levels downstream of the spring, although Hassan Saffi (*pers. comm.* Sept 2013) indicates that the Shor Darya's surface water salinity creeps up downstream of the Ateh Khan Khwaja spring, due to seepage of saline groundwater in the bed of the Shor Darya, suggesting the water table is close to the surface.

On the cross-sections of Figures 6.10a and b, it is noticeable that the depth of the water level below ground does not show a smooth trend. Indeed, there are four clear locations where the water table approaches more closely to the surface:

(i) In the Maimana valley, in the vicinity of Kariz Qala / Jar Qala springs.

(ii) In the Maimana valley, in the vicinity of Ateh Khan Khwaja (but based on very few data).

(iii) In the Shirin Tagab valley, just downstream of Boimoghli spring.

(iv) In the Shirin Tagab valley, along the stretch of river north of Jar Qala.

...in other words, in the vicinity o0f the major springs, and the zone of the Shirin Tagab where flow accretion is registered (see Chapter 3 and below).

Thus, it appears that the major spring discharges emerge where the water table approaches the surface (and, although the registered groundwater levels still appear well below the surface in nearby wells, this could simply be a topographic effect if the springs occur in incised springflow channels or the incised recent valley of the river itself).

The reasons why the rest water table appears to approach this surface in these locations could include:

(i) constrictions of the permeable alluvial channel, reducing its transmissivity. These constrictions could be lateral (width of channel) or vertical (depth of channel), forcing groundwater flow to the surface.

(ii) The fact that a major lateral groundwater flow joins the main alluvial channel, e.g. from a side channel. The excess groundwater flow being

constricted in a single channel could force it to emerge at the surface. This could be the reason for the location of the Ateh Khan Khwaja spring at the confluence of the Maimana and Qaysar rivers.

The Jar Qala spring appears (on Google Earth) to emerge from the western valley side. If so, it would appear to originate in loess / Neogene deposits. Given the name of the location (Kariz Qala), it is not inconceivable that the feature is not really a spring at all, but a karez construction into the valley side. The Kariz Qala spring in the valley floor could simply be a re-emergence resulting from the excess water entering the alluvial deposits.

Flow Accretion in the Lower Shirin Tagab

It was noted, in Chapter 3, that the Shirin Tagab loses the majority of its flow to the Araba irrigation channel, at the border between Shirin Tagab and Dowlatabad districts. However, flow re-accretes in the Shirin Tagab downstream.

The slope on the irrigation channel is less than that of the river and the river thus sinks progressively below the level of the irrigation channel northwards. We speculate that the irrigation channel loses water, either by leakage, or direct application to fields, to the ground. This leakage may flow north and west towards the river channel to gradually re-emerge as baseflow to the river channel. There may even be some direct overland flow from the irrigation channel to the river, via irrigated fields, or interflow via shallow soils and drains.

Figure 6.11. The Jar Qala region of Dowlatabad district, some 3 km north of Araba. The irrigation channel (pale blue) is to the right and the River Shirin Tagab (dark blue) is to the left. Dark blue dots show wells with groundwater levels around 25-30 m bgl, pale blue around 15 m bgl and white around 7-8 m bgl.

At Jar Qala, the river and irrigation channel are separated by only some 500 to 700 m. The irrigation channel is at an elevation of 455 m asl, while the River Shirin Tagab is at some 435 m asl. In wells near the river, the groundwater level is less than 10 m from the surface, suggesting the potential for upwelling of groundwater discharge and flow accretion, in addition to possible overland flow and interflow. Indeed, Hassan Saffi (*pers.*

comm., Sept. 2013) confirms that there are numerous groundwater springs in the bed of the River in this region of Dowlatabad district.

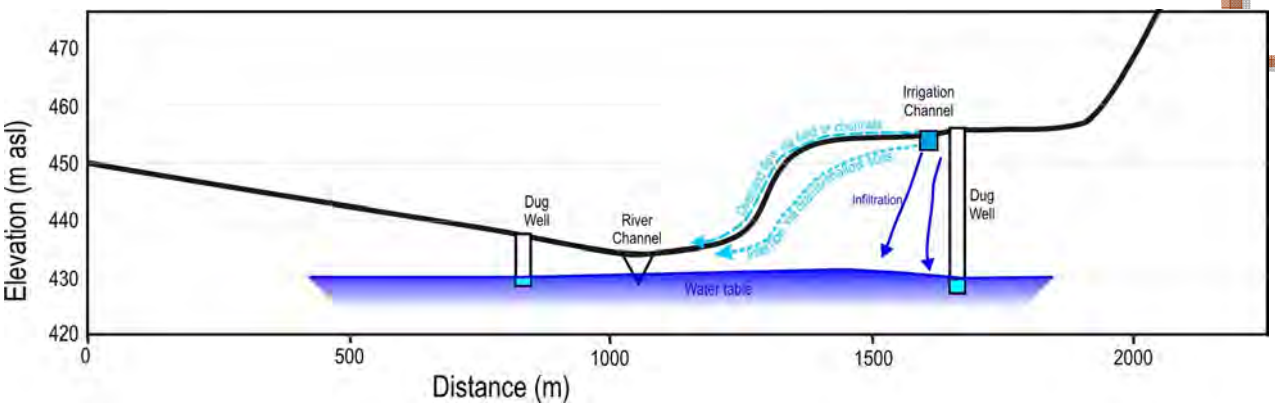

Figure 6.12. Schematic cross-section across the Jar Qala region of Dowlatabad district, some 3 km north of Araba, based on Figure 6.11, showing the various mechanisms for flow re-accretion in the river channel. This interpretation is highly speculative, using terrain elevations extracted from Google Earth. The correctness of this possible interpretation would depend on highly accurate surveying of ground and groundwater levels.

A similar situation pertains further to the north, in the Khairabad, Qoraish and Dowlatabad areas, where a large area of groundwater levels of <10 m bgl is located between the irrigation channel and the river.

In all cases, the explanations for the emergence of groundwater and spring flow discharges at these locations are very tentative. Much depends on accurate surveying or terrain and water levels, as any groundwater gradients involved would be very shallow. Research projects to investigate the hydrogeology of these areas would undoubtedly be most productive in terms of increased hydrogeological understanding.

7. Faryab: Thermogeology

7.1 What is thermogeology?

The term "thermogeology" simply refers to the science of the distribution and movement of heat within the ground, and to its exploitation by human beings for the purposes of heating and cooling. The existence and movement of heat in the ground is governed by the distribution of temperature within the ground.

The temperature of the shallow subsurface is largely governed by the annual average air temperature. At depths of a few metres, the ground heats up and cools down with the seasons, although the amplitude of the temperature swing diminishes with depth and the time lag becomes greater. Below around 6-10 m depth, the temperature of the ground, and its groundwater, becomes almost constant, at a level slightly higher than the annual average air temperature. In fact, snow cover tends to insulate the ground against the worst extremes of winter temperature, so the greater and longer the snow cover the higher the ground temperature will be, relative to annual average air temperature.

We have already seen (Chapter 2) that the annual average air temperature is around 14-15°C in Maimana, 17-18°C in Andkhoi, and 6-7°C in parts of Kohistan.

As one goes deeper into the ground, the temperature increases slowly according to the "geothermal gradient", which is typically between 1-3°C per 100 m in geologically stable areas (which Afghanistan, being part of a geologically recent orogenic belt, is not). In fact, Saba et al. (2004) cite a geothermal gradient of 2.5 to 3°C per 100 m as being typical for Afghanistan. The geothermal gradient $\Delta T/\Delta z$ is governed by Fourier's Law (Banks 2009, 2012):

$$\frac{\Delta T}{\Delta z} = \frac{q}{\lambda}$$

where T is temperature (K), z is depth (m), q is the geothermal heat flux (W/m^2) and λ is the bulk vertical thermal conductivity of the rock sequence (W/m/K).

7.2 Shallow subsurface temperatures

During groundwater sampling campaigns of 2013, 67 springs, 335 dug wells and 33 drilled boreholes (435 total) were visited and field pH, electrical conductivity and temperature were recorded. The sources were <100 m deep and, in most cases, <60 m deep (Figure 7.2b). These sources were in:

- Kohistan
- Bilchiragh
- Gurziwan
- Qaysar
- the area around Maimana Airport
- the four northern districts of Andkhoi, Qurgan, Qaramqol and Khani Chahar Bagh.

Figure 7.1 shows a map of the recorded groundwater temperatures. Although every effort was made to obtain representative "fresh" groundwater from the sources, it cannot be guaranteed that all samples would have been wholly adequately "purged" and thus representative of aquifer *in situ* temperatures.

Figure 7.2 shows the temperatures distributions by district as boxplots.

It will be seen that temperatures are broadly as expected, ranging from 11-13°C in Kohistan (most of the sampled points were in the lower-lying, and hence warmer, valleys of the district) to around 20°C in the northern districts around Andkhoi. In Maimana district, groundwater temperatures were typically 16-17°C, around 2°C warmer than annual average air temperatures.

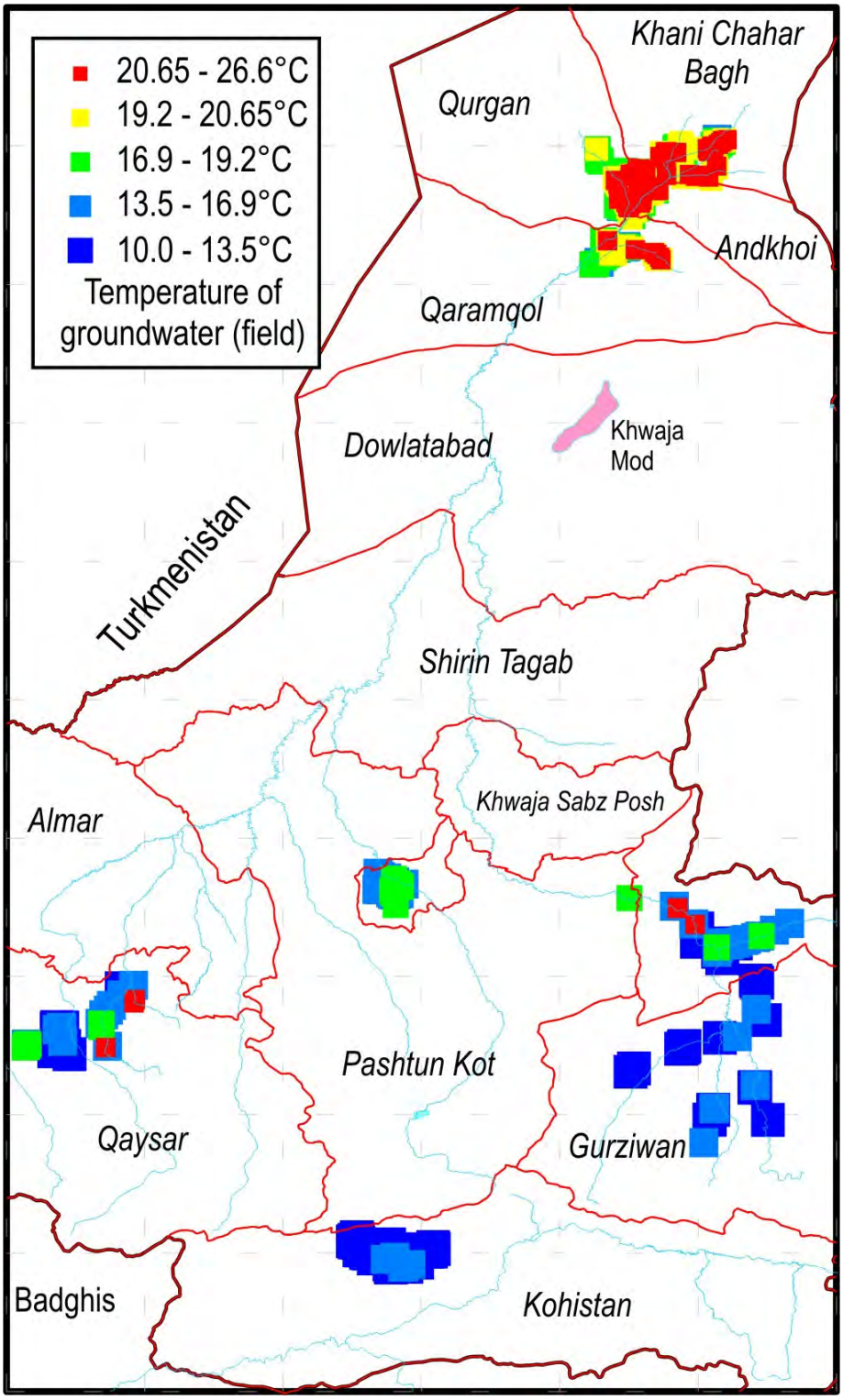

Figure 7.1. Recorded groundwater temperature (2013) in dug wells, boreholes and springs of Faryab.

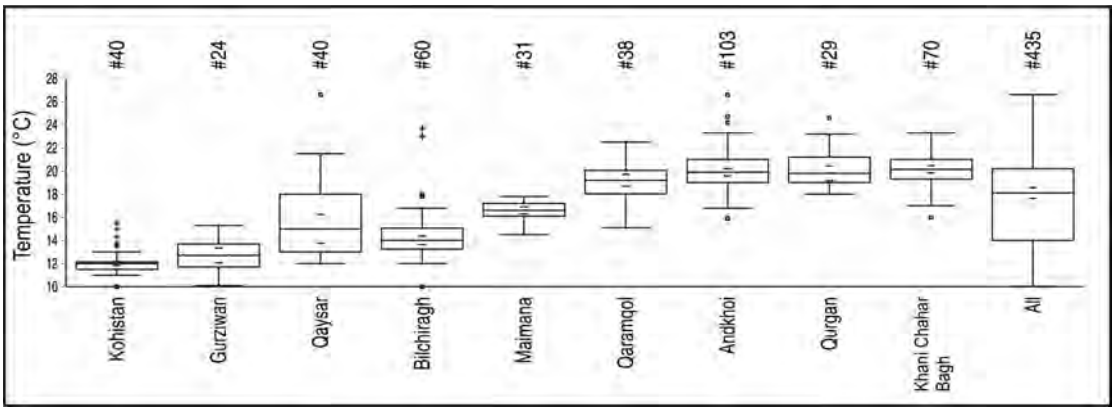

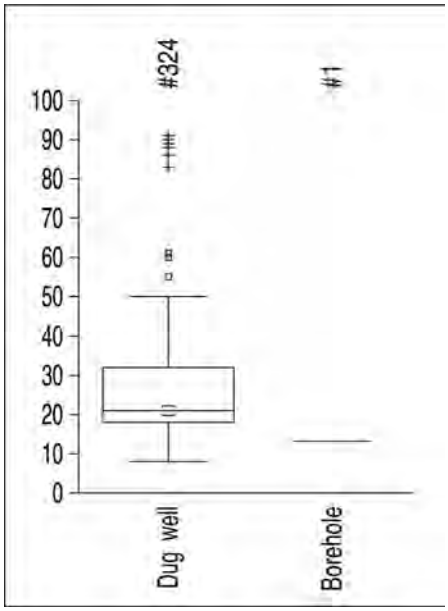

Figure 7.2a (above). Distribution of groundwater temperature (2013) by district as boxplots (435 readings total). In boxplots, the central "box" represents the interquartile range with a horizontal line as the median. The "whiskers" represent the non-outlying extraquartile range, with outliers shown as small squares (near outliers) or crosses (far outliers). Parentheses around the median represent a robust 95% confidence interval on the median. The #numbers along the top represent the number of data in each subset.

Figure 7.2b (left). Depth distribution of the 324 dug wells where temperature was recorded and the well depth was known. At only 1 drilled borehole was the depth recorded.

Temperature data have also been plotted against estimated ground elevation in Figures 7.3 and 7.4, showing how groundwater temperature increases as ground elevation drops and the climate becomes warmer towards the north. Figure 7.4 indicates a lapse rate of some 0.5°C per 100 m elevation.

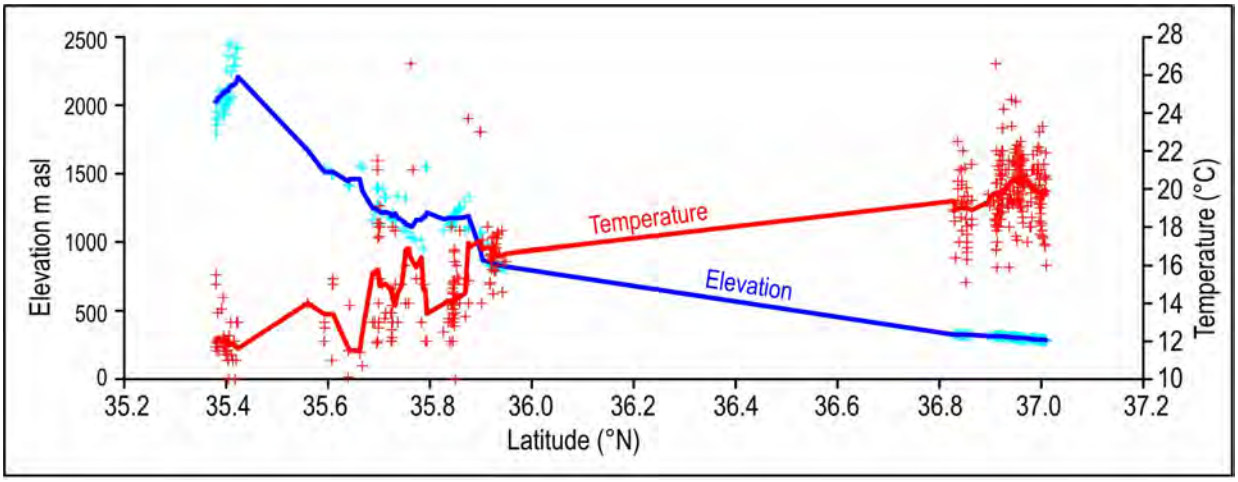

Figure 7.3. Groundwater temperature and altitude of sample location plotted against latitude in Faryab. The lines represent a moving average through the real data points (crosses).

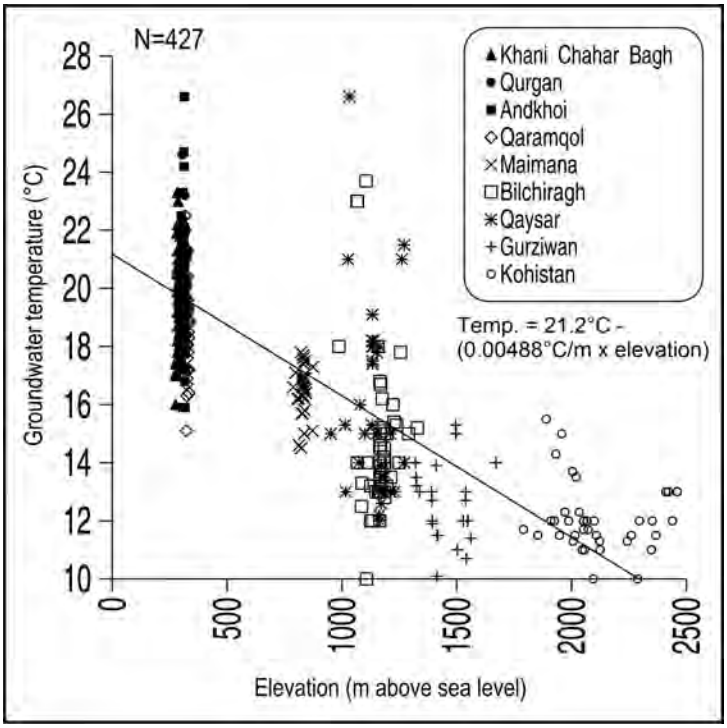

Figure 7.4. Groundwater temperature (°C) from the sampling campaign of 2013 plotted against elevation of sampling point above sea level. The line shows a best-fit linear regression, indicating an approximate lapse rate of 0.5°C per 100 m elevation.

The *lapse rate* is the rate at which atmospheric temperature decreases with increase in altitude. According to Wikipedia, the average global atmospheric lapse rate is around 0.64°C per 100m, which approximately corroborates the data from Faryab.

Where the depth of dug wells has been recorded, data have been examined to ascertain if there is any discernable increase in groundwater temperature with well depth. No such correlation has been found (Figure 7.5).

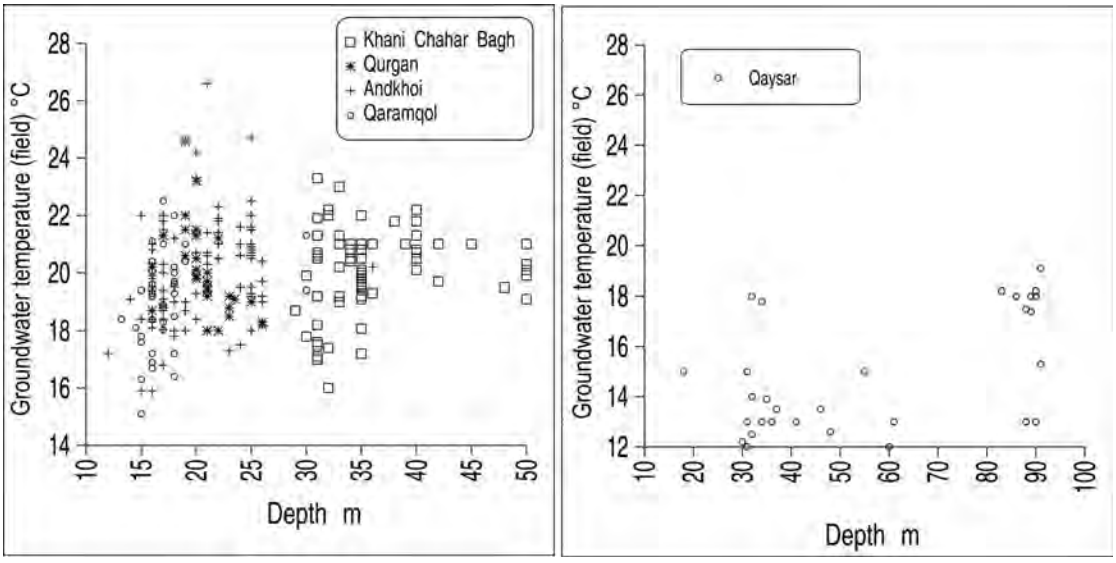

Figure 7.5. Groundwater temperature plotted against well depth for the four northern districts around Andkhoi and for Qaysar. These are almost exclusively dug wells, which do not penetrate a great distance below the water table. Hence, well depth is a good indicator of the depth of the horizon from which groundwater is derived.

7.3 Ground heating and cooling in Faryab

Areas of continental climate (extremely cold winters and hot summers) offer excellent potential for ground sourced heating and cooling. This is because, in summer, the ground is much cooler than the air, yet in winter it is much warmer.

Thus, in summer in Andkhoi, it is much more efficient to use a ground source heat pump (GSHP) to reject waste heat from buildings to the ground or to groundwater at 20°C, than to use a conventional air conditioner to reject waste heat to the outdoor air, which may have a temperature in the upper 30s°C.

In Kohistan, where the groundwater temperature may be as low as 10-11°C, one could even use the groundwater directly for space cooling, without the use of a heat pump.

In winter, when air temperatures fall close to, or below 0°C, the warm ground or groundwater, in the range 10-20°C could be very efficiently used for space heating, via a ground source heat pump.

The beauty of such systems is that the waste heat rejected to the ground in summer will tend to warm the ground up. This heat will be "stored" in the ground until winter, when it can be re-extracted again, using a ground source heat pump.

Such GSHP technology can run using brackish or even saline groundwater. By drilling heat exchangers into the ground (a so-called closed-loop system), it can even function where no groundwater is present. A modern GSHP does, however, require a reliable source of reasonably cheap electricity. In many parts of Faryab, this may be present via the import power lines running from Turkmenistan. Ground source heating and cooling technology, using the heat stored in shallow ground and groundwater, thus has considerable potential in Afghanistan.

7.4 Deeper geothermal prospects

The report by Saba et al. (2004) does not list any surface indications of geothermal prospects in Faryab Province. They suggest that the main geothermal prospects lie further south, along the Herat-Panjshir geosuture and the Chaman-Moqor fault systems of central Afghanistan. They do, however, note that high fluid temperatures can be encountered in so-called "geopressurised systems" - porous, high pressure sedimentary strata associated with the hydrocarbon reserves of the northern Afghan provinces at several km depth.

Klett et al. (2006; based on Gotgilf et al., 1969) report the following geothermal gradients from the Afghan-Tajik sedimentary basin of northern Afghanistan:

- 2.5°C per 100 m for the Neogene strata
- 3.2°C per 100 m for the Eocene-Oligocene strata
- 2.0°C per 100 m for the Palaeocene strata

Based on Krylov (1980), Klett et al. (2006) also report (again for the Afghan-Tajik basin):

- 2.4 to 3.0°C per 100 m for the upper 4.5 km of strata
- 2.5 to 2.9°C per 100 m to 6-7 km depth

Finally, Brookfield & Hashmat (2001) report a somewhat higher typical geothermal gradient of c. 3.46°C per 100 m for oil-producing wells of northern Afghanistan. Ulmishek (2004) also cites a gradient of 3.0 to 3.5°C per 100 m for the Amu Darya sedimentary basin.

A geothermal gradient of 3°C per 100 m, and a surface temperature of 20°C (annual average) would imply:

- a temperature of 50°C at 1 km depth
- a temperature of 100°C at 2.7 km depth
- a temperature of 200°C at 6 km depth.

Where porous and permeable sedimentary aquifers exist at these depths, thermal water may potentially be extracted to provide direct heating potential, or even electrical power production potential. In practice, these aquifers are most typically sandstones with intergranular porosity (as fractures tend to "close up" with great depth) but, occasionally, limestone aquifers can also retain permeability at considerable depth, depending on their karstification and weathering history.

It is anecdotally reported by hydrogeologists active in Faryab that the Ministry of Mines, Department of Oil and Gas, drilled an exploratory well into Lower Cretaceous/ Jurassic sandstones in the area to the NE of the Astana inlier in Faryab. They obtained a reported artesian flow of c. 25 L/s of overflowing saline groundwater at 45-50°C. The depth of the well is not clearly known. Such a water flux could be used for direct heating purposes. If a temperature differential of 15°C could be extracted from the water, the flux represents:

15 K x 4.2 kJ/L/K x 25 L/s = 1.6 MW of heating potential.

Unless the thermally spent water were reinjected, however, it is unlikely that such a flow rate would be sustainable in the long term.

8. Faryab: Groundwater Salinity

8.1 Previous Studies

As we have previously seen, from Chapter 1, historical writings imply that salinity has always been the greatest water supply problem for the northern districts of Faryab.

Mishkin's (1968) delineates zones of groundwater salinity (total dry residue in g/L), as shown in Figure 8.1.

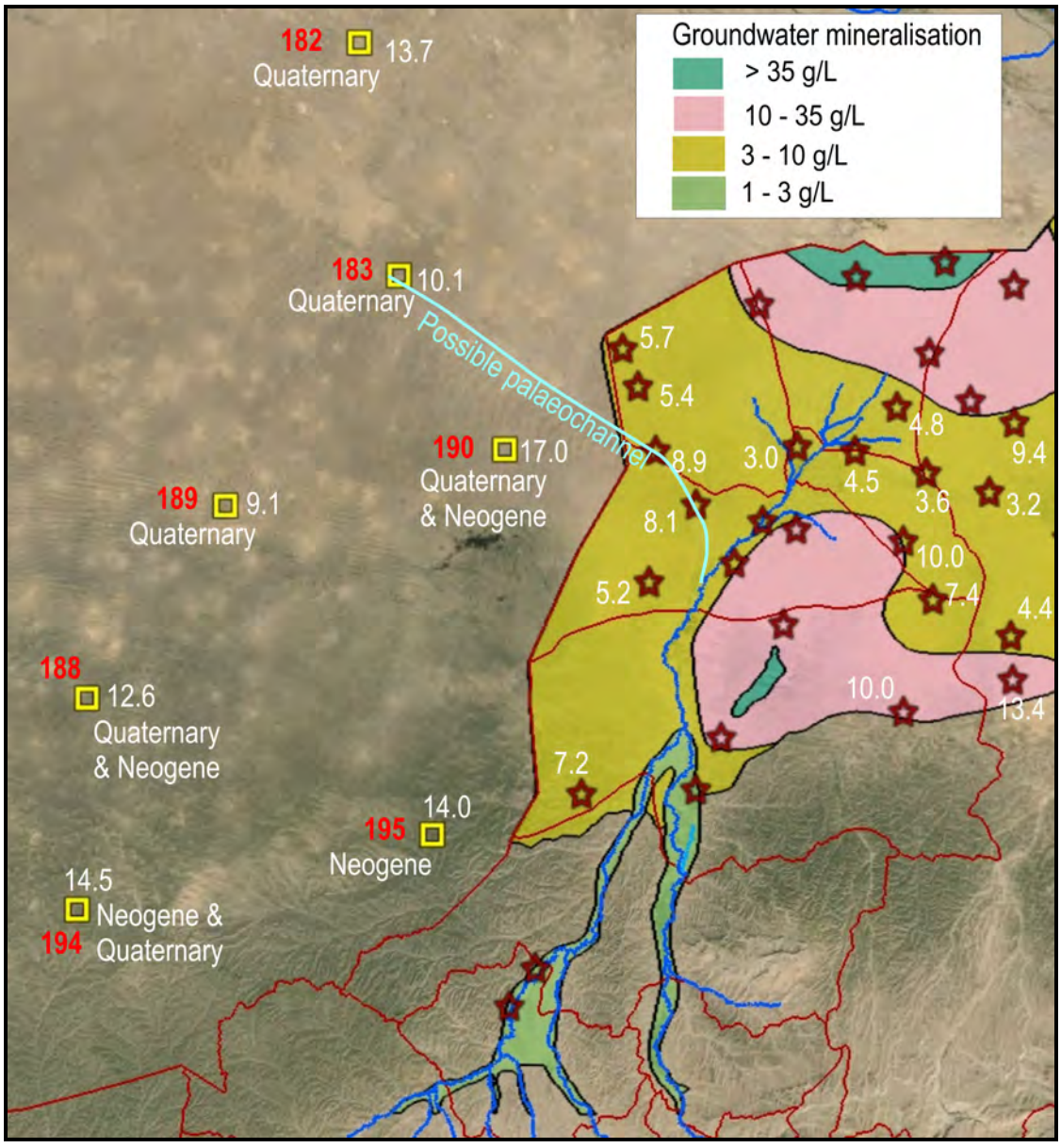

Figure 8.1. Aerial image showing Mishkin's (1968) groundwater salinity zones (in g/L of total dry residue) for the Quaternary deposits of northern Faryab. Red stars show the wells, boreholes and springs that Mishkin used to delineate his zones. White figures show groundwater total dry residue in g/L at individual boreholes and wells. Yellow squares show wells/boreholes in Neogene and/or Quaternary deposits in the Turkmen desert, taken from Krizhanovskii (1972). White text shows the aquifer horizons in these boreholes, while the red number is the Soviet borehole number. Red lines show district boundaries, blue lines show rivers.

Mishkin's map clearly shows:

- That groundwater salinity increases northward from values of 1-3 g/L in the alluvial deposits of the Maimana and Shirin Tagab valleys of Khwaja Sabz Posh, Pashtun Kot and Shirin Tagab districts, to >35 g/L in the far north of the Province.
- That there is also a zone of high groundwater salinity surrounding the regional groundwater discharge point of the Khwaja Mod saline lake.
- That there are generally lower salinities in the immediate vicinity of the main river channels. It should be noted, however, that zone of fresh groundwater along the Shor Darya in Mishkin's (1968) map is *not* supported by current data, which indicates saline groundwater along the Shor Darya.
- That around Andkhoi, groundwater salinity is generally > 3 g/L, even at depth (see Figure 6.8).
- That even further to the north (not shown on Figure 8.1), as one approaches the Amu Darya, groundwater salinity decreases again, and that a zone of fresher groundwater borders the Amu Darya valley (MUMTAZ 2007).
- That the intermediate salinity waters are often of sulphate type (sometimes chloride), while the highest salinity waters have more of a tendency to be of chloride type (not shown on Figure 8.1).

Across the border in Turkmenistan, groundwater salinities are even greater than in Faryab, typically > 10 g/L (Krizhanovskii 1972). There is no evidence from Figure 8.1 that a tentatively identified palaeochannel (Figure 6.1) stretching from the Shirin Tagab in Qaramqol to the Turkmen Unguz is associated with fresh groundwater reserves.

8.2 Salinity and Electrical Conductivity

Electrical conductivity is measured in µS/cm and characterises how easily the water conducts an electric current. There is a direct relationship between the electrical conductivity (EC) and the water's content of charged ions - i.e. its salinity. In general, at 25°C (Misstear et al. 2006):

1 meq/L of cations (or 1 meq/L of anions) results in 100 µS/cm of EC (8.1)

up to around 2000 µS/cm

or

M (mg/L) = EC (µS/cm) x f (8.2)

where f = 0.55 for a water dominated by sodium chloride

f = 0.75 for a water dominated by calcium bicarbonate

M = total dissolved solids, mineralisation, dry residue or salinity in mg/L

Guidance

A former edition of the SPHERE standards (2000) for humanitarian relief indicated that total dissolved solids in drinking water should be less than c. **1000 mg/L** (**EC < 2000 µS/cm**). The most recent edition (2011) merely states that the water must be palatable.

The WHO (2011) drinking water guidelines suggest that water typically becomes significantly and increasingly unpalatable at TDS levels greater than about **1000 mg/L**.

In most cases, the data held in the NORPLAN project database for Faryab represent direct measurements of EC, although it is not always clear whether the measurements are representative of a field temperature or have been corrected to a standard temperature (25°C).

In a few cases, the groundwater's total mineralisation M has been cited (this is especially the case for a small number of typically saline wells derived from Soviet literature for Turkmenistan or northern Afghanistan). For the purposes of plotting, this has been back-estimated to electrical conductivity using the algorithm:

IF (M <= 1500 mg/L) THEN (EC = M/0.7) ELSE (EC = M/0.6) (8.3)

on the basis that the more saline waters are more likely to be dominated by sodium chloride.

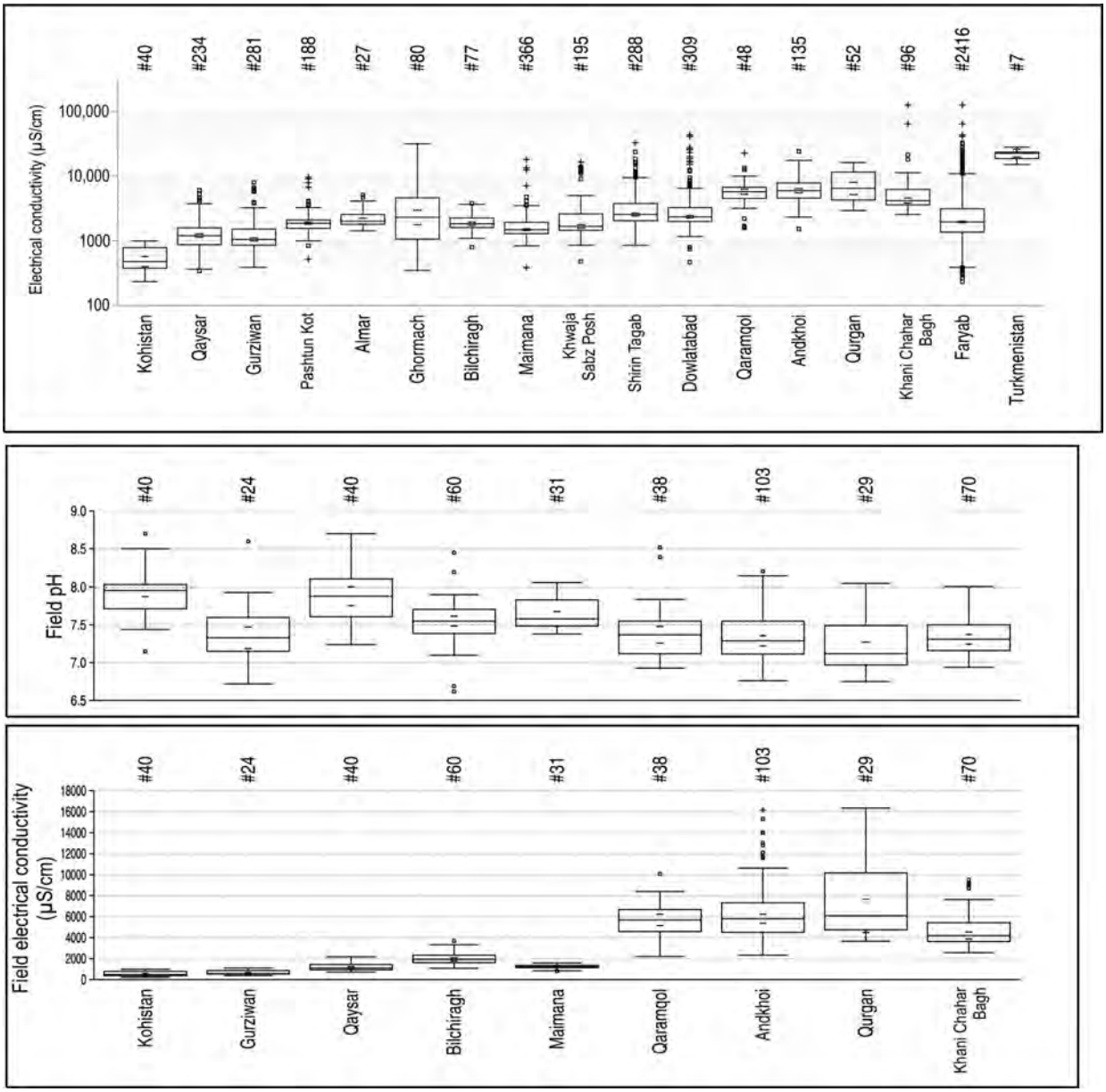

Figure 8.2. Boxplots showing the distribution, by district, of (top) **electrical conductivity from the entire NORPLAN database**, in Faryab and adjacent areas of Turkmenistan. The lower two diagrams show (middle) **field pH** and (bottom) **field electrical conductivity** from 435 wells, boreholes and springs visited during the field survey of 2013/early 2014. See text box below for an explanation of the boxplot.

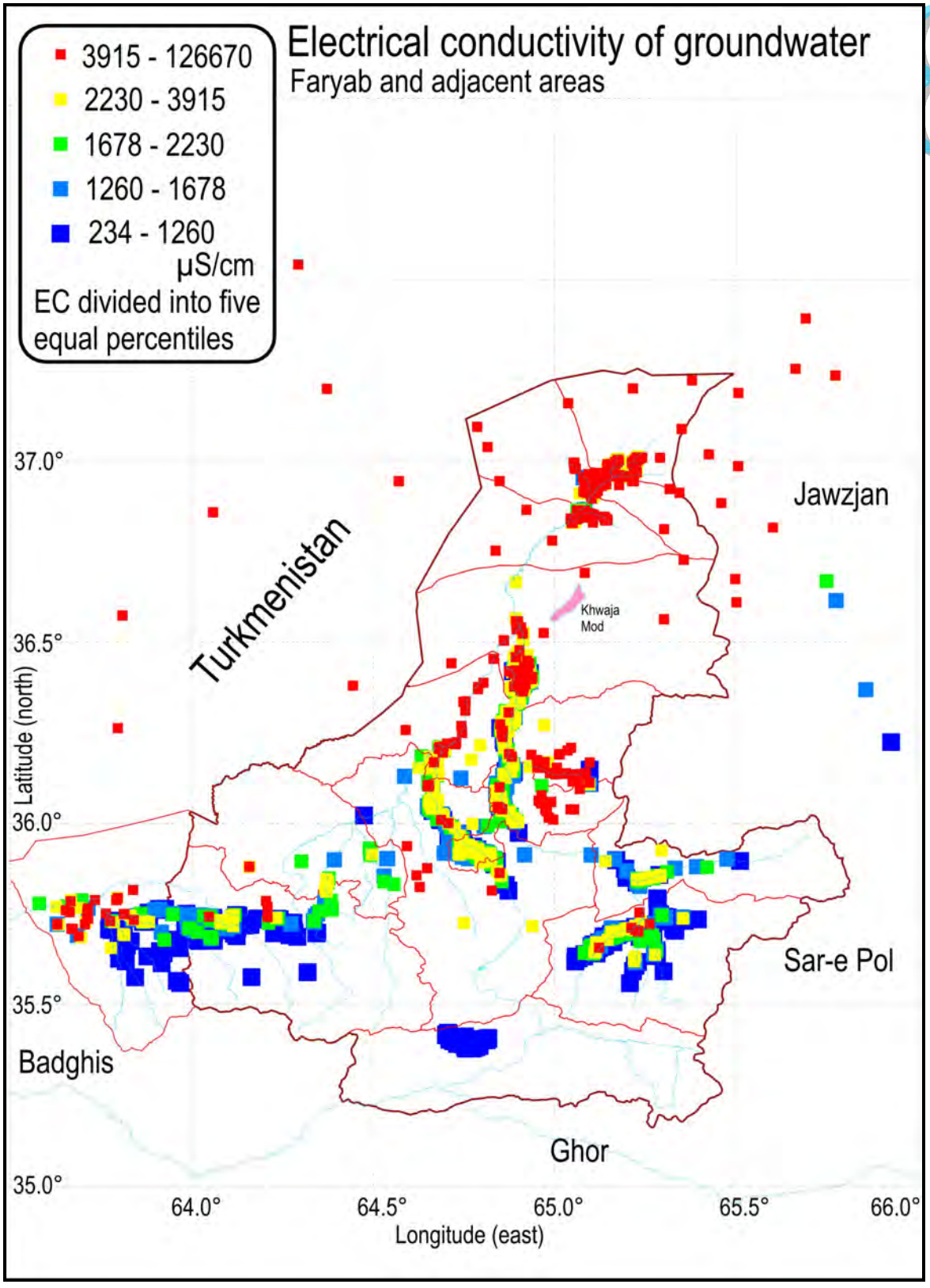

Figure 8.3. Electrical conductivity of groundwater in Faryab and adjacent areas, using all data in NORPLAN database as of April 2014. Note that data are concentrated in valleys and symbols for red "high" values can obscure lower values behind them. Also note that the EC of a few very saline waters may be somewhat overestimated due to the conversion algorithm from mineralisation (Equation 8.3).

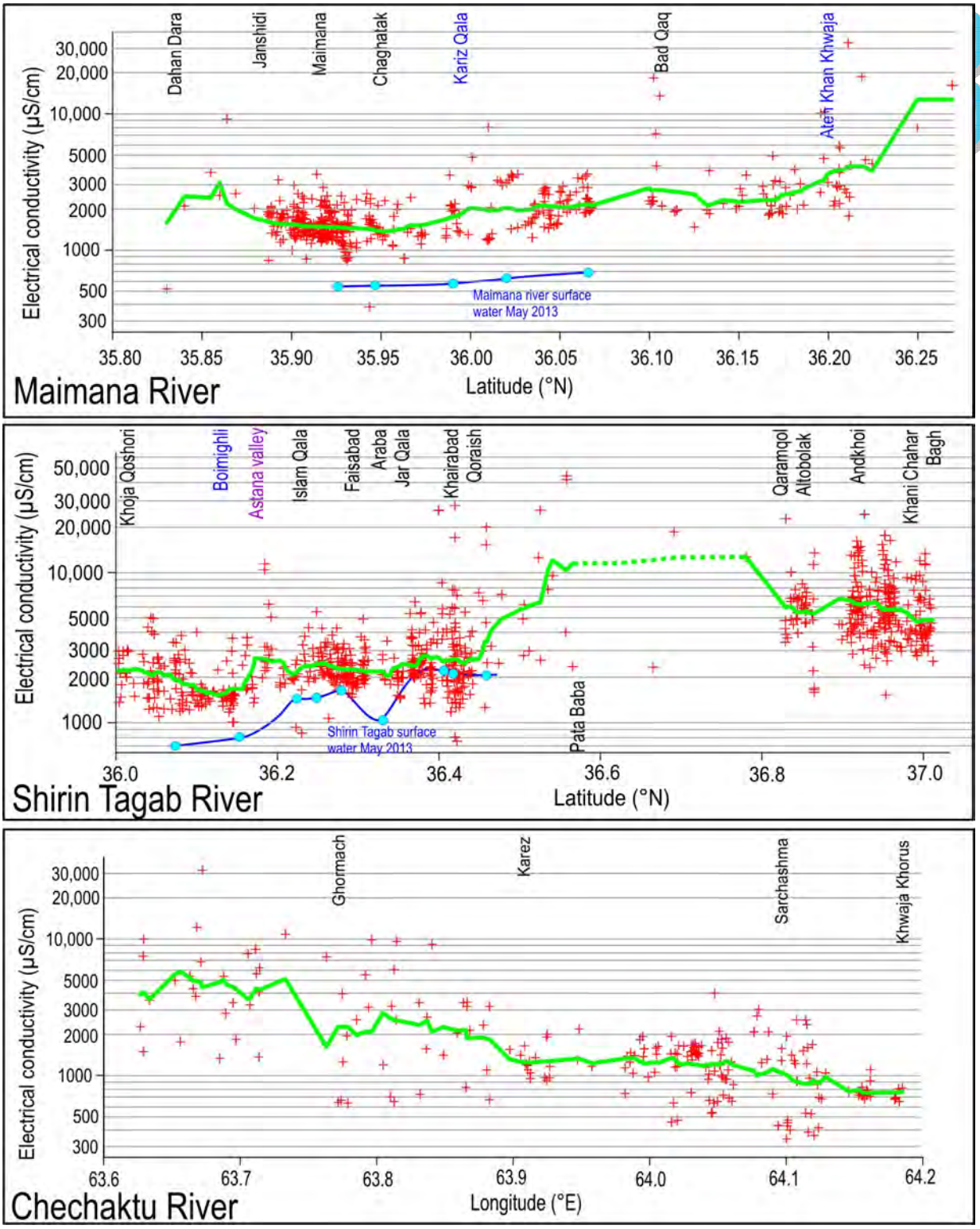

Figure 8.4. Electrical conductivity of groundwater in (top) the Maimana valley (middle) Shirin Tagab valley and (bottom) Chechaktu valley corridors, using all data in the NORPLAN database for these areas as of April 2014. The green line shows a running average; red symbols show actual data points. Note that the EC of a few very saline waters may be somewhat overestimated due to the conversion algorithm from mineralisation (Equation 8.3). In the Maimana and Shirin Tagab profiles, the blue symbols and lines show the electrical conductivity in the rivers' surface water (Chapter 3).

Figure 8.2 shows the total distribution of groundwater electrical conductivity by district, as boxplots, while Figure 8.3 shows a map. Figure 8.4 shows the variation in groundwater electrical conductivity along three alluvial valley corridors.

Boxplots

In boxplots, the central "box" represents the interquartile range with a horizontal line as the median. The "whiskers" represent the non-outlying extraquartile range, with outliers shown as small squares (near outliers) or crosses (far outliers). Parentheses around the median represent a robust 95% confidence interval on the median. The #numbers along the top represent the number of data in each subset.

It should be noted that EC has a tendency to increase northward (Figure 8.2). In Kohistan, EC is in the range 200-1000 µS/cm. In Qaysar and Gurziwan, values in the range 800-1600 µS/cm are more typical, while in the central districts of Faryab values 1200-2500 µS/cm are normal. In Shirin Tagab and Dowlatabad, EC values in excess of 3000 µS/cm begin to become common, while in the four northern districts are often in the range 4000 to <10,000 µS/cm. In the northernmost district of Khani Chahar Bagh, where groundwater levels become deeper (see Chapter 6), the salinity decreases a little again, with values of 3000-6000 µS/cm becoming typical.

8.3 Maimana Valley

From Figure 8.4, it should be noted that the groundwater salinity in the Maimana valley actually appears to decrease slightly in a downstream direction above and around Maimana.

In the section of the valley just downstream of Maimana, it is noteworthy that the salinity of the river water, as sampled in May 2013 (see Chapter 3) was significantly lower than that of the groundwater. This may simply be due to the fact that river sampling was at a time of snowmelt in the mountains (abundant fresh surface water, with the possibility that surface water salinity increases later in the year), but it may also indicate that some amount of river water has the potential to infiltrate the ground, mix with higher salinity regional groundwater and create a zone of fresher groundwater near the river.

Figure 8.5 shows the variation of electrical conductivity in the immediate vicinity of the Maimana River near Maimana. It is clear that, although there is a very large variability in the data, the very lowest salinity groundwater sources are in the immediate vicinity of the river channel, strongly supporting the hypothesis that recharging river water creates a zone of fresh groundwater near the river channel. This progressively mixes with more saline "ambient" groundwater with distance from the river.

Downstream of Maimana, groundwater salinity creeps up until the junction with the River Qaysar and the Shor Darya (Figure 8.4). Afghan hydrogeologists with experience from the area state that, although the Qaysar River's surface water is already relatively saline (c. 4000 µS/cm) at the confluence, its salinity creeps up downstream of the confluence (where the relatively low salinity Ateh Khan Khwaja spring is located) to values of around 8000 µS/cm, due to seepages of saline groundwater into the bed of the Shor Darya (Hassan Saffi, *pers. comm.* Sept. 2013).

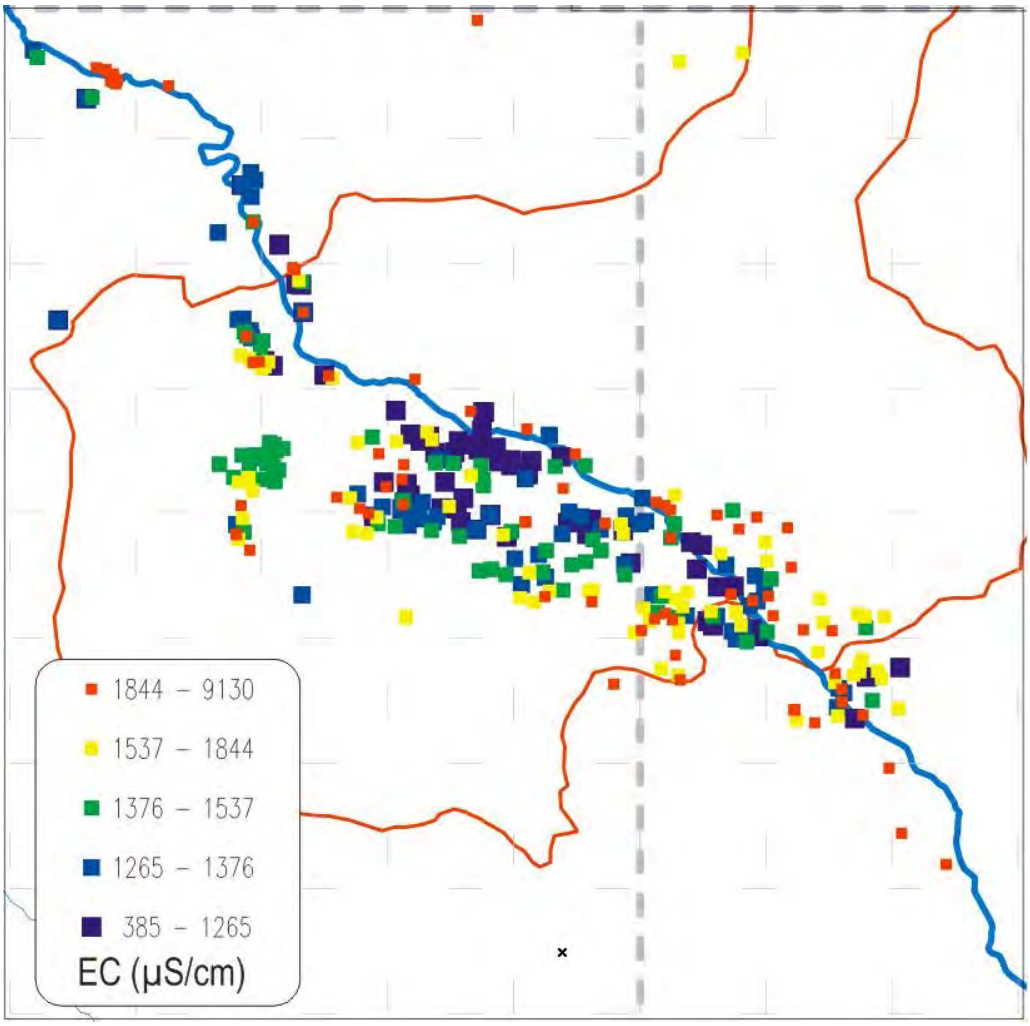

Figure 8.5. Groundwater electrical conductivity in wells, boreholes and springs in and around Maimana district (red outlines show district boundaries, blue line shows Maimana River). All available data in the NORPLAN database as of April 2014 have been used. For location, see Figure 8.3. Symbols are based on 5 equal percentile classes of 20%.

8.4 Shirin Tagab Valley

In the left hand section of the middle diagram of Figure 8.4, we can see that groundwater salinity has a weak tendency to decrease in a downstream direction, while surface water salinity in May 2013 is lower than groundwater salinity. This is again suggestive that recharging river water has the potential to create a zone of fresh groundwater near the river channel.

Groundwater salinity increases downstream of the Astana Valley, as does river water salinity. We know that the Astana River is itself saline, being fed by saline groundwater baseflow from the Neogene (and stratigraphically lower) aquifers of the area. It is also possible that the Astana Valley is also associated with a discharge of saline *groundwater* into the alluvial deposits of the Shirin Tagab valley.

Downstream of the Astana confluence, the salinity of both river and groundwater increases, although the river water salinity (as of May 2013) is still lower than the groundwater salinity.

Figure 8.6 shows the variation of electrical conductivity in the immediate vicinity of the Shirin Tagab in the southernmost part of Shirin Tagab district (near Islam Qala). As in Figure 8.5, the very lowest salinity groundwater sources are in the immediate vicinity of the river channel, strongly supporting the hypothesis that recharging river water creates a zone of fresh groundwater near the river channel. This progressively mixes with more saline "ambient" groundwater with distance from the river.

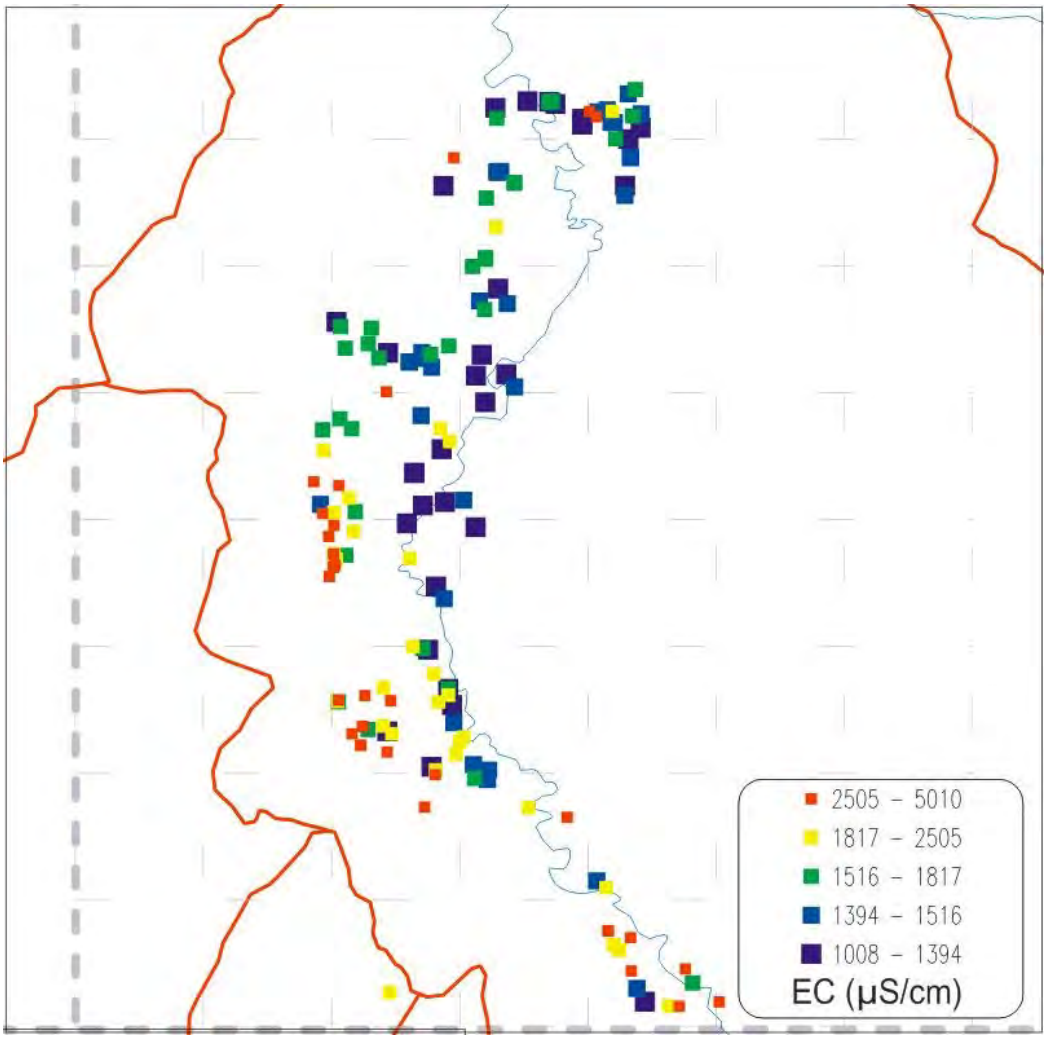

Figure 8.6. Groundwater electrical conductivity in wells, boreholes and springs in the Islam Qala area of Shirin Tagab district (red outlines show district boundaries, blue line shows Shirin Tagab River). All available data in the NORPLAN database as of April 2014 have been used. For location, see Figure 8.3. Symbols are based on 5 equal percentile classes of 20%.

Downstream of Araba and Jar Qala there is no great increase in the mean electrical conductivity of groundwater (Figure 8.4), although its variability seems to increase. We will recall from Chapter 6, that at Araba, the river loses almost all its flow to irrigation offtake, and then regains it by groundwater baseflow. It is thus no surprise to see, in Figure 8.3, the river water gaining an electrical conductivity comparable to the groundwater's in this section.

Below Qoraish, there are very few groundwater abstractions and the apparent increase in salinity (green line) is probably partially an artefact of very few data. However, the very fact that there are few registered abstractions is probably an indication that the groundwater is saline. This zone coincides with an influx of saline water from the Shor Darya (which means "salty river").

8.5 *Andkhoi area*

By Andkhoi (Figure 8.4), the salinity is up in the several thousands of µS/cm, although salinity does appear to decrease northwards (Figure 8.2) as the groundwater level becomes deeper in the Khani Chahar Bagh region (Figure 6.10b). This can be clearly seen in the map of Figure 8.7.

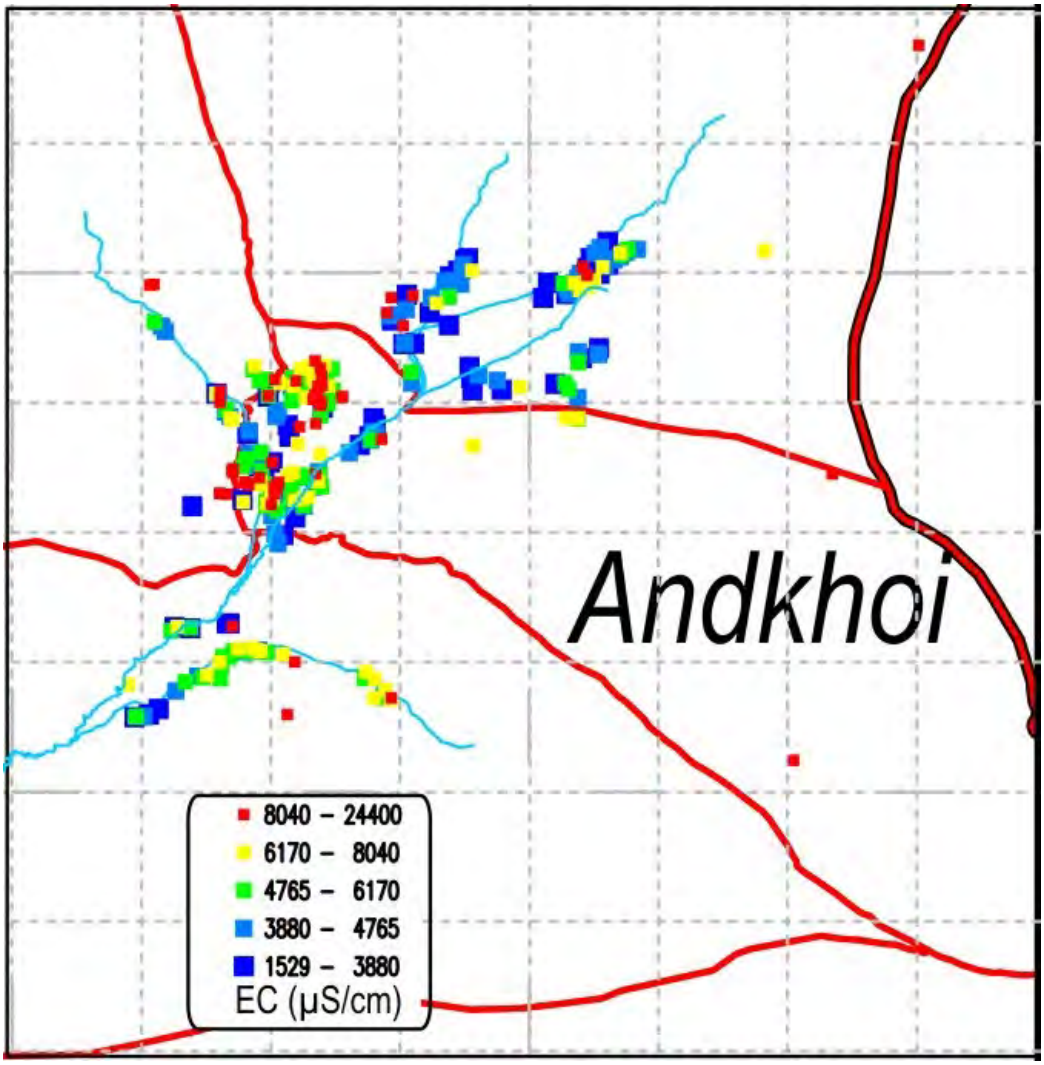

Figure 8.7. Groundwater electrical conductivity in wells, boreholes and springs in the Andkhoi area (red outlines show district boundaries, blue line shows Shirin Tagab River and distributaries). All available data in the NORPLAN database as of April 2014 have been used. For location, see Figure 8.3. Symbols are based on 5 equal percentile classes of 20%.

In NORPLAN's opinion, the question of the reason for the less saline groundwater at the northern end of the Andkhoi delta should form an important research topic for future years: is it because the groundwater is deeper here, and, if so, could fresher groundwater be found at depth throughout Andkhoi? Or is it because very little evapoconcentrated surface water reaches the northern end of the Andkhoi delta to recharge and "contaminate" the groundwater? Are we looking at resources of "fresher" river recharge water from a wetter geological epoch (pluvial period)?

In fairness it should be pointed out the concept of "fresh" is relative: the least saline water of the Andkhoi area (Figure 8.7) has a conductivity of 1529 µS/cm and over 80% of the groundwaters have a salinity exceeding 3800 µS/cm.

8.6 Chechaktu Valley

Finally, the alluvial corridor of the Checkaktu and associated rivers shows a very similar picture (Figure 8.4): i.e. one of steadily increasing groundwater salinity in a downstream (westerly) direction.

8.7 Empirical relationship between electrical conductivity and dissolved solids

In 2013 132 wells, boreholes and springs were sampled in Kohistan, Qaysar, Gurziwan, Bilchiragh and the four northern districts around Andkhoi. The samples were analysed at the laboratory of the British Geological Survey (BGS) at Keyworth, Nottinghamshire, UK. The BGS calculated total dissolved solids (TDS) in mg/L for the samples. The analyses also allowed us to calculate the anion and cation contents in meq/L.

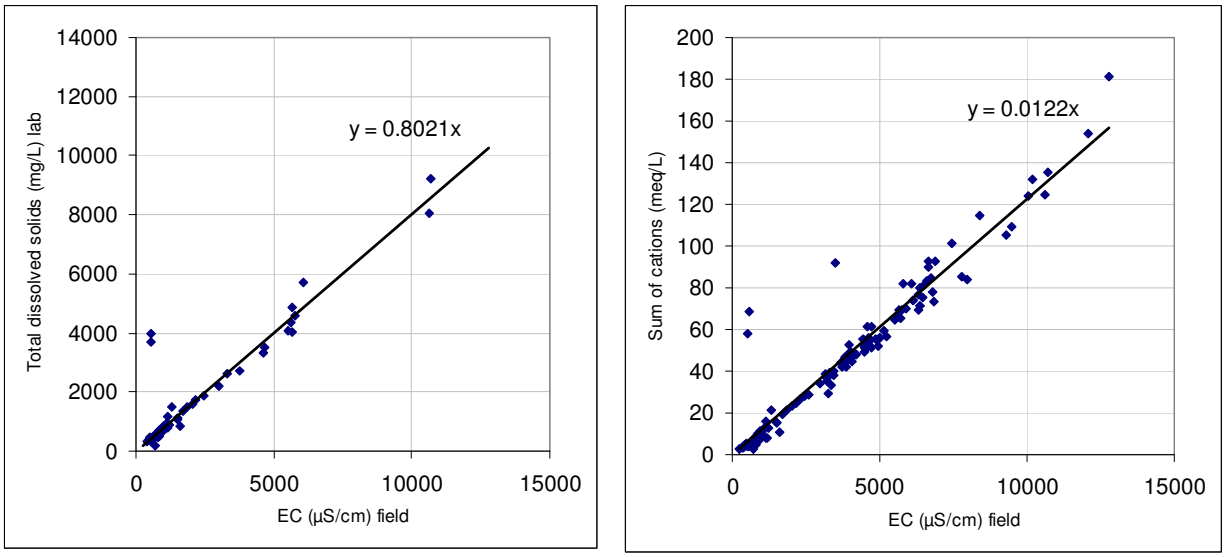

Figure 8.8. Relationship between field electrical conductivity (µS/cm, x axis) and (left) **Total dissolved solids (mg/L) according to analyses by BGS and** (right) **cation content in meq/L.** A couple of "rogue" field EC values occur in the data-set.

From these empirical data it appears that, for this data set:

1 meq/L of cations (or 1 meq/L of anions) results in 82 µS/cm of EC (8.4)

or

M (mg/L) = EC (µS/cm) x 0.8 (8.5)

The use of Equation 8.3 to convert groundwater mineralisations from Soviet literature to equivalent electrical conductivities will therefore have probably led to a modest overestimation of a few of the highest electrical conductivities in the plots of this Chapter.

9. Faryab: Groundwater Hydrochemical Types

9.1 Ion Balance Error

In 2013, 132 wells, boreholes and springs were sampled in Kohistan, Qaysar, Gurziwan, Bilchiragh and the four northern districts around Andkhoi. The samples were analysed by inductively coupled plasma mass spectroscopy (ICP-MS), ion chromatography and other techniques at the laboratory of the British Geological Survey (BGS) at Keyworth, Nottinghamshire, UK. The analytical data from this sampling round will be discussed further in Chapter 10.

The major ion concentrations in the samples were converted to milliequivalents per litre (meq/L) - i.e. millimoles per litre of charge - and ion balance errors were calculated. The vast majority of samples (88%) had an ion balance within ±5%, while 93% were within 10%. The larger ion balance errors were typically in favour of anions and were from the earliest batches of samples from Gurziwan and Bilchiragh, where filtration techniques had not yet been perfected and where any particulates in the water may have led to overestimates of bicarbonate alkalinity.

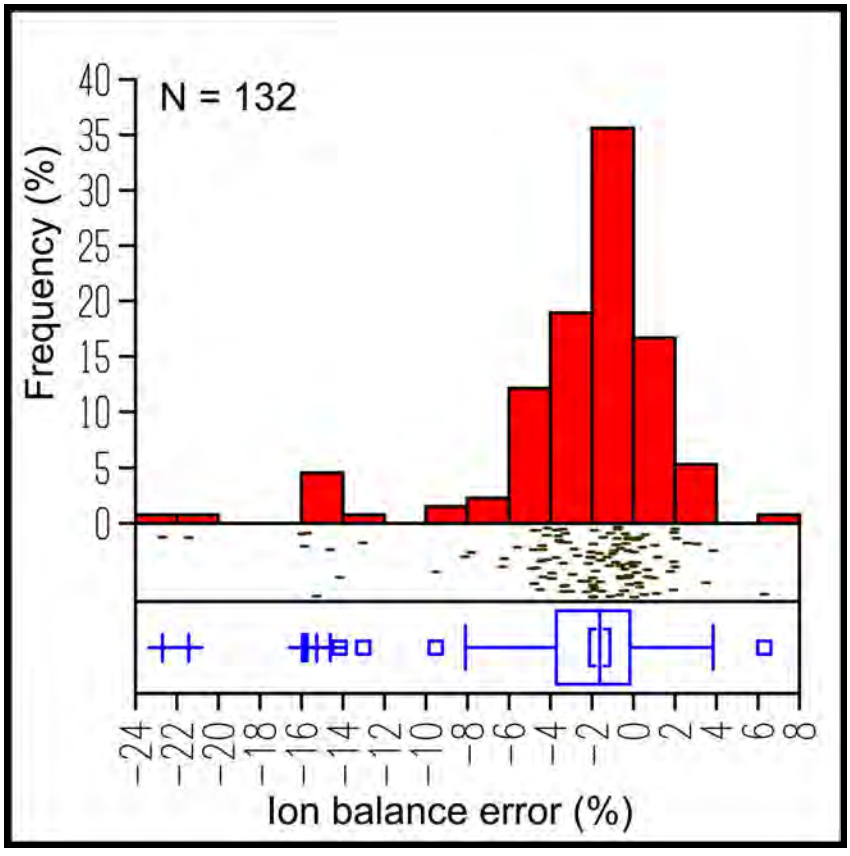

Figure 9.1. Distribution of ion balance errors in 132 samples from Faryab, shown as a histogram, scatterplot and boxplot.

9.2 Durov diagram

Having converted the 132 analyses to meq/L, they could now be plotted on a so-called Durov diagram (Figure 9.2), kindly prepared for us by the Geological Survey of Norway.

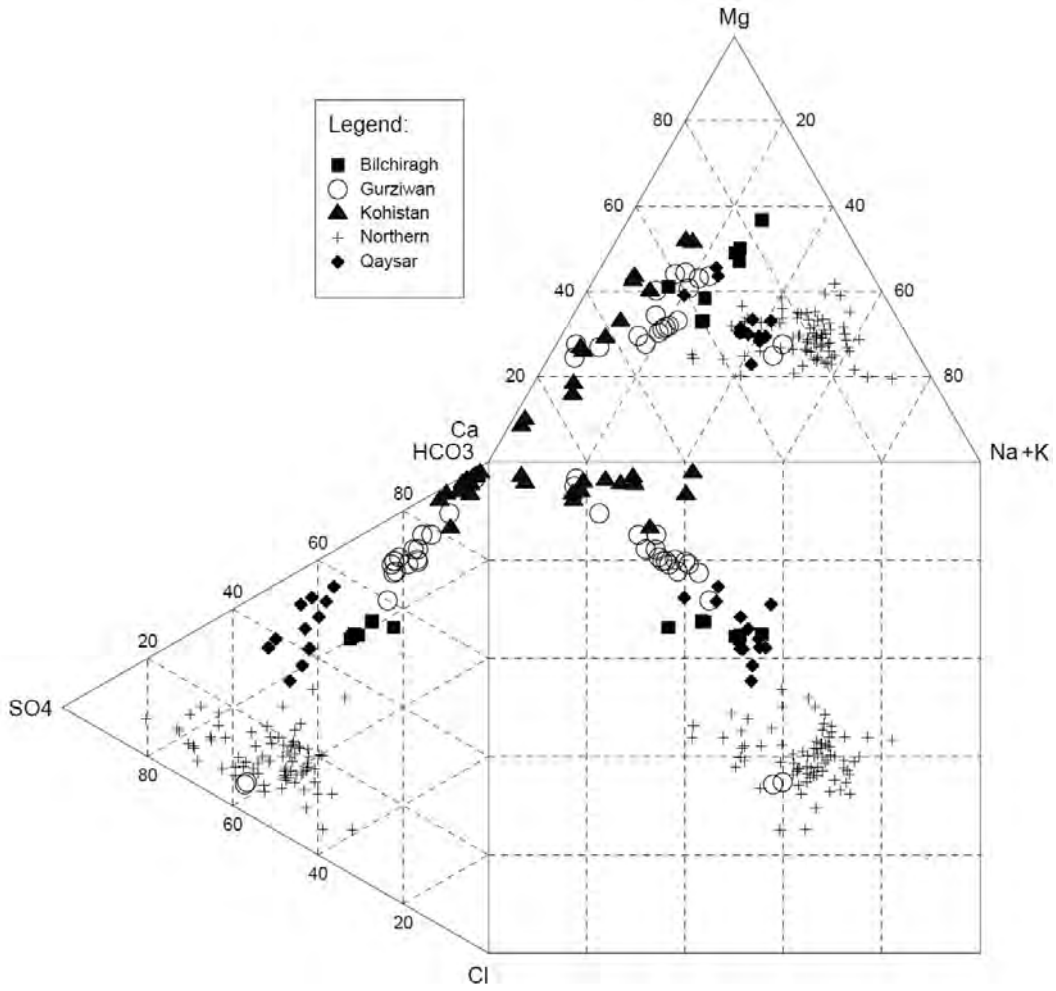

Figure 9.2. Durov diagram showing the major ion composition of 132 groundwaters in Faryab (sampled 2013) in terms of Na-Ca-Mg / SO_4-HCO_3-Cl ion composition. Plotted according to meq/L concentration (K is added to Na in the plot). Many thanks to Dr. Bjørn Frengstad, of the Geological Survey of Norway, for plotting this diagram.

It will be seen that the southern samples from Kohistan and Gurziwan (also the least saline) are dominated by calcium (sometimes magnesium) as the main cation and bicarbonate as the main anion. We say therefore that these are Ca-HCO_3 or Mg-HCO_3 waters.

Further north, in Bilchiragh, groundwaters are more likely to be Mg-HCO_3. In Qaysar samples are without a characteristic dominant ion. The dominant anion could be sulphate or bicarbonate, whereas the cations are relatively evenly balanced, the dominant one being either sodium or magnesium.

In the four northern districts, sodium becomes the dominant cation, with sulphate (or sometimes chloride) becoming the dominant anion. The groundwaters with the sodium chloride composition are typically beneath the very centre of Andkhoi city (Figure 9.3). In the north of the Andkhoi delta, in Khani Chahar Bagh, there are even a few groundwaters of dominant calcium sulphate composition.

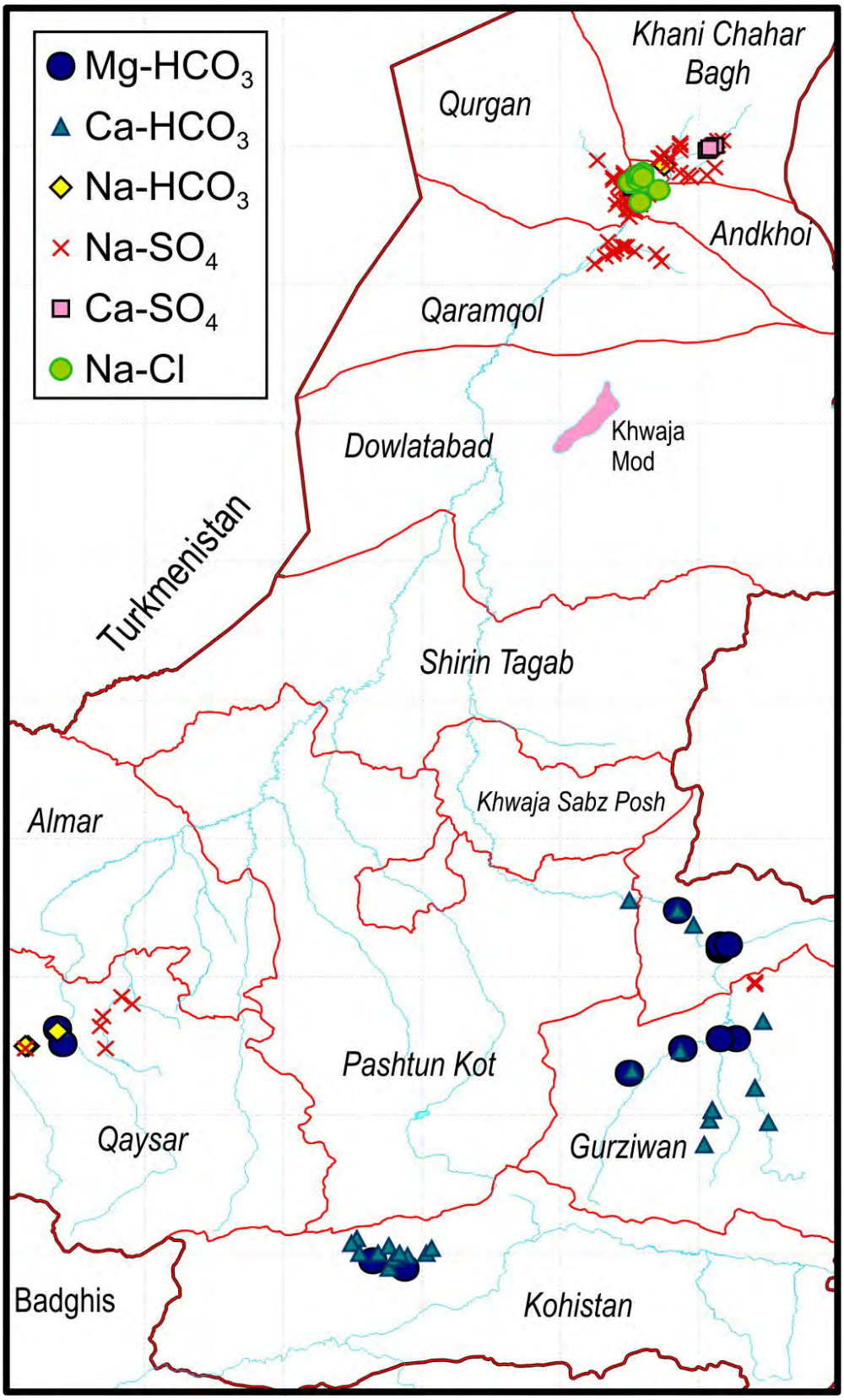

Figure 9.3. The 132 groundwaters sampled in 2013, classified according to dominant cation and anion, according to meq/L concentration.

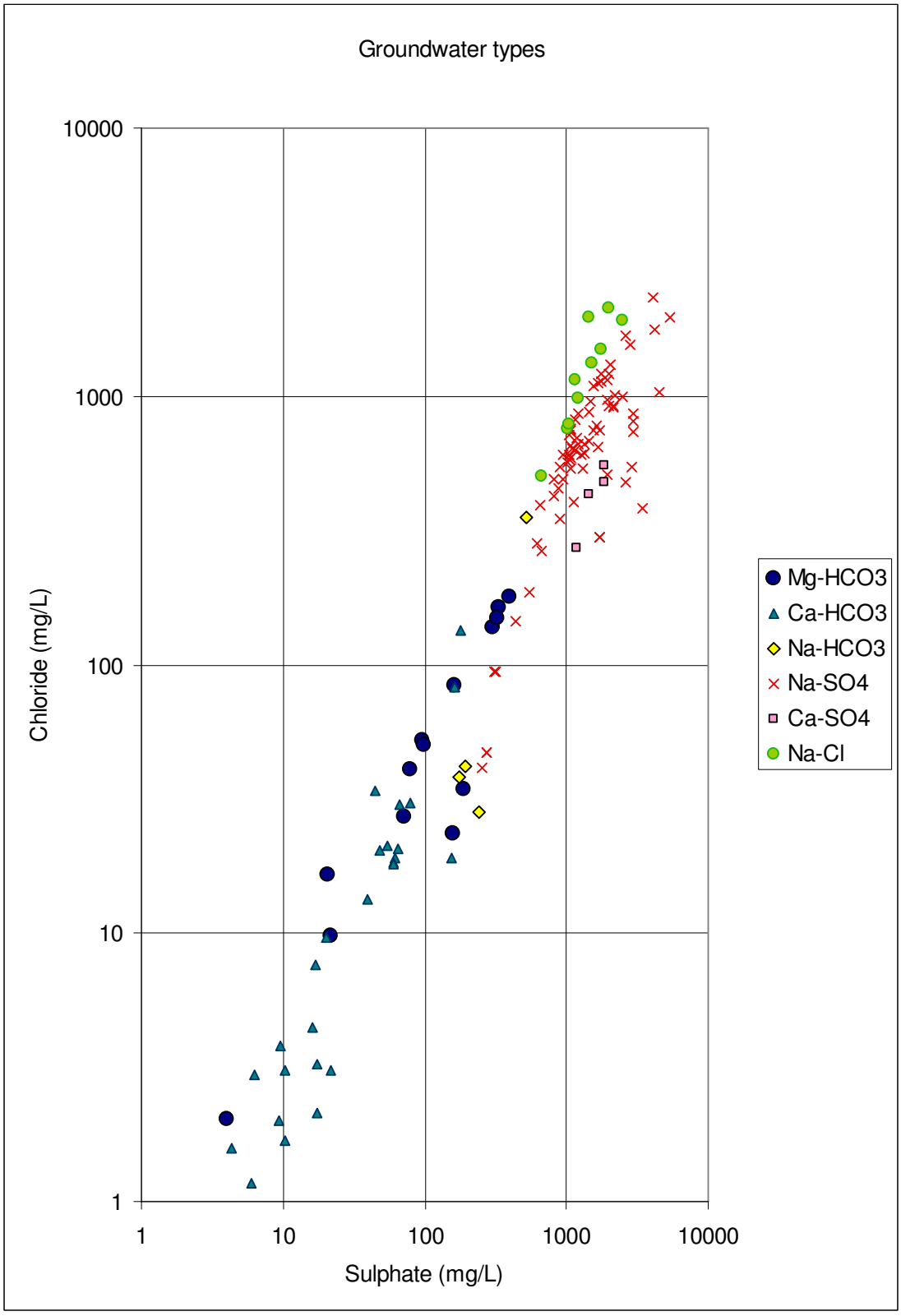

Figure 9.4. Chloride concentrations in the 132 groundwaters sampled in 2013, plotted against sulphate concentrations, and subdivided according to water type. Note the logarithmic scales in both axes.

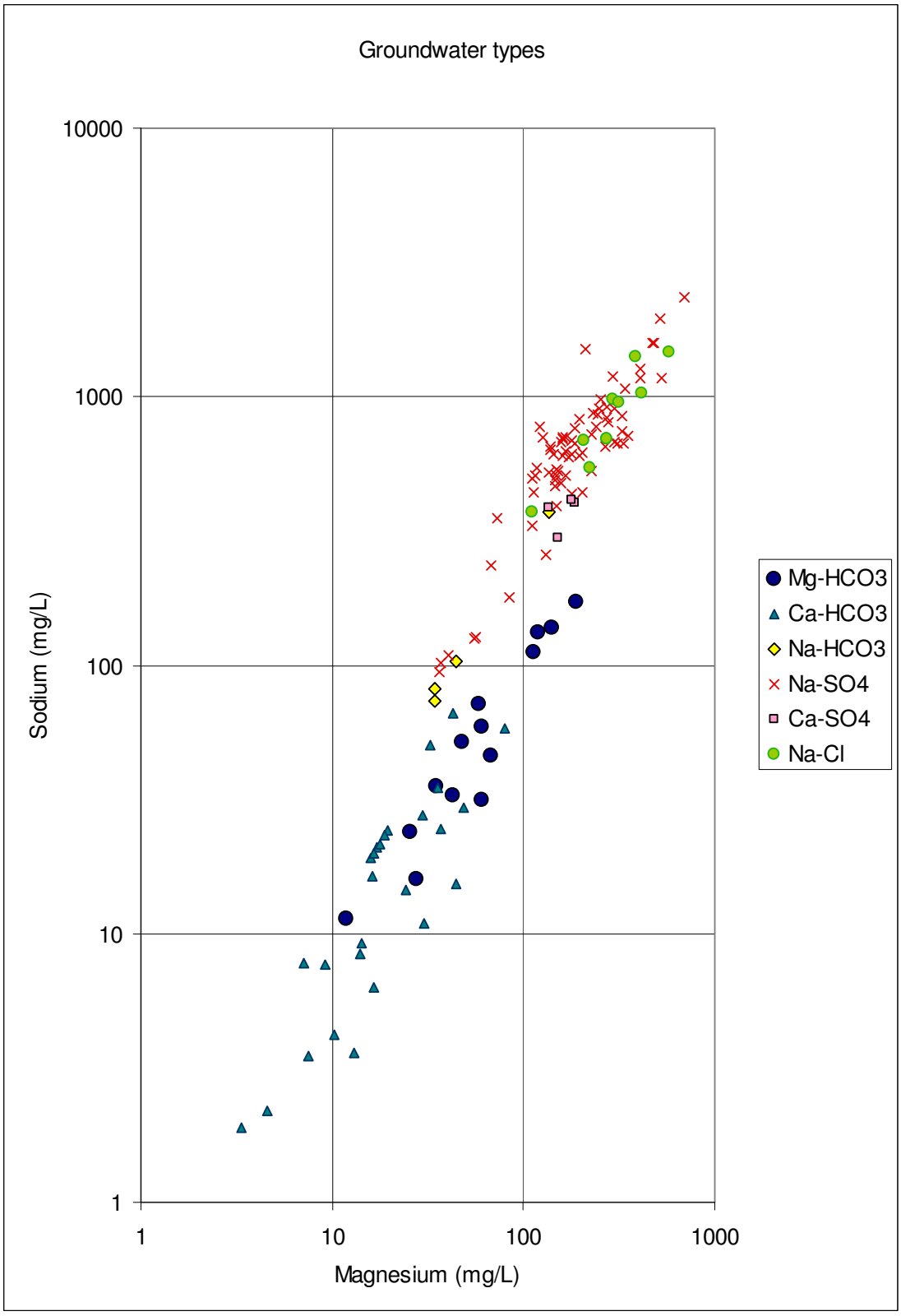

Figure 9.5. Sodium concentrations in the 132 groundwaters sampled in 2013, plotted against magnesium concentrations, and subdivided according to water type. Note the logarithmic scales in both axes.

We can create a large number of plots to clarify the evolution of major ion concentrations in the groundwaters. A small selection of these is shown in Figures 9.4 - 9.7.

Figure 8.4 shows chloride concentrations, plotted against sulphate concentrations, and subdivided according to water type. The following features should be noted:

- That the plotted waters appear to largely fall on a *continuum*;
- The chloride and sulphate concentrations increase roughly in proportion with each other (the gradient of the line is almost, but not exactly, 1:1).

These two observations are strongly indicative of evaporative processes driving up-concentration of the waters from south to north.

- The dominant cation in the water changes with increasing $SO_4^{=}/Cl^-$ concentration - from Ca in the lowest salinity waters, to Mg in the medium salinity waters and finally to Na in the most saline waters.
- The dominant anion in the water changes with increasing salinity - from HCO_3^- in the lowest salinity waters, to $SO_4^{=}$ or Cl^- in the most saline waters.

Figure 9.5 shows a similar plot for sodium concentrations against magnesium concentrations. This plot shows similar characteristics to Figure 9.4, except that the slope is greater than 1:1 - in other words, sodium accumulates in the water to a greater extent than magnesium (which should be unsurprising, as sodium "overtakes" magnesium as the dominant cation in the most saline waters).

9.3 Major ion ratios

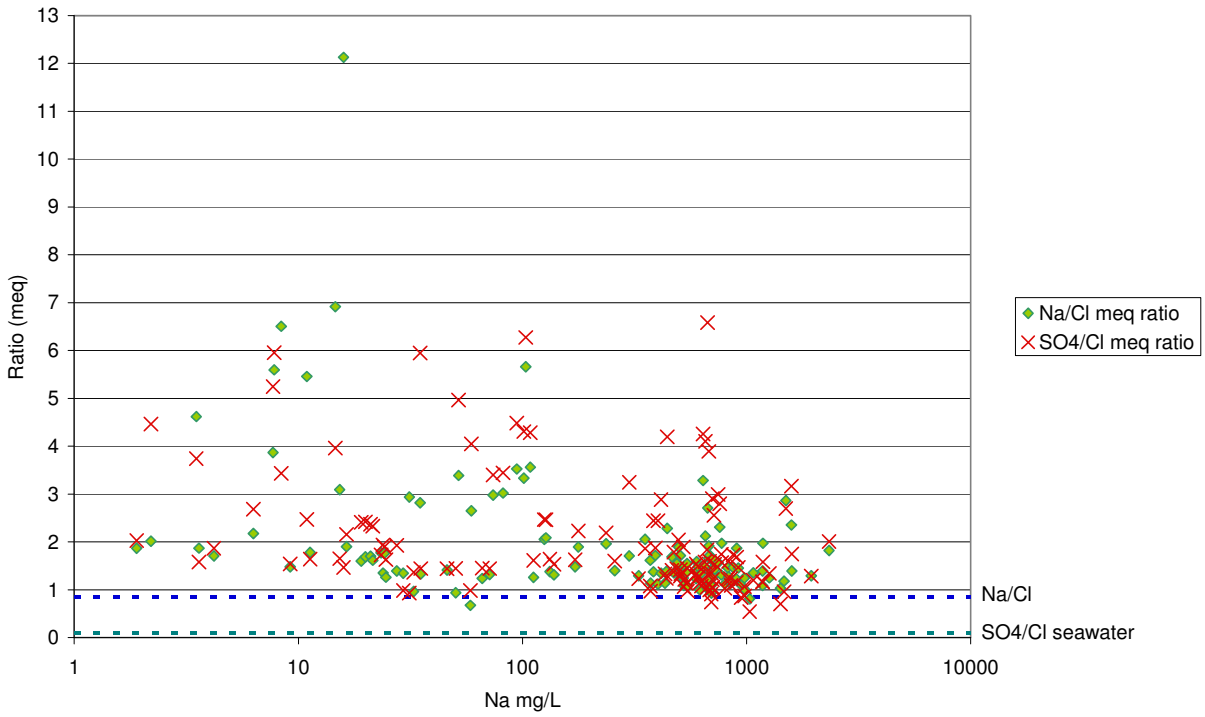

Figure 9.6. Milliequivalent ratios of Na/Cl^- and $SO_4^{=}/Cl^-$ in the 132 Faryab groundwater samples of 2013. Seawater ratios are shown by the dotted lines and are derived from data in Dickson & Goyet (1994).

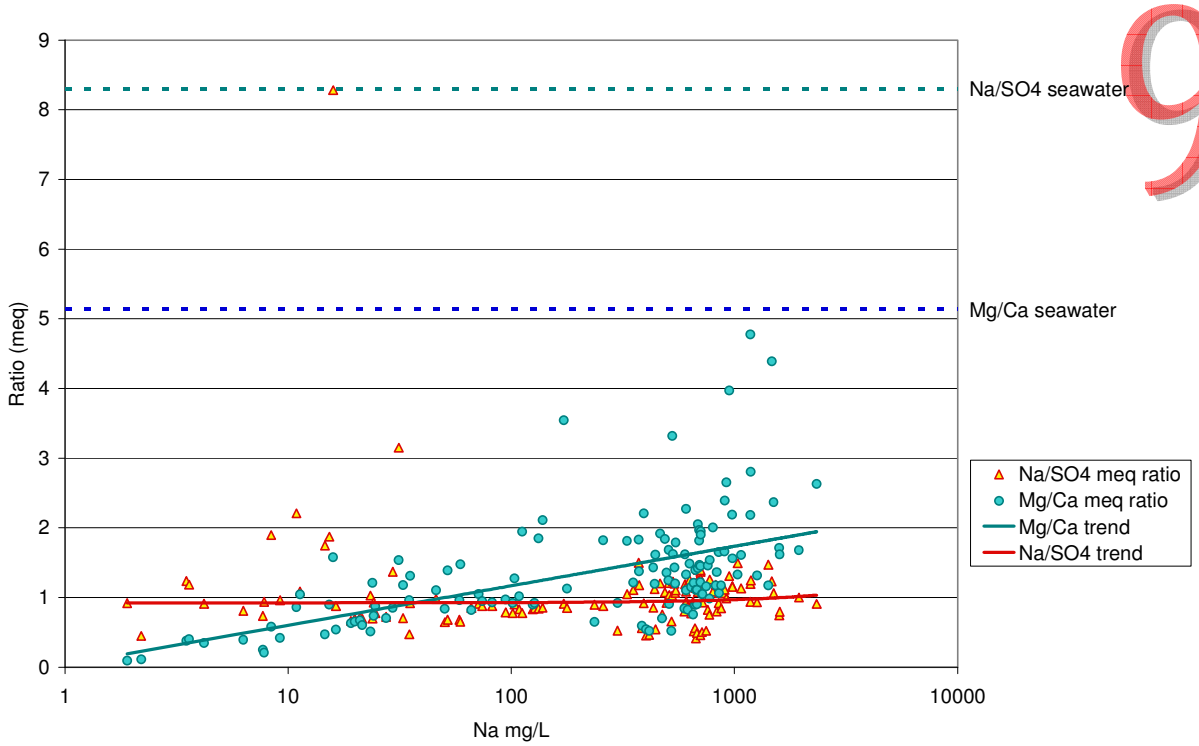

Figure 9.7. Milliequivalent ratios of Mg/Ca and Na/$SO_4^=$ in the 132 Faryab groundwater samples of 2013. Seawater ratios are shown by the dotted lines and derived from data in Dickson & Goyet (1994).

Figure 9.6 shows the ratios of sodium to chloride and sodium to sulphate as meq, with increasing sodium concentration. There is a very wide scatter in the data. However, at low salinities, the ratios tend to vary from 1 to 7. As salinity increases to high values, the ratios tend to converge towards values between 1 and 2, as the waters become dominated by Na^+, Cl^- and $SO_4^=$ in their major ion composition.

Figure 9.7 shows the ratios of sodium to sulphate and magnesium to calcium as meq, with increasing sodium concentration. The Mg/Ca ratio shows a steady increase with increasing salinity, from around 0.1 at low salinity to over 2 at high salinity. The ratio of 0.1 is characteristic of geologically recent intermediate-high magnesium calcite dissolution (Carpenter & Lohmann 1992, Railsback 2006 - see also Figure 9.11). In the most saline groundwaters of Faryab, the Mg/Ca ratio begins to approach the seawater ratio of c. 5. The sodium : sulphate meq ratio is relatively independent of salinity. It is typically around unity, although the variability decreases with increasing salinity.

9.4 Groundwater evolution

In Figure 9.9, the 132 waters have been sorted according to increasing sodium concentration and the relative proportions of their major cations and anions are shown as %-bar diagrams. In the top diagram, we can see that the proportion of sodium increases consistently throughout the series - in other words, **sodium is accumulated as a solute - there are few controls on its solubility.** In contrast, the proportion of calcium diminishes - **there appears to be a control on calcium accumulation**. Potassium is a minor, but consistent component of all samples. As regards anions, the proportion of bicarbonate diminishes - there appears to be a control on its accumulation. Sulphate and chloride concentrations appear to accumulate at the expense of bicarbonate, with few apparent controls on their solubility. It should be noted, however, that, in the lowest salinity samples, sulphate represents a considerably

greater proportion of the anion content than chloride, while the relative content of chloride is greater in the higher salinity samples.

Figure 9.10 shows how the absolute concentrations of the major ions increase as chloride concentration (a surrogate for salinity) increases. It will be seen that the trends for sodium and sulphate are generally identical, both typically exhibiting higher concentrations than chloride (though admittedly with significant variation: we know there are a number of waters where chloride is the dominant anion). Sodium, chloride and sulphate all exhibit approximately linear best-fit trends - they accumulate in proportion to each other with no apparent limits on solubility.

Calcium, on the other hand, does not accumulate in the same way. Its solubility appears to be limited at somewhere around 25 meq/L in the most saline samples and the trend line flattens out. The same applies to bicarbonate alkalinity: concentrations do not accumulate beyond c. 10 meq/L.

It is tempting to suggest that calcium and bicarbonate concentrations are limited by a calcite ($CaCO_3$) solubility ceiling. In the low salinity samples, calcium and bicarbonate dominate, as they can be dissolved relatively rapidly from calcite in the limestone and sedimentary rocks in the south of the province.

As regards magnesium (Figure 9.10) this accumulates more efficiently than calcium or bicarbonate, but its solubility also appears to be inhibited in the more saline samples. Magnesium could be being removed by re-precipitation as high-Mg calcite, dolomite ($CaMg(CO_3)_2$) or sepiolite ($Mg_4Si_6O_{15}(OH)_2 \cdot 6H_2O$), for example.

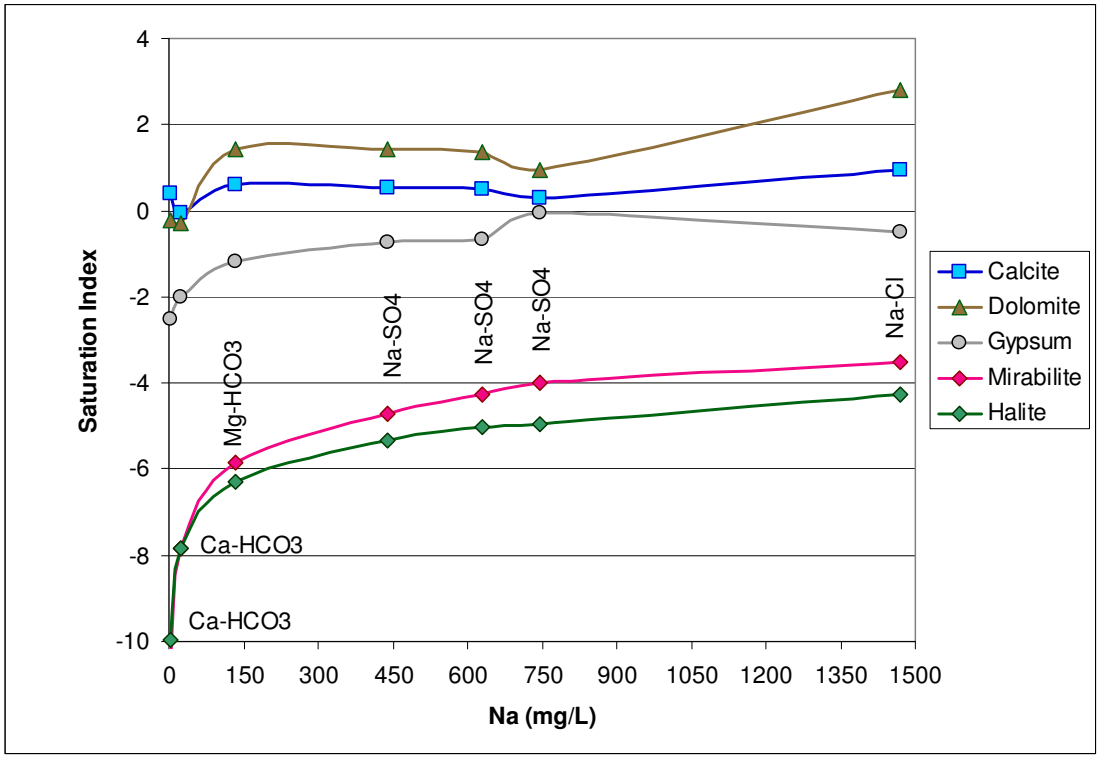

Figure 9.8. Results of PHREEQCI modelling of seven of the 132 Faryab groundwaters sampled in 2013. A saturation index of zero or above indicates that the water is saturated (or oversaturated) with the mineral in question. A negative index indicates that it is undersaturated. Water type is indicated for each sample.

The programme PHREEQC Interactive (PHREEQCI), described by Parkhurst (1995), was used to hydrochemically model seven of the 132 groundwaters, sampled in 2013, spanning the range of salinity variation. The waters selected for modelling had low ion

balance errors and did not have excessive nitrate concentrations (which might be indicative of contamination). The PHREEQC and MINTEQ v. 4 thermodynamic databases were utilised for the lower salinity groundwaters, while the PITZER database (see Plummer et al. 1988) was applied to the higher salinity waters (although the differences between the PITZER/MINTEQ/PHREEQC results were very modest). Figure 9.8 shows the results of the modelling for selected mineral phases.

All samples are saturated with respect to **calcite ($CaCO_3$)**. Calcite is ubiquitous in rocks and sediments and dissolution is rapid. A modest oversaturation appears to develop in the most saline samples. Calcite saturation means that, unless either calcium or carbonate alkalinity are removed from the water, these ions cannot efficiently accumulate further (as is demonstrated in Figure 8.10).

While **dolomite ($CaMg(CO_3)_2$)** is very slightly undersaturated in the two lowest salinity samples, it is saturated in all the other samples. At face value this would suggest that further accumulation of magnesium would be problematic. However, we empirically observe that magnesium continues to accumulate in the water (Figure 9.10) and that significant oversaturation with dolomite begins to develop (Figure 9.8). These observations suggest that dolomite is not effective at limiting Mg concentrations, possibly because of kinetic constraints on its precipitation from groundwaters. Some suppression of Mg accumulation is observed in the most saline samples (Figure 9.10), which could also be due to saturation with respect to the more soluble "disordered dolomite" structure or **magnesite ($MgCO_3$).**

Gypsum ($CaSO_4.2H_2O$) only approaches saturation in the most saline samples. This suggests that, if the salinity were to increase beyond the most saline samples, further sulphate accumulation in the system may be hindered by gypsum saturation. There is little sign of this in the samples collected in 2013 in the NORPLAN study, but it may help to explain why the most saline waters mapped by Mishkin (1968 - Figure 8.1) are predominantly sodium chloride, rather than sodium sulphate waters. Gypsum saturation would not completely prevent the further accumulation of gypsum, however, if sulphate exceeds calcium in the groundwater, and if the water is saturated with calcite, continued evaporative concentration, or exposure to sulphate minerals in sediments, might allow further sulphate accumulation at the expense of calcite precipitation to remove calcium.

None of the minerals **halite (NaCl)**, **mirabilite ($Na_2SO_4 \cdot 10H_2O$)**, **thenardite (Na_2SO_4)** or **epsomite ($MgSO_4 \cdot 7H_2O$)** reach saturation in the modelled samples. There are thus no solubility controls on sodium and chloride, which can continue to accumulate in the waters unhindered.

In summary, the evolution of the water systems in Faryab is very similar to that observed by Parnachev et al. (1999) and Banks et al. (2004) in the semi-arid steppe environment of southern Siberia. The fundamental features in the Siberian model were:

- Rainfall and recharge solutes in a continental environment are not characterised by marine or industrial salts (as is the case in Britain and Norway) but by dissolution of wind blown salts, potentially including halite, gypsum/anhydrite and mirabilite from saline soils or solonchaks.
- These salts are up-concentrated by evaporation during recharge, and are supplemented by Ca, Mg and HCO_3 from dissolution of calcite from limestone and sedimentary rocks, and by Na, Ca, HCO_3 and other base cations from hydrolysis of feldspars and other silicates.
- In the total hydrological system (recharge - surface water - [agricultural irrigation in the case of Faryab] - groundwater) solutes are steadily concentrated by evaporative processes and dissolution of evaporite minerals such as gypsum and halite from soils. This leads to parallel accumulation of Cl^-, Na^+, $SO_4^=$

- Saturation with respect to calcite hinders further accumulation of calcium and alkalinity in waters.
- Dolomite precipitation is not wholly effective at constraining Mg accumulation, due to kinetic factors.

All of these factors are also readily recognisable in Faryab. It should be emphasised that, when we talk of *evapoconcentrative processes* dominating groundwater evolution, this term could encompass:

- Direct evapoconcentration of dissolved salts in recharge water during evapotranspiration of rainfall on vegetation or in shallow soils.
- Dissolution of wind-blown evaporite salts by recharging rainfall or snowfall.
- Direct evaporation of river water and subsequent infiltration to the aquifer system.
- Evapotranspiration of river water or groundwater used for irrigation of fields, followed by re-infiltration to the ground.
- Dissolution of evaporite salts in the unsaturated or saturated zone of the groundwater system. These evaporite salts could be recent and represent salts deposited in shallow soil by evaporating surface water or rainwater (see Table 9.1). They could also represent geologically older palaeoevaporite salts, such as the gypsum and halite reportedly found in Neogene strata.

This latter may seem not to be an evapoconcentrative process - but the presence of evaporites in, say Neogene sediments, essentially represents geologically stored "evapoconcentration".

9.5 Soluble salts in soils

Let us therefore look briefly at the contents of soluble salts in soils of Faryab. Soils were sampled in January-March 2013. At each of eight sites, two samples of c. 1.5 kg were taken from 40 cm depth and two of 1.5 kg from 70 cm depth. Samples were returned to the laboratory of DACAAR and air-dried. Samples were then sieved through a 2 mm nylon mesh. Then:

- 20 g of the <2 mm dry soil fraction were added to 400 mL distilled water in a clean 500 mL flask and shaken for 1 hr.
- The flask was stood for 20 hours and the sediment allowed to settle.
- The supernatant liquid was then extracted with a clean polypropylene syringe and injected, via a new 0.45 µm filter, into a new clean 60 mL flask.
- The 60 mL flasks were shipped to the laboratory of the British Geological Survey at Keyworth UK, for analysis by ion chromatography and ICP-MS methods. Samples of the distilled water were also shipped for control analysis.

With the exception of modest concentrations of a very few elements, the distilled water was found to be of good quality. The samples were corrected for any minor element concentrations in the distilled water "blank". The concentration (Table 9.1) of the soluble element or ion (C_{sol}) in mg/kg of the air-dried, sieved sediment was back-calculated from the corrected concentration in the liquid extract (C_{liq}) by:

C_{sol} (mg/kg) = C_{liq} (mg/L) x (400 mL / 1 L) x (1 kg / 20 g) = C_{liq} x 20

Sample locations are shown in the map of Figure 9.11. Most of the soils sampled could be described as silty clays, while the underlying geology is indicated in Table 9.1.

There is no clear indication that the content of soluble salts increases in a northerly direction, nor that shallow soils on Neogene sedimentary rocks or loess always have high salt contents. We should remember that these soil samples are shallow and may not represent the soluble salt content of the underlying geological materials, which may have been dissolved / weathered away from the shallow soil profile. Figure 9.11, which plots the meq/L ratio of some soluble ion contents in the soils does show some interesting features, however.

In five of the eight samples, the calcium : sulphate ratio is much greater than unity, suggesting the calcite, or sorbed calcium on ion exchange sites, may be the main readily soluble calcium source in these soils. Figure 9.11 shows that the Mg/Ca molar ratio in the southernmost samples is around 0.1, probably representing the ratio in calcite ($CaCO_3$) and also reflecting the ratio in groundwaters of the southern area. The Mg/Ca ratio of soils (and groundwaters) increases to the north.

The sodium to chloride ratio is around 1 in the southernmost soil samples but tends to increase to the north. This may reflect the accumulation of other sodium minerals in the soil zone (in addition to halite - NaCl), such as mirabilite (sodium sulphate).

In each case, where the ratio is close to unity, this may be an indication that the mineral phase represented by that ratio may be a dominant salt component in the soil. For example:

- At Qezel Qul, both sodium : chloride and sodium : sulphate are close to unity suggesting that mirabilite and halite may be a dominant component in the soil or in windblown dust / precipitated salts impacting the soil.
- At Qara Sheikhy, Faizabad and Chakozi, the sodium : sulphate ratio is close to unity, suggesting the mirabilite may be a soil component. In these samples, both the calcium : sulphate ratio and the sodium : chloride ratio are greater than unity, suggesting that gypsum and halite are less important.
- At Yam Boleg, Tortqol Baloj and in the Qaramqol semi-desert, the calcium : sulphate ratio is close to unity, suggesting the gypsum may be an important soil component.
- In the Qaramqol sample, while the calcium : sulphate ratio is close to unity, the sodium : chloride ratio is greater than unity and the sodium : sulphate is less than unity. This is consistent with both modest amounts of halite and mirabilite being present, in addition to gypsum as the dominant component (if 1 mmol mirabilite and 1 mmol halite were present in addition to 5 mmol gypsum, the sodium sulphate ratio would be 1/2, the sodium : chloride ratio 3 and the calcium ratio 5/6)

9. Groundwater Types

Table 9.1. Soluble element / ion concentrations in soil samples	Depth	Ca	Mg	Na	K	Cl^-	SO_4^{2-}	Total S	NO_3^-	F^-	Total P	Sr	B	As	U
Sample location	cm	mg/kg	mg/kg	mg/kg	mg/kg	mg/kg	mg/kg	mg/kg	mg/kg	mg/kg	mg/kg	mg/kg	µg/kg	µg/kg	µg/kg
Qezel Qul, Pashtun Kot district Neogene sediments	40	436	25	12	27	24	27	<20	<0.4	2.5	<0.2	2.6	170	24	4
	40	418	23	12	32	19	25	<20	<0.4	3.2	<0.2	2.5	190	25	6
	70	468	27	16	23	21	34	<20	<0.4	3.1	<0.2	2.8	210	27	5
	70	402	26	14	17	15	32	<20	<0.4	3.6	<0.2	2.5	150	27	5
Median		**427**	**26**	**13**	**25**	**20**	**30**	**<20**	**<0.4**	**3.1**	**<0.2**	**2.6**	**180**	**26**	**5**
Yam Boleg, Maimana district Recent Quaternary alluvium	40	508	27	10	12	3	756	260	27	28	<0.2	34	250	31	31
	40	4812	74	12	17	2	12042	4240	17	28	<0.2	110	190	6.6	52
	70	518	31	14	87	121	670	240	15	14	<0.2	19	270	32	11
	70	4564	90	14	23	0.9	10936	3460	10	25	<0.2	83	230	11	61
Median		**2541**	**52**	**13**	**20**	**3**	**5846**	**1860**	**16**	**26**	**<0.2**	**59**	**240**	**21**	**42**
Sarbulaq, Maimana district Pleistocene loess	40	420	63	38	4.6	9	30	<40	21	4.2	<0.2	7.0	350	16	34
	40	390	56	44	4.2	11	40	<40	25	5.4	<0.2	6.6	370	21	43
	70	488	97	142	5.2	130	48	<40	46	8.0	<0.2	10	450	19	83
	70	418	92	90	5.2	45	207	100	45	8.4	<0.2	11	470	22	78
Median		**419**	**77**	**67**	**4.9**	**28**	**44**	**100**	**35**	**6.7**	**<0.2**	**8.8**	**410**	**20**	**61**
Qara Sheikhy, Shirin Tagab district DACAAR, who collected sample, believe site to be on Neogene (geol. map suggests site may just be on Quaternary alluvium)	40	508	44	16	100	14	77	<40	11	1.7	<0.2	4.2	210	26	7
	40	476	49	18	109	19	28	<40	8.6	1.7	<0.2	3.5	290	25	6
	70	432	46	12	128	13	41	<40	8.0	1.7	<0.2	3.8	210	15	7
	70	382	42	14	135	13	39	<40	5.6	2.1	<0.2	3.5	190	21	7
Median		**454**	**45**	**15**	**118**	**14**	**40**	**<40**	**8.3**	**1.7**	**<0.2**	**3.7**	**210**	**23**	**7**
Tortkol Baloj, Shirin Tagab district DACAAR, who collected sample, believe site to be on Neogene (geol. map suggests site may just be on Quaternary alluvium)	40	1858	96	20	30	8	3999	1460	11	19	<0.2	59	250	8.6	24
	40	1660	108	22	29	4	3747	1340	3.0	16	<0.2	42	230	7.8	18
	70	1342	150	18	25	50	3109	1100	48	3.6	<0.2	31	490	7.0	13
	70	1370	166	34	29	19	3259	1160	36	4.2	<0.2	38	550	9.4	15
Median		**1515**	**129**	**21**	**29**	**13**	**3503**	**1250**	**23**	**10**	**<0.2**	**40**	**370**	**8.2**	**17**
Faizabad, Shirin Tagab District Pleistocene loess	40	508	45	10	37	9	17	<20	<0.4	3.1	<0.2	4.5	190	24	12
	40	422	37	16	19	5	20	<20	<0.4	3.1	<0.2	3.4	270	24	10
	70	406	56	20	11	7	47	<20	3.4	3.7	<0.2	5.5	230	27	15
	70	418	82	16	14	5	14	<20	1.2	4.8	<0.2	7.7	170	18	23
Median		**420**	**50**	**16**	**16**	**6**	**18**	**<20**	**<1.2**	**3.4**	**<0.2**	**5.0**	**210**	**24**	**14**
Chakozi, Dawlatabad district Recent Quaternary alluvium	40	330	35	10	53	1	20	<20	28	2.1	<0.2	3.8	170	24	17
	40	366	35	14	53	4	32	<20	10	1.9	<0.2	4.2	130	34	14
	70	384	44	16	30	3	40	<20	43	2.6	<0.2	5.4	270	20	26
	70	558	54	14	41	2	24	<20	21	3.0	<0.2	7.0	110	14	36
Median		**375**	**40**	**14**	**47**	**3**	**28**	**<20**	**24**	**2.3**	**<0.2**	**4.8**	**150**	**22**	**22**
Semi-desert, Qaramqol district Recent Quaternary alluvium	40	540	110	376	45	278	1422	480	5.8	5.4	<0.2	25	1050	16	5
	40	408	78	212	47	63	878	300	5.8	3.5	<0.2	21	930	19	7
	70	426	76	176	51	37	794	280	5.6	4.6	<0.2	20	870	24	7
	70	402	73	140	52	18	683	240	8.1	4.9	<0.2	20	810	23	8
Median		**417**	**77**	**194**	**49**	**50**	**836**	**290**	**5.8**	**4.7**	**<0.2**	**20**	**900**	**21**	**7**

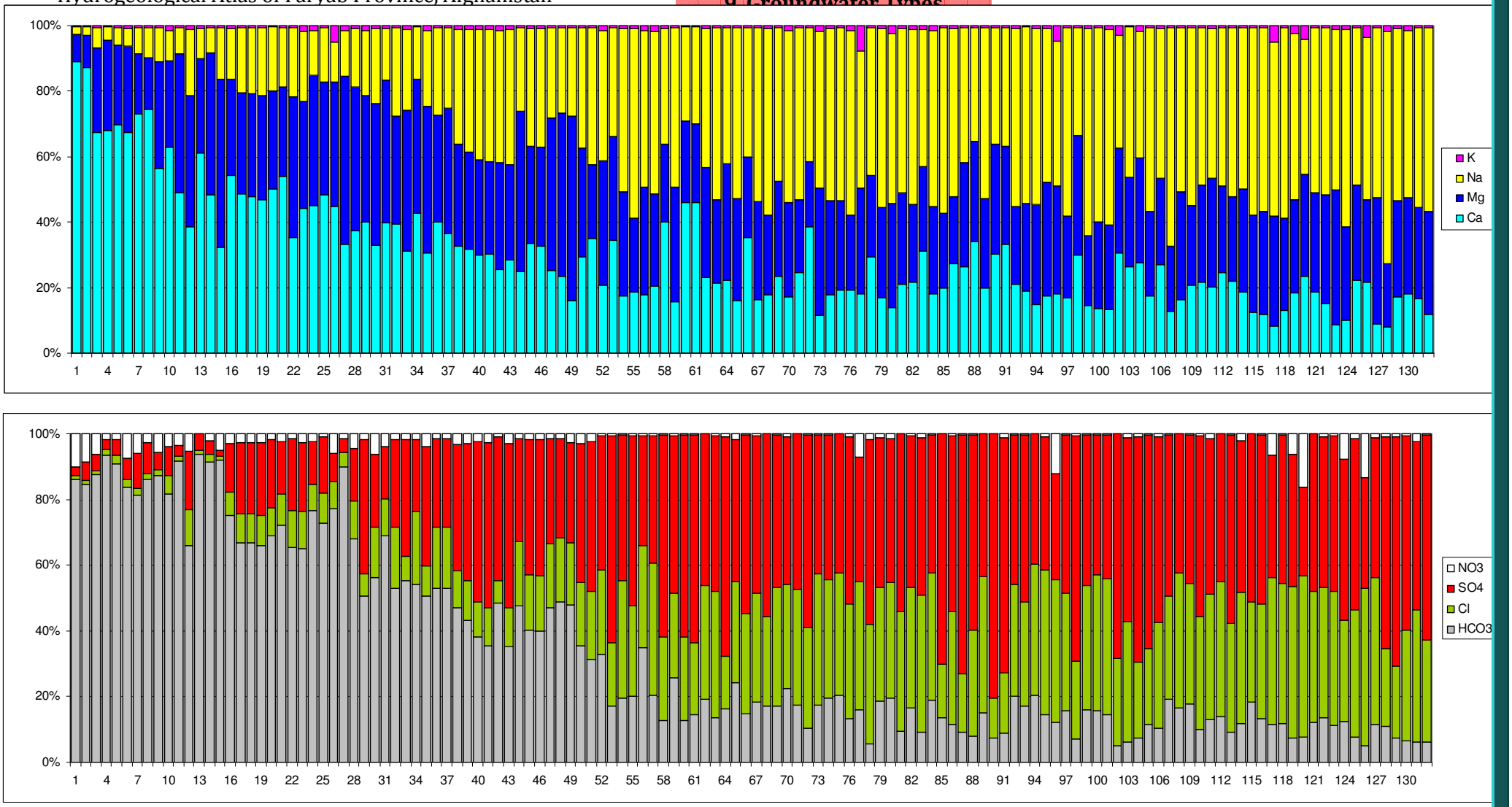

Figure 9.9. Percentage composition (as meq/L) of cation and anion content of the 132 groundwaters from Faryab, sampled in 2013, sorted according to increasing sodium concentration. The number on the x-axis represents the "rank" of the sample according to increasing Na concentration.

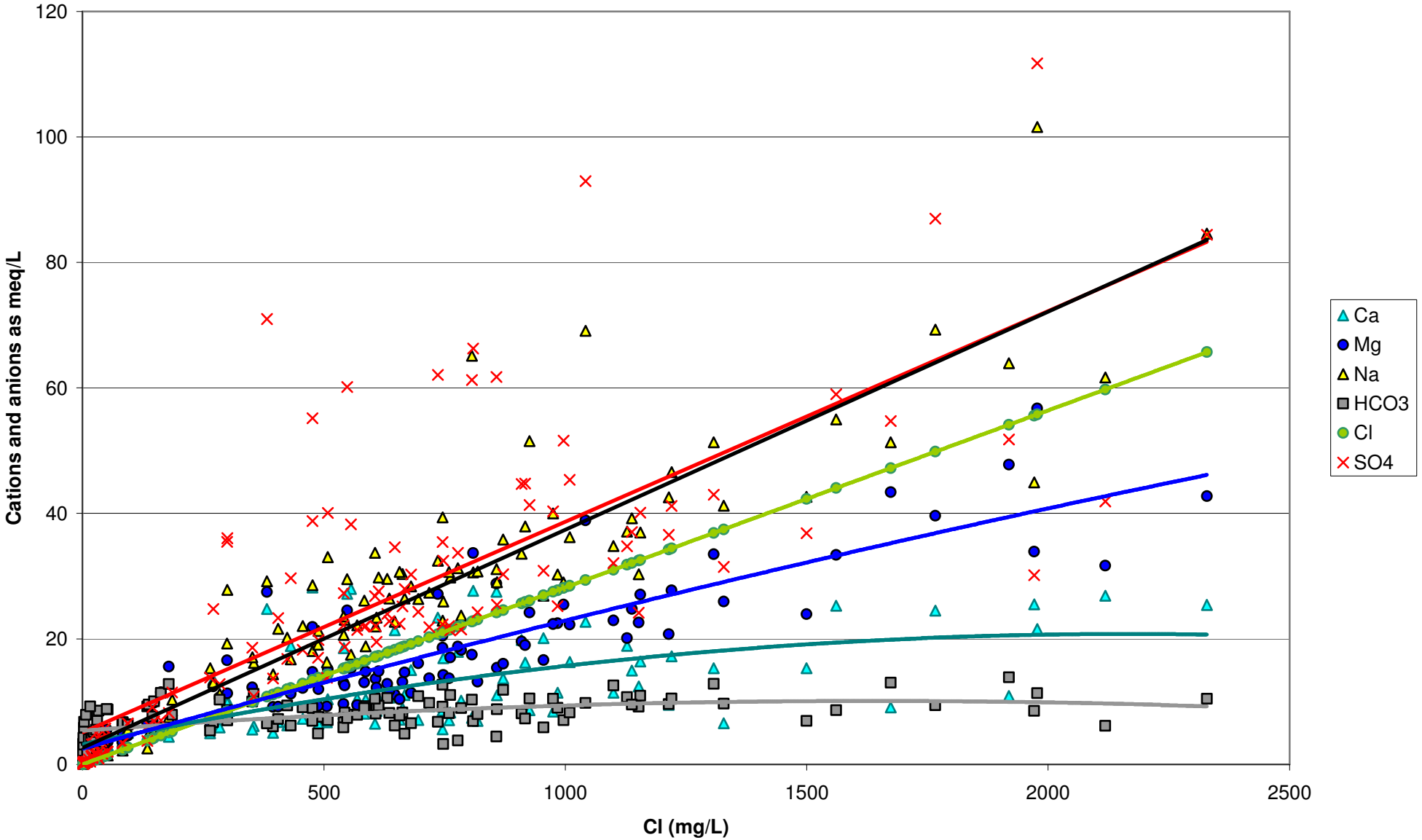

Figure 9.10. Major cation and anion concentrations (as meq/L) in the 132 groundwaters from Faryab sampled in 2013, plotted against chloride concentration (mg/L). Trend lines are either linear or parabolic best fits to widely spread data. Chloride, of course plots as a 1:1 line.

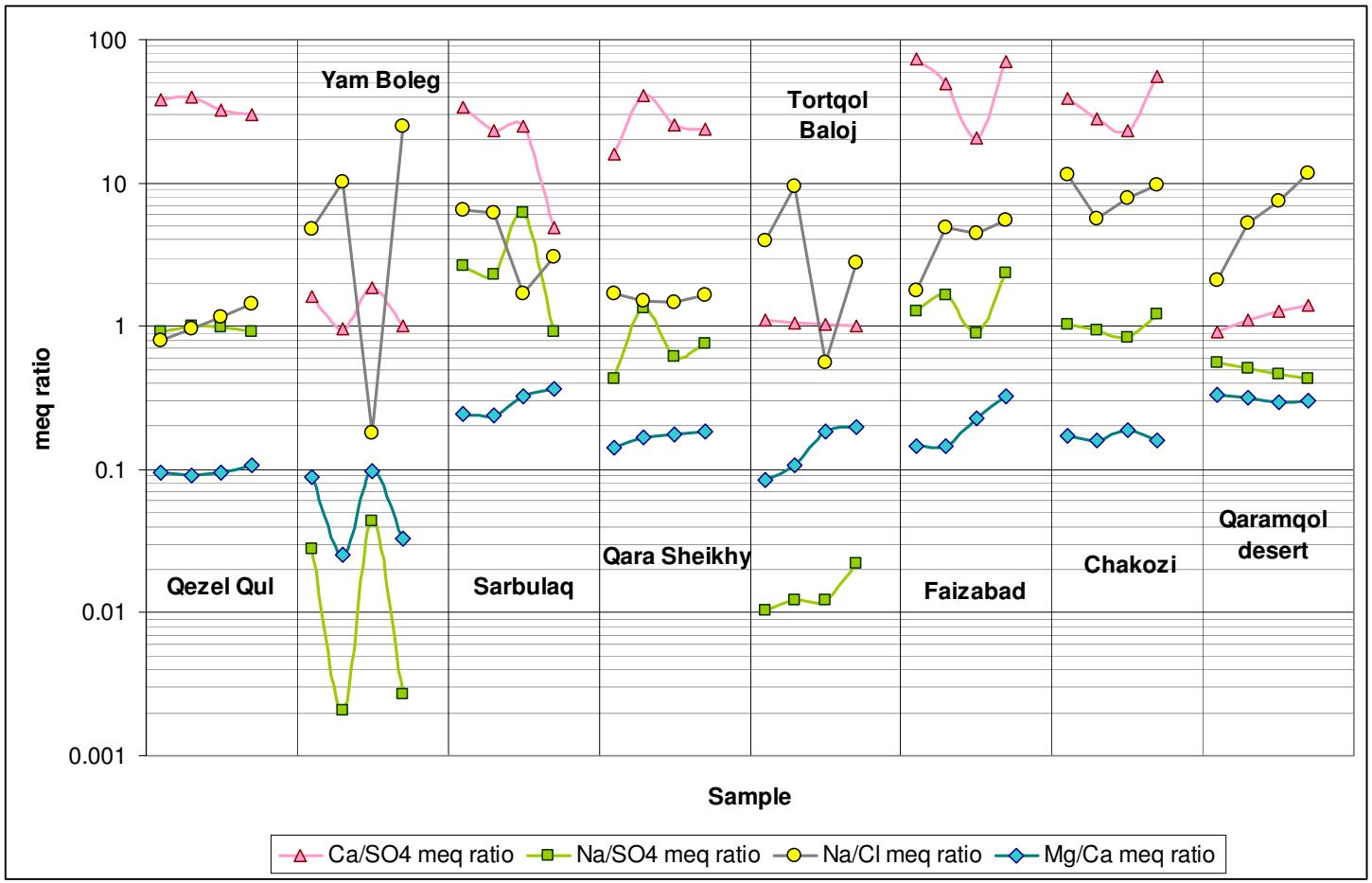

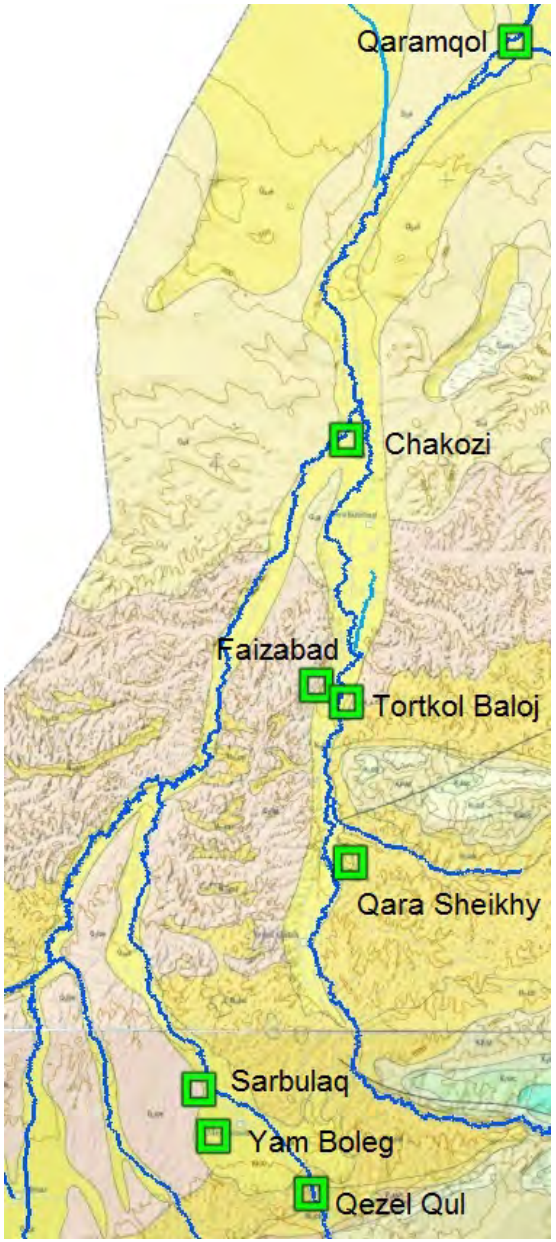

Figure 9.11. meq/L ratios of readily soluble components of soils in Faryab.

Contents represent meq concentrations in distilled water extracts from soil samples - see Table 9.1.

Samples are arranged from south-north from left to right.

10. Faryab: Groundwater Chemistry

10.1 Introduction

We have already examined, in Chapters 8 and 9, the topics of groundwater salinity, major ion hydrochemical types and possible groundwater hydrochemical evolution.

We will now examine some of the other components in groundwater, based on the 132 samples collected from the Kohistan, Gurziwan, Bilchiragh, Qaysar and northern (Andkhoi, Qaramqol, Khani Chahar Bagh and Qurgan) districts of Faryab in 2013. Of these samples, 40 were from springs, 91 from dug wells and 1 from a drilled borehole.

The data will typically be presented either as hydrochemical maps, or as **boxplots.**

Boxplots

In boxplots, the central "box" represents the interquartile range with a horizontal line at the median. The "whiskers" represent the non-outlying extraquartile range, with outliers shown as small squares (near outliers) or crosses (far outliers). Parentheses around the median represent a robust 95% confidence interval on the median. The #numbers along the top represent the number of data in each subset.

In the discussion of the presented parameters, the drinking water significance of the element will be commented in the light of:

- the WHO Drinking Water Guidelines: 4th Edition (WHO 2011)
- the European Drinking Water Directive 98/83/EC of November 1998

while recognising that neither of these documents has any legal authority within Afghanistan.

A large number of parameters were analysed, mostly either by ion chromatography (IC) or inductively coupled plasma mass spectrometry (ICP-MS) techniques at the laboratories of the British Geological Survey (BGS), Keyworth, UK. Only a relatively small number of parameters are discussed in this section. Those parameters selected for discussion are:

- those with health significance
- those where the large majority of samples returned values over the detection limit.

Where samples returned analytical values below the detection limit, we have elected to set the concentration to a value of half the lowest detection limit for the purposes of plotting diagrams (the reader should note that detection limit depends on salinity for many parameters and this arbitrary practice can be misleading in cases where large numbers of samples return values below detection limit).

10.2 pH

During 2013 and early 2014, pH was measured in the field (after pumping for c. 5 minutes to obtain fresh groundwater) at 435 groundwater survey locations in Faryab. This is referred to as the N=435 data set.

At N=132 of these locations, groundwater samples were collected and return to BGS for analysis. pH was also measured in the laboratory at BGS. The field measurements are to

be preferred, as transport and storage typically result in the samples losing dissolved CO_2, resulting in a pH increase. In fact, it can be seen that the majority of the waters, by the time they have been returned to the laboratory, have equilibrated at a pH of around 8.

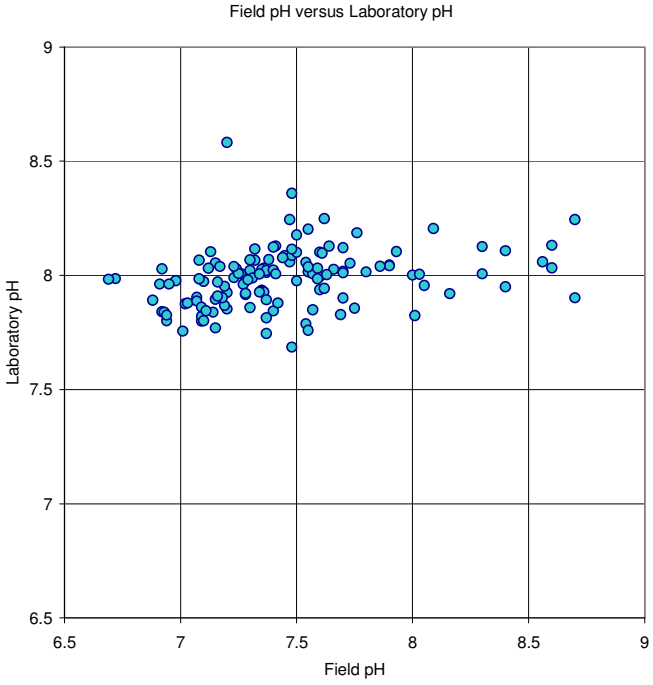

Figure 10.1. Plot of laboratory pH (measured at BGS) versus field-determined pH (N=132).

All the measured sources returned field pH values in the range 6.5 to 9, with vast majority between 7 and 8. The distribution of these according to district is shown in Figure 8.2. It will be observed that the generally higher pH values are observed in the southern districts, with pH generally decreasing slightly to the north. It is possible that this may be a temperature effect (the pH of pure water is 7.27 at 10°C, 7.08 at 20°C and 7.00 at 25°C), or it may represent some form of salinity-based interference.

pH

EC 1998 Directive: Indicator parameter. Should be between 6.5 and 9.5

WHO (2011): No guideline set. Not of health concern at levels found in drinking-water.

Field pH 25-percentile in Faryab =	7.18 (N=132)	7.23 (N=435)
Field pH 50-percentile in Faryab =	7.37 (N=132)	7.46 (N=435)
Field pH 90-percentile in Faryab =	8.01 (N=132)	8.00 (N=435)

For the N=435 data set, the relation between field pH, temperature (T, in °C) and electrical conductivity (EC, in µS/cm) is described by the following best-fit linear trend-lines:

pH = (51.903 - T) / 4.6029 r^2 = 0.2409

pH = (31859-EC) / 3740.8 r^2 = 0.2094

10

10.3 Arsenic (As)

Arsenic

EC 1998 Directive: < 10 µg/L

WHO (2011): Provisional guideline < 10 µg/L

25-percentile in Faryab	=	0.46 µg/L (N=132)
50-percentile in Faryab	=	0.70 µg/L (N=132)
90-percentile in Faryab	=	1.31 µg/L (N=132)

Arsenic can be harmful to human health in high concentrations in drinking water. Its hydrochemistry is complex. It can be released from sulphide mineralisations and may also occur in geothermal waters. It is often sorbed onto iron (III) oxyhydroxide minerals and can be released under moderately reducing conditions by reductive dissolution of these minerals. In neutral-alkaline solutions it can be rather soluble and can be concentrated by evaporative processes.

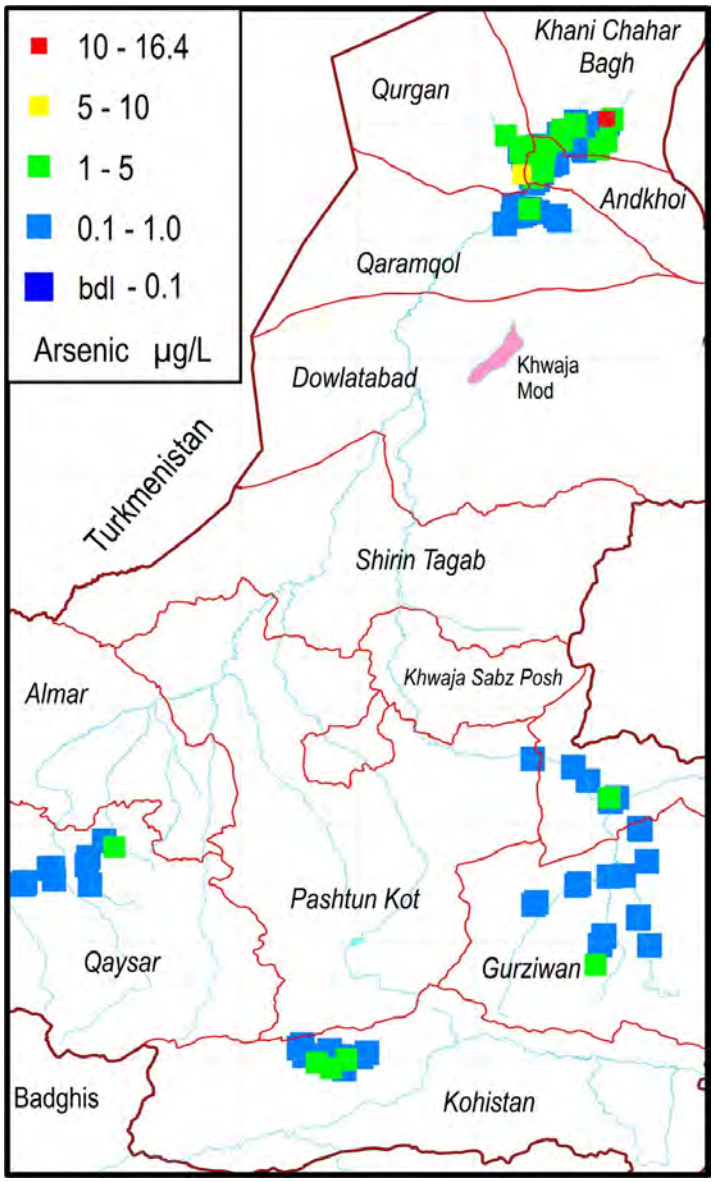

Figure 10.2. Distribution of As concentrations in groundwater in Faryab. One sample of 132 is below detection limit (bdl).

Only a single sample from Faryab exceeded the WHO (2011) guideline of 10 µg/L, from Khani Chahar Bagh district. The next highest concentration is a single sample at 5.1 µg/L in Qurgan district.

There is a slight tendency to increasing concentrations of arsenic in groundwater to the north.

10.4 Antimony (Sb)

Antimony

EC 1998 Directive: < 5 µg/L

WHO (2011): Guideline < 20 µg/L

25-percentile in Faryab	=	0.07 µg/L (N=132)
50-percentile in Faryab	=	0.10 µg/L (N=132)
90-percentile in Faryab	=	0.25 µg/L (N=132)

The antimony concentrations in the 132 groundwater samples from Faryab do not approach concentrations warranting health concern. The maximum recorded was 0.52 µg/L from a dug well in Andkhoi region. There is a weak tendency to increasing concentrations towards the north.

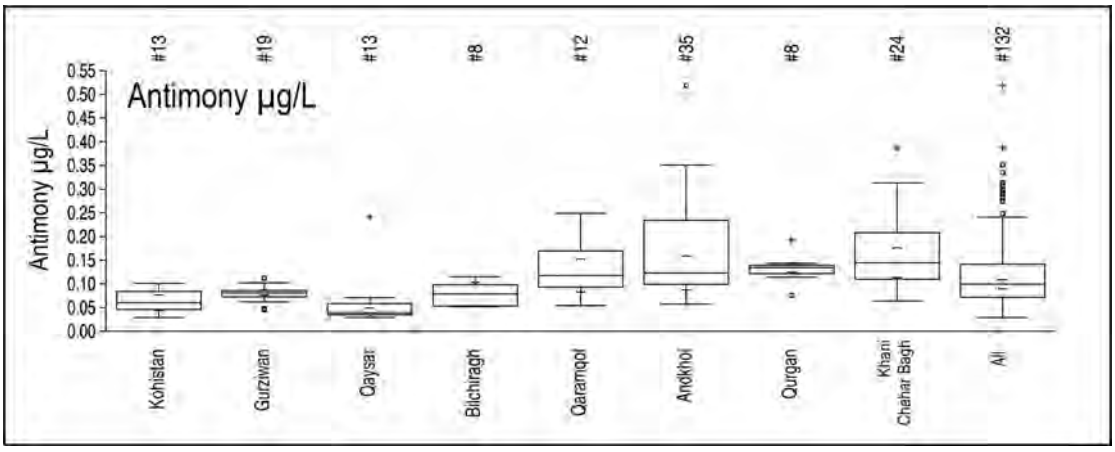

Figure 10.3. Boxplot showing distribution of antimony (Sb) in N=132 groundwater samples from Faryab. None of the 132 samples returned a value below the detection limit.

10.5 Barium (Ba)

Barium

EC 1998 Directive: No limit set

WHO (2011): Guideline < 700 µg/L

25-percentile in Faryab	=	14 µg/L (N=132)
50-percentile in Faryab	=	18 µg/L (N=132)
90-percentile in Faryab	=	52 µg/L (N=132)

The highest recorded barium concentration in Faryab is 218 µg/L, in a dug well in Kohistan, well below the WHO Guideline level.

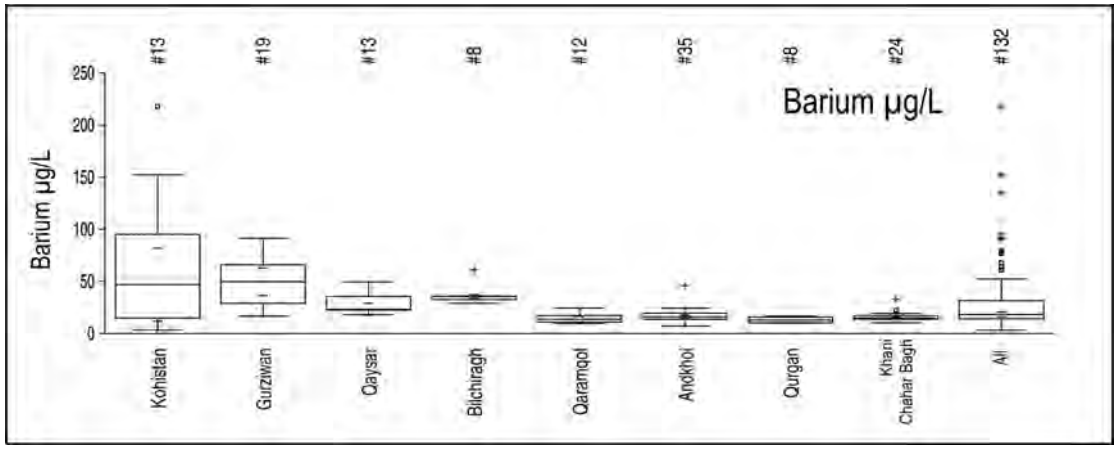

Figure 10.4. Boxplot showing distribution of barium (Ba) in N=132 groundwater samples from Faryab. None of the 132 samples returned a value below the detection limit.

There is a clear trend to decreasing concentrations of barium in groundwater to the north. It is believed that this is related to suppression of barium solubility by barite saturation, occasioned by high sulphate concentrations in groundwater of the northern areas. Barium exhibits a negative correlation with sulphate in the groundwaters.

10.6 Beryllium (Be)

Beryllium is a highly toxic element. The EU and WHO (2011) do not set drinking water guidelines for beryllium, but the USEPA (2009) sets a limit of 4 µg/L.

All of the 132 groundwater samples from Faryab returned concentrations below the detection limit, which varied from <0.01 µg/L to <0.05 µg/L. All samples were well below the USEPA limit, therefore.

10.7 Boron (B)

Boron

EC 1998 Directive: < 1000 µg/L

WHO (2011): Guideline < 2400 µg/L

25-percentile in Faryab	=	178 µg/L (N=132)
50-percentile in Faryab	=	859 µg/L (N=132)
90-percentile in Faryab	=	2474 µg/L (N=132)

14 of the 132 groundwaters sampled in Faryab exceed the recommended WHO (2011) Guideline value of 2400 µg/L, which is set from a human health perspective (possible effects on the male reproductive tract). The highest concentration of 7760 µg/L was from a groundwater from Andkhoi district.

It should be remembered that boron can be toxic to some plant species in smaller concentrations, making high-boron water unsuitable for irrigation of some species. For example, water containing more than 300 µg/L can be phytotoxic to sensitive plants such as avocado, bean or apple (Nable et al. 1997).

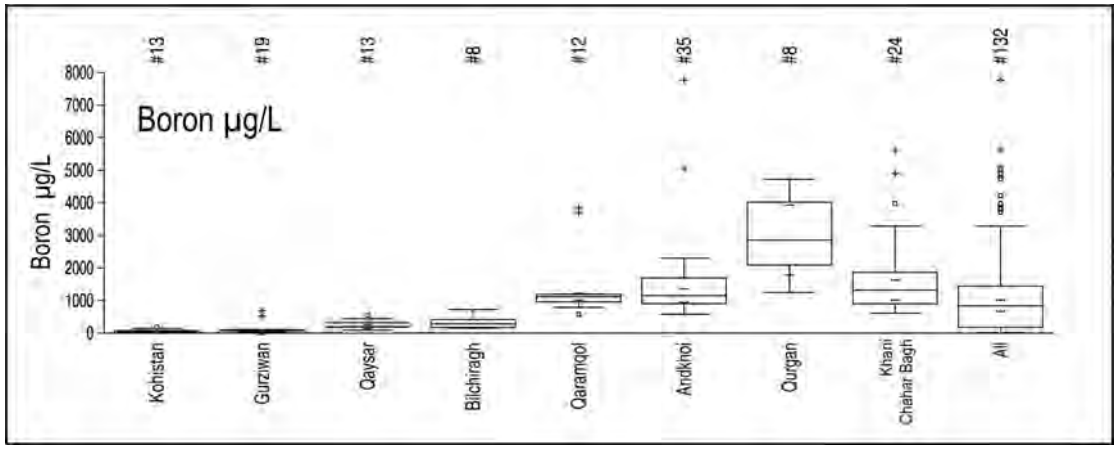

Figure 10.5. Boxplot showing distribution of boron in N=132 groundwater samples from Faryab. 1 of the 132 samples returned a value below the detection limit of <10 µg/L.

Boron concentrations exhibit a clear increasing trend from south to north. Boron typically occurs in alkaline groundwater in the form of a highly soluble borate anion and is susceptible to evapoconcentration.

10.8 Bromide (Br^-)

Bromide was measured as an anion on the ion chromatograph at BGS.

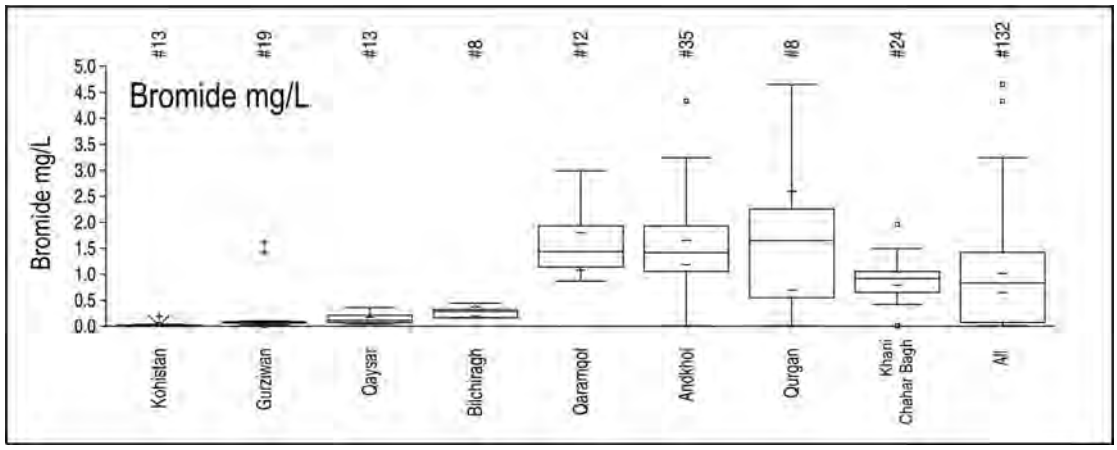

Figure 10.6. Boxplot showing distribution of bromide in N=132 groundwater samples from Faryab. 16 of the 132 samples returned a value below the detection limit and all 16 were arbitrarily set to 0.01 mg/L for the purposes of plotting, despite the fact that the detection limit varied from <0.02 to <1 mg/L depending on salinity. This erroneously give the impression of a few very low-bromide waters in the northern districts.

Chloride : Bromide mass ratios (Davis et al. 1998)

Atmospheric precipitation: 50 to 100

Shallow groundwater: 100 to 200

Seawater: 290

Domestic sewage: 300 to 600

Halite dissolution: 1000 to 10,000

Residual brine after halite precipitated: 50

The maximum concentration in groundwater was 4.65 mg/L in a dug well in Qurgan district. Bromide exhibits a strong correlation with salinity and the highest values clearly occur in the four northern districts.

.

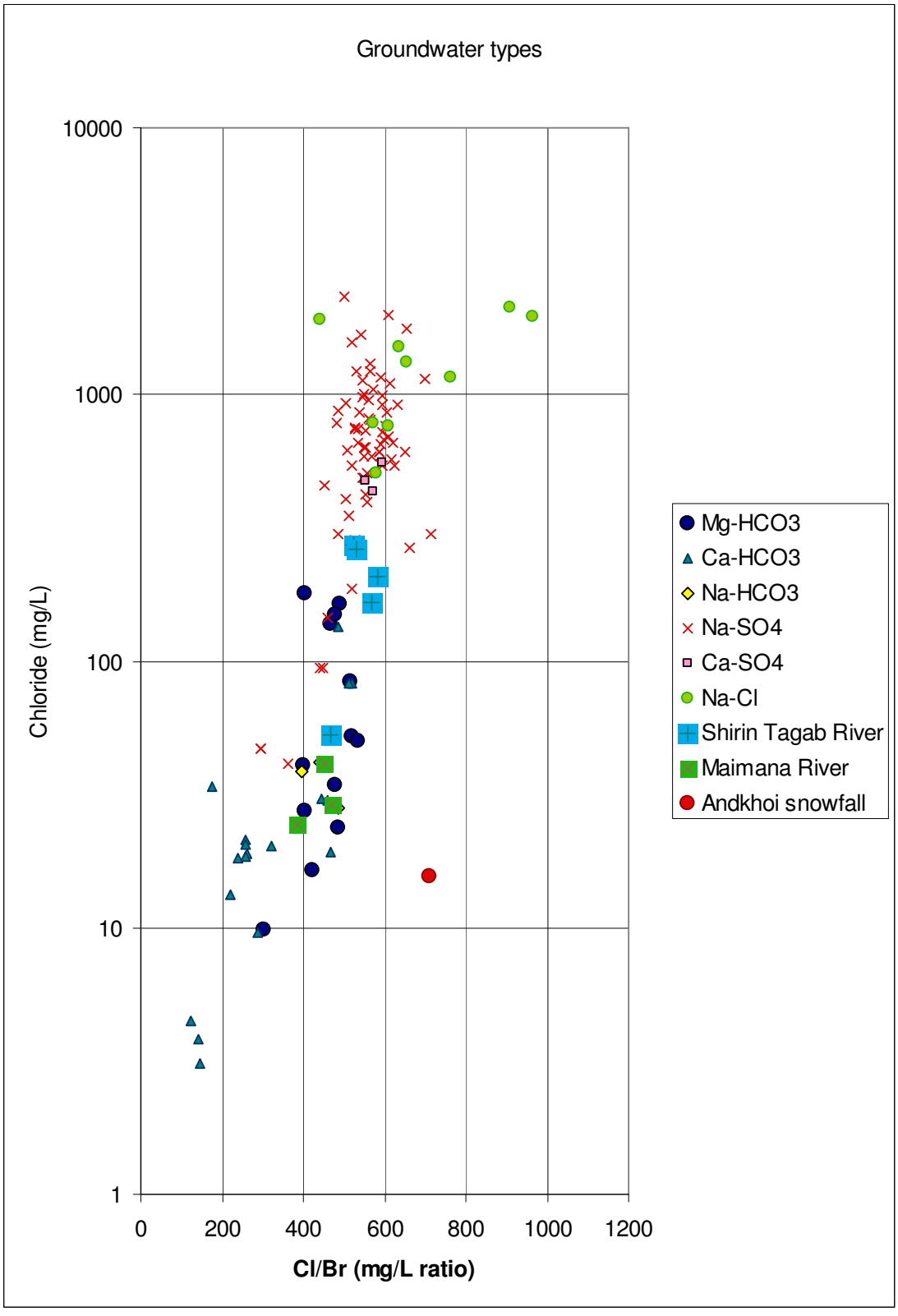

Figure 10.7. Chloride to bromide mass ratios, plotted against chloride concentration, for groundwaters sampled in 2013 (samples where bromide < detection limit omitted), subdivided according to water type (see Chapter 9). The diagram also shows river waters (sampling discussed in Chapter 3) and a single snowfall sample from Andkhoi where bromide was above detection limit.

Bromide

EC 1998 Directive: No guideline

WHO (2011): No guideline

25-percentile in Faryab	=	0.16 mg/L (N=116 samples above dl)
50-percentile in Faryab	=	0.92 mg/L (N=116 samples above dl)
90-percentile in Faryab	=	2.1 mg/L (N=116 samples above dl)

Figure 10.7 clearly shows that chloride : bromide ratio increases from south to north in groundwater, as salinity increases. In the southern districts, ratios as low as 200 occur, whereas, in the northern districts the typical ratio is around 580. River waters fall on the same trajectory.

Davis et al. (1998) wrote a key paper on Cl^-/Br^- ratios, where they report characteristic ratios for different sources (see text box above). They argue that evaporation in itself does not affect the Cl^-/Br^- ratio (although without clear evidence for this) and that the main influence on Cl^-/Br^- ratios is halite precipitation (lowers ratio in groundwater), halite dissolution (increases ratio) and admixture with halite-dissolution brines (increases ratio).

Davis et al. (2004), in their later paper, acknowledge that bromide chemistry is rather complex and that fractionation takes place at the seawater interface. Bubble-bursting and microbial processes mobilise bromine preferentially into the aerosol phase and leave precipitation enriched in bromide.

Conventional wisdom (Alcalá & Custudio 2004) holds that evapoconcentration during recharge does not affect Cl^-/Br^- ratios. One can only speculate (see Vengosh et al. 1992) whether fractionation *could* possibly take place during intensive evaporation in arid environments, leaving small quantities of recharge water depleted in bromide (high Cl^-/Br^- ratio). This hypothesis is certainly recognised by Wood & Sanford (2007) for an Arabian sabkha environment, Smoydzin, L. & von Glasow, R. (2009) for the Dead Sea and Zhou & McLennan (2011) for Mars!

Thus, using conventional models, we would conclude that the increasing Cl^-/Br^- ratios from south to north reflect increasing degrees of dissolution of evaporite minerals (such as halite) - possibly with a component of sewage / latrine leakage. Newer research does not preclude, however, the alternative model that intense evaporation can also cause the increase in Cl^-/Br^- ratios.

The high Cl^-/Br^- ratio in the single snowfall sample from Andkhoi could simply reflect windblown halite-containing dust being entrained in the sample.

10.9 Chromium (Cr)

The highest recorded chromium concentration in Faryab is 37 µg/L, from a dug well in Bilchiragh, below the WHO provisional health-based Guideline level of 50 µg/L.

There is no clear geographical trend in the chromium concentrations, both Bilchiragh and Khani Chahar Bagh districts exhibit median chromium concentrations well above most other districts.

Four of 132 samples returned values below the analytical detection limit.

Chromium

EC 1998 Directive: < 50 µg/L

WHO (2011): Provisional guideline < 50 µg/L

25-percentile in Faryab	=	0.49 µg/L (N=132)
50-percentile in Faryab	=	1.52 µg/L (N=132)
90-percentile in Faryab	=	10.9 µg/L (N=132)

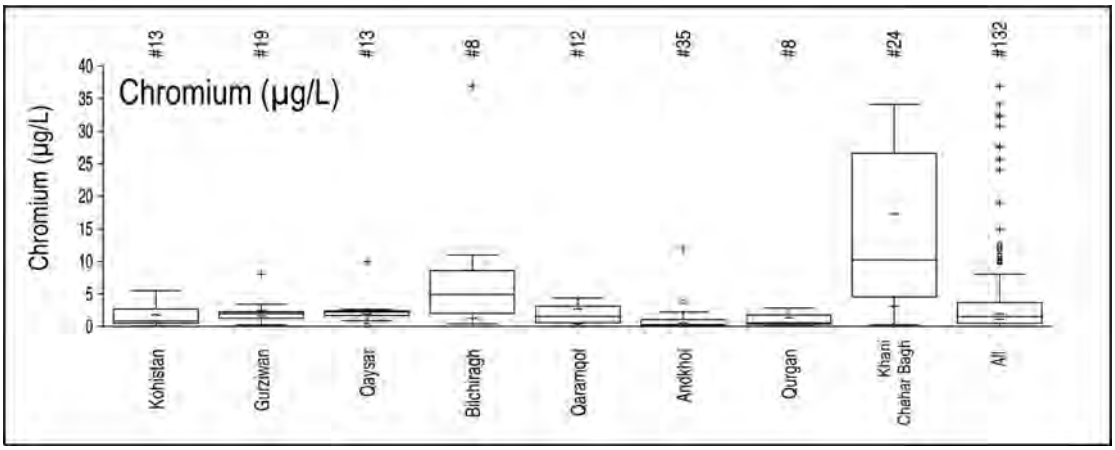

Figure 10.8. Boxplot showing distribution of chromium (Cr) in N=132 groundwater samples from Faryab. Four of the 132 samples returned a value below the detection limit (which varies between <0.05 and <0.3 µg/L) and these have been set to a value of 0.025 µg/L for plotting purposes.

10.10 Fluoride (F^-)

Fluoride was measured as an anion on the ion chromatograph at BGS. Modest quantities of fluoride are beneficial for correct bone and tooth development. A deficiency in fluoride can lead to increased vulnerability to dental caries.

Excessive fluoride intake can lead to fluorosis of teeth and, in extreme cases, of bones, in livestock and humans. Children are especially vulnerable.

Fluoride

EC 1998 Directive: < 1.5 mg/L

WHO (2011): Guideline < 1.5 mg/L

25-percentile in Faryab	=	0.3 mg/L (N=127 samples above dl)
50-percentile in Faryab	=	0.56 mg/L (N=127 samples above dl)
90-percentile in Faryab	=	1.13 mg/L (N=127 samples above dl)

In Faryab, the range of fluoride concentrations in groundwater is largely within an optimum window. Only six of the 132 samples exceed the WHO Guideline concentration of 1.5 mg/L, with the highest value of 2.3 mg/L occurring in a dug well in Qurgan district.

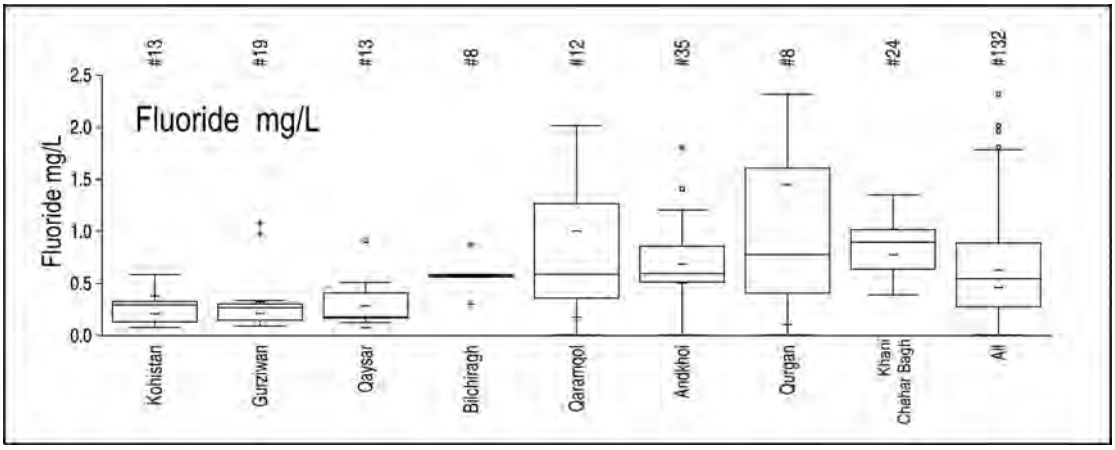

Figure 10.9. Boxplot showing distribution of fluoride (F^-) in N=132 groundwater samples from Faryab. Five of the 132 samples returned a value below the detection limit (which varies from <0.01 to <1 mg/L) and these have been set to a value of 0.005 mg/L for plotting purposes.

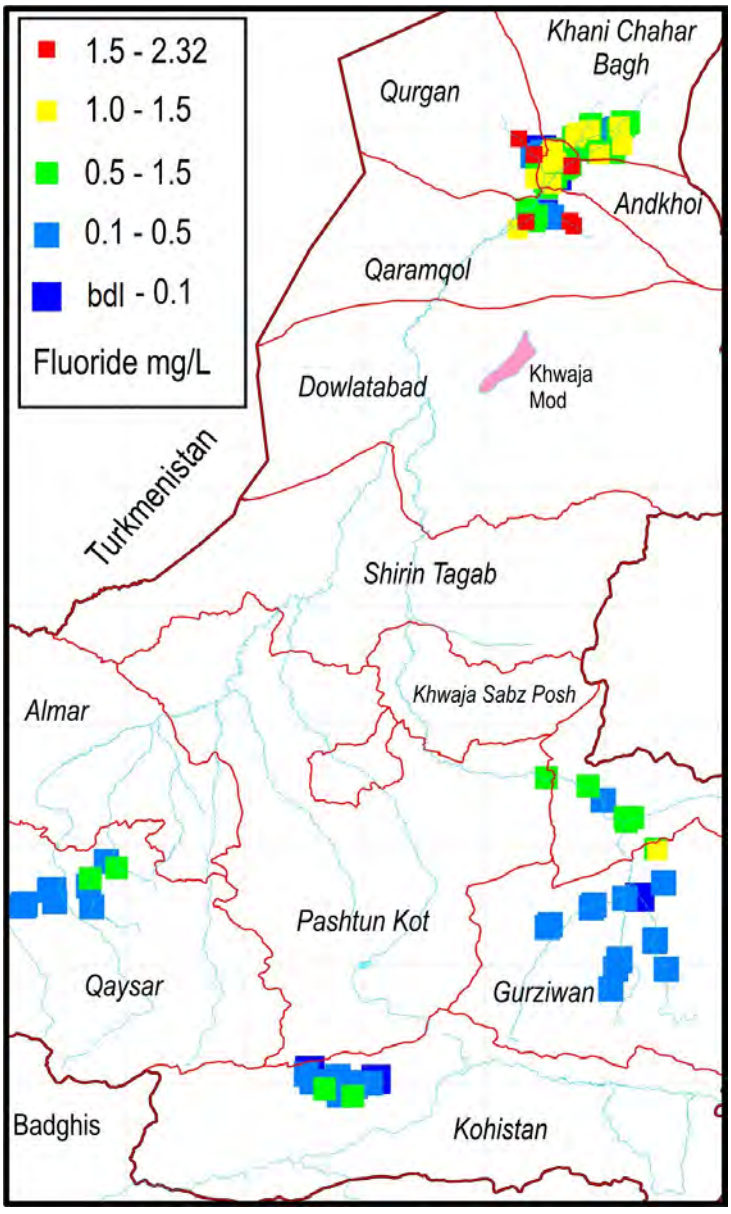

Figure 10.10. Distribution of F^- concentrations in groundwater in Faryab. Five samples of 132 are below detection limit (bdl).

Fluoride can be affected by anion exchange and thus tends to be more mobile in alkaline waters. It can also be affected, up to a point, by evapo-concentration, as it is relatively soluble. However, the presence of calcium in the groundwater hinders the accumulation of excessively high concentrations of fluoride, due to fluorite saturation being attained (CaF_2). Figures 10.9 and 10.10 confirm that the highest fluoride concentrations occur in the four northern districts.

10.11 Iron (Fe)

Iron

EC 1998 Directive: Indicator parameter <200 µg/L

WHO (2011): No guideline set. Not of health concern.

Only 31 of the 132 groundwater samples returned iron concentrations in excess of the detection limit (which varied from <1 to <12 µg/L). The highest iron concentration detected in the 132 Faryab groundwater samples was 11 µg/L, from a dug well in Andkhoi district.

Iron in drinking water is of aesthetic (colour, staining of sanitary ware) significance, rather than of health significance. It is typically found in reducing or acidic waters. The generally alkaline and oxidising nature of the sampled Faryab groundwaters is assumed to suppress iron solubility.

10.12 Lithium (Li)

Lithium belongs to the alkali metal group and is highly soluble in water. It thus tends to be evapoconcentrated along with potassium and sodium.

Lithium

EC 1998 Directive: No limit set

WHO (2011): No guideline set

25-percentile in Faryab	=	26 µg/L (N=132)
50-percentile in Faryab	=	83 µg/L (N=132)
90-percentile in Faryab	=	211 µg/L (N=132)

The maximum lithium concentration was 389 µg/L from a dug well in Andkhoi. Figure 10.11 clearly shows that lithium accumulates in groundwater to the north, along with the other salinity-related components.

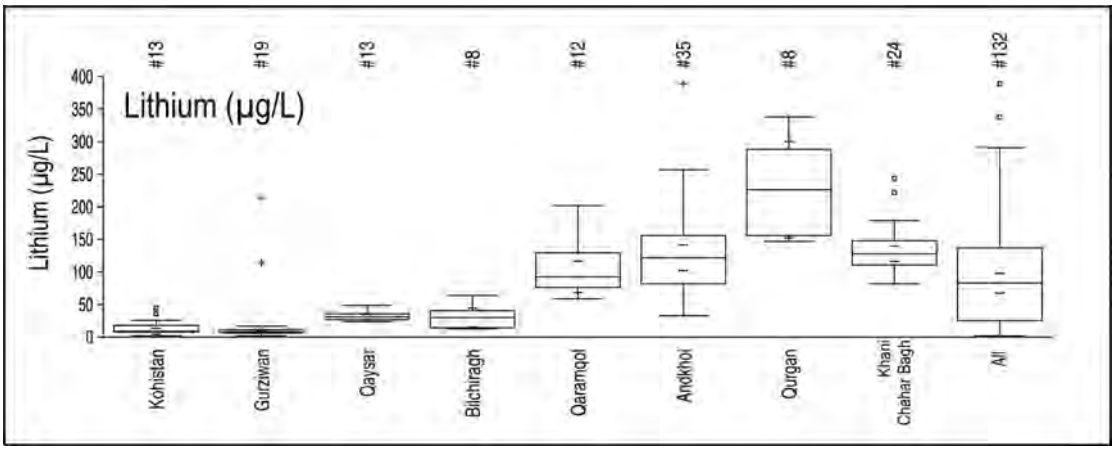

Figure 10.11. Boxplot showing distribution of lithium (Li) in N=132 groundwater samples from Faryab. None of the 132 samples returned a value below the detection limit.

10.13 Manganese (Mn)

Manganese

EC 1998 Directive: Indicator parameter <50 µg/L

WHO (2011): No guideline set. Not of health concern.

25-percentile in Faryab	=	<0.2 µg/L (N=132)
50-percentile in Faryab	=	0.9 µg/L (N=132)
90-percentile in Faryab	=	120 µg/L (N=132)

Only 85 of the 132 groundwater samples returned iron concentrations in excess of the detection limit (which varied from <0.2 to <0.7 µg/L). 20 of the 132 samples exceeded the EC guideline value of 50 µg/L. The highest manganese concentration detected in the 132 Faryab groundwater samples was 1310 µg/L, from Andkhoi district. Manganese is only found in concentrations of any significance in the samples from the four northern districts (Figure 10.12). Manganese in drinking water is of aesthetic (staining of sanitary ware) significance, rather than of health significance.

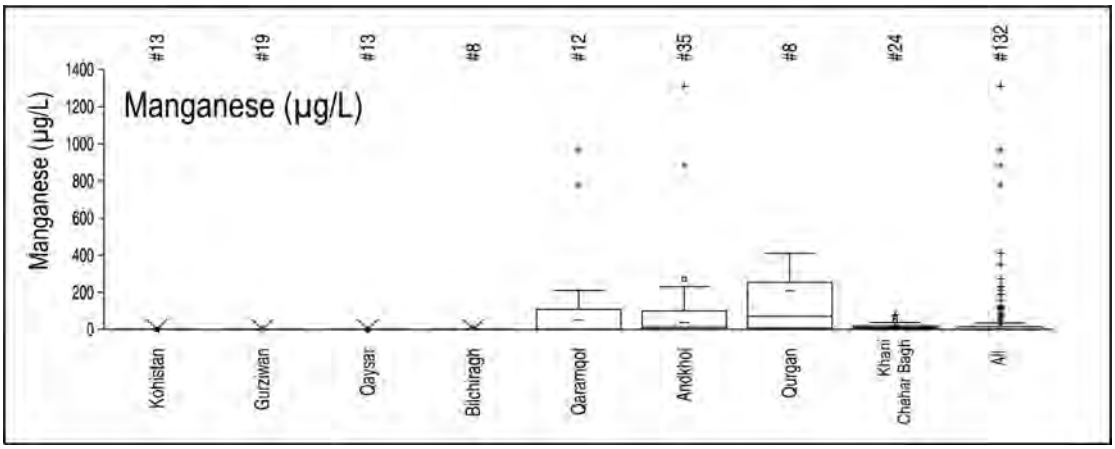

Figure 10.12. Boxplot showing distribution of manganese (Mn) in N=132 groundwater samples from Faryab. 47 of the 132 samples returned a value below the detection limit and these have been set to a value of 0.1 µg/L for plotting purposes.

10.14 Nitrate (NO_3^-)

Nitrate was measured as an anion on the ion chromatograph at BGS. It is one of very few of the analysed parameters that can degrade during storage and transport. While every effort was made to ensure cool and dark storage and swift transport, it cannot be excluded that some of laboratory analyses may underestimate the "as sampled" nitrate concentrations.

The WHO (2011) and EC limits of 50 mg/L nitrate as NO_3^- (equivalent to 11 mg/L as N) are set to protect infants against the possibility of methaemoglobinaemia ("blue baby" syndrome).

Sources of nitrate include agricultural practices (ploughing, application of organic and mineral fertilisers), sewage and leachate from pit latrines. Modest quantities of nitrate in rainfall can also be derived from vehicle exhausts, industry and nitrification of atmospheric nitrogen by lightning. Banks et al. (2002) have demonstrated a correlation

between nitrate concentrations in groundwater and urban areas / pit latrines. As a highly soluble anion, nitrate is susceptible to evapoconcentrative effects.

Nitrate

EC 1998 Directive: <50 mg/L (as NO_3^-)

WHO (2011): Guideline value <50 mg/L (as NO_3^-)

25-percentile in Faryab	=	9.0 mg/L (N=132)
50-percentile in Faryab	=	13.8 mg/L (N=132)
90-percentile in Faryab	=	62 mg/L (N=132)

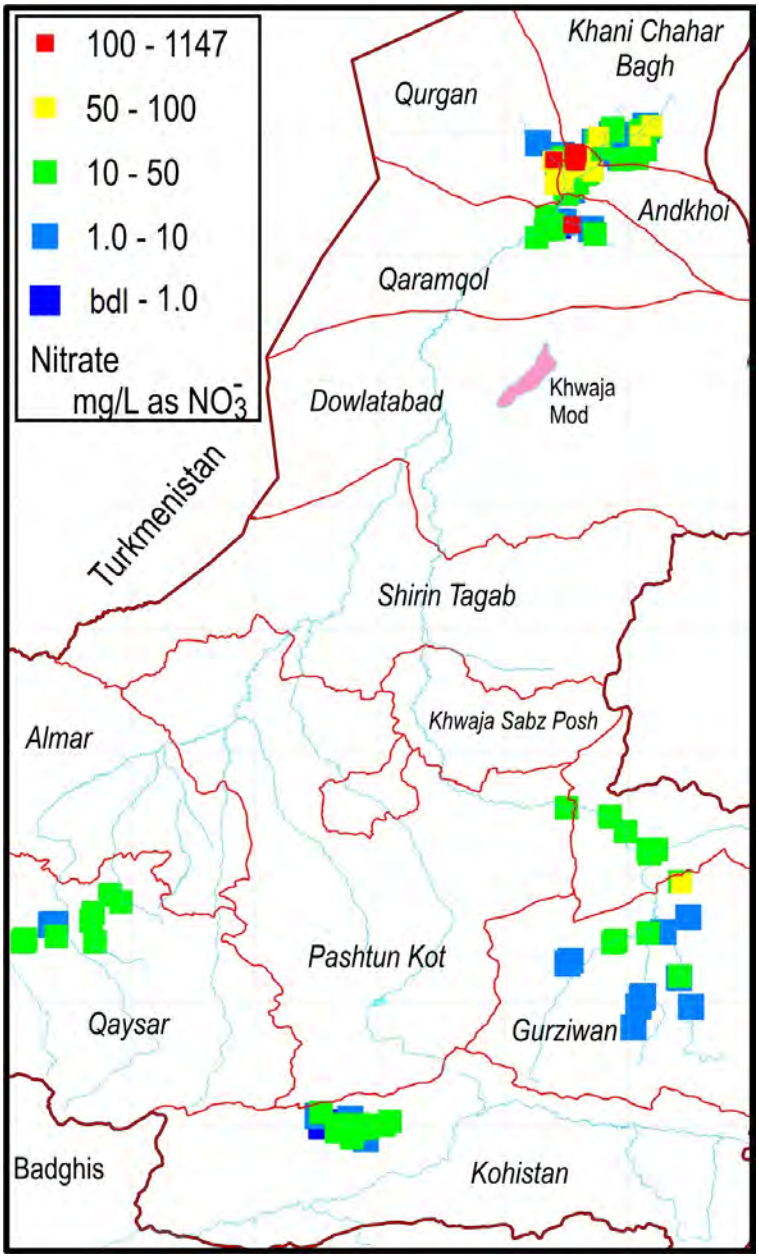

Figure 10.13. Distribution of nitrate (as mg/L NO_3^-) concentrations in groundwater in Faryab. One sample of 132 is below detection limit (bdl).

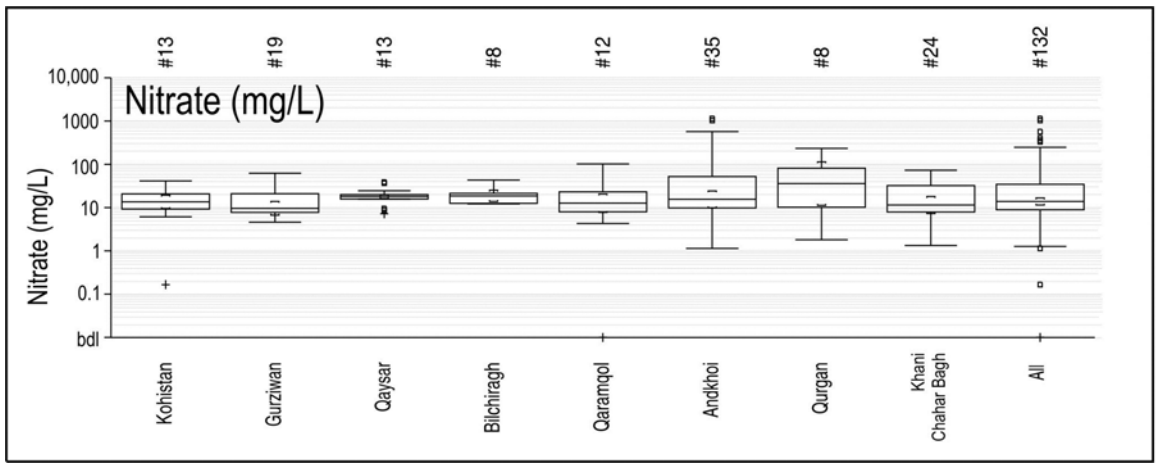

Figure 10.14. Boxplot showing distribution of nitrate (as mg/L NO_3^-) in N=132 groundwater samples from Faryab. 1 of the 132 samples returned a value below the detection limit (which varies between <0.02 and <1 mg/L) and this has been set to a value of 0.01 mg/L for plotting purposes.

20 of the 132 (15%) Faryab groundwater samples exhibited nitrate concentrations exceeding 50 mg/L. The highest value was an enormous 1147 mg/L from a dug well in Andkhoi, although a worrying 9 out of 132 samples exhibited nitrate concentrations in excess of 100 mg/L. The samples exceeding the WHO (2011) guideline value almost all came from the four northern districts around Andkhoi.

10.15 Potassium (K)

Potassium belongs to the alkali metal group and is highly soluble in water. It thus tends to be evapoconcentrated along with rubidium, lithium and sodium.

Potassium can be derived from hydrolysis of silicate rocks, but is also associated with organic matter and can be released from organic wastes (e.g. sewage effluents).

The maximum potassium concentration was 171 mg/L from a dug well in Andkhoi, which also exhibited a very high nitrate concentration of 1034 mg/L. Figure 10.15 clearly shows that potassium accumulates in groundwater to the north, along with the other salinity-related components.

Potassium

EC 1998 Directive: No guideline set

WHO (2011): Occurs at concentrations well below those of health concern

25-percentile in Faryab	=	4.2 mg/L (N=132)
50-percentile in Faryab	=	12.1 mg/L (N=132)
90-percentile in Faryab	=	44 mg/L (N=132)

When potassium is plotted against nitrate, it is found that the highest potassium concentrations tend to coincide with the highest nitrate concentrations. It is unclear if this is simply a reflection of mutual evapoconcentrative effects or whether it is due to a common derivation in infiltrating sewage effluent (for example) - or, quite possibly, both.

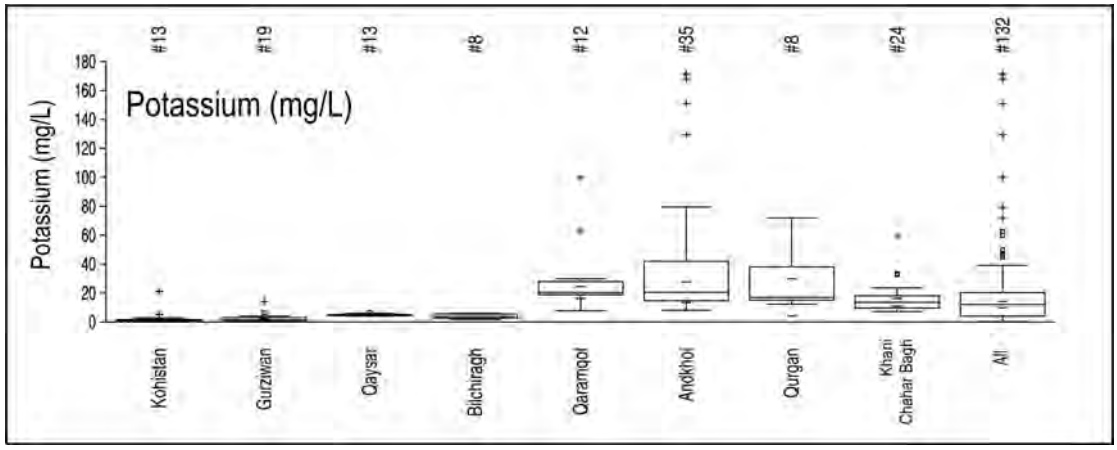

Figure 10.15. Boxplot showing distribution of potassium (K) in N=132 groundwater samples from Faryab. None of the 132 samples returned a value below the detection limit.

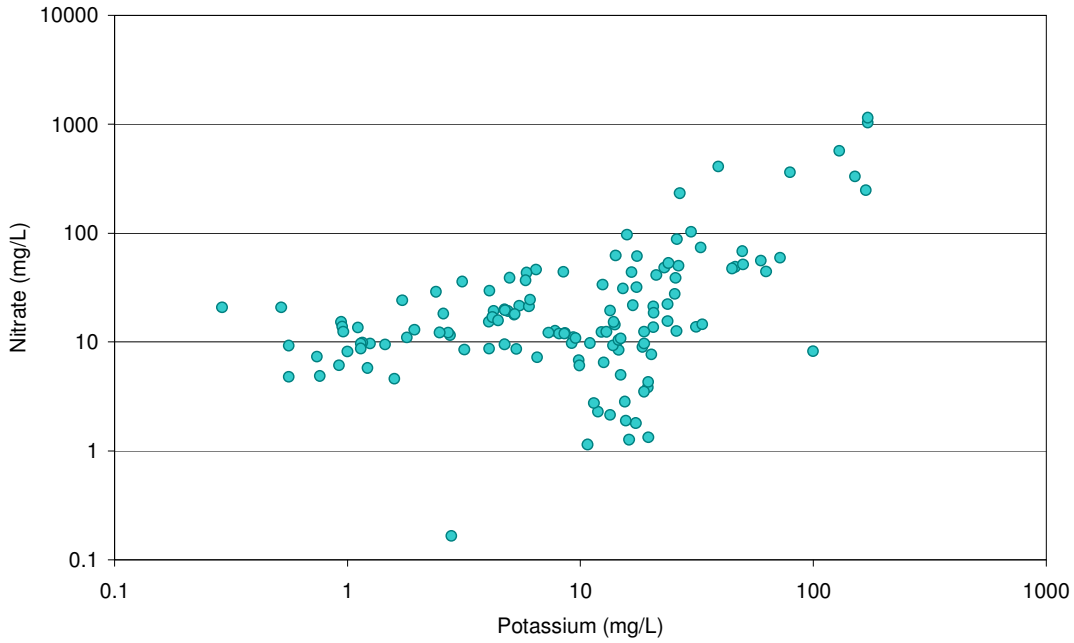

Figure 10.16. Scatterplot of groundwater concentrations of nitrate (as mg/L NO_3^-) versus potassium. N = 131 (one sample with nitrate below detection limit omitted).

10.16 Rubidium (Rb)

Rubidium belongs to the alkali metal group and is highly soluble in water. It thus tends to be evapoconcentrated along with potassium, lithium and sodium.

The maximum rubidium concentration was 19.8 µg/L from a dug well in Qurgan district. Figure 10.18 clearly shows that rubidium accumulates in groundwater to the north, along with the other salinity-related components. Especially high concentrations are observed in Qurgan district.

Rubidium is often regarded as a chemical analogue of potassium. Figure 10.17 shows a plot of the K/Rb mass ratio, plotted against chloride as a surrogate of salinity.

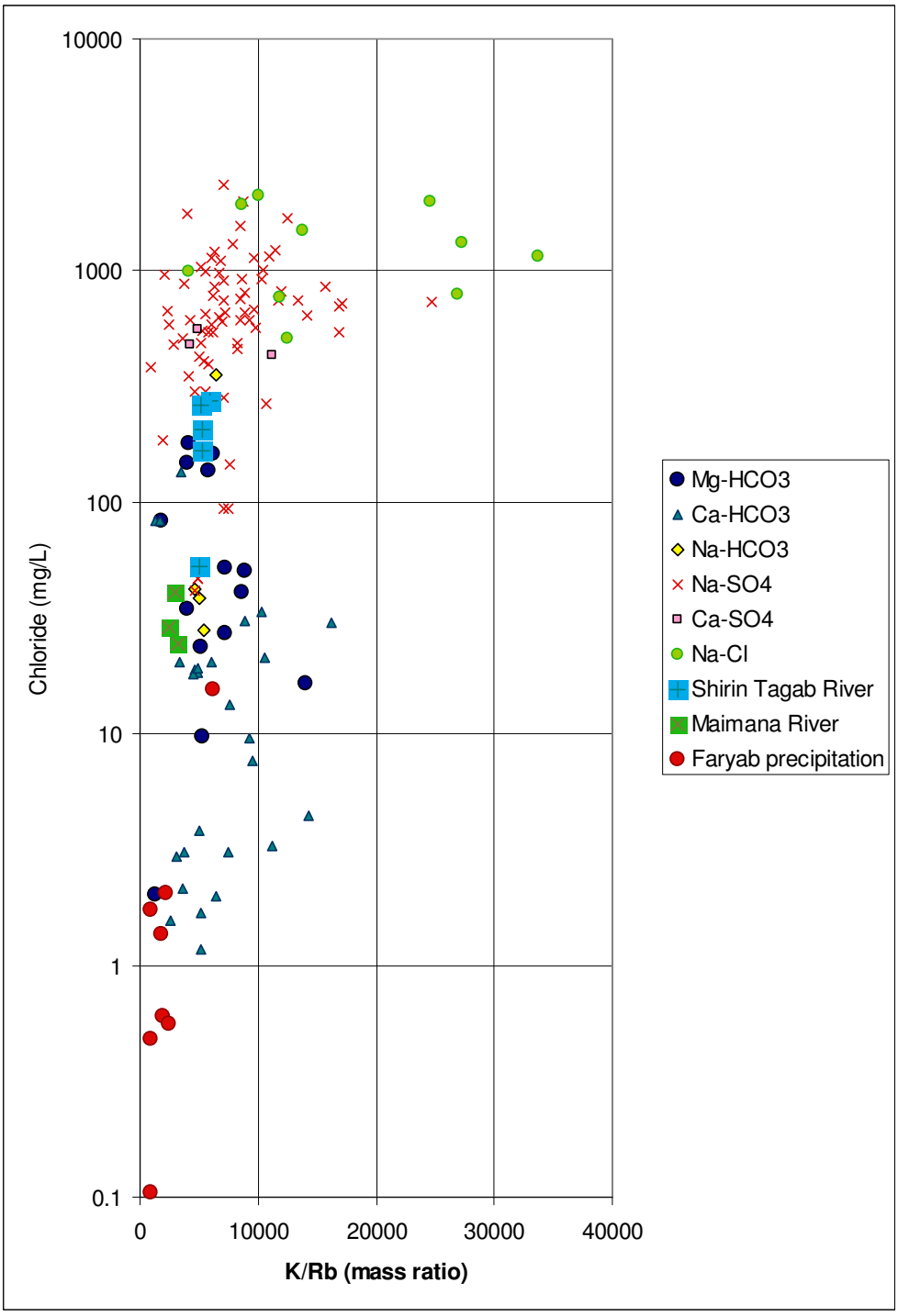

Figure 10.17. Potassium to rubidium mass ratios, plotted against chloride concentration, for groundwaters sampled in 2013 subdivided according to water type (see Chapter 9). The diagram also shows river waters (sampling discussed in Chapter 3) and precipitation samples (Chapter 2)

Figure 10.17 shows a fairly consistent K/Rb mass ratio of 3000-10,000 for most groundwaters, with river waters lying on the groundwater trend. A significant proportion of the Na-Cl groundwater types (and some Na-SO_4) groundwater types exhibit K/Rb ratios exceeding 10,000 and even exceeding 30,000 in one case.

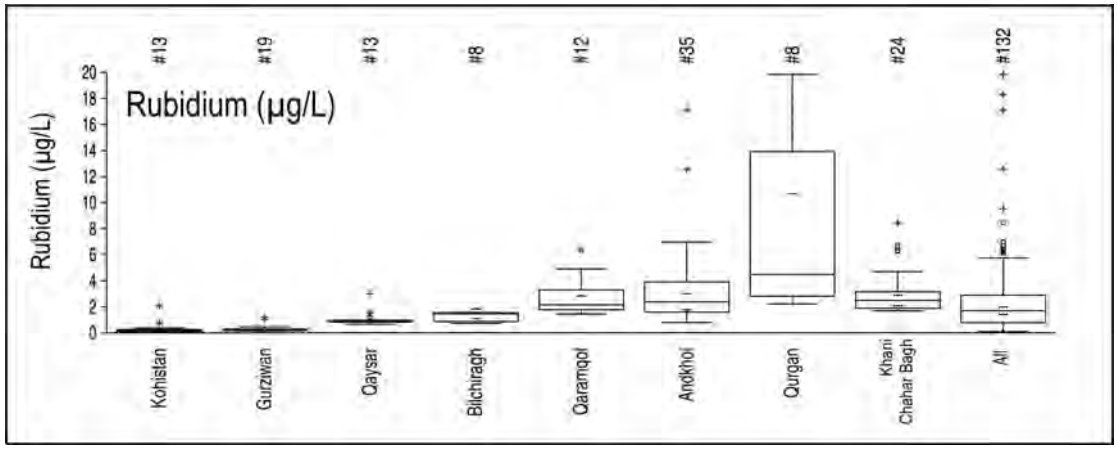

Figure 10.18. Boxplot showing distribution of rubidium (Rb) in N=132 groundwater samples from Faryab. None of the 132 samples returned a value below the detection limit.

Rubidium

EC 1998 Directive: No guideline set

WHO (2011): No guideline set

25-percentile in Faryab	=	0.79 µg/L (N=132)
50-percentile in Faryab	=	1.7 µg/L (N=132)
90-percentile in Faryab	=	5.5 µg/L (N=132)

10.17 Selenium (Se)

Selenium is an essential trace element, with the WHO (2011) recommending an adult daily intake of 26-35 µg. However, in excess, selenium can be toxic, with WHO (2011) recommending a maximum daily intake of 400 µg.

Selenium

EC 1998 Directive: <10 µg/L

WHO (2011): Provisional guideline <40 µg/L

25-percentile in Faryab	=	0.8 µg/L (N=132)
50-percentile in Faryab	=	4.8 µg/L (N=132)
90-percentile in Faryab	=	14.8 µg/L (N=132)

Of the 132 Faryab groundwater samples, four samples (3%) exceed the WHO (2011) provisional guideline of 40µg/L, while 30 samples (23%) exceed the EC limit of 10 µg/L. The highest concentrations are typically from the four northern districts and also from Bilchiragh.

The highest individual value of 98 µg/L was, however, from a spring in Gurziwan district.

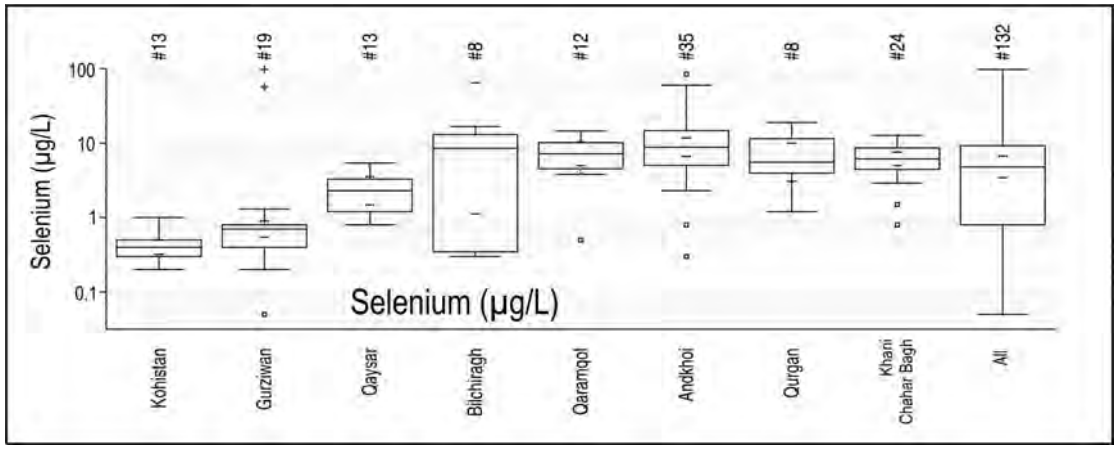

Figure 10.19. Boxplot showing distribution of selenium (Se) in N=132 groundwater samples from Faryab. 1 of the 132 samples returned a value below the detection limit (of <0.1 µg/L) and this has been set to a value of 0.05 mg/L for plotting purposes.

10.18 Silicon (Si)

Groundwaters typically contain 5-10 mg/L of dissolved silicon. This is typically in the form of monosilicic acid (H_4SiO_4) or, at higher pH, hydrogen silicate anions. The solubility of silicon increases with temperature; otherwise, groundwater dissolved silicon contents are seldom strongly affected by other aspects of the water's chemistry, typically being controlled by the solubility of cryptocrystalline silica (e.g. chalcedony or similar).

However, it has been found that (a) evapoconcentration can allow elevated concentrations of silicon to occur and for silica saturation to be exceeded, due to kinetic constraints on silica precipitation and (b) that other species in saline waters (e.g. sodium, by forming a $SiO_2(OH)_2Na^-$ complex ion) may be able to enhance silica solubility (Jones et al. 1967, Tanaka et al. 2004, Tanaka & Takahashi 2007).

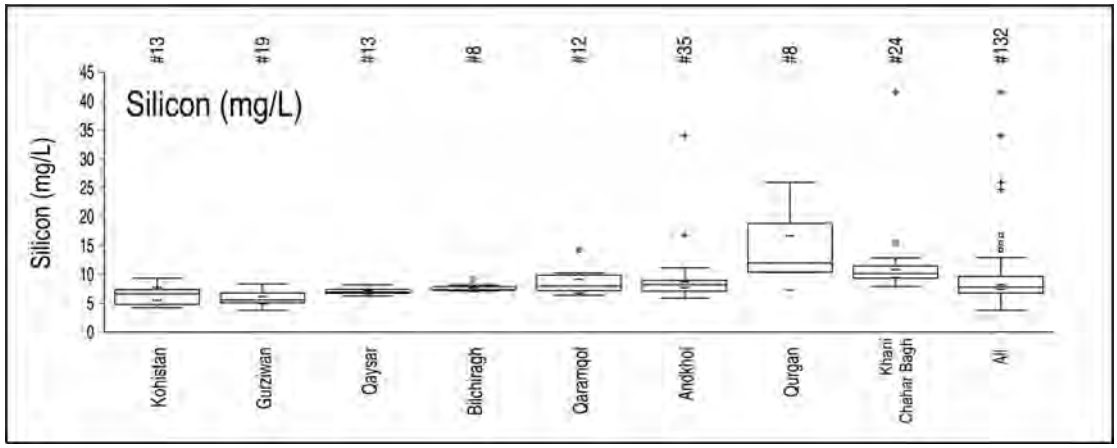

Figure 10.20. Boxplot showing distribution of silicon (as Si) in N=132 groundwater samples from Faryab. None of the 132 samples returned a value below the detection limit .

Indeed, it is found that the Faryab samples typically contain 5-10 mg/L Si. Concentrations significantly in excess of 10 mg/L only occur in a few locations in the northern districts, especially in Qurgan and Khani Chahar Bagh.

Figures 10.21a,b show that there is a weak correlation between silicon concentration and temperature and a slightly stronger one with sodium concentration. There are, however, a number of high Si concentrations (> 15 mg/L) that are not clearly explained by either of these factors.

Silicon

EC 1998 Directive: No guideline provided

WHO (2011): No guideline provided

25-percentile in Faryab	=	6.8 mg/L (N=132)
50-percentile in Faryab	=	7.8 mg/L (N=132)
90-percentile in Faryab	=	11.5 mg/L (N=132)

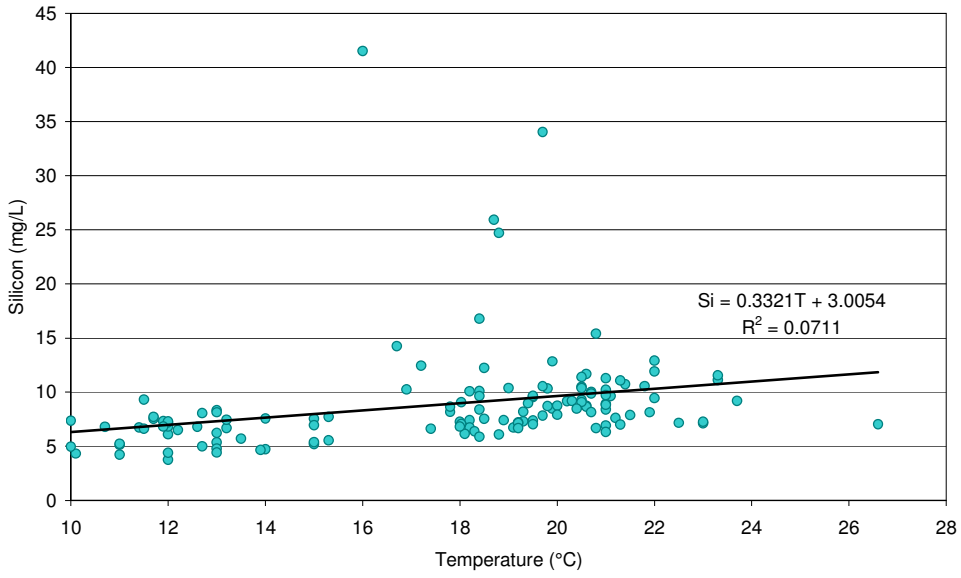

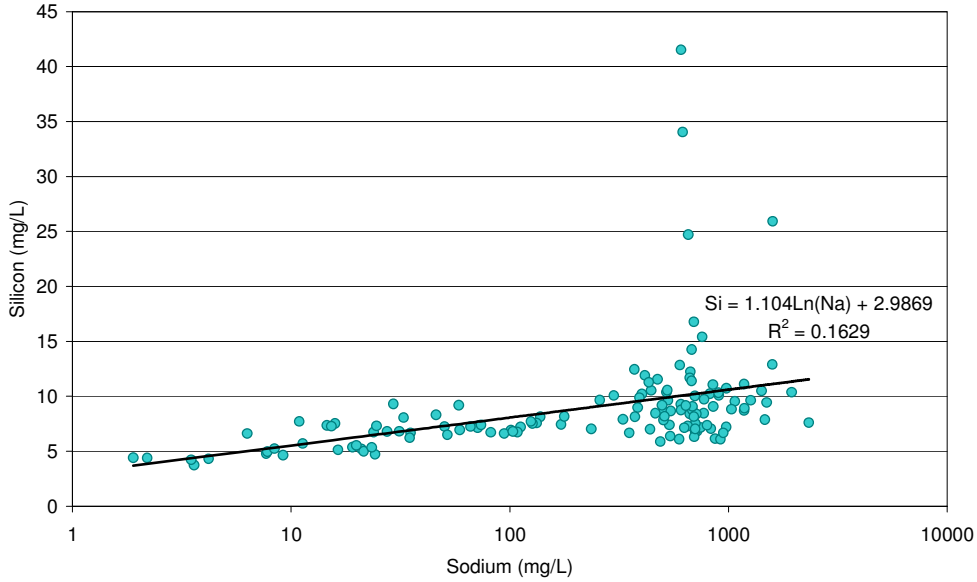

Figure 10.21. Scatterplots showing correlations of silicon in the 132 Faryab groundwater samples with (top) groundwater temperature and (bottom) sodium.

10.19 Strontium (Sr)

Strontium is an alkaline earth element, chemically analogous to magnesium.

Strontium

EC 1998 Directive: No guideline provided

WHO (2011): No guideline provided

25-percentile in Faryab	=	1.3 mg/L (N=132)
50-percentile in Faryab	=	9.5 mg/L (N=132)
90-percentile in Faryab	=	17.6 mg/L (N=132)

Concentrations of strontium in Faryab's groundwater are generally relatively high. The highest recorded concentration of 25.7 mg/L is from a dug well in Andkhoi. Like many other elements, strontium concentrations broadly reflect salinity, increasing towards the north.

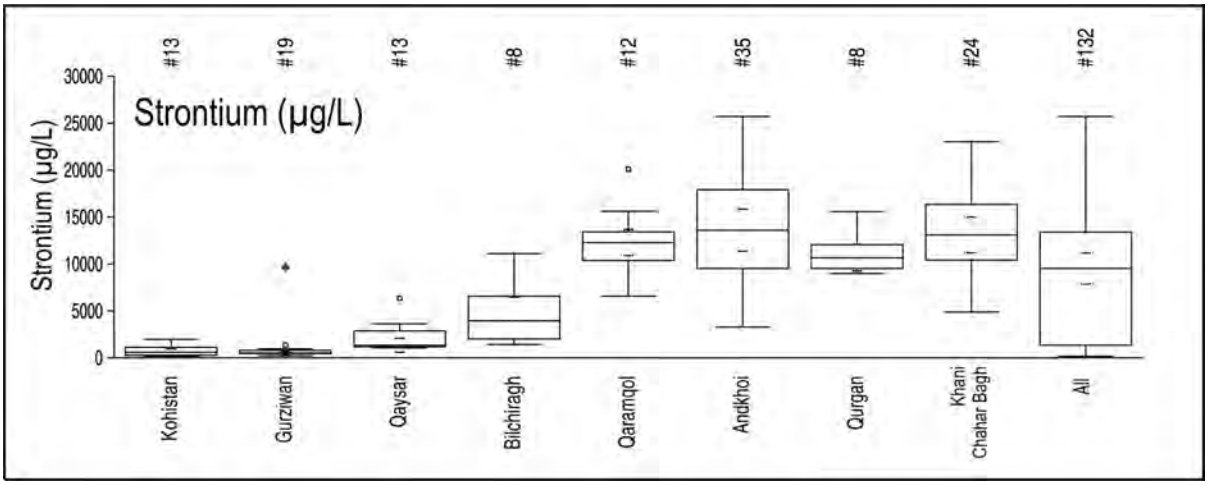

Figure 10.22. Boxplot showing distribution of strontium (Sr) in N=132 groundwater samples from Faryab. None of the 132 samples returned a value below the detection limit .

Figure 10.23 shows the mass ratio of Mg/Sr in groundwaters, river waters and precipitation in Faryab.

It will be seen that precipitation, river waters and many of the more saline groundwaters all exhibit a Mg/Sr ratio in the region of 10-20. The lower salinity groundwaters, however, exhibit a much higher Mg/Sr ratio in the region 20-60, together with some of the more saline groundwaters. For reference, the Mg/Sr ratio in modern abiotic marine calcite (Bahamas) is around 37. By contrast, modern biotic marine calcite has a much lower ratio 6-20 (Carpenter & Lohmann 1992). Seawater itself has a mass ratio of around 162 (Dickson & Goyet 1994).

As groundwater evolves and becomes saturated with calcite, one might expect the precipitation of abiotic calcite to remove magnesium preferentially from the groundwater, leaving groundwater enriched in Sr, and with a lower Mg/Sr ratio.

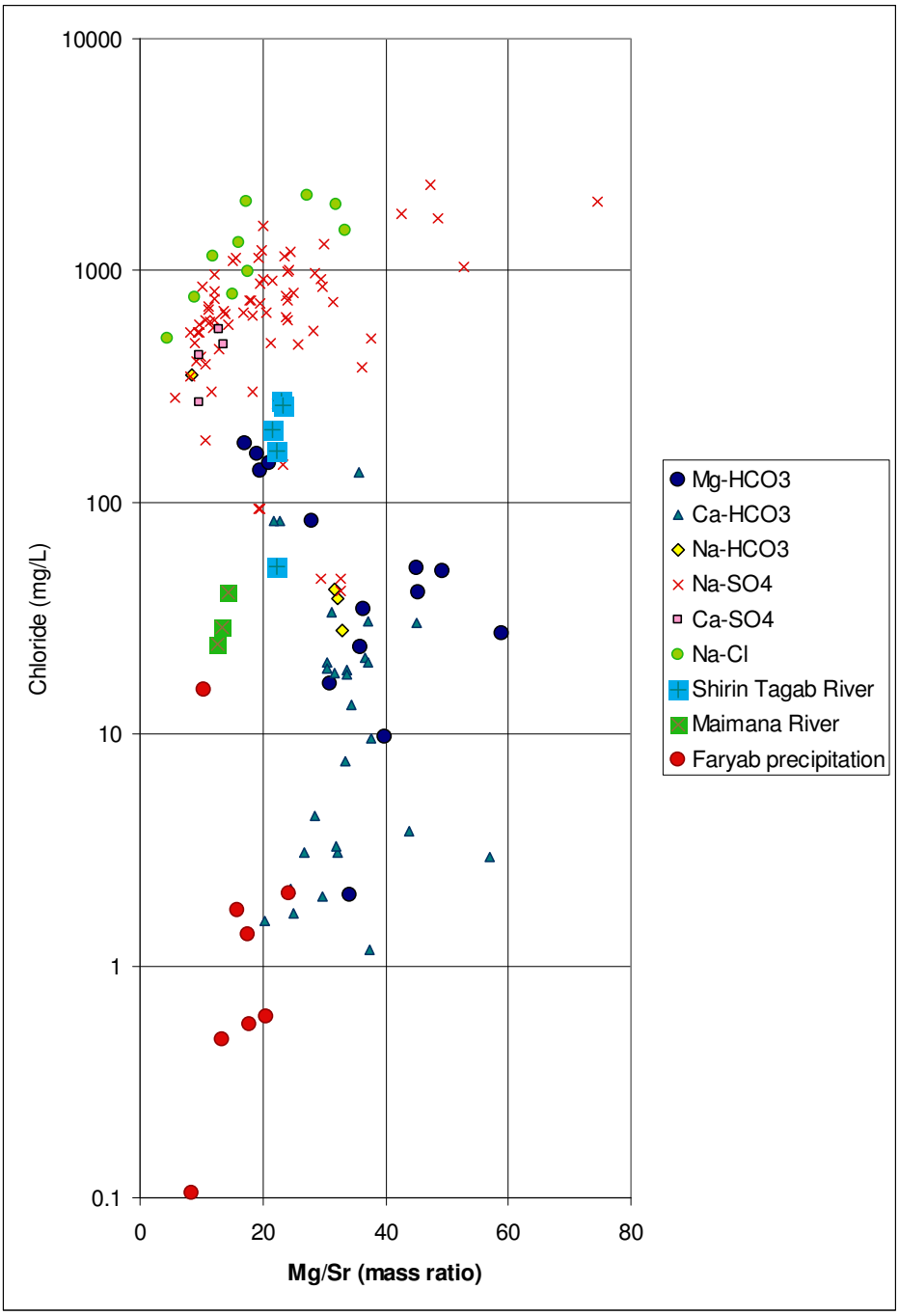

Figure 10.23. Magnesium to strontium mass ratios, plotted against chloride concentration, for groundwaters sampled in 2013 subdivided according to water type (see Chapter 9). The diagram also shows river waters (sampling discussed in Chapter 3) and precipitation samples (Chapter 2)

10.20 Thallium (Tl)

Thallium is a highly toxic element. The EU and WHO (2011) do not set drinking water guidelines for thallium, but the USEPA (2009) sets a limit of only 2 µg/L.

All but 7 of the 132 groundwater samples from Faryab returned concentrations below the detection limit, which varied from <0.01 µg/L to <0.2 µg/L. The highest recorded concentration was 0.05 µg/L. All samples were thus well below the USEPA limit.

10.21 Uranium (U)

Uranium is a mildly radioactive actinide element. Surprisingly, its chemotoxicity is regarded as being more important than its radiotoxicity, as discussed by Frengstad & Banks (2014).

Uranium

EC 1998 Directive: No guideline provided

WHO (2011): Provisional guideline <30 µg/L

25-percentile in Faryab	=	3.7 µg/L (N=132)
50-percentile in Faryab	=	16.2 µg/L (N=132)
90-percentile in Faryab	=	41 µg/L (N=132)

Although the solubility of uranium is limited in reducing environments, it forms stable oxyanions (and other ionic complexes) in oxidising environments, which can be highly soluble.

In Faryab, 26 of 132 samples (20%) exceed the WHO (2011) provisional guideline value of 30 µg/L, exclusively in the northern districts. The highest recorded uranium concentration was 62 µg/L from dug wells in Qurgan and Andkhoi.

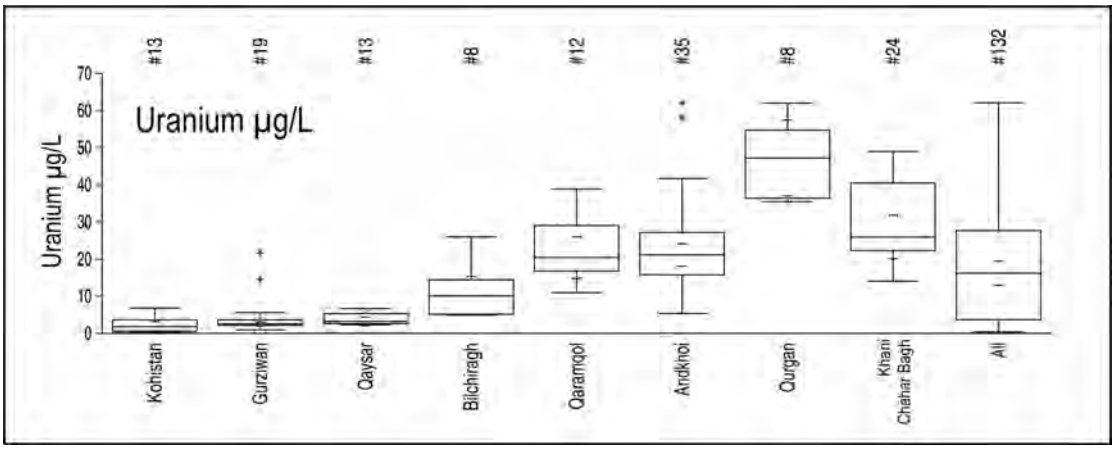

Figure 10.24. Boxplot showing distribution of uranium (U) in N=132 groundwater samples from Faryab. None of the 132 samples returned a value below the detection limit .

The map in Figure 10.25 is strongly suggestive of groundwater uranium concentrations increasing towards the north, which may also indicate the uranium anionic complexes are susceptible to the same evapoconcentrative processes as many other soluble elements. Alternatively, the high concentrations of uranium in saline groundwaters may be related to mobilization by complexation with salinity-related species, such as sulphate (Frengstad & Banks 2014). Figure 10.26 suggests that uranium complexation with sulphate is a highly plausible mechanism, as there is a much stronger correlation (r=0.90) with sulphate than with chloride (r = 0.70).

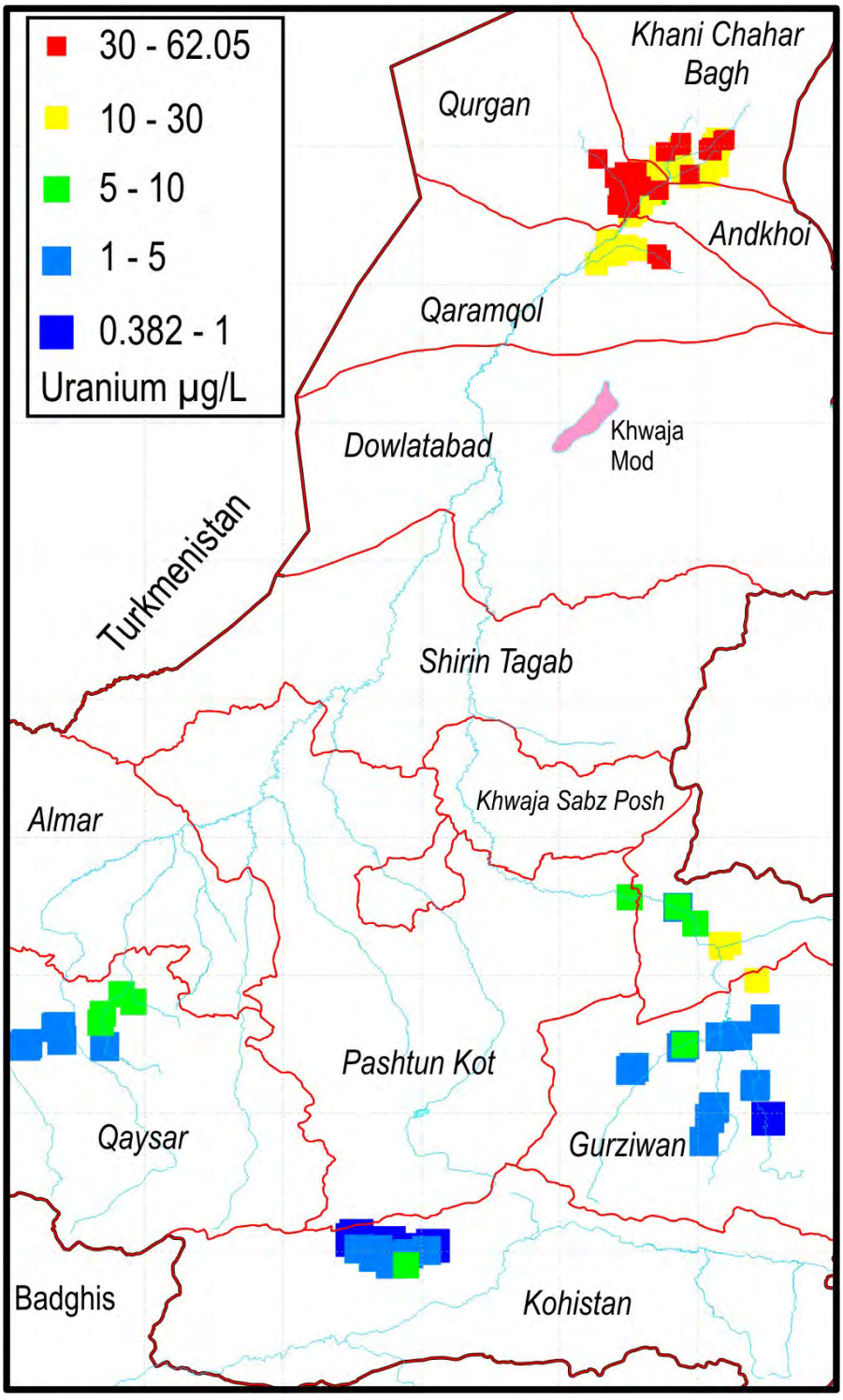

Figure 10.25. Distribution of uranium (U) concentrations in groundwater in Faryab. All 132 samples are above the analytical detection limit.

Ultimate sources of uranium can include:

- uranium minerals within igneous or metamorphic rocks (e.g. apatite, zircon)
- uranium within dark organic sedimentary marine mudrocks and shales
- some inorganic fertilisers, especially those derived from apatite.

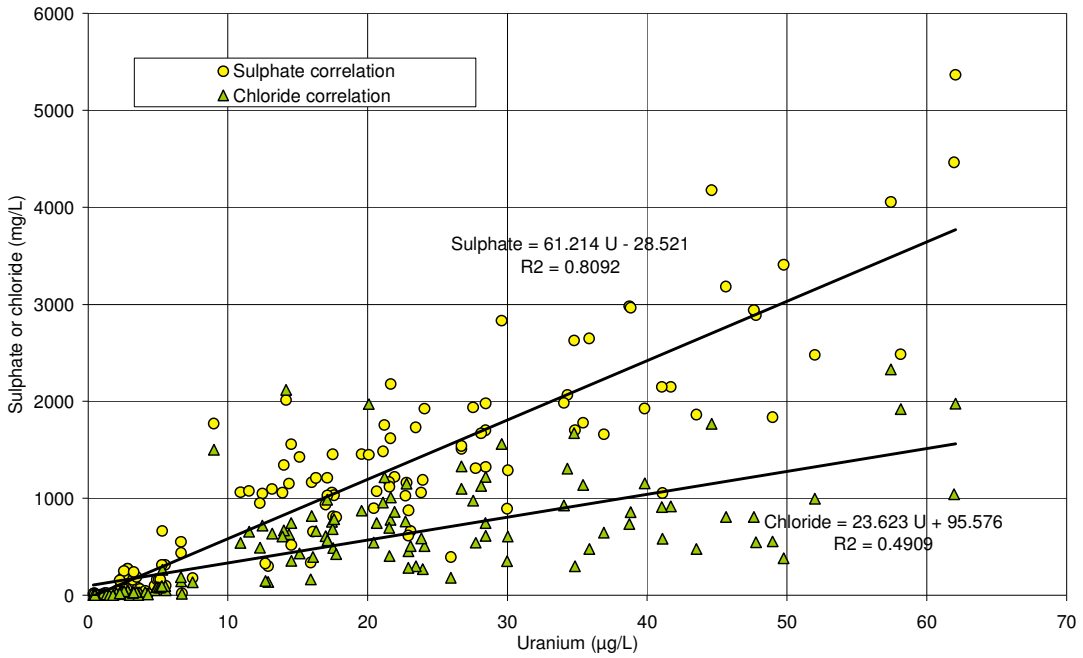

Figure 10.26. Scatter-plot showing correlation of uranium with sulphate and chloride. Best fit linear regressions shown.

10.22 Yttrium (Y)

The distribution of yttrium is presented here as a "hydrochemical curiosity" as it is not an element of any especial health significance. Yttrium is one of a group of chemically similar elements called the rare earth elements (REE) and relatively little is known about their occurrence and behaviour in groundwater systems (Banks et al. 1999).

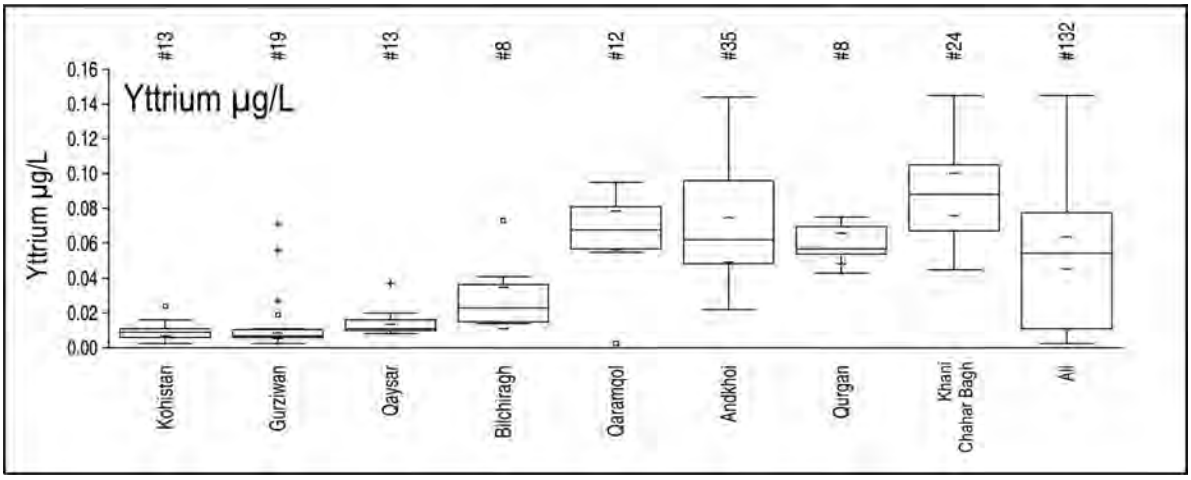

Figure 10.27. Boxplot showing distribution of yttrium (Y) in N=132 groundwater samples from Faryab. Six of the 132 samples returned a value below the detection limit (of <0.005 to <0.05 µg/L) and these have been set to a value of 0.0025 mg/L for plotting purposes.

From Figure 10.27 it seems that the occurrence of yttrium is not dissimilar to that of uranium, i.e. steadily increasing concentrations northwards, giving the appearance of broadly the same evapoconcentrative processes, or mobilisation by complexation with salinity-related species. Complexation of REE with chloride, sulphate and other species

is well-known - Lewis et al. 1998). Figure 10.27 does not show the same degree of correlation with chloride and sulphate as uranium does, however.

Yttrium

EC 1998 Directive: No guideline provided

WHO (2011): No guideline provided

25-percentile in Faryab	=	0.01 µg/L (N=132)
50-percentile in Faryab	=	0.05 µg/L ((N=132
90-percentile in Faryab	=	0.10 µg/L (N=132)

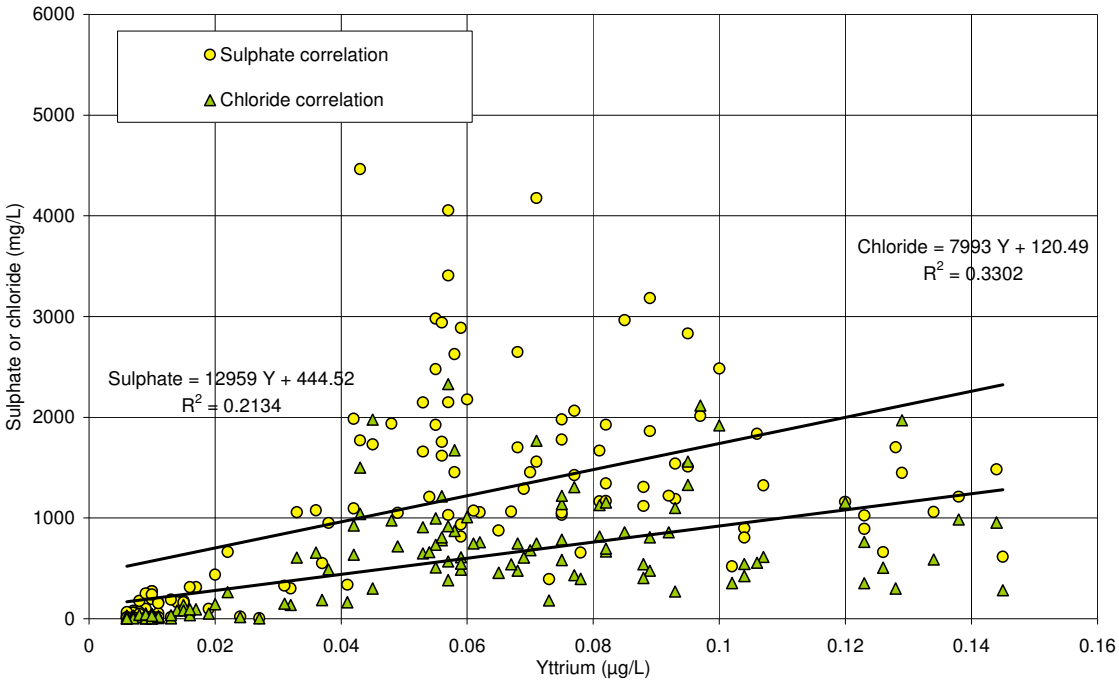

Figure 10.28. Scatter-plot showing correlation of yttrium with sulphate and chloride. Best fit linear regressions shown. Six values where yttrium is below detection limit are omitted.

10.23 Correlation with salinity

A number of the parameters discussed in this chapter show a clear correlation with salinity and an accumulation in groundwater towards the north.

The correlation coefficient (r) of these parameters in the 132 sampled groundwaters has been evaluated in the program DAS, by the Technical University of Vienna, after arbitrarily setting values less than the analytical detection limit to a value half of the lowest analytical detection limit. The result is Figure 10.29, which shows correlation coefficients with field electrical conductivity and with chloride. A correlation coefficient of +1 implies a perfect correlation, -1 implies a perfect negative correlation, while 0 implies no correlation.

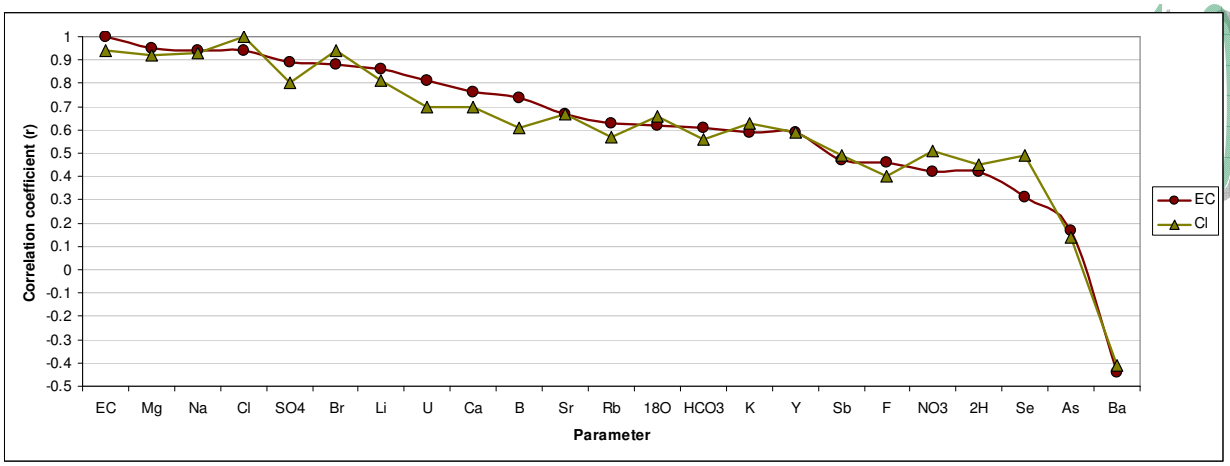

Figure 10.29. Correlation coefficients of selected parameters with electrical conductivity and chloride concentration, as surrogates of groundwater salinity. N = 132 groundwater samples from Faryab. 18O refers to the stable isotope $\delta^{18}O$ (see Chapter 11) and 2H to the stable isotope $\delta^{2}H$.

It will be seen that the most "salinity-related" parameters are magnesium, sodium, chloride, sulphate and bromide, followed by lithium and uranium.

The stable isotope $\delta^{18}O$ is susceptible to fractionation by evapoconcentration, and shows some correlation ($r>0.6$) with salinity, suggesting that at least some component of salinisation is related to evapoconcentrative processes.

Arsenic shows a rather poor correlation with salinity and barium shows a relatively good negative correlation.

11. Faryab: Stable Isotopes in Groundwater

11.1 Stable isotopes of oxygen and hydrogen

The most common isotope of oxygen has an atomic mass of approximately 16, and is called ^{16}O. Oxygen naturally contains a certain, modest percentage of a heavier isotope, with an atomic mass of 18, termed ^{18}O.

Similarly, the most common isotope of hydrogen comprises a single proton and a single electron, has an atomic mass of approximately 1, and is called ^{1}H. Hydrogen naturally contains a certain, modest percentage of a heavier isotope, comprising a proton, a neutron and an electron, with an atomic mass of 2, termed ^{2}H, or deuterium.

The water molecule H_2O thus has slightly heavier forms, containing either ^{18}O or ^{2}H (or, occasionally, both). The ^{18}O and ^{2}H contents of natural waters are often described by their deviation $\delta^{2}H$ / $\delta^{18}O$ from Standard Mean Ocean Water (SMOW), expressed in parts per thousand (‰).

Chemically, ^{18}O and ^{2}H are very similar to ^{16}O and ^{1}H, respectively, but certain processes cause a *fractionation* (enrichment or depletion). For example, water containing the heavy isotopes of oxygen and hydrogen does not evaporate as readily as "light" water. Thus, the water vapour is enriched in the lighter isotopes (has a lower $\delta^{2}H$ and $\delta^{18}O$), while the non-evaporated liquid residue is enriched in the heavier isotopes (has a higher $\delta^{2}H$ and $\delta^{18}O$).

Rainfall is, of course, derived from water vapour, usually evaporated from sea water. The rain (or snow) that condenses from the vapour thus also has a signature that is an isotopically "lighter" than sea water ($\delta^{2}H$ and $\delta^{18}O$ are negative), but heavier than the vapour from which it formed. Temperature (and altitude) affects the degree of fractionation during condensation of rain: in cold, upland situations, the rain (or snow) is often isotopically light (very negative $\delta^{2}H$ and $\delta^{18}O$), while in warmer, lowland climates the rain is isotopically heavier (less negative $\delta^{2}H$ and $\delta^{18}O$ - blue arrows on Figure 11.1).

It turns out that, on average throughout the world, precipitation samples lie on or around a global meteoric water line GMWL) when plotted on a $\delta^{2}H$ vs. $\delta^{18}O$ diagram. The typical equation for this line is often taken as

$$\delta^{2}H = (8.13 \times \delta^{18}O) + 10.8 \qquad \text{(Clark \& Fritz 1997)} \qquad (11.1)$$

The following websites provide good explanations of stable isotope fractionation in hydrologic systems:

USGS: http://wwwrcamnl.wr.usgs.gov/isoig/period/o_iig.html

SAHRA: http://web.sahra.arizona.edu/programs/isotopes/oxygen.html

If rainfall is highly continental, or not derived from the ocean, it may not fall on the GMWL, but on a local meteoric water line (LMWL), usually close and parallel to the GMWL. In arid regions (according to SAHRA 2014), precipitation tends to lie on a meteoric water line very slightly above, (but approximately parallel to) the GMWL, as shown by the orange dashed line in Figure 11.1. This deviation is often due to a component of locally evapotranspired water vapour (in addition to sea water vapour) and is referred to as the arid zone "deuterium excess" (Pang et al. 2011).

When rain falls on the ground and becomes groundwater or river water, it tends to retain its isotopic signature. If, however, it is subject to intense evaporation, it tends to move away below and to the right of the meteoric water line in a characteristic manner as shown by the green arrow in Figure 11.1. This deviation is simply because a water molecule containing an ^{18}O atom has a molecular weight of 20, while a water molecule containing a ^{2}H atom has a molecular weight of 19. Thus, the residual water subject to intense evaporation becomes enriched in ^{18}O more efficiently than in ^{2}H.

The data collected from Faryab Province clearly illustrates all these features.

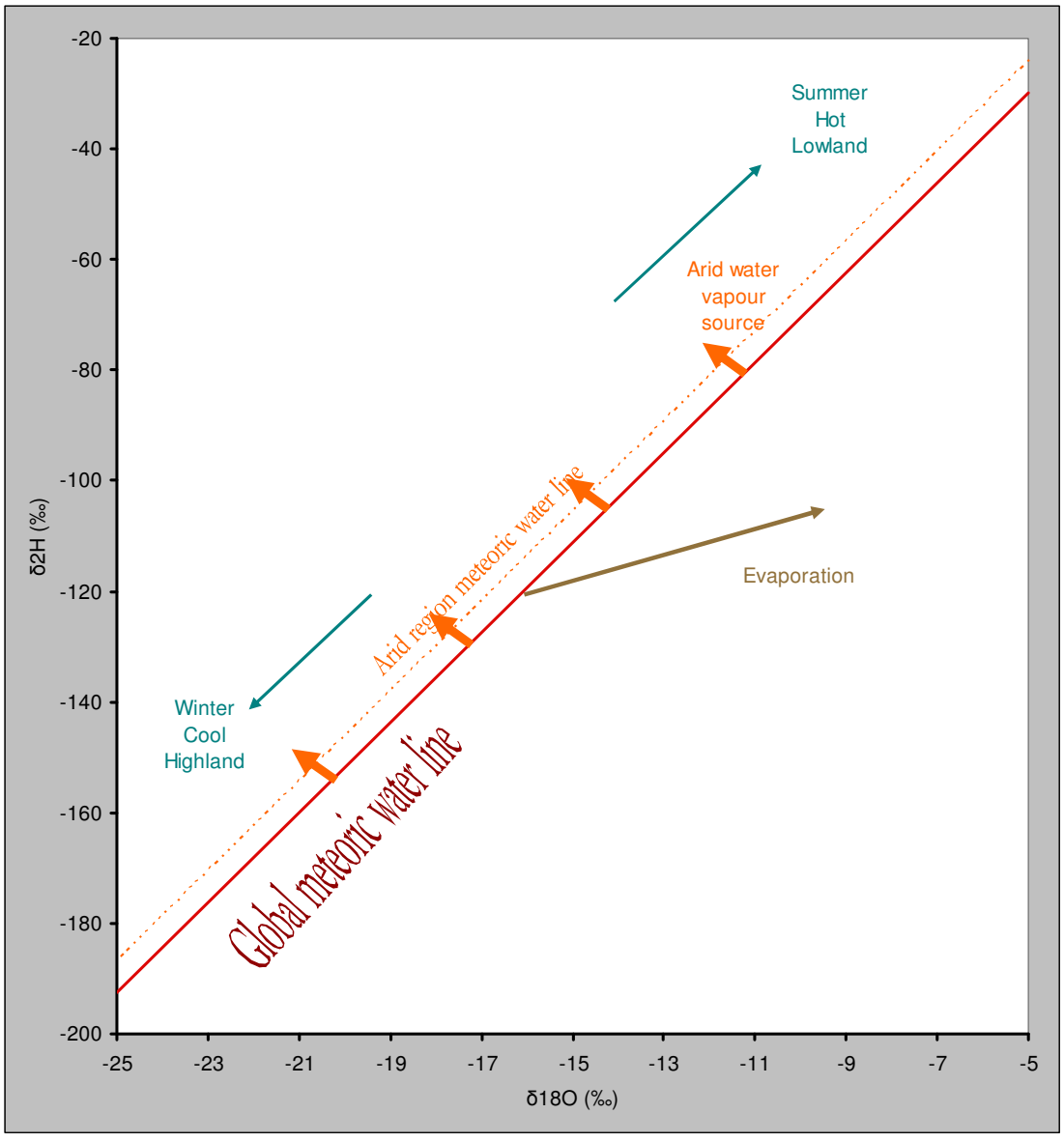

Figure 11.1. Generic stable isotope diagram, showing the global meteoric water line (red), an arid region meteoric water line (orange), seasonal effects (blue) and the effect of evaporation on surface water (or groundwater) bodies.

11.2 Precipitation and Rivers

We have already seen in Chapter 2 (Figure 2.8) that, as regards the isotopic signature of precipitation, the snowfall signatures are by far the isotopically lightest, with the

signatures becoming "heavier" throughout spring. The heaviest isotopic rainfall signatures typically come from Andkhoi, as one would expect, due to its hot, lowland climate. All the precipitation samples lie along, but slightly above, the global meteoric water line (GMWL). In fact, one can define a local meteoric water line, parallel to, but above the global meteoric water line, with the equation:

$$\delta^2H = (7.801 \times \delta^{18}O) + 15.08 \qquad (11.2)$$

The deuterium excess is thus around (15.08 - 10.8) = 4.3 ‰ greater than average global rainfall.

We have also seen, from Chapter 3.10d and 3.11d, that the waters of the Rivers Shirin Tagab and Maimana show a general tendency to become isotopically heavier downstream, which is strongly indicative of an evaporative fractionation effect.

We can now add (Figure 11,2) the river water samples from May 2013 to Figure 2.8.

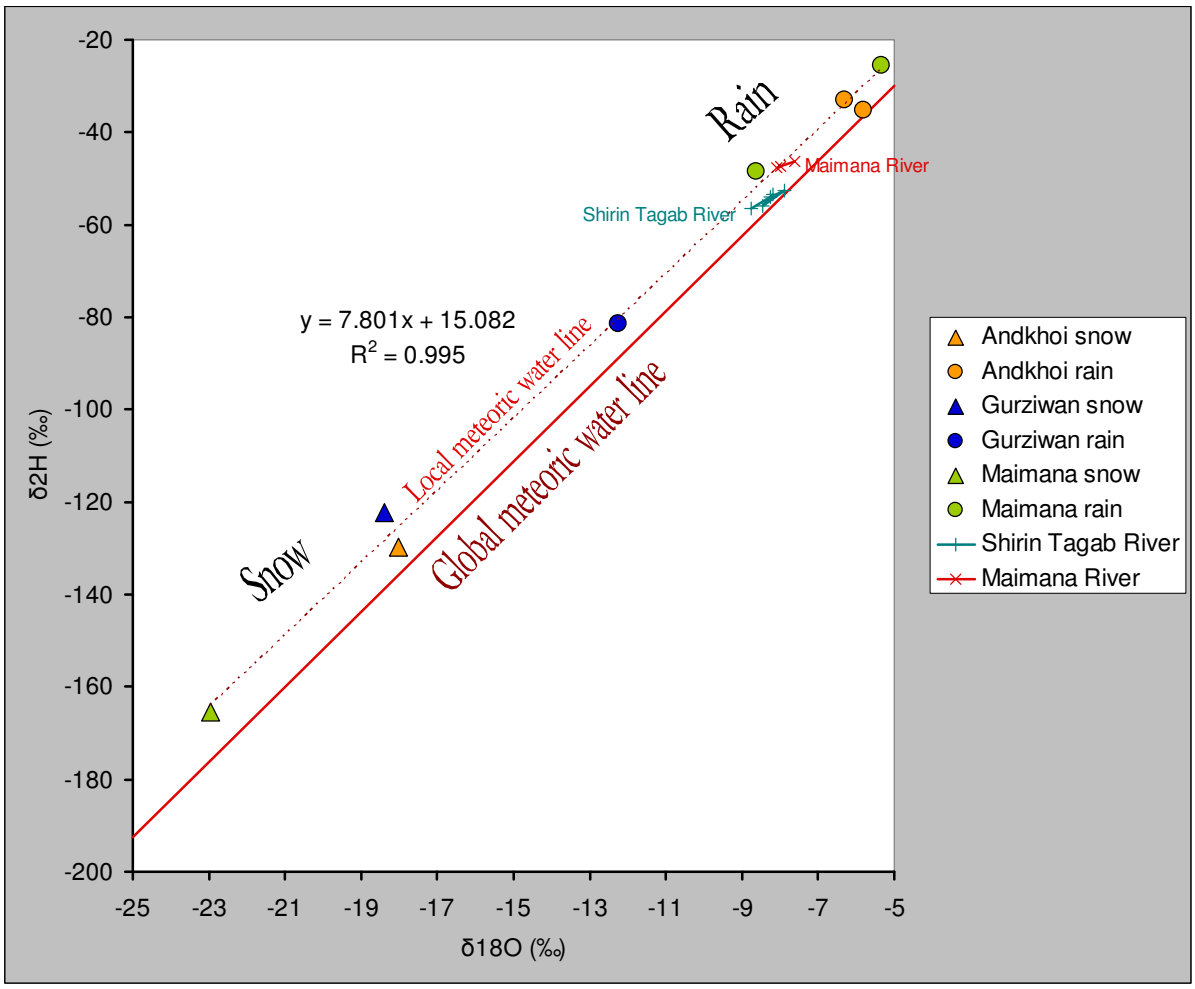

Figure 11.2. Stable isotope diagram comparing the isotopic composition of precipitation samples (from Figure 2.8) with river water samples from May 2013, described in Chapter 3. The GMWL is taken as $\delta^2H = (8.13 \times \delta^{18}O) + 10.8$ (Clark & Fritz 1997). The local meteoric water line is the linear best fit through all precipitation points and is defined by equation (11.2)

We find that the Maimana River samples plot slightly above the GMWL and close to the Maimana rainfall samples. The Shirin Tagab River samples are slightly lighter in ^2H; they plot between the Andkhoi rainfall samples and the Gurziwan rain/snow samples. This is

logical as they are from a location geographically between Gurziwan and Andkhoi in the catchment and will comprise a mixture of runoff with components both of up-catchment (Gurziwan) snowmelt and rain, and lower elevation rainfall. The trajectory described by the river water samples (see Figure 11.3) is characteristic of evaporative concentration of local meteoric water (see green arrow in Figure 11.1).

11.3 Groundwaters

60 of the 132 groundwaters sampled in 2013 were analysed for oxygen and hydrogen isotopes at the NERC Isotope Geosciences Laboratory located on the premises of the British Geological Survey at Keyworth, Nottingham, UK. The results are shown as boxplots in Figure 11.3.

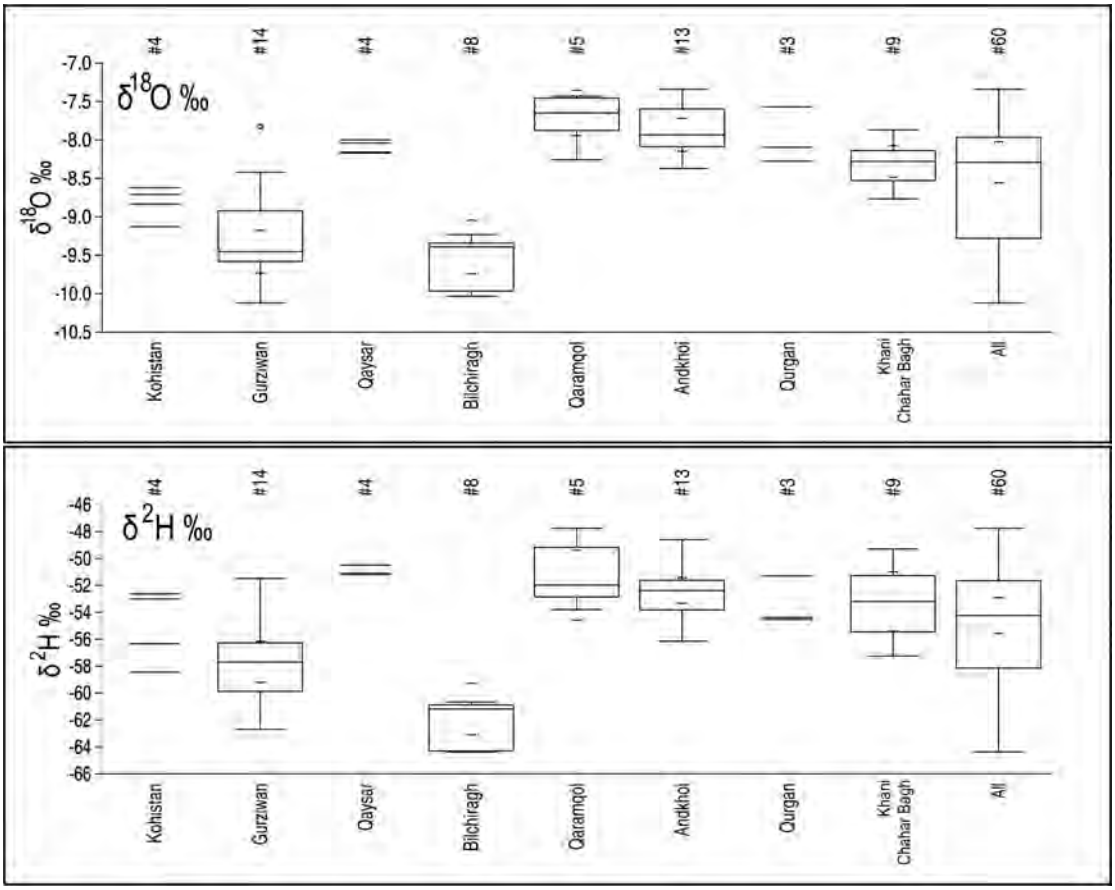

Figure 11.3. Boxplots showing distribution of oxygen-18 and deuterium in N=60 groundwater samples from Faryab.

On the δ^2H vs. $\delta^{18}O$ diagram (Figure 11.4), the groundwaters lie rather close to the Rivers. Thus, a small quadrant of Figure 11.2 has been taken and expanded to illustrate the stable isotopic composition of groundwaters.

The groundwaters from the upland districts (Kohistan, Bilchiragh, Gurziwan) plot, with isotopically lighter compositions, close to the local meteoric water line (LMWL). Further to the north, in the four northern districts around Andkhoi, the samples are isotopically heavier (which is consistent with the influence of either evaporation or isotopically heavier precipitation). However, the trajectory of the northern groundwater samples

(and those from the Shirin Tagab River) angles away from the meteoric water line in a direction that is wholly characteristic of evaporation (see green arrow in Figure 11.1).

The samples from the Shirin Tagab River lie within the groundwater field, strongly suggesting that there is an intimate linkage between groundwater and surface water (the Shirin Tagab being fed by groundwater baseflow to the north of Araba and in the Dowlatabad area, with groundwater resources being recharged by river infiltration in the Shirin Tagab delta area around Andkhoi).

Samples from Khani Chahar Bagh tend to have a slightly isotopically heavier δ^2H signature, relative to their $\delta^{18}O$ content, than the other samples from the Andkhoi area.

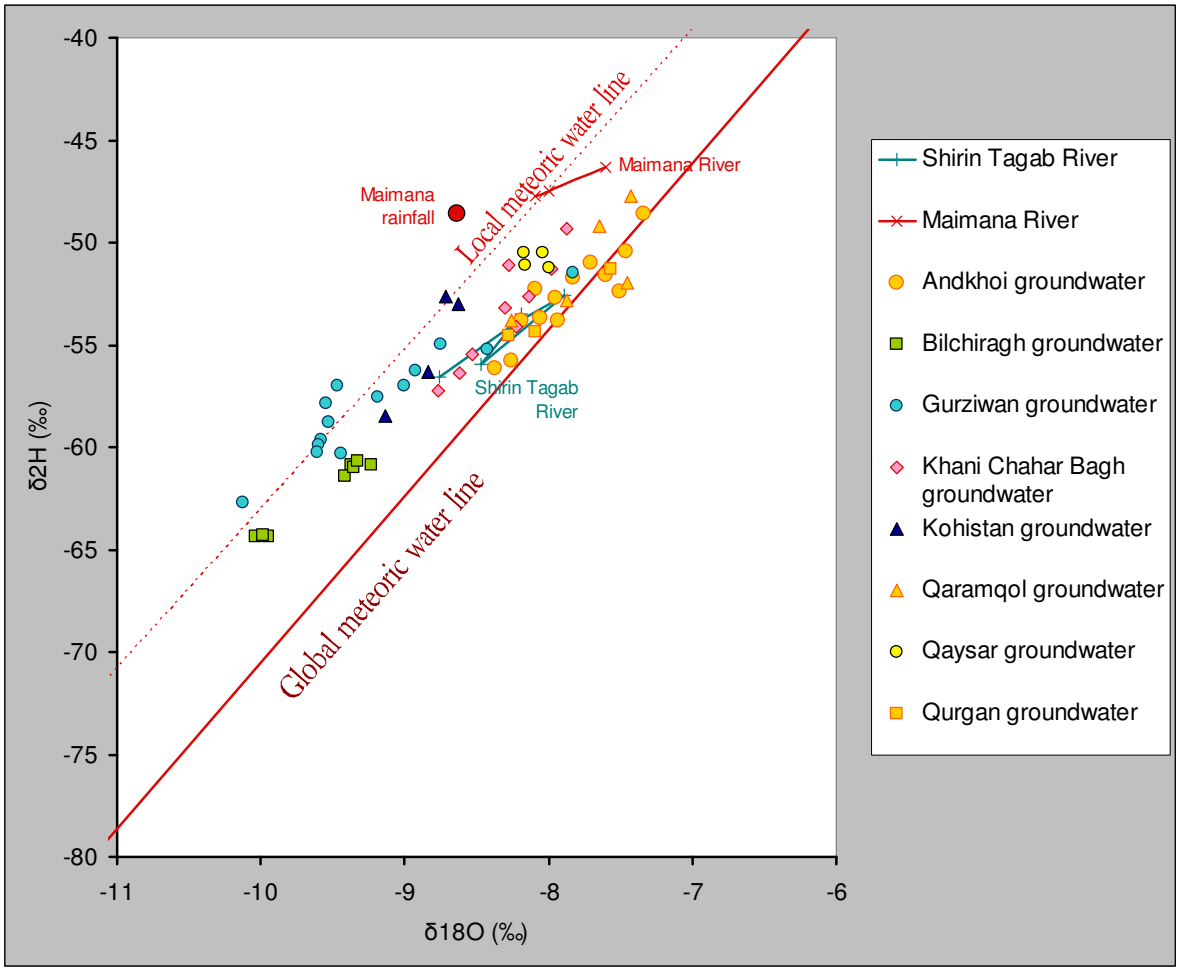

Figure 11.4. Stable isotope diagram comparing the isotopic composition of groundwater samples with river water samples from May 2013 and Maimana rainfall. The GMWL is taken as $\delta^2H = (8.13 \times \delta^{18}O) + 10.8$ (Clark & Fritz 1997). The local meteoric water line is taken from Figure 11.1.

The samples from Qaysar tend to lie slightly above the other groundwater samples in Figure 11.4, closer to the Maimana River, which is consistent with the samples being derived from the Maimana / Qaysar, rather than the Shirin Tagab, catchment).

In summary, stable isotope data confirms that groundwaters in the area appear to be ultimately derived from precipitation, but that, towards the north, groundwaters and river waters are strongly influenced by evapotranspirative effects.

Literature

References in Atlas Text

Abdullah, S.H. & Chmyriov, V.M. (1977a). *Hydrogeological Map of Afghanistan. Scale 1:2,000,000* Originally published as Annex No. 7 to Abdullah & Chmyriov (2008b).

Abdullah, S.H. & Chmyriov, V.M. (1977b). *Map of Mineral Waters of Afghanistan. Scale 1:2,000,000* Originally published as Annex No. 8 to Abdullah & Chmyriov (2008b).

Abdullah, S.H. & Chmyriov, V.M. (1977c). *Map of Mineral and Fresh Water Springs of Afghanistan. Scale 1:4,000,000* Originally published as Annex No. 9 to Abdullah & Chmyriov (2008b).

Abdullah, S.H. & Chmyriov, V.M. (eds.) (2008a). *Geology and Mineral Resources of Afghanistan.* Volume 1: Geology. Ministry of Mines and Industries of the Democratic Republic of Afghanistan / Afghanistan Geological Survey. British Geological Survey Occasional Publication No.15.

Abdullah, S.H. & Chmyriov, V.M. (eds.) (2008b). *Geology and Mineral Resources of Afghanistan.* Volume 2: Mineral Resources of Afghanistan. Ministry of Mines and Industries of the Democratic Republic of Afghanistan / Afghanistan Geological Survey. British Geological Survey Occasional Publication No.15.

Aladin, N., Létolle, R., Micklin, P. & Plotnikov, I. (2005). Uzboy and the Aral regressions: an hydrological approach. Preprint, *International Conference on Rapid Sea Level Change: A Caspian Perspective*, 2nd-9th May 2005 Rasht, Islamic Republic of Iran. 20 pp.

Alcalá, F. J. & Custudio, E. (2004). Use of the Cl/Br ratio as a tracer to identify the origin of salinity in some coastal aquifers of Spain. *In* Araguás, L., Custodio, E. & Manzano, M. (eds.) "Groundwater and saline intrusion", *Proceedings of the 18th Salt Water Intrusion Meeting, Cartagena, Spain, 2004*, 481-497. IGME.

Banks, D. (2001). *Guidelines for Sustainable Use of Groundwater in Afghanistan*. Report for Norwegian Church Aid. http://www.holymoor.co.uk/Poldok.PDF.

Banks, D. & Soldal, O. (2002). Towards a policy for sustainable use of groundwater by non-governmental organisations in Afghanistan. *Hydrogeology Journal* **10**, 377-392.

Banks, D., Karnachuk, O.V., Parnachev, V.P., Holden, W. & Frengstad, B. (2002). Rural pit latrines as a source of groundwater contamination; examples from Siberia and Kosova. *Journal of the Chartered Institution of Water and Environmental Management* 16, 147-152.

Banks, D. (2009). An introduction to "thermogeology" and the exploitation of ground source heat. *Quarterly Journal of Engineering Geology and Hydrogeology* **42**, 283-293.

Banks, D. (2012). *An Introduction to Thermogeology: Ground Source Heating and Cooling. 2nd Edition.* John Wiley & Sons, Chichester, 526 pp. ISBN: 978-0-470-67034-7.

Banks, D., Hall, G.M., Reimann, C. & Siewers, U. (1999). Distribution of rare earth elements in crystalline bedrock groundwaters: Oslo and Bergen regions, Norway. *Applied Geochemistry*, 14, 27-39.

Banks, D., Parnachev, V.P., Frengstad, B., Holden, W., Karnachuk, O.V. & Vedernikov A.A. (2004). The evolution of alkaline, saline ground- and surface waters in the southern Siberian steppes. *Applied Geochemistry* 19, 1905-1926. doi: 10.1016/j.apgeochem.2004.05.009

Berg, L.S. (1950). *Natural Regions of the USSR.* Translated from the Russian by O.A. Titelbaum and edited by J.A. Morrison and C. C. Nikiforoff, MacMillan, New York.

BGS (2014). *Geology of Afghanistan.* http://www.bgs.ac.uk/afghanminerals/geology.htm. Accessed February 2014.

Boomer, I., Aladin, N., Plotnikov, I. & Whatley, R. (2000). The palaeolimnology of the Aral Sea: a review. *Quaternary Science Reviews* **19,** 1259-1278.

Boomer, I., Wünnemann, B., Mackay, A.W., Austin, P., Sorrel, P., Reinhardt, C., Keyser, D., Guichard, F., & Fontugne, M. (2009). Advances in understanding the late Holocene history of the Aral Sea region. Quaternary International 194, 79–90.

Boroffka, N.G.O. (2010). Archaeology and its relevance to climate and water level changes: a review. *In* Kostianoy, A.G. & Kosarev, A.N. (eds.): "The Aral Sea Environment: The Handbook of Environmental Chemistry", 283-303. Springer - Verlag Berlin Heidelberg. doi: 10.1007/698_2009_1.

Breckle, S.W. & Geldyeva, G.V. (2012). Dynamics of the Aral Sea in geological and historical times. *In* Breckle S.W., Wucherer, W., Dimeyeva, L.A. & Ogar, N.P. (eds.): "Aralkum - a Man-Made Desert: The Desiccated Floor of the Aral Sea (Central Asia)", Ecological Studies 218, 13-35. Springer. doi: 10.1007/978-3-642-21117-1_2.

Brookfield, M.E. & Hashmat, A. (2001). The geology and petroleum potential of the North Afghan platform and adjacent areas (northern Afghanistan, with parts of southern Turkmenistan, Uzbekistan and Tajikistan). *Earth-Science Reviews* **55**, 41–71.

Byron, R. (1937). *The Road to Oxiana.* Macmillan.

Carpenter, S.J. & Lohmann, K.C. (1992). Sr /Mg ratios of modern marine calcite: empirical indicators of ocean chemistry and precipitation rate. *Geochimica et Cosmochimica Acta* 56, 1837-1849.

China Geological Survey (2012). *Groundwater Serial Maps of Asia: Hydrogeological Map, Groundwater Resources Map, Geothermal Map - Explanation.* Sinomaps Press, ISBN 978-7-5031-7398-1.

Clark, I.D. & Fritz, P. (1997). *Environmental Isotopes in Hydrogeology*. CRC Press, 352 pp. ISBN: 9781566702492.

Davis, S.N., Whittemore, D.O. & Fabryka-Martin J. (1998). Uses of chloride/bromide ratios in studies of potable water. *Ground Water* 36, 338-350.

Davis, S.N., Fabryka-Martin, J.T. & Wolfsberg, L.E. (2008). Variations of bromide in potable ground water in the United States. *Ground Water* 42, 902-909.

Dèzes, P. (1999). *Tectonic and metamorphic evolution of the Central Himalayan Domain in Southeast Zanskar (Kashmir, India).* PhD thesis; Institut de Mineralogie et Petrographie, Université de Lausanne.

Dickson, A.G. & Goyet, C. (eds.) (1994). *Handbook of methods for the analysis of the various parameters of the carbon dioxide system in sea water; version 2.* U.S. Dept. of Energy, ORNL/CDIAC-74.

Dronov, V.I. (2008a). Stratigraphy. Chapter 4 in Abdullah & Chmyriov (2008). 31-233.

Dronov, V.I. (2008b). The main stages of the geological history of the Afghan Territory. Chapter 7 in Abdullah & Chmyriov (2008). 394-428.

Dronov, V.I. & V.M. Chmyriov, V.M. (2008). Structure. Chapter 6 in Abdullah & Chmyriov (2008). 308-393.

Encyclopaedia Iranica (1988). *Band-**e** Torkestan.* http://www.iranicaonline.org/articles/band-e-torkestan.

Esenov. P.E. (2014). Groundwaters and salinization of soils in Turkmenistan. *In:* Zonn, I.S. & Kostianoy, A.G. (eds), "The Turkmen Lake Altyn Asyr and Water Resources in Turkmenistan". *Handbook of Environmental Chemistry* **28**, 141–150. doi: 10.1007/698_2012_215.

Fan, Y., & van den Dool, H. (2008). A global monthly land surface air temperature analysis for 1948-present, J. *Geophys. Res*. **113**, D01103, doi:10.1029/2007JD008470.

Favre, R. & Kamal, G.M. (2004) *Watershed Atlas of Afghanistan. 1st Edition: Working Document for Planners.* Ministry of Irrigation, Water Resources and Environment, FAO, SDC, AIMS and AREU.

Frengstad, B.S. & Banks, D. (2014). Uranium distribution in groundwater from fractured crystalline aquifers in Norway. *In:* Sharp, J.M. (ed.) "*Fractured Rock Hydrogeology*", International Association of Hydrogeologists Selected Papers **20**: 257-276. CRC Press/ Taylor & Francis, London.

Fyedorovich, B.A. (1978). Entry for *Karakum [Каракумы]* in the Great Soviet Encyclopaedia (1978).

Gapparov B.K., Beglov I.F., Nazariy A.M. & Usmanova O.K. (2011). Water Quality in the Amudarya and Syrdarya River Basins: Analytical Report. Scientific-Information Center Interstate Commission for Water Coordination in Central Asia (SIC ICWC) / United Nations Economic Commission for Europe (UNECE) / Central Asian Regional Environmental Center (CAREC). Tashkent, 2011. http://www.cawater-info.net/water_quality_in_ca/files/analytic_report_en.pdf.

Glantz, M.H. (1999). *Creeping Environmental Problems and Sustainable Development in the Aral Sea Basin*. Cambridge University Press. ISBN: 9781139429412.

Gotgilf, A.V, Atanasyeva, V.N. & Yusupov, I. (1969). Geothermal characteristic of Mesozoic-Cenozoic rocks of southwestern Tajikistan. *In:* Problemy neftegazenosnosti Tadzhikistana, vyp. 1, Dushanbe, Irfon, p. 143-145.

Great Soviet Encyclopedia (1978). *The Great Soviet Encyclopedia [Большая советская энциклопедия]*, (1969-1978). Found in Russian at http://slovari.yandex.ru and in English at http://encyclopedia2.thefreedictionary.com/.

Harris, D.R. (2010). Origins of agriculture in Western Central Asia: An environmental-archaeological study. University of Pennsylvania Press, 304 pp.

Hassan Saffi, M. (2010a). *Integrated Groundwater Study in Astana Valley, Shirin Tagab District of Faryab Province, Afghanistan*. DACAAR Report, Kabul. June 2010.

Hassan Saffi, M. (2010b). *Integrated Groundwater Study in Jalaier Valley, Shirin Tagab District of Faryab Province, Afghanistan*. DACAAR Report, Kabul. June 2010.

Ibrekk, H.A., Stoveland, S. & Ghani, S. (2006). *Analysis of the Water Situation in Faryab Province, Afghanistan: Water Resources, Drinking Water, Sanitation and Irrigation.* Royal Norwegian Embassy / NORAD / NORPLAN, Kabul, October 2006.

INTAS (2006). The rehabilitation of the ecosystem and bioproductivity of the Aral Sea under conditions of water scarcity. INTAS Project – 0511 REBASOWS; Final report. International Association for the promotion of co-operation with scientists from the New Independent States of the former Soviet Union (INTAS), 265 pp.

http://www.wau.boku.ac.at/iwhw/onlinepublikationen/nachtnebel/EU_INTAS_0511_Rebasows/Files/Final_report_EU_Intas0511_Aral_Sea.pdf.

Iranica Online (2014). *Band-e Torkestan.* http://www.iranicaonline.org/articles/band-e-torkestan, accessed February 2014.

Jones, B.F., Rettig, S.L. & Eugster, H.P. (1967). Silica in alkaline brines. *Science* 158(3806), 1310-1314.

Kharin, N.G. (2002). *Vegetation degradation in Central Asia under the impact of human activities.* Kluwer, 185 pp.

Klett, T.R., Ulmishek, G.F., Wandrey, C.J. Agena, W.F. (2006). Assessment of undiscovered technically recoverable conventional petroleum resources of Northern Afghanistan. *U.S. Geological Survey Open-File Report* **2006-1253**.

Kreibich, H. & Thieken, A. H. (2008): Assessment of damage caused by high groundwater inundation. *Water Resources Research (AGU)* **44(9)**, W09409. doi: 10.1029/2007WR006621.

Krizhanovskii, V.A. (Крыжановский, В.А.) (ed.) (1972). Гидрогеология СССР: том 38: Туркменская ССР. Институт Геологии Совета Министров Туркменской ССР. Издат. Недра, Москва. [*Hydrogeology of the USSR. Vol. 38. Turkmenistan. Nedra, Moscow - in Russian*]. 565 pp.

Krylov, N.A. - ed. (1980). *Neftegazonosnost bolshikh glubin [Petroleum potential at great depths - in Russian].* Nauka, Moscow, 142 pp.

Lee, J.L. (1987). The history of Maimana in Northwestern Afghanistan 1731-1893. *Iran*, **25**, pp. 107-124.

Létolle, R., Micklin, P., Aladin, N. & Plotnikov, I. (2007). Uzboy and the Aral regressions: A hydrological approach. *Quaternary International* **173–174**, 125–136.

Lewis, A.J., Komninou, A., Yardley, B.W.D. & Palmer, M.R. (1998). Rare earth element speciation in geothermal fluids from Yellowstone National Park, Wyoming, USA. *Geochimica et Cosmochimica Acta* **62(4),** 657–663.

Lyberis, N. & Mering, C. (2000). Evolution of the hydrographic network of the Karakum desert and environmental implications for the Aral Sea. Paper SP-461 *in Proc. ERS-Envisat Symposium*, "Looking down to Earth in the New Millennium", 16th-20th October 2000, Göteborg, Sweden.

Marinova, N.A. [Маринова, Н.А.] (ed.) (1974) Гидрогеология Азии *(Hydrogeology of Asia)*. Nedra, 576 pp.

McKinney, K.C. & Sawyer, D.A. (2005). Geologic map of quadrangle 3564, Chahriaq (Joand) (405) and Gurziwan (406) quadrangles, Afghanistan. Afghan Geological Survey in cooperation with the United States Geological Survey. *USGS Open-File Report* 2005-1099-A, *AGS Open-File Report* (405/406) 2005-1099-A.

McKinney, K.C. & Lidke, D.J. (2005). Geologic map of quadrangles 3560, 3562, and 3662, Sir Band (402), Khawja-Jir (403), Bala-Murghab (404), and Darah-i-Shor-i-Karamandi (122) quadrangles, Afghanistan. Afghan Geological Survey in cooperation with the United States Geological Survey. *USGS Open-File Report* 2005-1098-A, *AGS Open-File Report* (402/403/404/122) 2005-1098-A.

Mishkin, L.P. [Мышкин Л.П.] (1968). Схематическая карта гидроизогипси минерализации подземных вод четвертичных отложений центральной части Северного Афганистана. Масштаб 1:500,000 (*Schematic map if hydroisohypses of groundwater mineralization in the Quaternary deposits of the central part of*

northern Afghanistan. Scale 1:500,000). Reproduced in black and white as Figure 16 in Marinova (1974).

Misstear, B., Banks, D. & Clark, L. (2006). *Water Wells and Boreholes*. Wiley, Chichester, 514 pp. ISBN/ISSN: 978-0-470-84989-7

MRRD (2007). *Faryab PDP Provincial Profile.* Ministry of Rural Rehabilitation and Development, Kabul.

MUMTAZ (2007). *Design and implementation of Andkhoi city water supply pumping unit from the Amu Darya River.* Mumtaz Corporation Report MEW/530, 1386/2/20, dated 10th May 2007.

Nable, R.O., Bañuelos, G.S. & Paull, J.G. (1997). Boron toxicity. *Plant and Soil* **193**, 181–198. doi: 10.1023/A:1004272227886

Olson, S.A., and Williams-Sether, T. (2010). Streamflow characteristics at streamgages in northern Afghanistan and selected locations. U.S. Geological Survey Data Series 529, 512 pp. http://pubs.usgs.gov/ds/529/.

Orris, G.J. & Bliss, J.D. (2002). Mines and mineral occurrences of Afghanistan. USGS Open File Report 02-110.

Olbrycht, J.M. (2010). Some remarks on the rivers of Central Asia in antiquity. *In* Jackson, T.N., Konovalova, I.G. & Tsetskhladze, G.R. (eds.) "*Gaudeamus Igitur - Stuidies to Honour the 60th Birthday of A.V. Podossinov*", Russian Academy of Sciences - Institute of World History, 302-309. Moscow.

Pang, Z., Kong, Y., Froehlich, K.,Huang, T., Yuan, L., Li, Z. and Wang, F. (2011). Processes affecting isotopes in precipitation of an arid region. Tellus B **63(3),** 352-359. doi: 10.1111/j.1600-0889.2011.00532.x

Parkhurst, D.L. (1995). Users guide to PHREEQC – a computer program for speciation, reaction-path, advective-transport, and inverse geochemical calculations. *U.S. Geological Survey Water Resources Investigation Report* 95-4227.

Parnachev, V.P., Banks, D., Berezovsky, A.Y. & Garbe-Schönberg, D. (1999). Hydrochemical evolution of Na-SO4-Cl groundwaters in a cold, semi-arid region of southern Siberia. *Hydrogeology Journal* 7, 546-560. doi: 10.1007/s100400050228.

Plummer, L.N., Parkhurst, D.L., Fleming, G.W., Dunkle, S.A. (1988). A computer program incorporating Pitzer's equations for calculation of geochemical reactions in brines. *U.S. Geological Survey Water Resources Investigation Report* 88-4153.

Pravilova, E. (2009). River of empire: geopolitics, irrigation, and the Amu Darya in the late XIXth Century. *Cahiers d'Asie Centrale* **17/18**, 255-287.

Radojicic, S. (1978): Summary report on deep tube wells constructed by Water and Soil Survey Dept., Ministry of Water and Power, 1973-78.

Railsback, B.L. (2006). *Some Fundamentals of Mineralogy and Geochemistry*. Ebook available at http://www.gly.uga.edu/railsback/FundamentalsIndex.html.

Saba, D.S., Najaf, M.E., Musazai, A.M. & Taraki, S.A. (2004). *Geothermal energy in Afghanistan: Prospects and potential.* Prepared for the Center on International Cooperation, New York University (USA) and the Afghanistan Center for Policy and Development Studies (Kabul). February 2004, 38 pp.

SAHRA (2014). *Oxygen isotopes.* Sustainability of semi-arid hydrology and riparian areas (SAHRA) website. http://web.sahra.arizona.edu/programs/isotopes/oxygen.html. Accessed May 2014.

Schneider, U., Becker, A., Finger, P., Meyer-Christoffer, A., Rudolf, B., Ziese, M. (2011). GPCC Full Data Reanalysis Version 6.0 at 0.5°: Monthly Land-Surface Precipitation from Rain-Gauges built on GTS-based and Historic Data. DOI: 10.5676/DWD_GPCC/FD_M_V6_050.

Smoydzin, L. & von Glasow, R. (2009). Modelling chemistry over the Dead Sea: bromine and ozone chemistry. *Atmospheric Chemistry and Physics* 9(14), 5057-5072.

SPHERE (2000). *Humanitarian Charter and Minimum Standards in Disaster Response (1st edition).* The SPHERE Project, Geneva / Oxfam Publishing, Oxford. 330 pp.

SPHERE (2011). *Humanitarian Charter and Minimum Standards in Humanitarian Response (3rd edition).* The SPHERE Project, Practical Action Publishing, Rugby. 393 pp.

Steinshouer, D.W., Klett, T.R., Umlishek, G.F., Wandrey, C.J., Wahl, R.R., Hill, R.J., Pribil, M., Pawlewicz, M.J., King, J.D., Agena, W.F., Taylor, D.J., Amirzada, A., Selab, A.M., Mutteh, A.S., Haidari, G.N. & Wardak, M.G. (2006). Petroleum Resource Potential GIS of Northern Afghanistan. *U.S. Geological Survey Open-File Report* **OFR-2006-1179**. http://pubs.usgs.gov/of/2006/1179.

Struckmeier, W.F. & Margat, J. (1995). Hydrogeological maps: a guide and standard legend. *International Contributions to Groundwater*, **Vol. 17**, International Association of Hydrogeologists, Heise, Hannover. Available at http://www.bgr.bund.de/EN/Themen/Wasser/Projekte/laufend/Beratung/Ihme1500/standard_legend_hydro_maps.pdf?__blob=publicationFile&v=1 and at http://www.iah.org/downloads/pubfiles/IAHbook_ICH17.zip.

Tanaka, M., Takahashi, K. & Sahoo, Y.V. (2004). Speciation of dissolved silicates in natural waters containing alkaline and alkaline-earth ions. A case study--waters from arid lands (North West China). Analytical and Bioanalytical Chemistry 378(3), 789-797.

Tanaka, M. & Takahashi, K. (2007). The chemical behavior of silica in water in saline area; comparison for region and evaporation process. Spectrochim Acta Part A Molecular and Biomolecular Spectroscopy 68(1), 21-28.

Tarn, W.W. (1901). Patrocles and the Oxo-Caspian trade route. *Journal of Hellenic Studies* **21**, 10-29.

Thomas, V. & Ahmad, M. (2009). *A Historical Perspective on the Mirab System: A Case Study of the Jangharoq Canal, Baghlan.* Afghanistan Research and Evaluation Unit / Aga Khan Foundation. March 2009. 66 pp. Available from http://www.areu.org.af/Uploads/EditionPdfs/908E-The%20Mirab%20System-CS-web.pdf.

Ulmishek, G.F. (2004). *Petroleum Geology and Resources of the Amu-Darya Basin, Turkmenistan, Uzbekistan, Afghanistan, and Iran*. U.S. Geological Survey Bulletin 2201–H.

USEPA (2009). *National Primary Drinking Water Regulations.* United States Environmental Protection Agency, document EPA 816-F-09-004, May 2009. Available at http://water.epa.gov/drink/contaminants/upload/mcl-2.pdf, last accessed January 2014.

Vámbéry, A. (1865). *Reise in Mittelasien von Teheran durch die Turkmanische Wüste an der Ostküste des Kaspischen Meeres nach Chiwa, Bochara und Samarkand ausgeführt im Jahr 1863. [Travels in Central Asia from Teheran through the Turkman Deserts on the east side of the Caspian Sea towards Chiwa, Bochara and Samarkand].* Brodhaus, Leipzig.

Vengosh, A., Starinsky, A., Kolodny, Y., Chivas A.R. & Raab, M. (1992). Boron isotope variations during fractional evaporation of sea water: New constraints on the marine vs. non-marine debate. *Geology* 20, 799-802.

Wahl, R.R. (2005). Geologic map of quadrangles 3764 and 3664, Jalajin (117), Kham-Ab (118), Char Shango (123) and Shebergan (124) quadrangles, Afghanistan. Afghan Geological Survey in cooperation with the United States Geological Survey. *USGS Open-File Report* 2005-1092-A, *AGS Open-File Report* (117/118/123/124) 2005-1092-A.

Whitney, J.W. (2006). *Geology, Water, and Wind in the Lower Helmand Basin, Southern Afghanistan.* U.S. Geological Survey Scientific Investigations Report 2006–5182.

WHO (2011). *Guidelines for Drinking Water Quality (4th edition).* World Health Organisation, Geneva.

Wood, W.W. & Sanford, W.E. (2007). Atmospheric bromine flux from the coastal Abu Dhabi sabkhat: A ground-water mass balance investigation. *Geophysical Research Letters* 34, L14405. doi:10.1029/2007GL029922.

Zavialov, P. (2005). Physical Oceanography of the Dying Aral Sea. Springer / Praxis, 146 pp. ISBN: 0123415567816.

Zhou, Y. & McLennan, S.M. (2011). Experimental evaluation of photochemical influences of bromine and chlorine geochemistry on Mars. Proceedings of the 42nd Lunar and Planetary Science Conference (2011), 7-11th March 2011, Texas, USA.Paper 1667

Zonn, I.S., Kostianoy, A.G., Kosarev, A.N. & Glantz, M.H. (2010). *The Caspian Sea Encyclopedia.* Springer-Verlag, Berlin / Heidelberg.

Zonn, I.S. (2014). Karakum Canal: Artificial River in a Desert. *In:* Zonn, I.S. & Kostianoy, A.G. (eds), "The Turkmen Lake Altyn Asyr and Water Resources in Turkmenistan". *Handbook of Environmental Chemistry* **28**, 95-106. doi: 10.1007/698_2012_194.

Further Reading

Ahmad, M. & Wasiq, M. (2004). *Water Resource Development in Northern Afghanistan and its Implications for Amu Darya Basin.* World Bank Working Paper No. 36.

Aladin N., Plotnikov, I., Bolshov, A. & Pichugin, A. (undated). Biodiversity of the Caspian Sea. Caspian Sea Biodiversity Project, http://www.zin.ru/projects/caspdiv/biodiversity_report.html, last accessed 11/1/13.

Ashworth, J.M. (2005). *Groundwater Assessment of the Downstream Sections of the Balkh and Khulm Watersheds. Inception Report.* Ministry of Energy and Water, 2005.

Breckle, S.W. (1983). Temperate deserts and semi-deserts of Afghanistan and Iran. Pages 271-319 *in:* West, N.E. (ed.) *Temperate deserts and semi-deserts.* Elsevier, Amsterdam.

CAWater (2012). *Hydrogeology and groundwater.* http://www.cawater-info.net/afghanistan/groundwater.htm.

CSO (2013). *Estimated Population of Afghanistan 2012-13. Settled Population of Faryab province by Civil Division, Urban, Rural and Sex-2012-13*. Islamic Republic of Afghanistan, Central Statistics Organization. http://cso.gov.af/Content/files/Faryab(1).pdf

DACAAR (2011). *Update on "National Groundwater Monitoring Wells Network activities in Afghanistan". From July 2007 to December 2010.* DACAAR Report, Kabul.

Hassan Saffi, M. (2007). *Groundwater at risk in Afghanistan.* DACAAR Report, Kabul.

Hassan Saffi, M. (2011). *Groundwater natural resources and quality concern in Kabul Basin, Afghanistan*. DACAAR Report, Kabul.

Klemm, W. & Shobair, S.S. (2010). *The Afghan Part of the Amu Darya Basin. Impact of Irrigation in Northern Afghanistan on Water Use in the Amu Darya Basin*. http://www.unece.org/fileadmin/DAM/SPECA/documents/ecf/2010/FAO_report_e.pdf.

Nathan Berger (1992). *Afghanistan Water Constraints. Overview Analysis.* Report submitted to the Office of the A.I.D. Representative for Afghanistan Affairs by Nathan Associates Inc. and Louis Berger International, Inc.

Oberhänsli, H., Novotná, K., Píšková, A., Chabrillat, S., Nourgaliev, D.K., Kurbaniyazov, A.K. & Grygar, T.M. (2011). Variability in precipitation, temperature and river runoff in W Central Asia during the past ~2000 yrs. *Global and Planetary Change* **76**, 95–104.

Qureshi, A.S. (2002). *Water Resources Management in Afghanistan: The Issues and Options.* International Water Management Institute, Working Paper 49, Pakistan Country Series No. 14.

Rakhmatullaev, S., Huneau, F., Kazbekov, J., Le Coustumer, P., Jumanov, J., El Oifi, B., Motelica-Heino, M. & Hrkal, Z. (2010). Groundwater resources use and management in the Amu Darya river basin (Central Asia). *Environmental Earth Sciences* **59**, 1183-1193.

Rawlinson, H.C. (1879). The Road to Merv. *Proceedings of the Royal Geographical Society and Monthly Record of Geography - New Monthly Series* **1(3),** 161-191.

Rout, B. (2008). *How the Water Flows: A Typology of Irrigation Systems in Afghanistan*. Afghanistan Research and Evaluation Unit (AREU).

Rycroft, D.W. & Wegerich, K. (2009). The three blind spots of Afghanistan: water flow, irrigation development, and the impact of climate change. *China and Eurasia Forum Quarterly* **7(4),** 115-133.

Salama, R.B., Otto, C.J. & Fitzpatrick, R.W. (1999). Contributions of groundwater conditions to soil and water salinization. *Hydrogeology Journal***, 7(1),** 46-64.

Shobair, S.S. (2001). *Irrigation water management – crop water requirements.* Food and Agriculture Organisation of the United Nations (FAO), Peshawar (Pakistan), June, 111 pp.

Shobair, S.S. & Alim, A.K. (2004). *The effects of calamities on water resources and consumption in Afghanistan*. Food and Agriculture Organization of the United Nations (FAO).

Tünnermeier, T., Houben, G. & Niard, N.; edited by Himmelsbach, T. (2005 / 2006). *Hydrogeology of the Kabul Basin* (3 parts). Bundesanstalt für Geowissenschaften und Rohstoffe (BGR), Hannover, Germany.

Uhl, V.W. & Qasem Tahiri, M. (2003). Afghanistan. An overview of groundwater resources and challenges. Uhl, Baron, Rana & Associates, Inc. http://www.vuawater.com/pages/Afghanistan_GW_Study.pdf.

USAID (1976). *Helmand River Basin. Soil and Water Survey Study Report.* Government of Afghanistan and USAID.

Zonn, I.S. (2002). *Water resources of Northern Afghanistan and their future use.* Paper presented at workshop on water, climate and development issues in the Amu-Dar'ya basin, Philadelphia, PA, 2002.